



UNIVERSITY OF  
BIRMINGHAM

**A Comparison of Cell Wall Properties of  
*Arabidopsis thaliana***

By

**Robert John Palin**

A thesis submitted to the  
University of Birmingham  
for the degree of  
**Doctor of Philosophy**

School of Engineering  
University of Birmingham  
United Kingdom

UNIVERSITY OF  
BIRMINGHAM

**University of Birmingham Research Archive**

**e-theses repository**

This unpublished thesis/dissertation is copyright of the author and/or third parties. The intellectual property rights of the author or third parties in respect of this work are as defined by The Copyright Designs and Patents Act 1988 or as modified by any successor legislation.

Any use made of information contained in this thesis/dissertation must be in accordance with that legislation and must be properly acknowledged. Further distribution or reproduction in any format is prohibited without the permission of the copyright holder.

---

## *Abstract*

---

Mechanical properties of the plant cell wall are important in many industrial applications including bio-fuels, food quality and biotechnology. The plant cell wall consists of a network of cellulose microfibrils cross-linked with hemi-cellulose and interpenetrated by pectin. It is known that changes in the composition and architecture of the cell wall lead to detectable differences in the mechanical properties, but the relationship is not yet fully understood. In this work, three cell wall mutations of *Arabidopsis thaliana*, *ida*, *mur1* and *qua-2* (Snakeskin/*sk*s), were compared to the *Columbia* (*col0*) wild type. Shoot and root growth were characterised to evaluate the effects of the mutations on plant growth. The *ida* mutation behaved like *col0*, with *mur1* and *sk*s showing increasingly severe effects of mutation on growth. Cells were also grown in suspension culture and an investigation of the wall components of both plant tissue and suspension cultured cells was conducted. An increase in pectin caused by the culturing process, and differences in cellulose content due to the mutations were found. The mean force required to break the suspension cultured cells (the rupture force) and deformation at rupture were obtained by compression testing. Force-deformation data from cell compressions were mathematically modelled up to deformations below the elastic limit of the cell walls, allowing the derivation of a low strain elastic modulus (E). Significant reductions in E for *mur1* compared to *col0* and *ida* and between *sk*s compared to *ida* were observed. Similarities were drawn between the effects of genotype changes at both plant and single cell levels in that *mur1* and *sk*s were significantly different to *ida* and *col0* for shoot, root and cell wall material properties.

---

## *Acknowledgments*

---

Firstly to my supervisors Professor Colin Thomas (Chemical Engineering) and Dr Jeremy Pritchard (Biosciences), their guidance and advice has been invaluable and their patience commendable.

To the staff of Chemical Engineering and Biosciences I would like to express my thanks for their help and support through the trials of navigating postgraduate education.

Colleagues and friends of the micromanipulation research group and W204 in the past and present for their encouragement and support, you have my eternal gratitude.

Finally to my family and friends, even though only ever likely to read the first few pages, I cannot begin to imagine what I would have done without you.

---

## *Table of Contents*

---

<b>Abstract .....</b>	<b>I</b>
<b>Acknowledgments .....</b>	<b>II</b>
<b>Table of Contents.....</b>	<b>III</b>
<b>List of Figures .....</b>	<b>VIII</b>
<b>List of Tables.....</b>	<b>XIV</b>
<b>List of Appendices.....</b>	<b>XV</b>
<b>Chapter 1: Introduction .....</b>	<b>1</b>
<b>Chapter 2 Literature Review .....</b>	<b>3</b>
2.1 The Significance of Plant Cell Wall Mechanical Properties .....	3
2.2 The Plant Cell .....	5
2.3 The Plant Cell wall .....	6
2.4 The Cell Wall Components .....	6
2.4.1 Cellulose .....	6
2.4.2 Hemi-cellulose.....	7
2.4.3 Pectin.....	9
2.4.4 Lignin .....	10
2.5 Fiber Orientation and Cell Wall Architecture.....	11
2.5.1 The Covalently Cross-Linked Model .....	11
2.5.2 The Tether Model.....	11
2.5.3 The Diffuse Layer Model .....	12
2.5.4 The Stratified Layer Model.....	13
2.6 Regions of the Plant Cell Wall .....	13
2.6.1 Middle Lamella .....	13
2.6.2 The Primary Cell Wall .....	14

2.7 Plant Cell Wall Proteins .....	15
2.8 Plant Water Relations .....	16
2.8.1 Turgor Pressure .....	16
2.8.2 Aquaporins .....	17
2.9 Plant Growth .....	18
2.9.1 Primary Growth .....	18
2.9.2 Cell Wall Loosening and Cell Expansion .....	20
2.9.3 Radial Restriction by Microtubules .....	21
2.10 Cell Division .....	22
2.11 Plant Growth Regulators.....	24
2.11.1 Auxin.....	25
2.11.2 Cytokinin.....	26
2.12 Plant Cell Culture .....	27
2.13 Arabidopsis thaliana .....	27
2.13.1 Genetics.....	27
2.13.2 Mutations in Cell Wall Genes .....	28
2.14 Investigations into the Mechanical Properties of Plant Cells .....	29
2.14.1 Pressure Probe .....	29
2.14.2 Compression Testing by Micromanipulation.....	31

## **Chapter 3: Characterising Phenotype.....33**

3.1 Selection of Mutants in Appropriate Candidate Genes .....	33
3.2 Plant Growth Characteristics (PGC) and Bulking up Seed Stocks .....	34
3.2.1 Methods .....	35
3.2.2 Results .....	35
3.2.3 Discussion.....	37
3.2.4 Conclusions.....	42
3.3 Plant fresh weight: dry weight.....	42
3.3.1 Method.....	42
3.3.2 Results and Discussion .....	43
3.3.3 Conclusions.....	46
3.4. Root Growth Assay (RGA).....	47
3.4.1 Method.....	47
3.4.2 Results .....	49
3.4.3 Discussion.....	51
3.4.4 Conclusions.....	53
3.5 Root Cell Length Profile (RCLP).....	54
3.5.1 Method.....	55
3.5.2 Results .....	55
3.5.3 Discussion.....	57

3.5.4 Conclusions.....	59
3.6 Chapter Conclusion .....	60

## **Chapter 4: Optimising Arabidopsis thaliana Cell Suspension Cultures for the Generation of Single Cells. ....61**

4.1 Initiation of Cellular Suspension Cultures .....	62
4.1.1 Seed Surface Sterilisation .....	62
4.1.2 Investigation of Optimum Explant location.....	62
4.1.3 Germination .....	63
4.1.4 Media Compositions for Explant Investigation .....	63
4.1.5 Composition of the Root Induction Media (RIM) .....	64
4.1.6 Composition of the Shoot Induction Media (SIM).....	64
4.1.7 Composition of the Callus Induction Media (CIM) .....	64
4.1.8 Liquid Culture .....	65
4.2 Maintenance .....	66
4.3 Callus Reserve .....	66
4.4 Quantifying Cell Culture Composition .....	66
4.5 Cell Viability .....	67
4.6 Likely Problems to be Encountered .....	67
4.7 Results .....	68
4.7.1 Explant which Produces the Highest Number of Single Cells.....	68
4.7.2 Media investigation.....	73
4.8 Discussion .....	73
4.9 Conclusions .....	75

## **Chapter 5: The Biochemical Analysis of the Polysaccharide Composition of the Arabidopsis thaliana Primary Cell Wall .....76**

5.1 Cellular Material .....	77
5.2 Method .....	78
5.3 Results and Discussion .....	79
5.3.1 Hemicellulose .....	79
5.3.2 Pectin.....	82
5.3.3 Cellulose .....	83
5.4 Conclusions .....	86

## **Chapter 6: Compression Testing by Micromanipulation .....88**

6.1 An Introduction to Compression Testing by Micromanipulation.....	88
6.2 Probe Manufacture and Transducer calibration.....	89
6.2 Current Techniques .....	89
6.2.1 Low Strain Rate Tester (LSRT).....	90
6.2.2 High Strain Rate Tester (HSRT) .....	92
6.4 Interpreting the Data .....	94
6.5 Adapting the current techniques for single <i>A. thaliana</i> cells .....	96
6.6 Results.....	101
6.6.1 The relationship between cell diameter and rupture force .....	104
6.6.2 The relationship between the cell diameter and the percentage deformation at rupture.....	105
6.6.3 The relationship between the percentage deformation at rupture and the rupture force .....	106
6.6.4 Non-bursting cells.....	107
6.6.5 Elastic limit .....	107
6.7 Discussion .....	108

## **Chapter 7: Determining Mechanical Properties by Mathematical Modelling .....112**

7.1 Using a Mechanical Model to Determine Intrinsic Mechanical Properties .....	112
7.2 Adapting the existing software for <i>Arabidopsis thaliana</i> cells .....	113
7.2.1 Number of Data Points.....	114
7.2.2 Baseline Identification .....	114
7.2.3 The Initial Point of Contact.....	116
7.2.1 Input Parameters .....	119
7.3 The Cell Wall Thickness .....	120
7.4 Results and Discussion .....	121
7.4.1 Transmission Electron Microscopy (TEM) .....	122
7.4.2 Low Strain Elastic Modulus (E) .....	126
7.4.3 Elastic limit .....	128
7.4.4 Initial Stretch Ratio ( $\lambda_s$ ) .....	130
7.5 Conclusions .....	130

## **Chapter 8: Further Work and Discussion .....132**

8.1 Chapter 3.....	132
8.1.1 Root Growth Assay.....	132
8.1.2 Root Cell Length Profiling .....	133
8.2 Chapter 4 .....	134
8.2.1 Flowcytometry .....	134

8.2 Chapter 5 .....	135
8.2.1 Alternative Methods for Analysis of Cell Wall Biochemical Composition .....	135
8.2.2 Confocal Raman Microscopy .....	135
8.3 Chapter 6 .....	138
8.4 Chapter 7 .....	139
8.4.1 Improvements to the Software/Model .....	139
8.5 General Observations .....	139
8.6 Final Conclusions .....	140
<b>References.....</b>	<b>145</b>
<b>Appendices.....</b>	<b>162</b>

---

## *List of Figures*

---

- Figure 2.1: The plant cell, in which the main components are shown (not shown to scale).....5
- Figure 2.2: glucose monomer demonstrating a polymeric cellulose chain. Monomers are joined by a  $\beta(1\rightarrow4)$ -glycosidic link. This is representative of every bond found in a cellulose fibre. Each protein in the hexameric rosette complex creates cellulose chains that combine to form a cellulose microfibril. ...7
- Figure 2.3: An example of a hemicellulose fibre, xyloglucan. The glucose (Glc) molecules are bonded using a  $\beta(1\rightarrow4)$ -glycosidic link, the same as in cellulose. Xylose (Xyl) are bonded to the glucose backbone using an  $\alpha(1\rightarrow6)$  glycosidic link to which the branches can be attached, in this case a Galactose (Gal) and Fructose (Fru) molecule. Each of these bonds is formed by a specific enzyme designed to attach the correct sugar to the correct molecule already in the chain. ....8
- Figure 2.4: Schematic structure of pectin showing the three main pectic polysaccharides rhamnogalacturonan I (RG-I), rhamnogalacturonan II (RG-II) and homogalacturonan (HG). The examples highlight the backbone structure in addition to any monosaccharides that can potentially be used to form the side chain branches. .... 10
- Figure 2.5: The four potential models for the architecture of the primary cell wall. A: the covalently cross-linked model; B: the tether model; C: the diffuse layer model and D: the stratified layer model. These are theoretical models extrapolated from the known properties of the polysaccharides of which the wall is composed. (Copied from <http://www.crc.uga.edu/mao/intro/outline.htm>) ..... 12
- Figure 2.6: cross-sectional diagram of the plant cell wall (not to scale) showing the layering of the regions, the plasma membrane not part of the wall but is integral to several cell properties especially growth. It is shown here for orientation. The cell wall, its architecture is unknown but it thought to take the form of one of the four models presented in section 2.5 but is known to contain cellulose, hemicellulose. Lastly, the pectin rich middle lamella..... 14
- Figure 2.7: the modification of the cell wall to accommodate the plasmodesmata between two cells (Not to scale). Plasmodesmata are involved in cell-to-cell communication and require significant modification to the wall to accommodate this structure ..... 15
- Figure 2.8: A cross sectional diagram showing the different zones involved in a growing root, the root cap; the zone of cell division; the zone of elongation and the zone of differentiation. A nascent cell is produced from a cell division in the apical meristem of the zone of division. As the root grows the cell enters the zone of elongation where it undergoes longitudinal expansion. Elongation arrests and acquires a cell fate dependant on its relative position in the organ, e.g. root hair or transport vessel. . 19
- Figure 2.9: The cell growth cycle. This illustrates the process by which new cells leaving the zone of division, undergoing expansion through turgor mediated longitudinal elongation of the cell wall and become mature cells. ....24
- Figure 2.10: a schematic showing the major components of the pressure probe used for work on the individual cells. The pipette pierces a cell; the cytoplasm is forced into the pipette due to the elevated internal pressure. This pressure is measured by returning the meniscus to its original position. The force required is equal to that of the internal turgor pressure.....30
- Figure 3.1: a top view of a tray of 20 plants of each genotype at day 30. Clockwise from top left: col0, ida, sks and mur1. This figure is not representative of the position in the green house, but arranged to aid comparison. For the purpose of scale, the pots seen as brown rings are 8cm in diameter. ....36

Figure 3.2: a top view of a tray of 20 plants of each genotype at day 35. Clockwise from top left: col0, ida, sks and mur1, This figure is not representative of the position in the green house, but arranged to aid comparison. For the purpose of scale, the pots seen as brown rings are 8cm in diameter. ....	36
Figure 3.3: The average time taken for the seedlings to germinate. This was taken as the point at which the hypocotyl was first visible. Error bars show the standard error. Using the student's t test, mur1 and sks genotypes take significantly longer to germinate than col0 ( $P>0.05$ ). Three biological replicates of twenty plants were used. ....	38
Figure 3.4: the number of leaves in the rosette and the width of the rosettes taken on day 20. Error bars show the standard error. The sks and mur1 mutations have a significantly reduced rosette width compared to col0 and IDA. In addition to this mur1 also have significantly fewer rosette leaves than <i>ida</i> ( $P>0.05$ ). Three biological replicates of twenty plants were used. ....	38
Figure 3.5: Average time taken for the plants to flower. This was taken as the time until the first flower was observed on the plant. Error bars represent the standard error. The sks took significantly longer to flower than the col0 and IDA genotypes ( $P>0.05$ ). Three biological replicates of twenty plants were used. ....	39
Figure 3.6: Measurement taken from the plants on the day of flowering. Error bars show standard error. Mur1 show significant decreases to col0 and IDA in the number of cauline leaves and rosette width. Sks shows significant increased numbers of rosette leaves and decrease rosette width. In addition, sks has a significantly increased number of cauline leaves to mur1 ( $P>0.05$ ). Three biological replicates of twenty plants were used. ....	41
Figure 3.7: Average heights of the plants on days 30 and 35. Height was taken as the distance from the soil to the highest point of the plant. Sks are significantly shorter than col0 plant by day 35 and on both day 30 and 35 when compared to IDA ( $P>0.05$ ). Three biological replicates of twenty plants were used. ....	41
Figure 3.8: The results of the fresh weigh/dry weight investigation. (A) Shows the fresh weight of each genotype over 45 days. (B) Shows the dry weight of the same plants over the same period. (C) Shows the percentage moisture content of the plants calculated from the results from (A) and (B). The results are taken from the pooling of 5 plants and counts as an average. ....	44
Figure 3.9: Diagram showing a plate from the Root Growth Assay. (A) The sterilised seeds were placed on the zero line and allowed to germinate; the roots will grow vertically down the plate (direction shown by the red arrow). (B) Shows the plate after several days of growth monitoring with dots marking the root growth every 24 hours. The fourth root from the left has reached the bottom of the plate, this was taken as the end of the experiment as no more information can be accurately recorded and so the data were collected. ....	48
Figure 3.10: (A) shows the average root length of the four genotypes over the first 216 hours of growth. Sks and mur1 show statistically significant differences to col0 from 120 hours and 216 hours respectively. (B) Shows the average root growth rate calculated at the mid-point of each of the 24-hour periods. The sks and mur1 mutations show statistical significant differences to col0 from 84 hours and 180 hours respectively ( $P>0.05$ ). All error bars are the standard error. Results are taken from the averages of 5 sets of data 16 roots for each mutation paired with 16 col0 (WT). ....	50
Figure 3.11: shows an example of roots grown in the root growth assay. Three roots visible, the furthest left was a col0 root and the two right of the line were mur1. The second mur1 root to the right of the line demonstrates both root curved growth and adventitious root emergence, two additional growth processes that could not be accurately measured but may have affected the maximal root growth. ....	51
Figure 3.12: The region over which the root cell lengths were measured. In the photograph, cells in the root tip can be seen (the area above the scale bar) as it had been crushed between the slide and coverslip to expose them. Root hairs can also be seen as they emerge towards the distal end of the root section shown. Scale bar is 1000 $\mu$ m. ....	56

Figure 3.13: the average root cell length moving away from the root tip. All error bars are shown as the standard error. Between 750 and 1000  $\mu\text{m}$  mur1, IDA and sks root cells are significantly longer than col0. After 1250  $\mu\text{m}$  col0 cells are significantly longer than sks and mur1, and from 1500  $\mu\text{m}$  significantly longer than IDA. From 2000  $\mu\text{m}$  IDA cells are significantly longer than mur1 and sks. ( $P>0.05$ ).....56

Figure 3.14: the average distance to the emergence of root hairs from the root tip. All error bars are shown as the standard error. Statistically col0 and IDA show lateral root emergence further along the root than sks and mur1. ( $P>0.05$ ).....57

Figure 4.1: The protocol for producing the explant material by tissue regeneration. These regenerated tissues were tested to discover the optimum explant for the initiation of the suspension cultures. Liquid cultures were inoculated with similar amount of tissue and the numbers of single cells produced were scored. The results of this investigation can be seen in figure 4.3 (Adapted from Che et.al. 2006). .....65

Figure 4.2: samples cultured cells stained with NR protocol. (A) Examples of 3 different categories of cell class large cell aggregate (1); small cell aggregate (2) and single cell (3). Similar diameters of single cells and individual cells in the aggregates can be seen. (B) Gives an enlarged example of a single cell stained with NR. NR proves the cell is viable as only the vacuole is stained .....68

Figure 4.3: Shows the average number of single cells generated from different explants of two-week-old col0 cultures. Also shown is the effect of absence of light. As the cells have been subjected to the same conditions throughout the growth phases, all other variables have been standardised allowing paired analysis. Callus cells generate significantly more single cells than either root or shoot cells, with root cells also showing a significant increase over shoot cells. All cell types show a significant difference when the dark and light grown samples were compared. ( $P>0.05$ ).....69

Figure 4.4: shows the fluctuations of pH of the suspension cultures for 21 days after initiation. This was seen as the life of a culture as sub-culturing was done at 28 days. Each genotype has error bars representing the standard error. ....71

Figure 4.5: shows the number of viable single cells as a percentage of an estimated total cell count. The number of cells in the large aggregates was very difficult to measure correctly. Therefore an estimate for the cell number for each large aggregate was made based on size, shape and density. Error bars represent the standard error. The ida mutation shows significantly lower levels of all genotypes throughout the experiment. sks and col0 are significantly higher than mur1 from day 7. The sks mutation has a significantly higher percentage of single cells from day 10, presumably caused by the reduction of cell-to-cell adhesion as a result of the mutation ( $P>0.05$ ).....71

Figure 4.6: shows the average diameters of the single cells and cells contained within the small aggregates. Each point has an error bar represented by the standard deviation. No significant differences can be seen between either of the cell states or genotypes. Cell diameters for all genotypes and cell state appear to be converging at an average diameter of 25  $\mu\text{m}$ . Error bars represent standard error.....72

Figure 5.1: Data from each stage where hemicellulose was extracted cultured tissue shown in light grey plant tissue shown in dark grey. (A) Stage 1 and (B) stage 3 contain a proportion of the native hemicellulose. (C) Stage 4 contains the mannose rich hemicellulose. (D) Stage 5, (E) stage 6 and (F) stage 7 all show a large proportion of the total hemicellulose, which has been de-acetylated due to the nature of the extraction. The error bars show the standard error. The differences are discussed at length in the results chapter 5.5.1. ....80

Figure 5.2: Amount of hemicellulose extracted per gram of fresh weight. Stages 1, 3, 4, 5, 6 and 7 extract a portion of the total hemicellulose present, a combination of the data shown in figure 5.1. Each data set contains three replicates with three measurements taken from each sample. The pooled data shows total hemicellulose liberated for plant and cultured tissue of each genotype. The total hemicellulose liberated is not influenced by either genotype or culture stage. ....81

Figure 5.3: Estimated amount of pectin produced per gram of initial fresh weight for both cultured (dark grey) and plant (light grey) of tissue from each genotype. Error bars give the standard error.

Statistically there is significantly more pectin produced by the *col0* and *ida* compared with *sk5* and *mur1* in both cultured and plant tissue. The amount of pectin present in the cultured tissue is significantly higher than that produced by the plant tissue of *ida*, *mur1* and *sk5* ( $P > 0.05$ ). *Col0* also shows this difference but at a non-significant level. ....82

Figure 5.4: Dry weight of the residue. The residue contains remaining polysaccharides that remain insoluble from the extraction. (A) Cultured tissue (dark grey) and (B) plant tissue (light grey) error bars represent the standard error. Residue constitutes mostly of the cellulose present in the wall, as all other polysaccharides have been removed. The *mur1* mutation shows significantly lower levels of residue from the plant tissue that *col0* and *ida*. The *sk5* mutation resulted in significantly lower amounts of residue than *ida* for both plant and cultured tissue ( $P > 0.05$ ) and non-significant differences to *col0* for both culture and plant. The *ida* mutation shows a slight increase in residue compared with *col0* (not significant) in both cultured and plant tissue. ....84

Figure 5.5: The percentage of the original fresh weights that corresponds to the dry weight residue. (A) Comparison between values for cultures (A) from chapters 5 and 4. (B) Comparison between values for plants from chapters 5 and 3. (C) Comparison between the plant and culture values from chapter 5. ....85

Figure 6.1: schematic diagram of the compression of an individual cell between a large flat probe and a glass slide. (Not to scale). ....89

Figure 6.2: Schematic of the low strain Rate Compression Testing Apparatus (LSRT). The main components can be seen, the probe mounted on the force transducer, which is attached to a stepping motor. This is positioned above the sample chamber, which is held in a stage attached to a micromanipulator. Two microscopes are used for lateral and inverted views of the sample chamber.91

Figure 6.3: Schematic of the High Strain Rate compression testing apparatus (HSRT). The transducer mounted probe is positioned above the sample chamber and attached to a stepping motor in a similar manner of the LSRT. Additions include the high power light source and condenser, to improve illumination for the high-speed camera. The inverted microscope has been removed for piezo electric drive below the sample chamber. A mirror unit and camera allow an inverted view. ....92

Figure 6.4: an example of a voltage/time graph from a compression of a single *Arabidopsis* cell using the HSRT at  $3000 \mu\text{m s}^{-1}$ . (A) Gives the point of initial contact between the probe and the cell. Cell rupture occurs at (B). (C) Shows the initial point of contact with the base/debris, compression then continues until the probe rests on the chamber base (D). This figure is the opposite to all other figures in this chapter as the voltage is recorded negatively away from zero. The calculations made from this data express the values positively. ....94

Figure 6.5: an example force/displacement graph generated from raw voltage/time data. (A) The initial point of contact of the probe with the cell. (B) The rupture point. (C) The point of contact with the base/ debris. (D) The point at which the probe rest on the chamber. From this example the diameter of the sample can be taken as approximately  $25 \mu\text{m}$ , the distance between (A) and (D). ....96

Figure 6.6: shows the stages in development of the compression of *Arabidopsis thaliana* single cells. Each curve demonstrates a typical example of a force/deformation curve calculated from the data at each stage. The triangle curve represents cells compressed at  $68 \mu\text{m s}^{-1}$  using the LSRT. The circles represent cells compressed at  $200 \mu\text{m s}^{-1}$  using the stepping motor on the HSRT. The diamonds represent cells compressed at  $3000 \mu\text{m s}^{-1}$  using the piezo-electric stack on the HSRT with the output voltage from the transducer amplified  $10\times$ . The diamond curve follows the pattern seen in figure 5.9, typical of what is expected of a cell rupture. ....99

Figure 6.7: (A) Average diameter of the cells from the compression data for each genotype; (B) average force required for rupture for each of the genotypes; (C) the average percentage deformation at rupture for each of the genotypes. The error bars show the standard error. The *mur1* and *sk5* mutations show a statistically higher ( $p > 0.05$ ) force required to rupture the cells when compared to the *ida* mutation. ....103

Figure 6.8 shows the relationship between cell diameter and the rupture force for each of the genotypes. For each a linear trend line represents the general trend for the cells compressed. All trend lines show a positive agreement for this relationship. ....	104
Figure 6.9: shows the relationship between cell diameter and the percentage deformation at rupture. Each genotype has a general line demonstrating a general relationship between the points. For all but mur1, a negative trend was seen. ....	105
Figure 6.10: the relationship between the percentage deformation at rupture and the rupture force. Each genotype has a linear trend line, all of which show a positive trend. ....	106
Figure 7.1: Highlights the change in baseline calculation for Arabidopsis thaliana. The data are force/displacement information from the compression of a single Arabidopsis cell approximately 25µm in diameter. Before this modification any cells where the average of the first two blocks (1 block = 25 data points) was not with a user set tolerance the cell was dismissed as dead and not processed. Due to the noise of the baseline this meant that the majority of the cells were initially classed as dead, which NR staining (section4.5) had suggested these cells were viable. Therefore, the software was modified to calculate the baseline as the average of the first block. In the figure the points in black (block 1) demonstrates this region. ....	115
Figure 7.2: gives an example of the selection of the initial point of the compression using the manual intervention function. The data are the force/displacement data for the compression of an Arabidopsis single cell approximately 25 µm in diameter. The model would have selected the white point as the initial point of contact however the cell would therefore fail on other criteria. Therefore manual intervention was utilised to select the black point as the initial point of contact as this is the point from which the data does not return to the base line before rupture. ....	116
Figure 7.3: The selection of the elastic limit using the manual intervention. The cell no longer behaves elastically after approximately 30% dimetral deformation. This required the selection of the data between the initial point of contact of probe and cell and elastic limit. The manual intervention function was utilised to select the elastic limit as the rupture point ensuring the model was fitted the desired range. The white point is the point at which the cell ruptures and was chosen by the software as the busting point. The black point is the elastic limit; this was manually selected as the rupture point to omit the plastic region from the fitting procedure. Although the elastic modulus was found from a reduced set of data points, the bursting force was still identified correctly (as the white point in this illustration) .....	117
Figure 7.4: a selection of transmission electron microscopy micrographs. (A) Cross section of a single col0 cell at 5000× magnification, the primary wall can be seen as the black band. On the outer edge an area of what is presumed to be pectin can be observed. (B) IDA cell contained within a cellular aggregate, 5000× magnification. The primary walls of the adjoining cells are clearly visible, separated by a thin middle lamella. The triangular regions at the corners of the cells were also observed. (C) A cross-section of an sks wall from a single cell at 40,000× magnification. The two regions of the wall, primary wall and the pectin rich region are clearly distinguishable. From this micrograph it can be seen that the two regions are of comparable thickness of approximately 300 nm. From the TEM micrographs (not all shown) the initial diameters were measured, to determine the initial thickness ratio for the input parameters. ....	122
Figure 7.5: The average primary cell wall thickness of the four Arabidopsis thaliana genotypes, for samples of the cultured cells. Error bars represent standard error. 25 measurements were taken for each of the genotypes. Sks has significantly thinner primary walls than col0. ....	124
Figure 7.6: the average diameters of the cells, observed during the microcompression and those determined by the modelling. The pattern of the diameters is the same between the two data sets; however the observed diameters are significantly higher than those given by the model (P>0.05)....	125
Figure 7.7: The average low strain elastic moduli for the four genotypes. Error bars represent the standard error. T test analysis shows that col0 and IDA have a significantly higher low strain elastic modulus than mur1 (P.0.05). IDA also shows a non-significant difference to sks. Number of samples, col0=66; IDA=56; mur1=65 and sks = 86. ....	127

Figure 7.8: the average value for the elastic limits of the genotypes. This is the point at which the wall no longer behaved in an elastic manor and took on plastic traits. This is the point to which the data was used for the calculation of the low strain elastic modulus. The results show that the col0 cells had a significantly lower elastic limit than ida and mu1 ( $P>0.05$ ). ..... 129

Figure 7.9: the average initial stretch ratio ( $\lambda_s$ ) for each genotype. The error bars represent the standard error. Significant differences can be seen, mur1 is higher than sks and col0; ida is higher than col0. .... 129

Figure 8.1: Results from a preliminary investigation into the raman spectra of Arabidopsis thaliana cell wall mutations. (A) A confocal image of a sample of sks suspension cultured cells. (B) A confocal image of a sample of col0 suspension cultured cells. Both (A) and (B) are coloured to represent the raman spectra generated at that point. (C) Raman spectra recorded on snake skin (red) and sample C019 (blue). The spectra presented, are average spectra from the image scans (16384 spectra each). Both spectra show Raman bands at the same wave numbers, with variations of peak intensities. To compare peak intensities, both spectra were normalized to the peak at 1458/cm. .... 136

---

## *List of Tables*

---

<b>Table 2.1: Potential genotypes that contain mutations in genes that affect the cell wall, all are from the Columbia background and are therefore comparable. ....</b>	<b>29</b>
<b>Table 3.1 contains a summary of the main point from the chapter. ....</b>	<b>60</b>
<b>Table 6.1: Shows the average cell diameter, the average rupture forces and the percentage deformation at rupture for 1 and 2 week old suspension cultures of the four genotypes analysed. Error is equal to the standard error. There is no significant effect of age, enabling the pooling of the data sets (P&lt;0.05) .....</b>	<b>102</b>
<b>Table 7.1: The initial input parameters required by the model. These values are used in the constitutive equations of the model, and are values that must be specific for the specimen. Compression speed and data capture are parameters chosen during the compression development (chapter 6.5). Volts and compliance are parameters of the transducer and were determined during calibration (appendices 8-10). The initial thickness ratio, is calculated from the initial diameters and the wall thicknesses (section 7.3) .....</b>	<b>119</b>
<b>Table 7.2: output values from the parameters calculated by the model. Values are averages of those output by the software and are shown with the standard errors. ....</b>	<b>121</b>

---

*List of Appendices*

---

<b>Appendix 1: Long Ashton Solution.....</b>	<b>162</b>
<b>Appendix 2: The Protocols for Surface Sterilisation.....</b>	<b>163</b>
<b>Appendix 3: De-proteinisation by phenol/ acetic acid / water (PAW) .....</b>	<b>164</b>
<b>Appendix 4: Preparation of Alcohol Insoluble Residue (AIR) .....</b>	<b>165</b>
<b>Appendix 5: Sequential Extraction of Polysaccharide from Primary Walls.....</b>	<b>166</b>
<b>Appendix 6: De-salting by Dialysis .....</b>	<b>168</b>
<b>Appendix 7: Analysis by Spectrophotometry .....</b>	<b>169</b>
<b>Appendix 8: Probe Manufacture.....</b>	<b>172</b>
<b>Appendix 9: Force Transducer.....</b>	<b>174</b>
<b>Appendix 10: Transducer Calibration - Sensitivity.....</b>	<b>175</b>
<b>Appendix 11: Transducer Calibration - Compliance .....</b>	<b>176</b>
<b>Appendix 12: Compression Rig Control and Calibration.....</b>	<b>177</b>
<b>Appendix 13: Immunolocalisation TEM staining .....</b>	<b>180</b>

---

## *Chapter 1: Introduction*

---

A single plant cell is the basic building block of the plant organism, differentiated to form tissues that are combined to create the organs of the whole organism. All of the characteristics of the whole plant can therefore be determined as a sum of the properties of all the individual cells in the organism and their interactions.

The structure of the plant is of particular importance and interest in biomechanics, but understanding the biomechanical role played by each single cell in a plant is a near impossibility due to the complex nature of plants. For example, cellular packing, geometry and the inclusion of intracellular spaces are all factors that can influence tissue strength. However, a reductionist approach studying cells is a means of obtaining a better understanding of the role of some cells of whole plants.

Plant physiology has shown that plant cells are surrounded by a cell wall and under the influence of internal pressure that is essential to the mechanical integrity of each individual cell. In addition, the 'omics' branches of biology have led to a better knowledge and understanding of the cell wall and its biosynthesis. Combining these two streams of research might illustrate the effects caused by genomic differences in the synthesis of plant cell walls on the physical properties of those walls.

Therefore the aims of this project were to investigate differences (if any) in shoot and root growth and cell wall properties of single cells suspension cultures between various genotypes of the genetic model plant *Arabidopsis thaliana* containing known cell wall mutations.

Chapter 2 contains a literature review covering biological aspects affecting the project including the growth of plant cells and the plant cell wall. In addition to this, previous experiments that have been used to investigate the mechanical properties of the plant cell wall have been discussed.

In chapter 3, experiments on shoot and root growth of the phenotypes are described. These experiments were preliminary to investigations to score the effects of the mutations on the growth.

Analysis of the roots and shoots in parallel allowed the growth phenotype to be determined, highlighting areas where mutations are most likely to affect.

Chapter 4 outlines a protocol for the generation of *Arabidopsis thaliana* suspension cultures. These cultures were optimised for the generation of single cells. Investigations into several aspects affecting the culture were trialled to discover those conditions most conducive for single cell production.

To compare fully the biochemistry and the mechanical properties, the effects of the mutations on the cell wall compositions were investigated, as described in chapter 5. Samples of tissue and suspension cultured cells were analysed for the main components of the cell wall, determining the differences in relative abundances caused by the mutations.

Chapter 6 describes the technique of compression testing by micromanipulation. Through this method experimental force-deformation data were extracted directly from the single cells. There is a discussion of the problems encountered during the development of the method.

From the data yielded from the compression of the single cells, (intrinsic) cell wall material properties had to be extracted. This was done using a computer model, achieved by fitting numerical solutions to the experimental data. Modification of the model to allow the interpretation of the *Arabidopsis* cell data is explored in chapter 7.

Chapter 8 considers the whole investigation pulling it together in a general discussion and suggests possible avenues of future investigation that have become apparent during the course of the project.

## *Chapter 2 Literature Review*

---

### **2.1 The Significance of Plant Cell Wall Mechanical Properties**

Many industrial and commercial processes require plants to function. Of course this is well known in agriculture, but in recent years for the production of chemicals for pharmaceuticals (Fischer et al., 2004) and for fuels (Ragauskas et al., 2006) has also increased. With space limited and demand ever increasing, processes in the modern world require plants which are efficient and yield more products (Tester and Langridge, 2010).

Farming is the most obvious application of plants in industry, particularly the production of edible fruits, vegetables and cereals. However, land available for agriculture is being reduced by the growth of the human population and with it the amount of food required (Tilman et al., 2001). Encroaching cities and the constant need for housing leaving land value at a premium This leads to a reduction in agricultural output leaving many countries heavily reliant on imports (Godfray et al., 2010). The continual expansion of the global population leading to a deficit in food production, applying pressure on existing producers causing expansion into areas not necessarily applicable for farming, such as deserts or forests. Converting existing forests to farmland has massive implications mainly deforestation which is linked to global warming (Fearnside, 1996). Crop plants can be potentially manipulated to produce variants with increased viability in harsher environments (Valliyodan and Nguyen, 2006), e.g. areas with low rain fall (Vinocur and Altman, 2005). Cereals such as wheat and maize require large amounts of water so will only grow in certain climates. Areas of low annual precipitation support only the hardest of plant life, adapted to the conditions over millennia of evolution. Unfortunately these species very rarely produce consumable items. These adaptations could be applied to more agriculturally significant species, creating hardier varieties through genetic manipulations (Thomson et al., 2007). For example, creating roots which grow deeper to anchor the plants better and tap into deep-water sources or stronger walls to maintain structure under severe drought stress.

Once produce has been harvested it begins to ripen (Neal, 1965), leaving a finite amount of time before they become unusable (Brady, 2003). This is a combination of many factors, ripening (Yamaki et al., 1979) is caused by decomposition of the intracellular regions, very noticeable with over ripe tomatoes (Burg and Burg, 1965).

Besides this, plants are used to produce many items of commercial interest (Fischer et al., 2004) e.g. pharmaceuticals (Fischer et al., 2000) and many other bio-molecules production (Guda et al., 2000). Plant cells can be grown in suspension cultures (Hellwig et al., 2004), in bioreactors. Allowing artificial growth environments to be established and the physical conditions can be controlled (Decker and Reski, 2004) in bioreactors. Commonly used to generate pharmaceutical products from mammalian or bacterial cells, they are also applicable for plant cells. Bioreactors (Fischer et al., 1999) could be used to increase quantities of plant products for commercial use (Hellwig et al., 2004). However the yield is dependent on the survivability of cells in the reactors. It is possible that hardier cells would be more resistant to damage from constant mechanical shear (Scragg et al., 1988) will give higher yields. The resistance to mechanical damage is probably highly dependent of the cell wall properties (Dunlop et al., 1994) although its effects may also be important (Namdev and Dunlop, 1995).

The ability of plants to produce large quantities of carbohydrates is one of their main bonuses as biological system. This is evident in the production of bio-fuels which is dependent on the amount of biomass produced by growing the plants (Himmel et al., 2007). Bio-fuels (Pauly and Keegstra, 2010) are seen as a low carbon and renewable alternative to fossil fuels (Demirbas, 2007). The use of cellulose-based materials to make biofuels requires significant pre-treatments (Uslu et al., 2008) that also depend on the composition, structure and possibly the mechanical properties of the cell walls.

These industrial reasons justify the investigation of the mechanical properties of plant cell walls. It would be convenient if this could be done on single suspension cultured cells, which are more tractable to study. However, it is not known if genotype changes affect (parts of) whole plants and cultured cells in related ways. This is the basis of the present study. However, there are broader implications to studying the effects of genotype on cell wall mechanical properties in developing a

better understanding on the roles of polysaccharides in the walls and better understanding the cell properties

## 2.2 The Plant Cell

The plant cell (Hooke, 1664) figure 2.1 is the basic unit of the plant organism, upon which it relies for all its growth and strength. The cell must have structures that are light but strong enough to support the weight of the organism without compromising its ability for continued expansion whilst maintaining access to nutrients. The mechanical properties of these structures of each cell must depend on several factors, such as the amount of material present, interactions between the materials, with other cells surrounding them, the growth state of the cell and whether there are any other factors affecting the wall. This leads to the question of whether changing any of these factors will some detectable differences in growth and ultimately the mechanical properties.

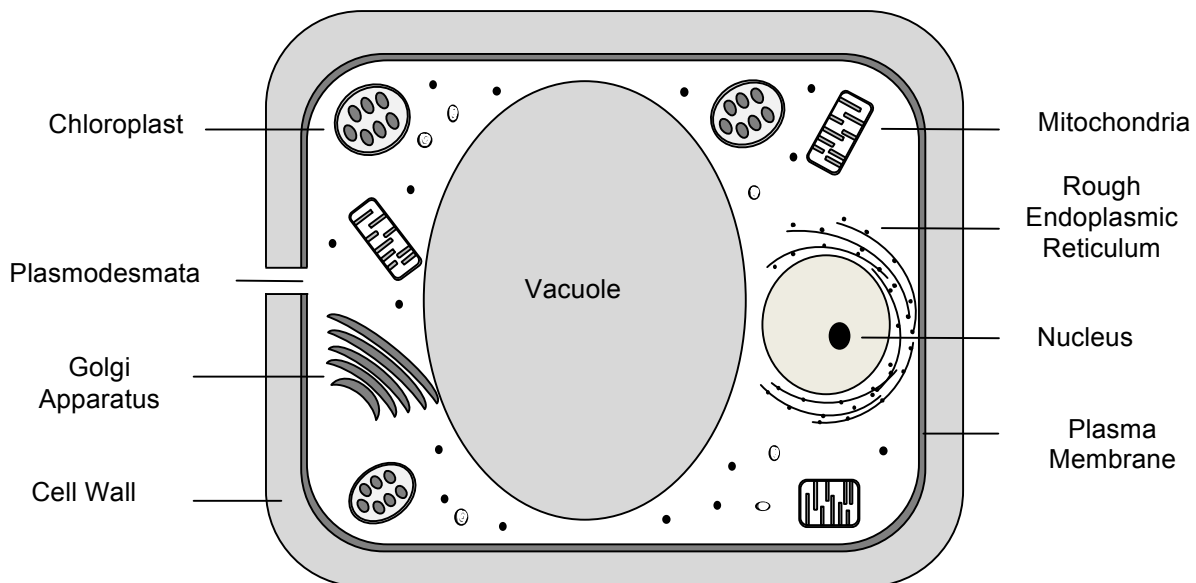


*Figure 2.1: The plant cell, in which the main components are shown (not shown to scale)*

### **2.3 The Plant Cell wall**

Plant cells encase themselves within a complex polysaccharide wall (Popper, 2008). The presence of the cell wall is essential for distinguishing plant cells from other eukaryotic cells. The roles played by the cell wall are not only varied, but essential to the survival of the organism, including cell growth, differentiation, communication, defence (Vorwerk et al., 2004) in addition to being the major structural component of the cell (Jaquinod et al., 2007) and organism (Chivasa et al., 2002).

### **2.4 The Cell Wall Components**

The wall demonstrated in figure 2.1 is vastly oversimplified. The wall is a dynamic and layered region under constant flux, changing to reflect the needs of the cell and the plant. Components of the plant cell wall have been extensively researched and are known to be made of carbohydrate polymers, primarily cellulose (Arioli et al., 1998), hemi-cellulose (Hayashi, 1989; Fischer et al., 2004), pectin (Reiter, 2002) and lignin (Lewis and Yamamoto, 1990). These components occur in varying amounts and at different stages of cellular development. These polymers generally form fibres in the wall and have specific roles and associated regions in which they are mainly found (MaCann *et al.*, 1992).

#### **2.4.1 Cellulose**

Cellulose is the main structural component of the primary plant cell wall. The basic monomeric subunit of the cellulose fibre is glucose, these monomers are bound in a  $\beta$ - (1,4) motif into cellulose (Figure 2.2), which is the most abundant biopolymer on earth and can be as long as 15,000 subunits. The structure of cellulose enables it to be highly resistant to hydrolysis. Cellulose is synthesised by the cellulose synthase (CESA) protein (Richmond, 2000), in *Arabidopsis thaliana* there are 10 genes (Somerville, 2006) in the CESA family (Richmond and Somerville, 2000) that are expressed in different tissues and cell types (Brett, 2000).

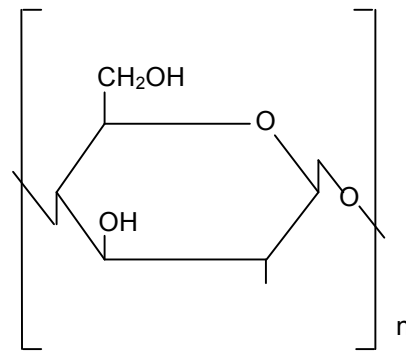


*Figure 2.2: glucose monomer demonstrating a polymeric cellulose chain. Monomers are joined by a  $\beta(1\rightarrow4)$ -glycosidic link. This is representative of every bond found in a cellulose fibre. Each protein in the hexameric rosette complex creates cellulose chains that combine to form a cellulose microfibril.*

Cellulose synthesis (Saxena and Brown, 2005) requires two separate processes, chain initiation and elongation of the polymer chain. Elongation utilizes UDP-D-glucose precursors, adding to the existing glucan chain to generate microcrystalline cellulose however the initiation of the process is also not very well understood. Recent studies indicate that sterol glucoside might function as the initial acceptor for chain elongation. Due to the location of the CESA in the cell membrane, the cellulose microfibrils are released into the extracellular region and incorporated into the wall (Emons and Mulder, 2000). Due to the size of the cellulose microfibrils, it would be difficult to do this release using vesicles; as such the membrane bound enzymes increase efficiency.

#### **2.4.2 Hemi-cellulose**

Hemi-cellulose fibres are branched polysaccharides that are structurally homologous to cellulose because they have a backbone composed of (1,4)- $\beta$ -D-hexosyl residues. Hemicellulose fibres are much shorter than cellulose fibres, usually consisting of approximately 200 subunits. The most commonly occurring subunit in the hemi-cellulose is glucose, but they can also contain mannose, rhamnose, galactose and especially xylose. This allows hemi-cellulose increased viability allowing more specific interactions. The most commonly occurring hemi-cellulose fibre found in many primary walls is xyloglucan (Hayashi, 1989). Other hemicelluloses that are found with less frequency in primary and secondary walls include glucuronoxylan, arabinoxylan, glucomannan, and galactomannan. An example can be seen in figure 2.3.

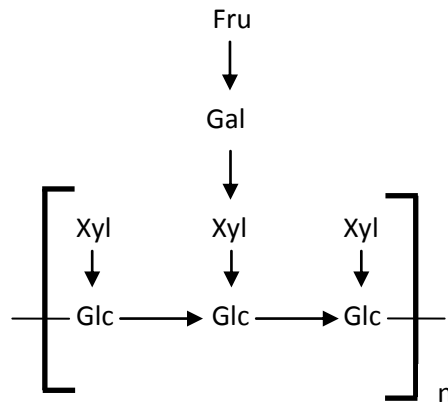


**Figure 2.3:** An example of a hemicellulose fibre, xyloglucan. The glucose (Glc) molecules are bonded using a  $\beta(1\rightarrow4)$ -glycosidic link, the same as in cellulose. Xylose (Xyl) are bonded to the glucose backbone using an  $\alpha(1\rightarrow6)$  glycosidic link to which the branches can be attached, in this case a Galactose (Gal) and Fructose (Fru) molecule. Each of these bonds is formed by a specific enzyme designed to attach the correct sugar to the correct molecule already in the chain.

The main function of hemi-cellulose is to cross-link other fibres in the primary wall (Pena et al., 2004). They give lateral strength across the matrix, control cell shape and growth. The branched nature of hemi-cellulose gives it the necessary points from which the cross-links can be formed. Changes in composition of the fibres allows for variation in binding specificity (Edouard et al., 2004).

Weak acids and bases, in addition to many enzymes, can easily hydrolyse hemi-cellulose fibres. For this reason they are an easy target for modification compared with the stable cellulose molecules. As such they are heavily involved in the process of cell expansion and this will be discussed further in section 2.9. Hemi-cellulose synthesis stems from cellulose synthesis. Both begin with the same UDP-glucose precursor, but the former allows for the incorporation of different sugars, leading to the branched motif (Ebringerova, 2005).

### 2.4.3 Pectin

Pectin is the sole component of the middle lamella which is responsible for cell-to-cell adhesion (Jarvis et al., 2003). They are a group of polysaccharides that are rich in galacturonic acid (GalA). GalA occurs in two major structural features that form the backbone of three polysaccharide domains (Vincken *et al.*, 2003) that are thought to be found in all pectin species (Ridley et al., 2001) of which there are three main families (Willats et al., 2001); (a) homogalacturonan (HGA), made up of linear chains of galacturonic acid residues. The carboxyl groups of HGA are often methyl esterified, reducing their ability to form gel. (b) Rhamnogalacturonan-I (RG-I), consisting of alternating residues of galacturonic acid and rhamnose, has additional branched side chains containing other pectin domains. (c) Rhamnogalacturonan-II (RGII) (O'Neill et al., 2004), complex pectin domain that contains 11 different sugar residues and forms dimers through borate esters. (Figure 2.4) These three polysaccharide domains can be covalently linked to form the pectin networks that make up the middle lamella and contribute to the primary cell wall matrix.

These matrices can be modulated by enzymes to change the structure depending on the position of the cell in the organism, thereby determining the mechanical properties (Ishii and Matsunaga, 2001). The pectin (Cumming et al., 2005b) chains also penetrate in to the primary cell wall; this is to anchor the lamella to the primary wall regions and thus holding the two cells together. However, it would appear that the pectin has little structural significance to the properties of the primary cell wall (Jarvis, 1984). The middle lamella is a special region of the cell wall that is created during cytokinesis (Bacic, 2006). It requires ion interactions (e.g.  $Mg^{2+}$ ) with the pectin molecules for intermolecular bonds between the pectin chains.

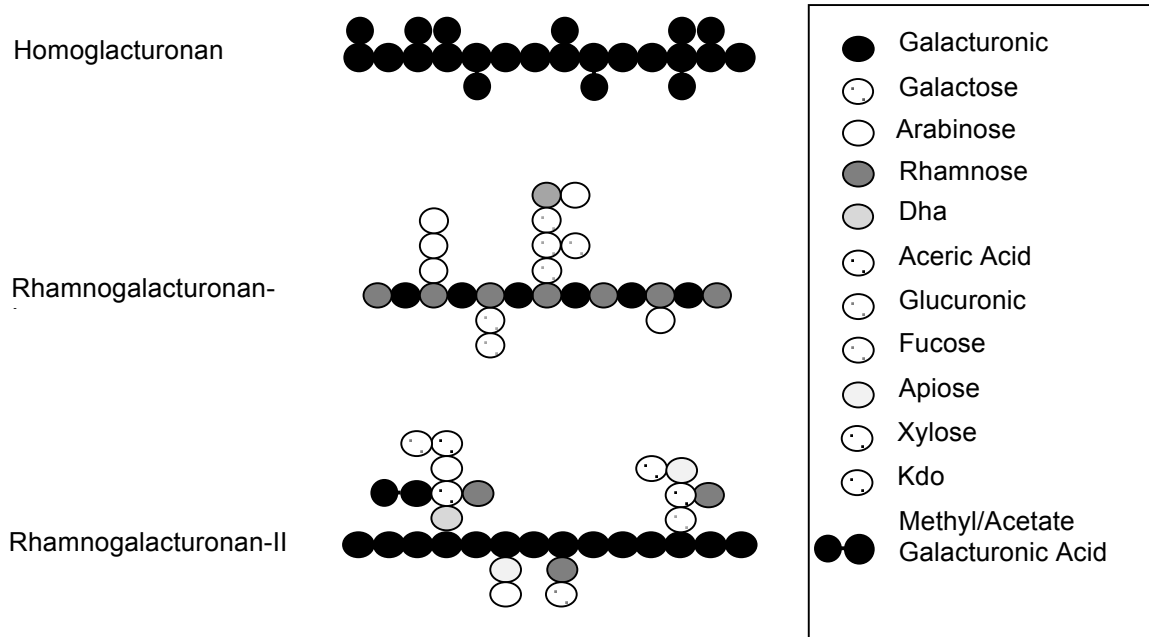


**Figure 2.4:** Schematic structure of pectin showing the three main pectic polysaccharides rhamnogalacturonan I (RG-I), rhamnogalacturonan II (RG-II) and homogalacturonan (HG). The examples highlight the backbone structure in addition to any monosaccharaides that can potentially be used to form the side chain branches.

As the middle lamella is a region shared between adjacent cells it houses the plasmodesmata (Fig 2.7). These are inter-connecting channels of cytoplasm that connect to the protoplasts of adjacent cells across the cell wall and allow intercellular communication as signals can pass through the plasmodesmata between the two cells.

#### 2.4.4 Lignin

At certain points in plant development the cell wall goes through a process of maturation where a secondary cell wall composed largely of lignin is deposited beneath the primary cell wall. Lignin (Lewis and Yamamoto, 1990) is primarily composed of polymerised phenolics, which are layered between the primary cell wall and the plasma membrane. This is the development of a rigid wall containing large amounts of lignin; this is a permanent alteration, fixing the cells at its current dimensions. The process of lignination is most obvious in trees and shrubs (Levine et al., 2001) and is involved in *Arabidopsis* secondary cell wall synthesis (Turner et al., 2001).

## **2.5 Fiber Orientation and Cell Wall Architecture**

The organization and interactions of wall components (Keegstra *et al.*, 1973; Talmadge *et al.*, 1973) is not known with certainty and there is still considerable debate about how wall organization is modified to allow cells to expand and grow (Our, 1973). This is due to lack of any conclusive evidence clearly defining the cell wall architecture, as current methods cannot analyse the intact cell wall to sufficiently high resolution. The layered construction of the cell wall further complicates things as a model for one region may not represent another (MaCann *et al.*, 1990).

For the architecture of the primary cell wall (Carpita and Gibeaut, 1993), several hypothetic models have been proposed to account for the mechanical properties of the wall: the covalently linked cross model, the tether model, the diffuse layer model and the stratified layer model.

### **2.5.1 The Covalently Cross-Linked Model**

This model proposes that the wall matrix polymers (cellulose, pectin etc) are covalently linked to one another. It suggests that cellulose will be covalently cross-linked with xyloglucan fibres, resulting in the creation of a cellulose-hemi-cellulose network that will give the wall tensile strength. However there is a lack of evidence for the presence of covalent linkages between the other known matrix polymers (e.g. xyloglucan with pectin) and thus the model has been questioned. (Valent and Albershelm, 1974) (Figure 2.5 A)

### **2.5.2 The Tether Model**

The tethered model suggests the Xyloglucan molecules are hydrogen bonded to cellulose microfibrils resulting in the formation of cross-links between the cellulose fibres. The cellulose-xyloglucan network is then suggested to combine in a non-covalently cross-linked pectic network. (Bacic *et al.*, 1988) (Figure 2.5 B)

### 2.5.3 The Diffuse Layer Model

The diffuse layer model suggests that xyloglucan molecules are hydrogen bonded to the surface of cellulose microfibrils but do not directly cross-link them. A layer of less-tightly bound polysaccharides surrounds the tightly bound xyloglucan. The cellulose and xyloglucan are embedded in a pectic matrix (MaCann and Roberts, 1992). (Figure 2.6 C)

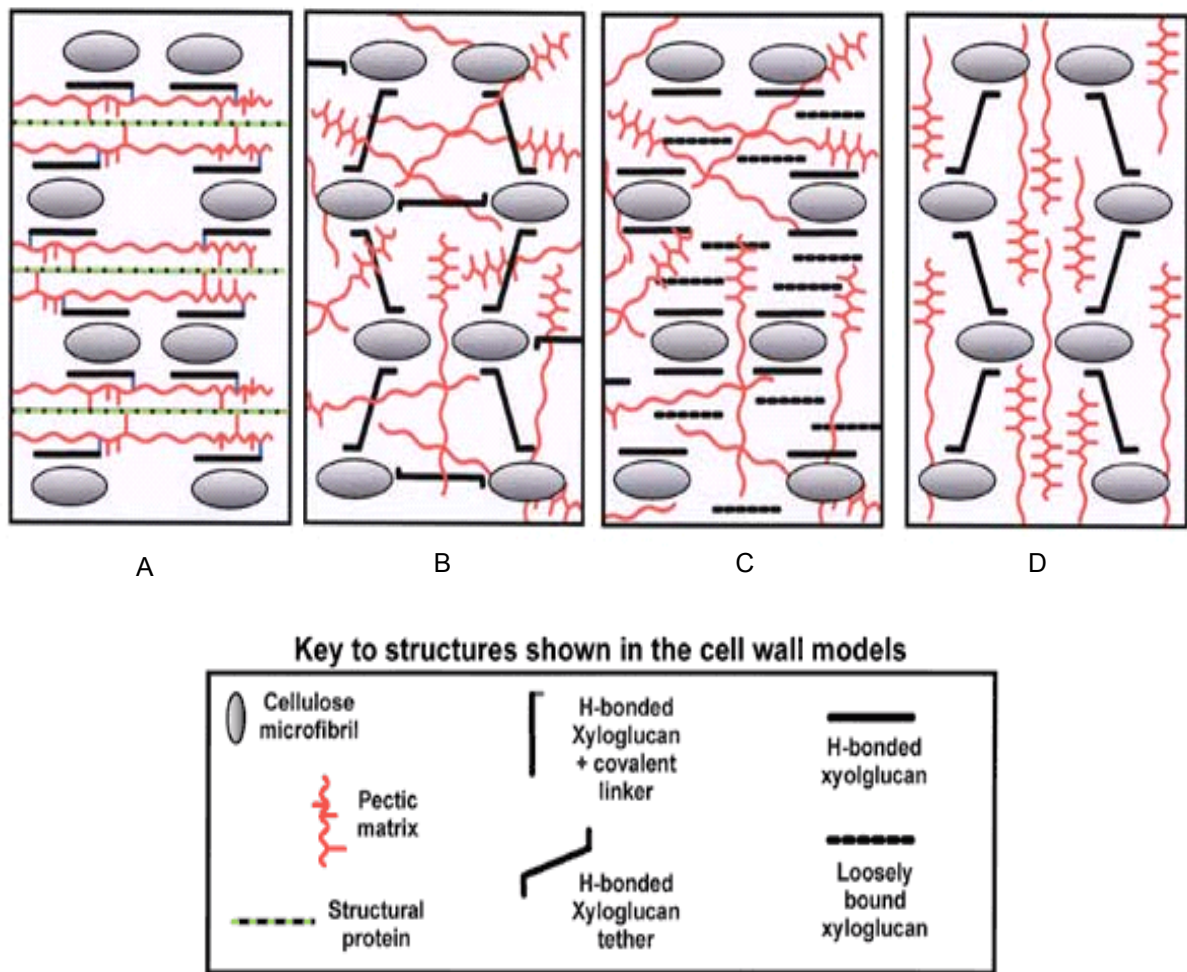


Figure 2.5: The four potential models for the architecture of the primary cell wall. A: the covalently cross-linked model; B: the tether model; C: the diffuse layer model and D: the stratified layer model. These are theoretical models extrapolated from the known properties of the polysaccharides of which the wall is composed. (Copied from <http://www.cerc.uga.edu/mao/intro/outline.htm>)

### **2.5.4 The Stratified Layer Model**

The stratified layer model suggests that the matrix components are arranged in to more defined layers composed of a single component with little or no linking between the layers. Xyloglucan molecules are hydrogen bonded to and cross-link cellulose microfibrils. Layer of pectic polysaccharides separates these layers of cellulose-xyloglucan complexes. (Figure 2.5 D)

Much research is still required to provide a complete description of the primary wall at the molecular level. There is however, an increasing amount of evidence to suggest that primary walls are dynamic structures whose composition and architecture changes during plant growth and development. This may be dependent on the stage of growth and position of the cell in the plant due to their differing requirements.

## **2.6 Regions of the Plant Cell Wall**

The purpose of the plant cell wall as a whole have already been discussed; however there are several regions to the cell wall all of which are composed of different polymers and therefore have different roles. The main two regions in *Arabidopsis* walls are discussed in this section. Figures 2.6 and 2.7 give examples of wall architecture.

### **2.6.1 Middle Lamella**

The middle lamella (Allen, 1901) is a matrix of polysaccharide that is predominantly composed of pectin (Fry, 1986). The main function of this region is to maintain cell to cell adhesion (Jarvis, 1984). To anchor the region, pectin fibres permeate the primary cell wall but are thought to have no mechanical significance.

The middle lamella is laid first, formed from the cell plate during cytokinesis. Once this has formed the primary cell wall is expanded inside it. The middle lamella (Allen, 1901) is made mostly of pectin chains which form the linker region between adjacent cells. It is assumed that the middle lamella (Cumming et al., 2005a) has little or no structural significance to the individual cells, however, will

have some part to play in the overall structure of the plant organism (Jarvis et al., 2003). The middle lamella also houses the plasmodesmata (Turgeon, 1996), as part of the cell to cell communication network (Figure 2.7). The middle lamella is affected by intercellular separation forces generated by internal turgor pressures (section 2.8.1) (Jarvis, 1998)

## 2.6.2 The Primary Cell Wall

The primary cell wall (McNeil et al., 1984) is the major structural region of plant organisms, especially in *Arabidopsis thaliana*. It is composed of long cellulose fibrils arranged in a matrix cross linked with hemi-cellulose fibres (Whitney et al., 1999). This region also contains several types of cell wall associated proteins such as expansins (Rose et al., 2004). This means that the primary cell wall is responsible for the expansion of the individual plant cells and therefore the growth of the whole organism. Pectin fibres also infiltrate the primary cell wall, as an anchor for the middle lamella.

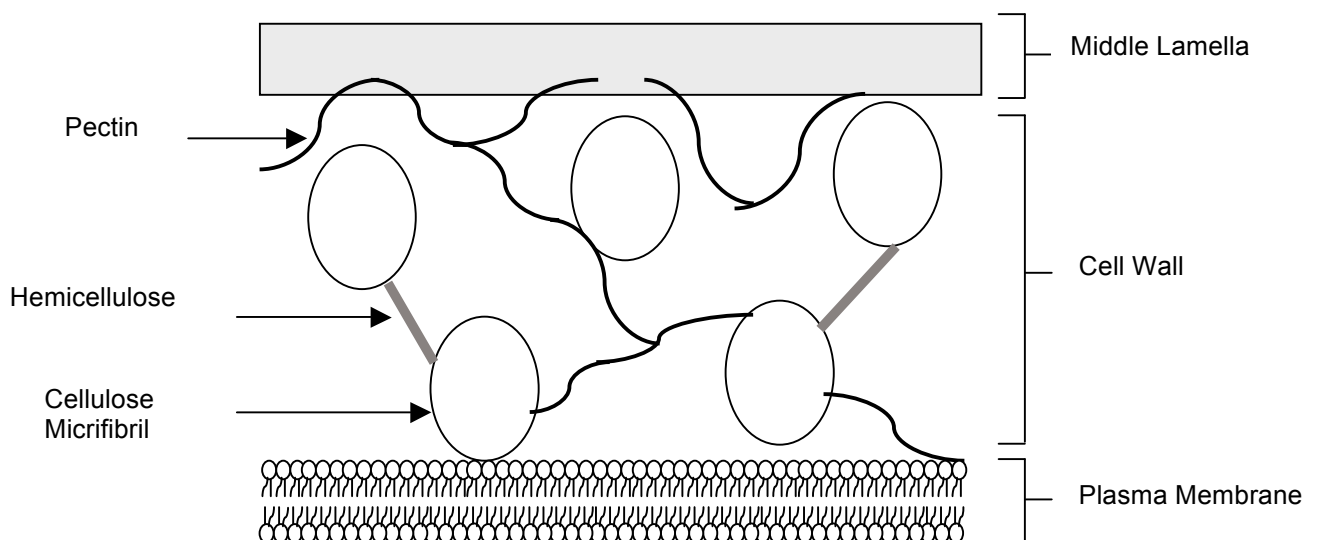


**Figure 2.6:** cross-sectional diagram of the plant cell wall (not to scale) showing the layering of the regions, the plasma membrane not part of the wall but is integral to several cell properties especially growth. It is shown here for orientation. The cell wall, its architecture is unknown but it thought to take the form of one of the four models presented in section 2.5 but is known to contain cellulose, hemi-cellulose. Lastly, the pectin rich middle lamella

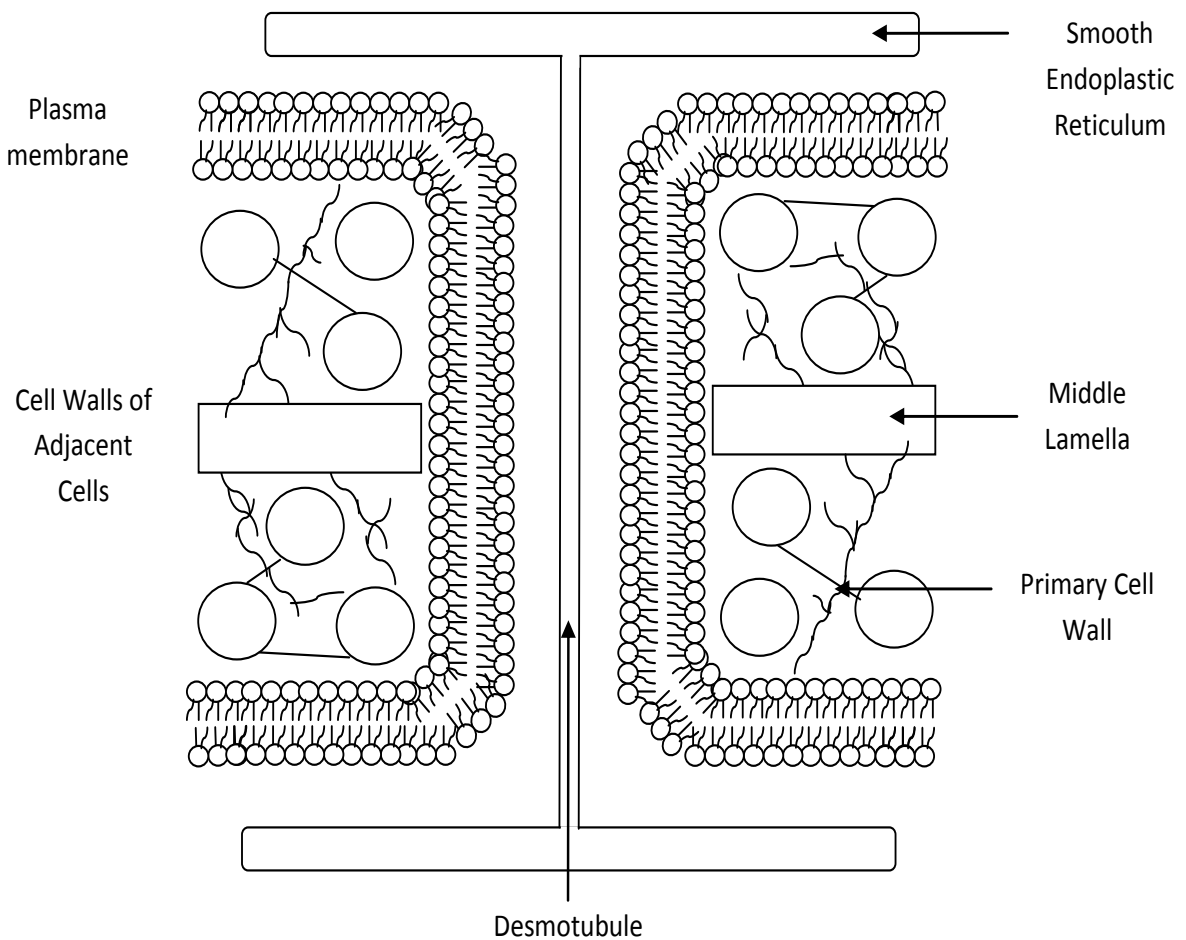


*Figure 2.7: the modification of the cell wall to accommodate the plasmodesmata between two cells (Not to scale). Plasmodesmata are involved in cell-to-cell communication and require significant modification to the wall to accommodate this structure*

## 2.7 Plant Cell Wall Proteins

Plant cells walls are not only made up of carbohydrates, they also incorporate a number of proteins (Morrow and Jones, 1986). The function of the individual protein (Cassab and Varner, 1988) is dependant entirely on its composition and structure (Showalter, 1993), with many effecting the deposition and modification of wall polysaccharides (Fry, 1995). The most abundant include hydroxyproline-rich glycoproteins (HRGP), also called the extensins (Tierney and Varner, 1987) and are involved in cell wall expansion (Cosgrove, 2000b) (section 2.9.2).

## 2.8 Plant Water Relations

Plant survival is dependent on water for so many things. Constantly required to drive essential processes and maintain the existence from the constitutive level to the more specialised, for example photosynthesis (Rabinowitch, 1952; Krause and Weis, 1991)

### 2.8.1 Turgor Pressure

All cells are enclosed by a semi-permeable plasma membrane, called the plasmalemma, which is encompassed by the rigid cell wall (sections 2.3-2.6). This is not to be confused with the tonoplast, the membrane that encloses the central vacuole (Marty, 1999). This vacuole may equate for up to 90% of the total volume and contains more transport mechanisms than the plasmalemma for aid in the active transport of solutes. The osmotic pressure is the result of the intracellular accumulation of these solutes, e.g. ions, across the plasma membranes. An increase in osmotic pressure generates a concentration gradient across the semi-permeable membrane enabling water to move freely across the membrane attempting to reach equilibrium between the osmotic pressure difference across the membrane and the hydrostatic (turgor) pressure across the wall. This increase in osmotic pressure can only generate the concentration gradient if mass transport of solutes occurs. The influx of water causes the plasmalemma to swell, causing it to push against the inside of the cell wall creating a positive pressure inside the cell. A stable turgor pressure (Zimmermann, 1978)( $P$ ) is created once the internal and external solutions reach equilibrium, with the net movement of water across the membrane being zero. It is possible to measure this internal pressure using the plant cell pressure probe, often showing pressures in excess of 1.0 MPa (section 2.14.2).

Water will flow across a semi-permeable membrane so long as a potential difference exists in the free energy of water across that membrane. This is described as the water potential gradient ( $\Delta\Psi_w$ ) and may arise as a result of concentration, pressure differences or gravity (Blancaflor and Masson, 2003; Morita *et al.* 2002). On the scale of the plant cell, gravitational effects can be said to be negligible. The presence of the wall allows the intracellular pressure to be established that much higher than that of the apoplast. As water moves into the cell the vacuole swells and the plasmalemma is forced against the wall (Steudle *et al.*, 1977). The wall has little compliance, limiting the maximum volume of

the cell. However the cell continues to accumulate water in an attempt to equilibrate the osmotic pressures. This leads to a further increase in the turgor pressure and it is this turgor pressure that is vital in the growth processes of the organism.

### 2.8.2 Aquaporins

Water movement through the cell membrane was until the 1950's believed to be the principal method of water exchange. An alternative method of water transport using 'aqueous pores' (Powell and Weaver, 1986) has been suggested. Previous experiments showed water flux across the membrane occurred at a much higher rate than could be explained simply by diffusion and that there must be some form of biological pore that allowed water transport between the cell and external solutions (Johansson et al., 2000).

Aquaporins (Maurel et al., 2008) are found in most biological membranes, with a structure consisting of 6- $\alpha$  helices. These are arranged to form a pore, positioning several essential amino acids into the channel wall. Water molecules are move through the channel by orientating themselves in the local electrical field formed by these essential amino acids. This method of transportation limits the use of aquaporins to small, non-polar molecules suggesting that they are not water exclusive.

In plants there are several families (Borstlap, 2002) of aquaporins optimised for an individual membrane in the cell, e.g. plasma membrane intrinsic protein (PIP) (Beebo et al., 2009). Aquaporins are used in the symplastic (transcellular) pathway and importantly the establishment and maintenance of turgor. Due to the reliance of plant cells on water control, plant aquaporins have been adapted to stop water flux. Gating of aquaporins caused by a conformational change in response to several stimuli, blocks the channel preventing water flow. It is thought that different stimuli affect aquaporins via two mechanisms. In response to drought, specific serine residues are dephosphorylated (Johansson, 1998). Flooding causes protonation of specific histidine residues (Chakrabarti et al., 2004).

Plant aquaporins have been found to be highly susceptible to blockage from heavy metals, in particular Mercury ( $\text{Hg}^{2+}$ ) (Savage and Stroud, 2007).

## **2.9 Plant Growth**

One of the seven fundamental aspects of life is the growth of the organism as a whole (Srivastava, 2002a). Growth of an organism has two mechanical contributors, the expansion of the existing cellular material and the addition of new cells through cellular division. To explain these mechanisms involved in growth, the root system (figure 2.8) will be used as an example (Beemster and Baskin, 1998). Roots played an important role in this project as described later. However, the growth of shoot systems (Evans and Hughes, 1962) is fundamentally the same (Gendreau et al., 1997). In every root there are specific regions, which are responsible for different stages of the growth process.

### **2.9.1 Primary Growth**

Primary growth is the method by which the central root extends downwards into the soil. There are two factors influencing growth, the production of new cells and the longitudinal elongation of the mature cells (Lee and Yang, 2008). Different regions of the root are designated for different processes, which can be seen in figure 2.8.

The zone of cell division contains the apical meristem, which is an area of rapid division of undifferentiated cells, majority of this division (Baskin, 2000) is directed away from the root cap (Mordhorst et al., 1998). Contained within the apical meristem are quiescent centers (Clowes, 1958) that divide much more slowly than the other meristematic cells. These cells are resistant to radiation and chemical damage and act as a reserve to be used if the apical meristem is damaged. The root cap protects the delicate apical meristem as the root moves through the soil. As the root moves the cap secretes lubricating polysaccharide slime which reduces friction. As the root moves, cells are constantly being lost; these are replaced by cells produced by mitosis in the apical meristem (Berger et al., 1998).

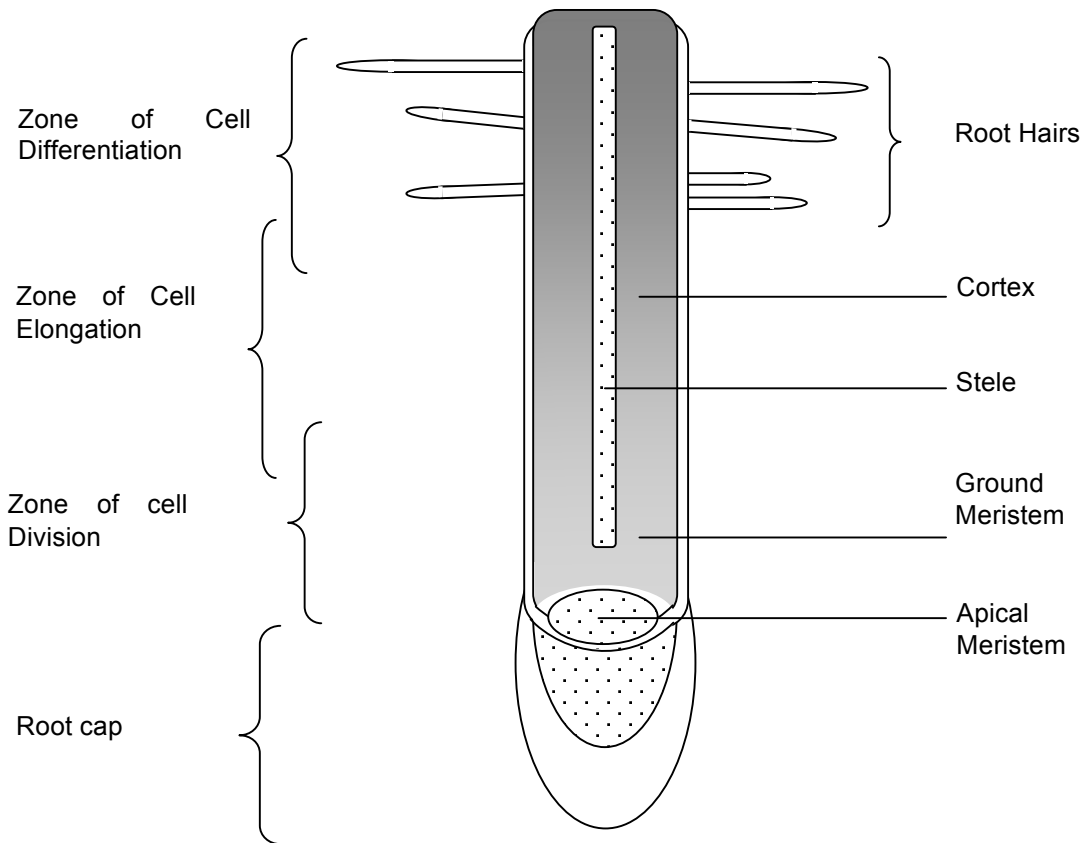


**Figure 2.8:** A cross sectional diagram showing the different zones involved in a growing root, the root cap; the zone of cell division; the zone of elongation and the zone of differentiation. A nascent cell is produced from a cell division in the apical meristem of the zone of division. As the root grows the cell enters the zone of elongation where it undergoes longitudinal expansion. Elongation arrests and acquires a cell fate dependant on its relative position in the organ, e.g. root hair or transport vessel.

Also included in the zone of cell division are three regions just above the apical meristem, the primary meristem that continues to divide for some time. The protoderm produces cells which will become dermal tissue, the ground meristem produces cells that will become ground tissue and the procambium which produces cells that will become vascular tissue.

Behind this region of division is the zone of elongation the cells, in which cells no longer divide and are tasked with longitudinal expansion (Mathur, 2004; De Smet et al., 2006). It is this cellular elongation that drives the root tip forward, further down into the soil (Beemster and Baskin, 1998). This is further discussed in section 2.9.2.

In the zone of differentiation, cells differentiate according to position in the root to take on their terminal cell fates. In this region the emergence of root hairs occurs, leading to the emergence of lateral roots (Casimiro et al., 2003). External and internal factors can contribute to the emergence of lateral roots (De Smet et al., 2006).

### **2.9.2 Cell Wall Loosening and Cell Expansion**

As discussed in section 2.9.1, the process of establishing an elevated internal pressure, the turgor pressure is the first step in cellular expansion (Nicol and Hofte, 1998). The following sections will discuss the processes prior to cellular expansion (Taiz, 1984).

Once the cell has reached a sufficient turgor and moved into the zone of elongation, the cell will begin to expand longitudinally. It is sum of all these expansions that can be said to be the growth of the organism. However this process is very complex. The cell must have some way of restricting growth to only one dimension, as any lateral growth would be wasteful. In addition to this the cell must also not damage wall components that have been deposited in the wall.

#### **2.9.2.1 Expansins**

It was observed that walls in acidic conditions underwent an expansion called 'acidic creep' (Schneitz et al., 2002) whereby the wall would expand (Cosgrove, 1998). Wall expansion must have additional factors which cause the walls to expand. The presence of an acidic solution in the apoplast would be a poor choice for a control mechanism. This would be very difficult to control, leading to systemic expansion rather than the localised expansion that is observed. Therefore, additional factors that are triggered by the acidic conditions must exist.

One possible family of proteins with the potential for causing these changes is known as the expansins. Expansin treated walls relax faster than controls, but when the expansins are inactivated (heat) the walls behave like controls that were not treated with expansins. This suggests that

expansins do not affect the covalent structure of the wall, instead their loosening effects are only observed while the wall is under tension.

### **2.9.2.2 Tentative Model for Expansin Activity**

Expansins transiently displace short stretches of hemicelluloses that are bonded to the surface of the cellulose microfibrils (Li et al., 2002). If the wall is in tension, the polymers creep, inevitably dragging along other structural components. If the wall is relaxed, no polymer movement occurs (Cosgrove, 2000a). This highlights the role played by the turgor pressure that was discussed in section 2.8. Additional enzymatic involvement is possible at this stage, reducing crosslinking increase the rate and overall expansion. However it is possible to overcome expansin mediated expansion with sufficient crosslinking (Li et al., 2003). This appears to occur as the cells mature, and can be observed as cells move from the growing zone to the differentiation zones in the roots. The cessation of cell expansion is clearly visible and is used as a marker to define the regions. The family of expansin genes is continually expanding, as continued investigation uncovers new proteins and functions (Lee *et. al* 2001; Lee *et. al.*, 2006)

### **2.9.3 Radial Restriction by Microtubules**

To this point, the discussion has covered the roles of turgor pressure and cell wall loosening in the process of cellular expansion (Cosgrove, 1999). However, these factors alone cannot account for the highly controlled expansion that is seen in plants. The 1-dimensional longitudinal expansion of the cells to increase the lengths of the organs must have additional control mechanisms. Nothing described so far is able to regulate the expansion to solely longitudinal growth.

There are several possibilities ranging from the simple to the complex. It is possible that the position of the cell in the plant may have some influence (Emons and Mulder, 1998). Cellular density and cellular packing may restrict the radial expansion of the cells within the root. However this would also effect longitudinal expansion in the same way. It also does not explain why the epidermal cells do not undergo dramatic radial expansion as they are not under the same spacial limitations as those cells within the root. Therefore must be discounted as a major factor, but may have some role to play. It is

possible that large amount of wall material (i.e. cellulose fibres) are deposited circumferentially around the organ. This would restrict the maximum possible diameter. A structure this significant would clearly be visible under a light microscope. Unfortunately no such structure is visible, suggesting that the restriction must be at the cellular level. Each cell must be able to regulate radial expansion in favour of longitudinal expansion to drive growth. It is possible that highly specific enzymes could be used to increase or decrease the levels of crosslinking at certain sites to effect expansion. This too must be discounted due to the homogeneity of the wall, preventing any enzyme from targeting a site specifically. Therefore there must be a non-wall component that is responsible for limiting radial expansion. One structure that is present in all cells in the cytoskeleton (Dubel and Little, 1988).

Research has suggested that the cytoskeleton has a role to play in the control of longitudinal cellular expansion (Smith, 2003; Smith and Oppenheimer, 2005). Filaments arranged helically in the direction of the proposed expansion (Kropf et al., 1998). The coils of cytoskeleton allow the cell to expand in the desired direction, whilst preventing the radial expansion (Mineyuki and Gunning, 1990). This is achieved by allowing the filaments to creep with the expansion with the gaps between the coils increasing (Yuan et al., 1994). A suitable analogy would be the way a spring expands as it is pulled from both ends (Sugimoto et al., 2000).

It is now possible to propose a suitable model for longitudinal cellular expansion that satisfies all the necessary criteria. The driving force is the turgor pressure created in an attempt to equilibrate the osmotic potentials. This pressure triggers the expansin and enzymatic creep allowing the wall to expand. The expansion is channeled by the restriction of growth in the radial direction by the cytoskeleton.

### **2.10 Cell Division**

Having investigated the primary factor in growth, it is important to understand the mechanisms by which new cells are created. It is these new cells that allow the organs to continue to grow after the older cells have matured. Understanding these processes and the potential for manipulation will be essential for the subsequent investigations.

## Chapter 2: Literature Review

The second factor in plant growth is the addition of new cell to the organs from apical meristems which in turn elongate to drive growth (Staiger and Doonan, 1993). If the number of cell available were finite, growth would be limited to the accumulated maximum lengths of all cells in the organ. However, the continued production of new cells through the plant cell cycle (Dewitte and Murray, 2003) allows for additional growth (Smith, 2001). However the maximum size of the organism is limited, determined by a factor of expression of all the genes that correspond to any aspect of growth.

The cell cycle (Genschik, 2001) itself is made up of four sections with mitosis the region where DNA replication, karyokinesis and cytokinesis occur, resulting in two daughter cells. This process is influenced and regulated (Menges et al., 2002) by many factors (Doonan and Fobert, 1997), both external and internal (Jacobs, 1992). These factors can have a great bearing on the output of the apical meristem and therefore the maximum growth (Green and Bauer, 1977).

After a cell division, the new cell is laid down, into its position in the root. This is where it will remain, as no cells are produced behind. The ultimate fate of cells is determined by the relative position in the plant and by the concentrations of certain growth factors that cause this differentiation (section 2.11). As the root tip moves forward, the cell moves through the zone of division, beginning its cellular functions. The turgid cell enters the zone of elongation; this is where cell wall loosening begins. Nascent cells from the apical meristem enter what can be seen as a second cycle, a growth or maturation cycle (Sussex et al., 1995). The growth of root will be used as example to explain this.

Figure 2.9 shows the cycle of cellular maturation, as the journey of a hypothetical cell leaving the apical meristem having been produced through cell division (Berger et al., 1998). Undergoing expansion through the process of turgor driven, expansins mediated longitudinal elongation. Leaving the elongation zone a mature cell, able to be differentiated into the required cell fate. This process of differentiation is driven by several factors, however most importantly plant growth regulators (Richard et al., 2002)

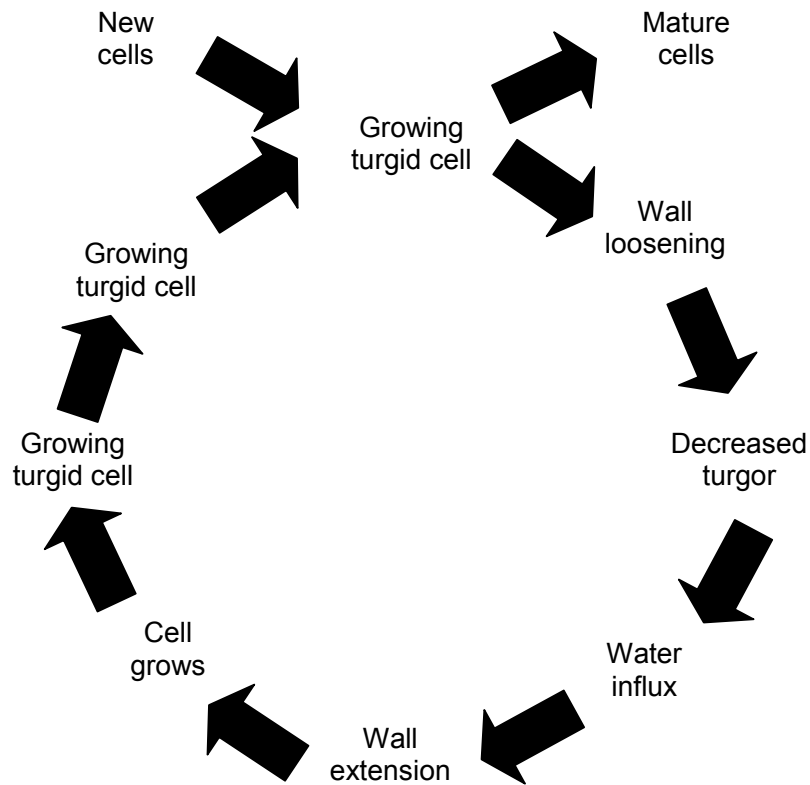


*Figure 2.9: The cell growth cycle. This illustrates the process by which new cells leaving the zone of division, undergoing expansion through turgor mediated longitudinal elongation of the cell wall and become mature cells.*

## 2.11 Plant Growth Regulators

The growth and differentiation of plant cells must have a method of control. It must be sensitive enough (Trewavas, 1982) to induce the catalogue of processes; but also robust to move long distances throughout the entire organism. This is achieved by chemical messenger molecules called hormones, or Growth Regulators (GRs) (Srivastava, 2002b). These hormones influence the expression of specific genes in order to direct the fates of the cells to those that are required. By regulating the concentration and composition of GRs a specific point of the plant, it is able to influence the differentiation of the cells in that region (Torrey, 1976). The fate of most cells is affected by its relative position in the plant. External stimuli can also affect the hormone distribution, e.g. sunlight which can influence the direction of stem growth to maximize photosynthesis (Morelli and Ruberti, 2002). Large quantities of GRs accumulate in these cells influencing the differentiation of those cells

around them by utilizing many control mechanisms, e.g. concentration gradients and feedback loops (Benjamins and Scheres, 2008). This knowledge is required in order to control the differentiation of the cells to produce the single cells required for compression. By exploiting the method of gene expression, the fates of cells can be artificially influenced by GRs in the external media. This method of regulation, replicates the method of controlled expression seen in plants with the growth media replacing the neighboring cells to deliver the GRs.

Plants use a combination of two main families of GR, which have a variety of affects that will change depending on concentration and composition of those available to the cells. These are Auxin and Cytokinin and are responsible for the control of all the gene expression in the plant.

### **2.11.1 Auxin**

Auxins were the first class of GRs to be discovered and shown to be involved in the coordinative signaling of plant development (Zhao, 2010). They are characterised by the presence of an aromatic ring and carboxylic group.

The most important member of the auxin family is indole-3-acetic acid (IAA), as it is the most potent auxin, and thus is responsible for the majority of the auxin effects in plants. Many synthetic analogues of IAA have been created, with reduced potency and including naphthalene acetic acid (NAA) and 2,4-dichlorphenoxyacetic acid (2,4-D). All maintain the characteristic aromatic ring and carboxylic acid group but alter the other side chains to produce a different molecule.

Other naturally occurring and synthetic auxins exist, but the IAA family of auxins is the most predominantly used in plant cell culture and as such was used in this research for the generation of suspension cultures (chapter 4). Auxins act as hormones to control plant development by influencing gene expression. This is achieved by targeting for degradation members of the Aux/IAA family of transcriptional repressor proteins by ubiquitination, catalysed by an ubiquitin-protein ligase. The ubiquitin tag marks the protein for destruction, acting as a marker for the ligase which breaks the bonds between the peptides, changing the space of the protein thus rendering the repressors unable to function (Fu and Harberd, 2003).

## Chapter 2: Literature Review

As a hormone, auxin is essential for the control of cell growth, affecting both cell division and expansion. Mostly responsible for influencing the root systems, e.g. promoting axial elongation and lateral expansion, auxins interact with other plant hormones in order to influence the development of the plant. Auxin concentrations gradients are responsible for defining the establishment of differentiation in the proximal regions of the roots and shoots in addition to the initiation of lateral root emergence.

### **2.11.2 Cytokinin**

Cytokinins are a different class of plant growth hormones to auxins. There are two types of cytokinins, adenine-type and phenylurea type (Mok and Mok, 2001). The adenine-type includes kinetin, zeatin and benzylaminopurine (BAP), which are commercially available. Kinetin does not naturally occur in plants but is a chemical analogue of some naturally occurring compounds and exhibits strong cytokinin activity in plants (Miller, 1961).

Adenine type cytokinins are synthesized in almost all cell types, stems, leaves and roots. However it is possible all dividing cells are responsible for the synthesis of these hormones. They are involved in both local and long distance signaling, utilizing the same transport system used for purines and nucleotides.

Like auxins, cytokinins are involved in the control of all aspects of plant development, but especially the control of shoot and leaf division and morphogenesis, chloroplast maturation and auxiliary bud release (Sakakibara, 2006).

However, the relationship between the two classes is how the plant is able to control cell differentiation more delicately. This is done by manipulation of the ratio of auxin: cytokinin that the cells in the developing region are exposed to. This ratio is crucial during cell division and the differentiation of plant tissues, especially considering that auxin is known to regulate the biosynthesis of cytokinin, an example of a feedback loop common this type of gene regulation.

## 2.12 Plant Cell Culture

The use of plant cell culture has become more prominent in recent years. This is to accommodate the increase of pharmaceuticals (Bonati, 1980) and other products (Ma et al., 2003) that have become available. Culturing cellular material has not been a recent development, with mammalian and bacterial cell culture used in many processes (Arathoon and Birch, 1986).

Culturing cellular material can be seen as any artificial system where the growth conditions are controlled. This can be simply the composition of the media in a petri dish to computer controlled environments for large bioreactors.

The use of cultures is one possible method to generate single cells. Previous work used culturing to generate single tomato cells (Blewett et al., 2000). This involved supplementing the media with sucrose and specific concentrations of GRs (chapter 2.10) to control the cellular fates and growth cycle (Olson et al., 1969). The technique of culturing has been applied to many plant species, including *Arabidopsis thaliana* (Encina et al., 2001)

## 2.13 Arabidopsis thaliana

*Arabidopsis thaliana*, more commonly known as thale cress. A small flowering plant related to cabbage and mustard. Although it has little agricultural significance it has several advantages that made it the model for understanding the genetic, cellular, and molecular biology of the flowering plant. It is used as a model because of its small size allowing many replicates in a small area. Fast growth, allows many generations in a relatively short space of time, approximately 5 per year. Finally *Arabidopsis thaliana* has a small genome (120Mbp) which is easy for sequencing and manipulation.

### 2.13.1 Genetics

By 2000 all of its 5 chromosomes had been sequenced (Theologis et al., 2000; Lin et al., 1999; European et al., 2000; Kazusa DNA Research Institute et al., 2000; Mayer et al., 1999) and lots of work has been done to analyse the results from this research and better understand the roles of the

individual genes (The, I, 2000). So far 22,500 genes have been identified and work is continuing to discover the functions of all of them (Swarbreck, *et. al.*, 2008).

This level of understanding of the *Arabidopsis thaliana* genome was a major factor in the choice to use it for this investigation. Through the genome sequencing (Bevan and Walsh, 2010), many genes have been discovered which affect the biosynthesis of cell wall components and their deposition into the wall and there is a plethora of possible mutations available that could affect the mechanical and physical properties. Many of these are available from seed stock centers, by-passing the need for genetic manipulation, which is costly, time consuming and carries with it certain ethical issues. Tomato cells have been used previously to generate mechanical information. This is beneficial as it is easier to generate single cells from the tomatoes. However, the genome is currently unsequenced and as such research on this system is limited. This required the move to a more understood system, hence the reasons for choosing *Arabidopsis thaliana* as the experimental system for the project, building on work that has previously been done with single tomato cells.

### **2.13.2 Mutations in Cell Wall Genes**

The cell wall (Fagard *et al.*, 2000) of the normal *Arabidopsis* plants found in the wild (the wild type – WT) is the control organism for all *Arabidopsis* experiments, Columbia (Col0). With the sequencing of the *Arabidopsis* genome (Bevan and Walsh, 2005) this enabled the identification of many new mutations via genomic analysis and reverse genomics. There are many naturally occurring and induced mutations in genes that affect the cell wall (Ossowski, *et. al.*, 2010). All of these have changes in the genomic sequence responsible for genes that control the metabolism or catabolism of the cell wall components. This means that each mutant genotype will cause a specific mutation affecting its cell wall; these mutations will have varying effects on its properties (Reiter *et al.*, 1997). *Arabidopsis* has many well documented gene mutations that affect the cell wall (Alonso, *et. al.*, 2003); most are caused by disruption of metabolic pathways, as the initial cell wall component precursor must go through many alterations (Benfey, *et.al.*, 2010).

Mutation	Encodes	Effect
<i>mur1</i>	GDP-D-mannose-4,5-dehydratase	Catalyses of the first step in the de novo synthesis of GDP-L-fructose is reduced
<i>mur2</i>	AtFUT1	Lacks frucosylated xyloglucan a cell wall component
<i>mur3</i>	Xyloglucan Galactosyltransferase	Absence of conserved a-L-fucosyl -b-D-dalactosyl side chains reduced fibre cross-links
<i>mur4</i>	Uridine Diphospho L-Arabinose	50% reduction in monosaccharide L-arabinose
<i>qua2</i> (SKS-Snakeskin)	Putative methyl transferase	Reduces methylation of homogalacturonan backbone
<i>ida</i>	Overexpression inflorescence Deficient in Abscission	Activates Cell separation in vestigial abscission zones
<i>qua1</i> (Quasimodo1)	Putative membrane bound glycosyltransferase required for normal pectin synthesis	25% reduction in galacturonic acid; reduced cell adhesion

**Table 2.1: Potential genotypes that contain mutations in genes that affect the cell wall, all are from the Columbia background and are therefore comparable.**

Table 1 shows some cell wall mutations have already been identified using genomics and proteomics. *mur1* (Bonin et al., 1997); *mur2* (Vanzin et al., 2002); *mur3* (Madson et al., 2003); *mur4* (Burget and Reiter, 1999); *pmr6* (Vogel et al., 2002); *qua2* (Mouille et al., 2007); *ida* (Stenvik et al., 2006b) and *qua1* (Bouton et al., 2002) are all cell wall mutations that result in altered cell wall properties. These have all been identified but the structural significance of each of the mutation on the individual cell wall is yet to be characterised.

## 2.14 Investigations into the Mechanical Properties of Plant Cells

### 2.14.1 Pressure Probe

The pressure probe (Tomos and Leigh, 1999) is an instrument used to measure hydraulic structure of individual cells, water movement in plant structures and the response (Zimmermann and Husken, 1979) of tissues to water stress (Husken et al., 1978) (Fig 2.10). A glass micro-capillary tube is

tapered to a point by heating and filled with silicone oil removing air. The silicone oil has a low friction and is incompressible, unlike air.

The capillary tube is used to pierce the cell wall of a cell, which results in the cell contents being pushed in to the tube due to the high internal cellular pressure. Restoring the meniscus to its original position required application of pressure that can be measured by a pressure transducer. The Meniscus between the cytoplasm and oil can be moved using the motor, micrometer and metal rod assembly. Through the manipulation of the pressure the volumetric elastic modulus can be derived, in addition to the hydraulic conductivity.

The pressure probe has been used successfully to analyse single cells in intact plants (Tomos D, 2000). This has produced large amounts of data on the cell walls of the individual cells the root system (Pritchard et al., 1989) and shoots (Zimmermann and Husken, 1979).

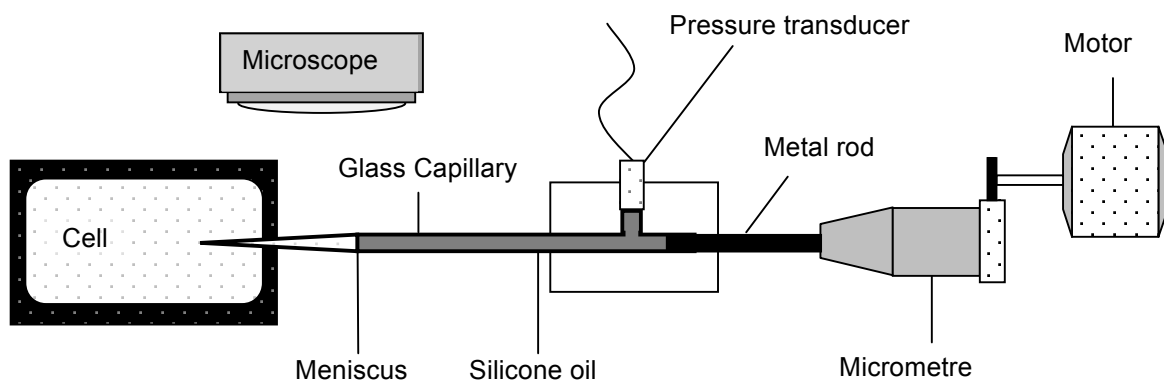


**Figure 2.10: a schematic showing the major components of the pressure probe used for work on the individual cells. The pipette pierces a cell; the cytoplasm is forced into the pipette due to the elevated internal pressure. This pressure is measured by returning the meniscus to its original position. The force required is equal to that of the internal turgor pressure.**

The technique has only had limited success when applied to the single cell suspension cultures as the cells need to be immobilised but not adhered to any surfaces as this will affect water relations (Wang et al., 2006). It may be possible to use a suction pipette as this allowed work with tomato cells in suspension which yielded some interesting results. Unfortunately, this technique will not be applicable to the *Arabidopsis* suspension cells as they are too small.

### **2.14.2 Compression Testing by Micromanipulation**

Compression testing put simply, is squeezing a cell in an attempt to gain information on its mechanical properties (Thomas et al., 2000). The first example of this technique is the compression of sea urchin eggs, visually measuring the surface deformation to determine the forces being imposed (Yoneda, 1964; Yoneda and Dan, 1972). However sea urchin eggs are quite large and other biological cells are not, so the technique was evolved, leading to the development of compression testing by micromanipulation (Zhang et al., 2009). The technique is capable of compressing small cells or particles (minimum of 1 $\mu$ m). The forces that are involved in these compressions are recorded (minimum force detectable is approximately 1 $\mu$ N) (Zhang et al., 1991). This technique will be discussed in greater detail in chapter 5. Micromanipulation involves samples being compressed between two flat parallel surfaces, usually until failure. The forces involved and the displacement of the surfaces allow force – deformation data to be calculated, giving comparative data for different sample populations e.g. genotypes.

Previously, the technique has been applied to many different experimental systems including animal cells (Zhang et al., 1991), yeast cells (Smith et al., 2000; Mashmouhy et al., 1998), bacteria (Shiu et al., 1999), microspheres (Wang et al., 2005) and single tomato cells from suspension cultures (Wang et al., 2005; Blewett et al., 2000). It is encouraging to see that plant cells have been compressed using this method before, although these were much larger and more easily obtained tomato cells. However, the method may require modification to cope with the differences in cellular properties, in particular cell size.

The forces needed to deform the cells can be influenced by many factors: sample factors such as cell size; wall thickness and internal pressure; and equipment factors such as compression speed and

equipment age. To remove this variation, a method of extracting values from the data that is independent from the method of measurement is required.

Through mathematical modelling of the force-deformation data gain from compression testing, intrinsic mechanical properties can be determined. An intrinsic property can be described as one that does not change dependant on the method used to derive it. Initially the elastic modulus data was extracted by measuring the contact area of between the sample and compressive surface, the forces involved and the principal radii of curvature at the point of contact (Cole, 1933; Hiramoto, 1963). Although this yielded the elastic modulus, it was very difficult to accurately measure the contact area, thus requires a method of calculating the elastic modulus without relying on measuring the contact area. This led to the development of two mathematical models, the 'liquid-drop' model (Yoneda and Dan, 1972) and the elastic membrane model (Pujara and Lardner, 1979). More recently, models have been developed specifically for the derivation of intrinsic mechanical properties from yeast (Stenson et al., 2009) and tomato cells (Wang et al., 2004). The tomato cells were found not to be linear elastic to rupture, after an elastic limit had been reached the cells were presumed to behave plastically. The model assumes that the wall is elastic (i.e. obeys Hooke's law) therefore only data ranging from the initial point of contact and elastic limit can be used. From this data the low strain elastic modulus was calculated for the single tomato cells.

## *Chapter 3: Characterising Phenotype*

---

The project aims were to investigate effects of cell wall mutations on the physical and mechanical properties of the plant cell wall. It was hypothesised that with the single cell compression approach, these changes can be quantified. The mechanism of plant growth by individual cell expansion has been discussed in section 2.8. Plants require the wall for establishment of turgor pressure that can be essential for growth. Modulation of cell wall properties by changes in wall biochemistry can allow turgor pressure to expand cells. Since expansion growth is a result of the accumulation of individual cell expansions it is likely that changes in cell wall properties induced by loss of function mutation may affect plant growth. By choosing mutations in genes with different putative effects on wall biochemistry the effect on the different wall components could be assessed.

The single cells that were assessed were generated from suspension cultures, chapter 3. However, to justify this investigation proof of the effects that these mutations caused were investigated (Went, 1958) using the phenotypes of the roots and shoots. This chapter investigates the effects the losses in functionality have on the growing plant, enabling the prediction of the intrinsic mechanical properties that were investigated in chapters 6 and 7.

### **3.1 Selection of Mutants in Appropriate Candidate Genes**

To investigate the effects of compositional change on the wall, mutations were selected in genes that correspond to aspects of cell wall biosynthesis. Wide ranges of mutants are currently available in *Arabidopsis thaliana* from sites such as National *Arabidopsis* Stock Centre (NASC) in Nottingham, UK. The use of existing mutants for this investigation has many benefits. Many of the mutations have already been partially investigated at some level. The generation of new mutants is a costly and time consuming and unnecessary in the present study, given the number of mutations available.

## Chapter 3: Characterising Phenotype

A search in the literature indicated over 25 mutants that are potentially available and whose annotation allowed hypothesis about alterations in wall mechanical properties. Investigation of 25 mutations is not an appropriate resolution, it would be time consuming and therefore not feasible.

However, comparison of mutations in different regions of the cell wall, primary wall, middle lamella or both (chapter 2.6), could give greater insight into regulation of wall properties. Accordingly, mutations were separated into those that affect these three categories. Four genotypes were chosen, the *Columbia* (col0) wild type, *qua2* (aka snakeskin/sks) representing middle lamella mutations, *mur1* representing primary cell wall mutants and *ida* that affect both regions. The Wild type genotype acts as the control for the experiments, to which the mutations will be compared. All mutations were acquired from NASC, Nottingham, except *sks*, a sample of which was donated by Alan Marchant from Southampton University. More information on these mutations is available in table 2.1 which can be found in chapter 2.13.

### 3.2 Plant Growth Characteristics (PGC) and Bulking up Seed Stocks

The first method of phenotype analysis looked at the aerial region of plants over the first 5 weeks of growth. During this time certain characteristics, e.g. height and rosette width, were scored for a population of each of the genotypes. Investigations were conducted using the University of Birmingham Bioscience greenhouse facility, which standardises the growth routine of the plants. The soil is standard, watering and light availability is automatically controlled, thus minimising environmental effects that could influence the growth, allowing any differences found can be attributed to the genetic differences between the genotypes. Once the characterisation is completed the seeds from these plants were harvested and formed the seeds stocks for the other experiments in this investigation.

A population of a single genotype will exhibit biological variability based on the availability external variables e.g. nutrients, water and sunlight. This explains the requirement of increased numbers of biological replicates to verify any differences through statistical analysis.

### 3.2.1 Methods

For each genotype five seeds were sown onto the surface of the soil of twenty 8 cm diameter pots. Seedlings were germinated for 10 days when all but the largest removed. This number of plants was selected as it was manageable, but allowed sufficient numbers for statistical analysis. Seedlings were then measured on ten different growth criteria, over the first 35 days of growth. The measurement criteria were chosen to maximise the information gained, the limit of 35 days was set as a measure of comparison to the col0, as this is the time in which col0 (the wild type) plants will have reached a mature state. Measuring was conducted at the same time each day to ensure consistency. The plants are subjected to a 16:8 lighting regime with Philips 400W 50N agro bulbs, temperature was maintained between 18-20 °C and watered for 2 minutes each day.

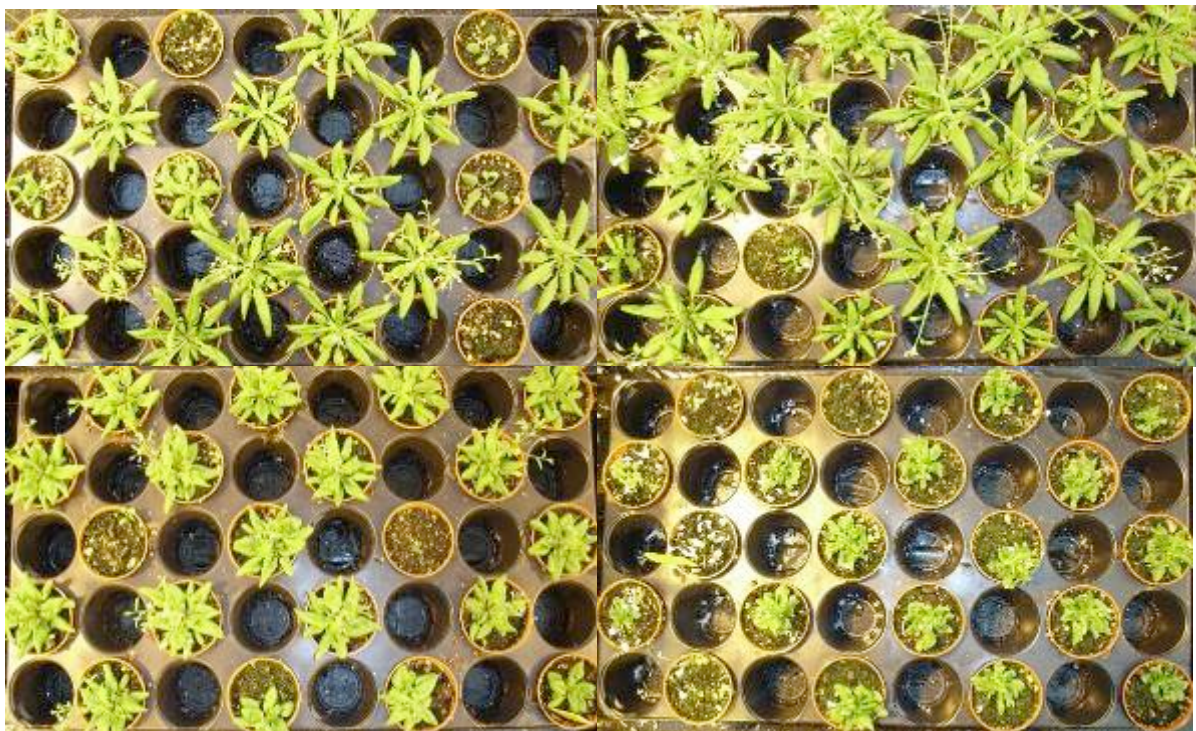
After 35 days the plants were enclosed upright in seed collection bags with cable ties securely fastened around the base of the stem. Pots were raised to dry out. Once dry the siliques were broken releasing the seeds. The plant debris was removed using tea strainers. The seeds were collected on sheets of paper stored in microfuge tubes. This procedure enabled the collection of large numbers of paired seeds required for all subsequent experiments. The seed was to be stored in microfuge tubes, in a dark and dry place, e.g. drawer in a lab bench. The collected seeds were allowed to mature; this process takes approximately 4 weeks.

### 3.2.2 Results

Figures 3.1 and 3.2 demonstrate some of the differences observed during the investigation. From the photographs it is possible to gauge the differences between the genotypes at the two time points but the growth of each plant between the time points. Each figure shows the differences visible in rosette width, in addition to leaf size and shape. The leaf shape was not directly analysed but will be discussed in 3.2.3



*Figure 3.1: a top view of a tray of 20 plants of each genotype at day 30. Clockwise from top left: col0, ida, sks and mur1. This figure is not representative of the position in the green house, but arranged to aid comparison. For the purpose of scale, the pots seen as brown rings are 8cm in diameter.*



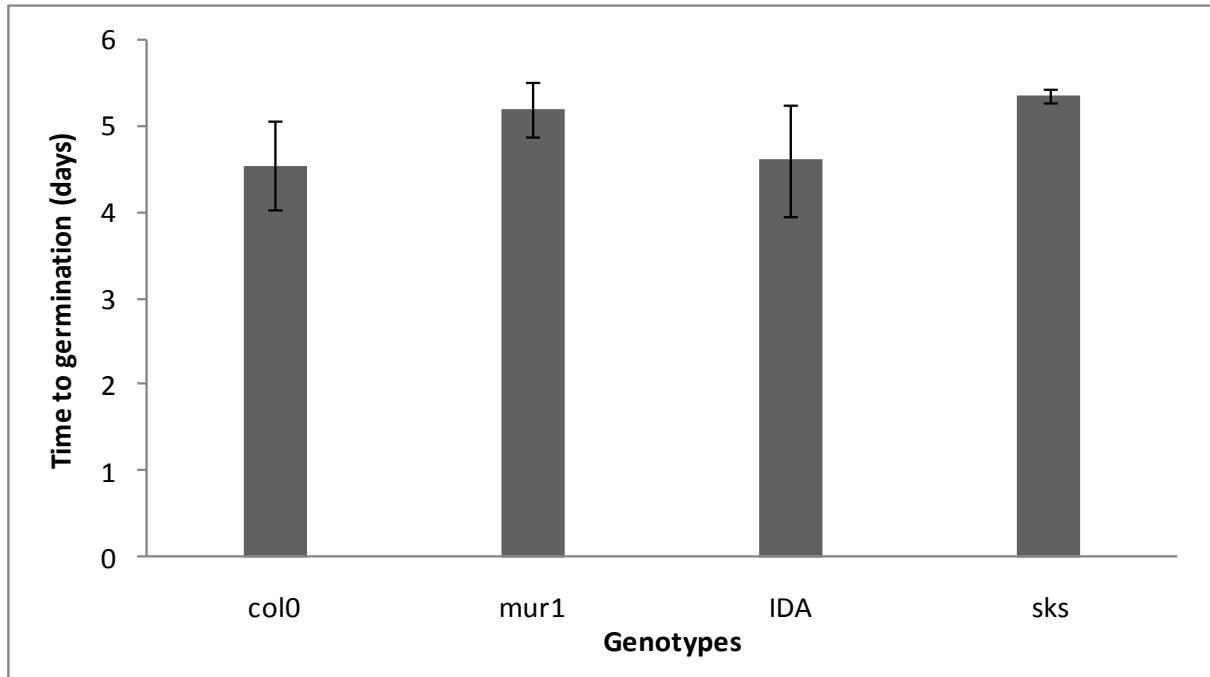
*Figure 3.2: a top view of a tray of 20 plants of each genotype at day 35. Clockwise from top left: col0, ida, sks and mur1, This figure is not representative of the position in the green house, but arranged to aid comparison. For the purpose of scale, the pots seen as brown rings are 8cm in diameter.*

Figure 3.3 - 3.6 are graphical representations of the 10 measurements made over the 5 weeks of the experiment. The averages of the three replicates are shown, totalling 60 plants for each genotype. For rosette widths and plant heights, the measurements were made at the maximal point for consistency.

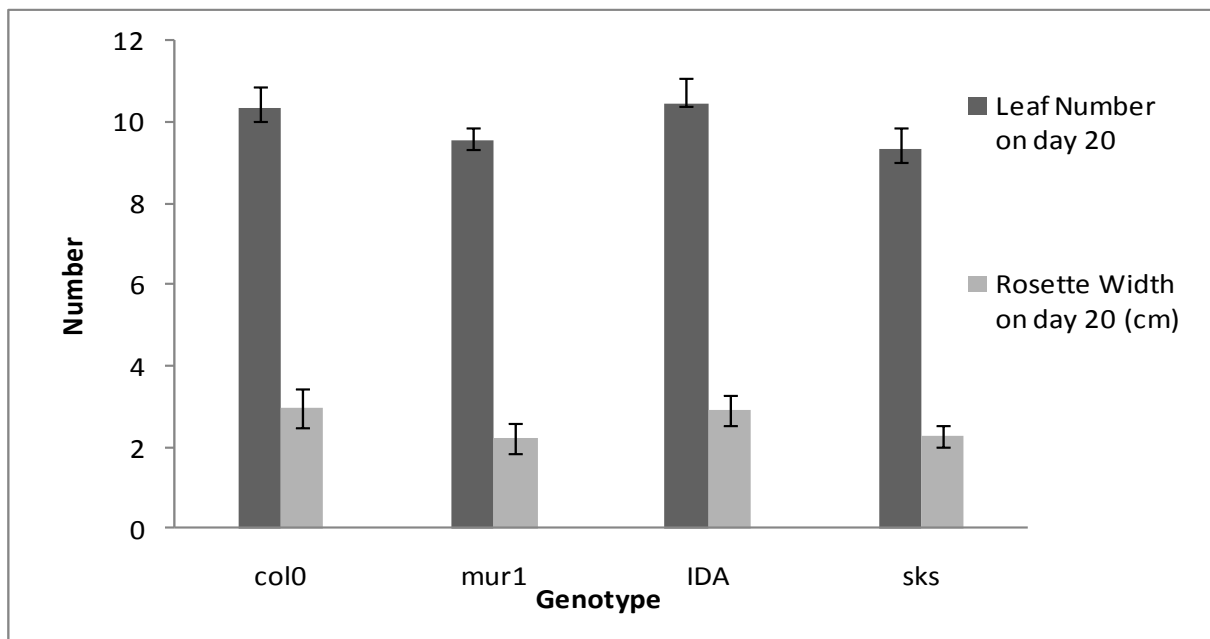
### 3.2.3 Discussion

Figure 3.1 and 3.2 are photographs taken looking down on trays of each genotype at day 30 and 35. Day 30 was approximately the time of bolting. Col0 and IDA appear similar in size and shape, mur1 shorter in leaf length but with similar leaf width and sks significantly shorter, narrower leaves and often curled. These effects contribute to greatly reduce the leaf surface area that perhaps influenced the plant into producing additional leaves. However this increase in leaf number often caused leaves to be partially or completely obscured to direct sunlight. These suggest that as far as the rosette is concerned, that the increase in leaf number may have little benefit. When the photographs are compared, only small increases in rosette width are seen. This evidence supports the suggestions in the paragraph above concerning the subsequent effects of delayed germination. It shows that all of the plants have started to grow vertically concentrating of the growth of the stem and flowers.

In figure 3.3 the average time taken for the seeds of each genotype to germinate can be seen. Col0 and IDA were very similar averaging approximately 4.5 days. It is therefore possible that the IDA mutation does not have an effect at this stage of development; this is not unexpected as there is no abscission. However, the mur1 and sks have significantly increase germination times. This lengthening in germination time could have been caused by the seedlings struggling to establish turgor limiting the early stages of growth or some effect of the mutation in the seed casing.



**Figure 3.3:** The average time taken for the seedlings to germinate. This was taken as the point at which the hypocotyl was first visible. Error bars show the standard error. Using the student's *t* test, *mur1* and *sks* genotypes take significantly longer to germinate than *col0* ( $P > 0.05$ ). Three biological replicates of twenty plants were used.



**Figure 3.4:** the number of leaves in the rosette and the width of the rosettes taken on day 20. Error bars show the standard error. The *sks* and *mur1* mutations have a significantly reduced rosette width compared to *col0* and *IDA*. In addition to this *mur1* also has significantly fewer rosette leaves than *IDA* ( $P > 0.05$ ). Three biological replicates of twenty plants were used.

At day 20 two characteristics were measured, rosette width and leaf number, this data is given in figure 3.4. The results for *ida* show close agreement to those of the *col0*. Compared to *col0* and *ida*, *mur1* shows a significant reduction to both, with *sks* showing a reduction in rosette width. Further leaves emerge from the central point of the plant and expand outwards. Similarity in leaf number suggests the plants are at similar levels in development, thus the differences in the rosette width caused by the mutations. With the *mur1* producing leaves similar in shape to the *ida* and *col0* but simply smaller.

This may be caused by mutations in hemicellulose affecting the expansive growth. The curled and shortened nature of the *sks* leaves, are highly likely to have been caused by the weak intercellular bonding resulting from the lack of pectin in the middle lamella. This is because growth in the plant is not only controlled by internal forces, but because of location in the plant and interaction with the surrounding cells.

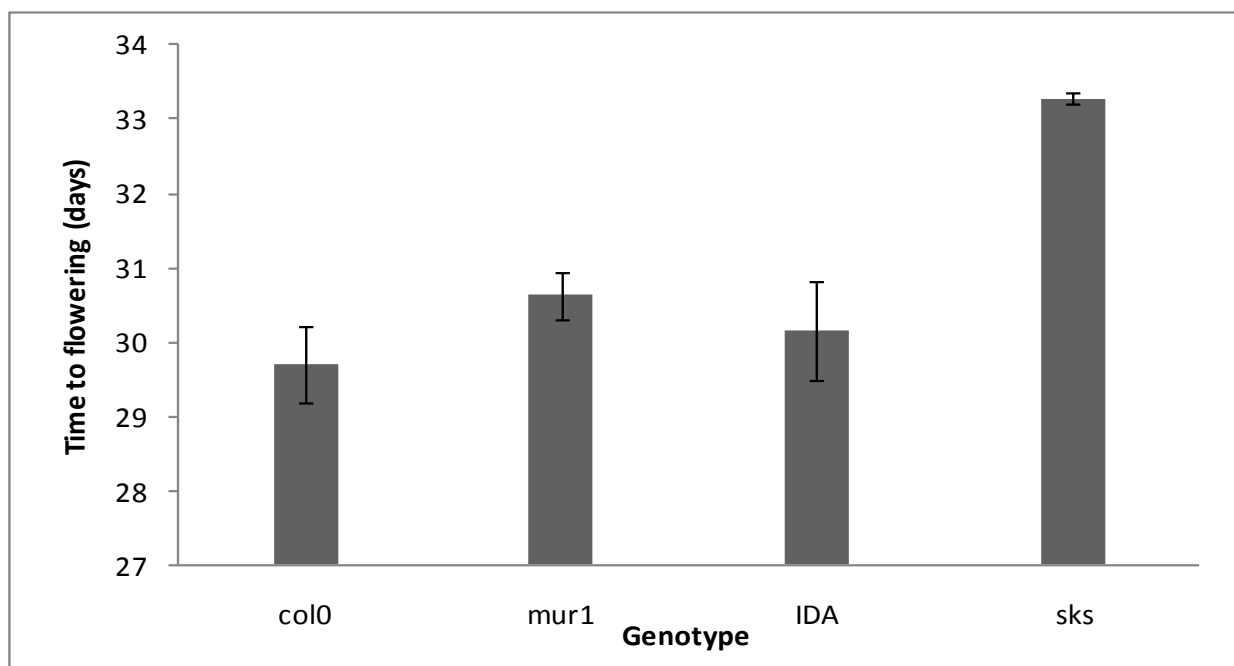


**Figure 3.5:** Average time taken for the plants to flower. This was taken as the time until the first flower was observed on the plant. Error bars represent the standard error. The *sks* took significantly longer to flower than the *col0* and *IDA* genotypes ( $P > 0.05$ ). Three biological replicates of twenty plants were used.

### Chapter 3: Characterising Phenotype

After germination, the next development stage is flowering. The time taken for the genotypes to flower is represented by figure 3.5. Compared with *col0* and *ida*, the *sk5* genotype takes significantly longer to flower. It would appear that the *sk5* mutation was causing additional developmental effect on the plants. This delay in flowering is more than would have been expected when compared to the patterns seen previously. Further evidence for this can be seen in figure 3.6 this shows the data from plants at flowering. The height of the plants shows a similar pattern to previous but with no significant differences. However with respect to the numbers of cauline and rosette leaves were higher in the *sk5* compared with the others. This may be a result of a smaller leaf area, and so in an attempt to generate more energy the plant produces more leaves to try and counter this deficit.

The additional expenditure in energy causes the additional delay to the flowering of the *sk5* plants, however this is speculation. The fourth bar chart of figure 3.6 compares the rosette width at flowering and shows *mur1* and *sk5* with significantly lower widths than *col0* and *ida*. This shows the same pattern as found in the day 20 results in fig 3.4; however the differences have been extenuated with time. At flowering the plant reduces the energy it is expending on rosette leaf production. This helps to show that the effect of increased germination time has not had affected the other measurements. This reduction in rosette expansion and the differences over time can be seen in figures 3.1 and 3.2.

Figure 3.7 represents this change in height that was suggested by figures 3.1 and 3.2. Once again the same patterns occurred. With the *col0* and *ida* similar at both 30 and 35 days, *mur1* showed only a slight reduction at day 30 but this difference increases at day 35 however neither difference is significant. The *sk5* mutation shows significant differences to all other genotypes at days 30 and 35. The increase in cauline leaves seen for *sk5* seems unlikely when shown with a short stem. This height deficit may be a combination of reduced cellular expansion and the production of additional rosette and cauline leaves to increase energy production.

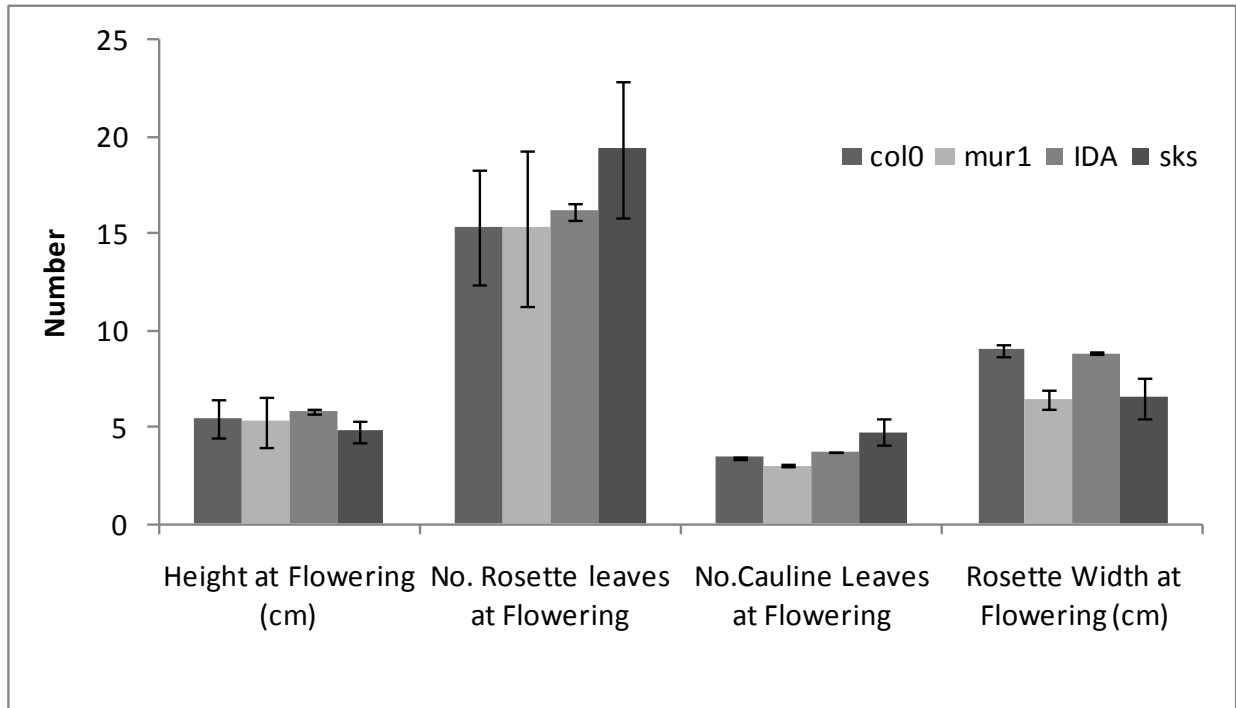


**Figure 3.6:** Measurement taken from the plants on the day of flowering. Error bars show standard error. *Mur1* show significant decreases to *col0* and *IDA* in the number of cauline leaves and rosette width. *Sks* shows significant increased numbers of rosette leaves and decrease rosette width. In addition, *sks* has a significantly increased number of cauline leaves to *mur1* ( $P > 0.05$ ). Three biological replicates of twenty plants were used.

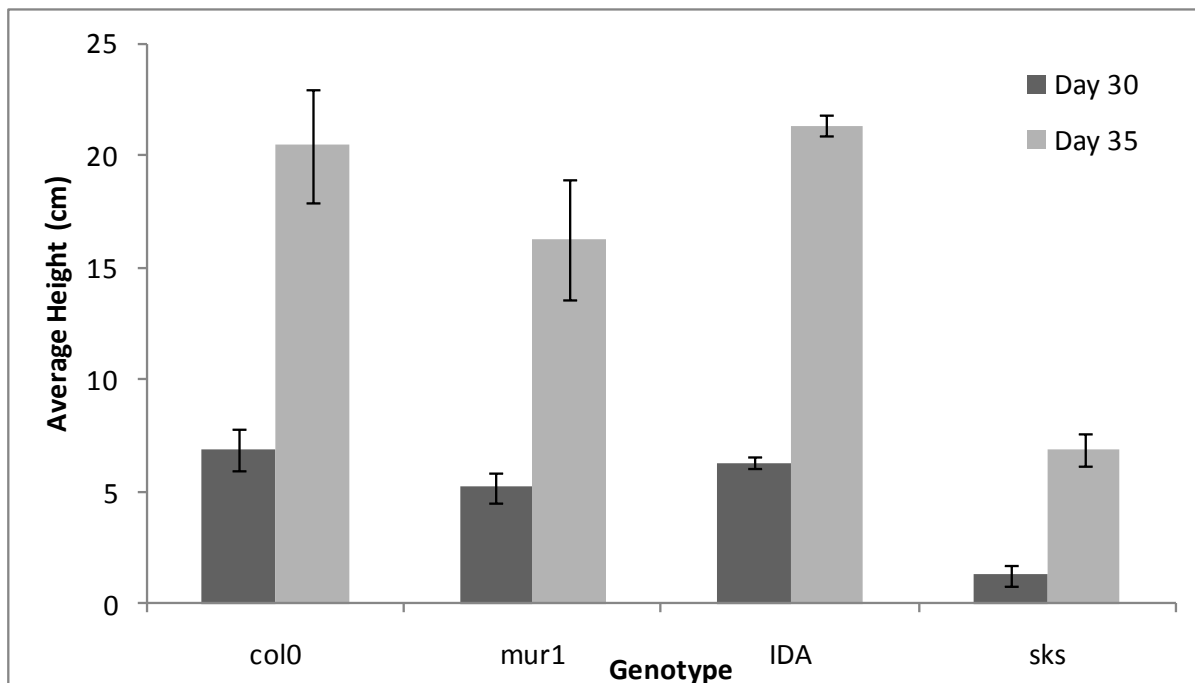


**Figure 3.7:** Average heights of the plants on days 30 and 35. Height was taken as the distance from the soil to the highest point of the plant. *Sks* are significantly shorter than *col0* plant by day 35 and on both day 30 and 35 when compared to *IDA* ( $P > 0.05$ ). Three biological replicates of twenty plants were used.

### 3.2.4 Conclusions

It is interesting that the middle lamella (*sks*) and primary cell wall (*mur1*) mutations have a reductive effect, causing the plants to develop slower and to a smaller maximal size. Results for the *ida* mutation show little affect at any stage of the plant development when compared to the WT. It is possible that the plant is able to compensate for the mutation and operate within normal parameters, masking the effects of the mutation when compared to more severe mutations in the middle lamella and primary cell wall, where the differences are clear. The evidence from the PGC encouraging, the mutations are clearly having an effect on growth. However, these preliminary measurements of growth must be supported by a simpler and more controllable system to validate the conclusions.

The *sks* mutation is obviously having additional developmental affects on the aerial region of the plant. With the increased number of leaves potentially attempting to compensate for the energy deficiencies caused by the small surface area of the existing leaves. The curling of the leaves resulting in the reduced surface may be due to the weakened reduction of pectin in the middle lamella. It is this altered cell adhesion that is responsible for the results observed.

### 3.3 Plant fresh weight: dry weight

The differences seen in the Plant Growth Characterisation (PGC) investigation 3.2 shows that the genotypes cause differences in leaf growth patterns and maximum heights. Unfortunately PGC does not suggest reasons why these differences occur. There are two possible causes, the mutations cause a reduction in material in the walls, or they affect the functionality of the fibres in the wall. It is known that the *sks* causes a reduction in pectin (Mouille et al., 2007). Whether this reduction has any subsequent effects or any of the other mutations cause differences an investigation into material present was conducted.

#### 3.3.1 Method

To investigate the differences in the plant growth with respect to cell wall quantity, the amounts present were recorded during the course of growth. Plants were grown in the same conditions as those of the PGC section 3.2, and harvested at 5-day intervals. 15 days were allowed at the start of

the experiment for germination and the seedlings to be of sufficient weight to measure. Five plants were pooled for each genotype, helping during the early stages after hypocotyl emergence when the plants are small. The above ground region was taken, pooled and weighted to find the fresh weight. These were then dried at 60°C for 24h and weighed to get the dry weight. The percentage moisture content was calculated from the fresh weight. It is presumed that the dry weights consist of mostly cell wall material. There will be cellular components remaining for example organelles however the weights of these will be discounted as significant as this is a preliminary experiment. For a more detailed investigation of the wall biochemistry see chapter 5.

### 3.3.2 Results and Discussion

Figure 3.8 (A) and (B) shows the fresh weight (FW) and dry weight (DW) respectively. A similar pattern in relationship of the WT and the mutations is visible. An initial lag period as the plants start to produce energy by photosynthesis followed by a rapid increase that begins to plateau towards as growth slows. The FW and DW for *col0* are higher from day 30 onwards when compared with all the mutations, however *IDA* shows a higher dry weight than the other two mutations in the later end of the experiment, but shows a similar fresh weight to the other mutations.

The PGC suggests that day 30 is the point at which the plants bolt, rapidly increasing stem height, which is then followed by flowering. This explains the sudden increase in both weights, with the stem and cauline leaves etc. causing the overall weight of wall material being produced to drastically increase to meet the higher demand. Variations in growth conditions are kept to a minimum. Factors that could influence growth, e.g. carbon, light and water availability are standardised. Mutational effects are the only variable influencing the weights, i.e. reduction in cell wall material production.

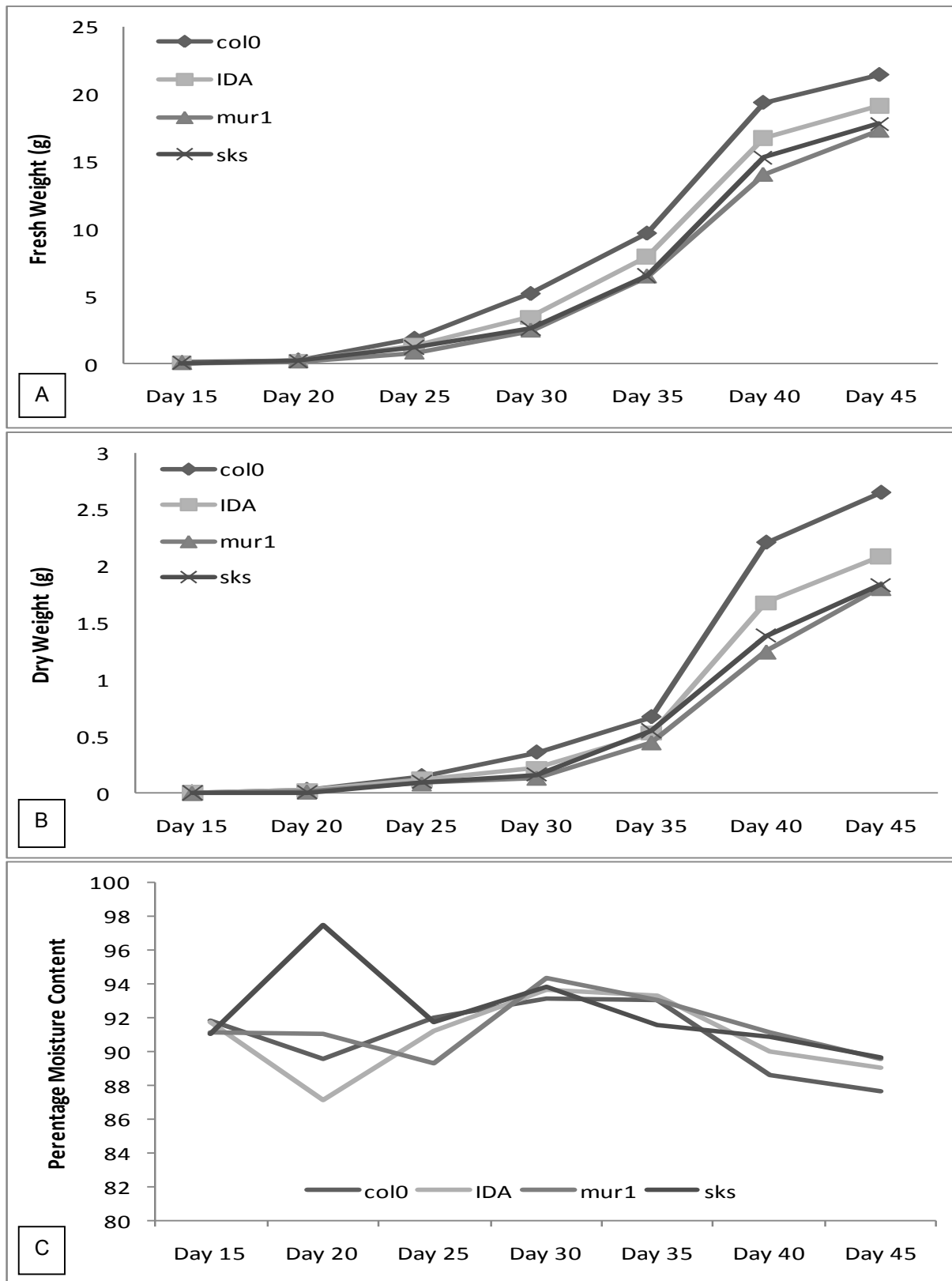


**Figure 3.8:** The results of the fresh weigh/dry weight investigation. (A) Shows the fresh weight of each genotype over 45 days. (B) Shows the dry weight of the same plants over the same period. (C) Shows the percentage moisture content of the plants calculated from the results from (A) and (B). The results are taken from the pooling of 5 plants and counts as an average.

### Chapter 3: Characterising Phenotype

The *ida* mutations showed many similarities to *col0* during the PGC. It is therefore possible that *ida* requires less polysaccharide or produces less polysaccharide in-order to act in a similar manner to *col0* figure 3.8 B., assuming the DW is proportional to the weight of cell wall material present. The *ida* mutant may possibly produce thinner primary walls, with more cross-links etc. giving similar properties to *col0*. The IDA mutation affects the abscission regions (Stenvik et al., 2006a) These areas are prominent in the aerial region with flowers. This may result in the lower dry weight. This mutation will not affect the main stem; hence the height is not affected 3.6. Theoretically, the effects of the *ida* mutation should not be noticed in the growth of the roots as no abscission zones occur in this region. This was investigated in section 3.4.

The results showing *mur1* and *sks* with similar levels of FW (figure 3.8 A) and DW (figure 3.8 B) were also interesting as the PGC shows differences which may affect the amount of material present. *Mur1* are taller and have larger rosette leaves, but *sks* has more rosette and cauline leaves. It may be speculated that these additional factors cancel out resulting in no net differences in weight.

Figure 3.8 (C) shows that throughout the experiment the moisture content of the genotypes throughout the experiment remain similar. Due to the destructive nature of sampling, it is not possible to maintain the samples throughout the experiment. From day 30 onwards the plants exhibited a slow but consistent decrease in moisture content, e.g. the percentage of wall component increases gradually.

During development plant tissues go through a process of maturation of the plant wall, which involves thickening and strengthening with additional cross links (Smith, 2001). It is also possible that lignin deposition occurs, but this is not likely to be a major factor at this stage. This percentage is a calculated from the FW and DW measurements, and converted into a percentage ignoring the different weights of material from the genotypes. This increases the relevance of this data, showing the plants are in a similar stage of development and the differences seen as actual, caused by changes in wall properties caused by the mutations.

### 3.3.3 Conclusions

The ability of the genotypes to produce and deposit material into the wall appears to have an affect on the FW and DW. The evidence from this investigation supports the results from the PGC that physical differences seen in the growth characteristics. The *sk*s and *mur1* mutations exhibit significant lower FW from day 30 and DW from day 35 to WT. In addition to this *ida* also shows non-significant differences from the WT in FW and DW from day 30. From day 30, the DW differences become significant.

Given the previous data in section 3.2 on the growth of the mutations, the results for *sk*s and *mur1* are not surprising. The reduction of the total amount of polysaccharide present in the walls could explain to a certain degree the large differences in growth that are observed. The mutations appear to reduce the amount of polysaccharide present in the wall to the extent that growth is significantly affected. However it is possible that this reduction in polysaccharide may not be directly resulting from the mutations but maybe developmental. It is also know from the literature (section 2.13.2) that *sk*s causes a reduction in the total pectin content of the cell wall. This evidence supports these conclusions.

The results for the IDA mutation were a little unexpected. This suggests that mature the *ida* plants produce a similar growth pattern of the above region to the WT, but with a significantly reduced amount of cell wall.

These data raises some questions about the *ida* mutation and supports previous data for *sk*s and *mur1*. However it is unable to differentiate between the two, justifying the need for more sensitive investigation into the polysaccharide composition. This can be found in chapter 5; the experiment was designed to determine the biochemical differences caused by the mutations, through investigation of the quantities of the 3 main types of polysaccharide present in the wall.

### **3.4. Root Growth Assay (RGA)**

In an attempt to validate the conclusions of the plant growth characteristic (PGC), a more controllable system must be used. It is very difficult to accurately measure the exact growth of stems, as they expand in three-dimensions. Investigating mutational effects on the growth of the roots simplifies the system to one dimension. Making accurate measurements of roots in soil is very difficult and removing the roots from the soil is not an option due to the chance of damaging them and disrupting their growth.

In contrast, the use of hydroponics could allow the overall length to be measured but would be time consuming. However, growth of roots on agar slopes allows visualisation and easy monitoring of root growth in the early stages of development.

#### **3.4.1 Method**

Due to limited space allowed in the plates the time of the experiment is limited. The effects of the energy production lag seen in the germination time of the PGC is now an additional problem. This is where the seedlings have used the limited stores of energy contained within the seeds and begin producing energy through photosynthesis. The germination of the seeds must therefore be removed as a limiting factor. It may be possible to overcome the lag by synchronising the germination of the seeds and by the addition of sugar to the media. This means that the experiment will be a measure of maximal root growth at optimal growth conditions rather than natural root growth. Removal of nutrients as a limiting factor means the limited time should no longer be a problem. Supplementing the media with a high concentration of sugar required an aseptic environment, as any subsequent infection could easily ruin the experiment.

The medium was composed of 1 litre long Ashton solution supplemented with 1% sucrose and 0.5% agar. Long Ashton solution contains all the micro/macro-nutrients that the seeds required for germination and early growth. This was made up using the stock solutions (see appendix 1), 2.5mls of each solution, added sequentially from 1-8 (to prevent precipitation), 1% sucrose and made up to 1

litre with sterile distilled water (SDW). The pH was adjusted to 5.6 using 1M NaOH and the agar added and thoroughly dissolved using a magnetic stirrer.

The flask is sealed with foil; the mixture is then heated and allowed to boil, whilst subjected to continuous stirring. This was allowed to boil for 10 min, removed from heat and allowed to cool. The solution was now clear. Once cool, in a flow hood, the medium was poured into 8cm square petri dishes. Time was allowed for the agar to set and for any excess water to evaporate as this could cause problems later (see discussion section 3.4.3).

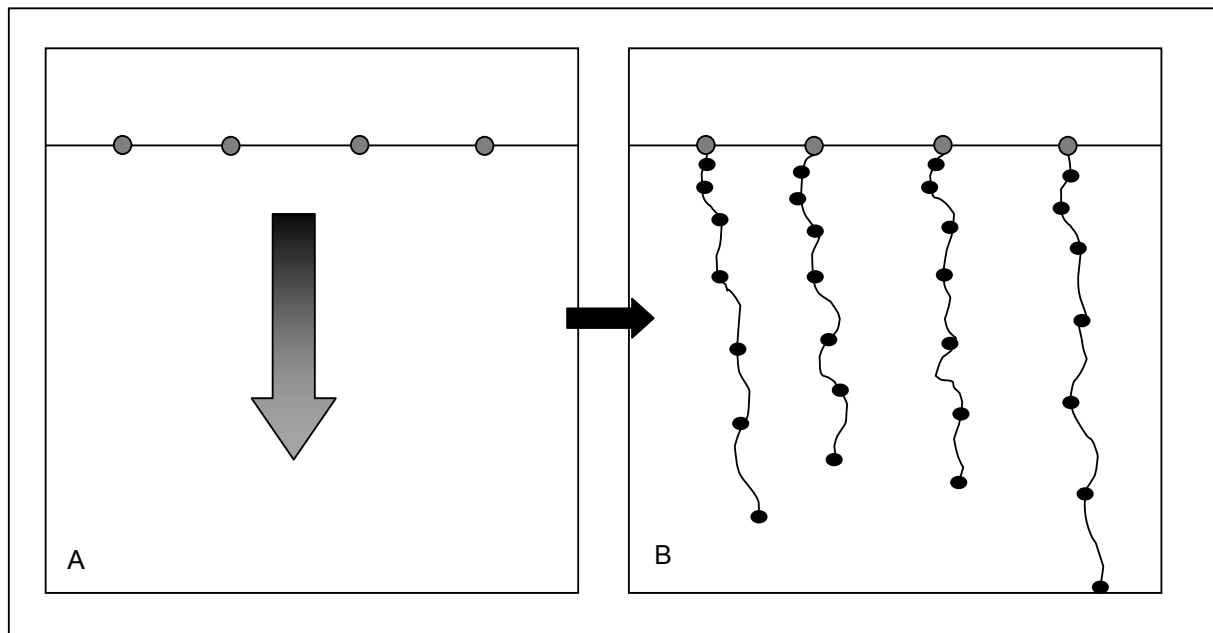


**Figure 3.9:** Diagram showing a plate from the Root Growth Assay. (A) The sterilised seeds were placed on the zero line and allowed to germinate; the roots will grow vertically down the plate (direction shown by the red arrow). (B) Shows the plate after several days of growth monitoring with dots marking the root growth every 24 hours. The fourth root from the left has reached the bottom of the plate, this was taken as the end of the experiment as no more information can be accurately recorded and so the data were collected.

## Chapter 3: Characterising Phenotype

Surface sterile (appendix 2) seeds were positioned using a fine paintbrush onto a line 1 cm from one end of the dish; this indicated the zero position. The plates were sealed using para-film 'M' and placed at 4°C for 2 days. Cold storage during the imbibition period prior to germination will greatly increase the uniformity of germination of the seeds. After 2 days at 4°C the plates are stood vertically at 22°C to promote natural vertical growth, through gravitropism. Plates were sellotaped in pairs along one side to prevent them falling over; this still allows access to the side of the plates where growth will be marked. Growth was marked on what would be the bottom of the plate.

The root growth assay gives raw data for the growth of each seedling root over each 24h period. From the raw data two major characteristics were determined; the root growth rate and the total root growth for each of the genotypes tested. 4 Wild type (*col0*) and 4 mutant seeds were grown in each plate enabling paired analysis to be used, this allowed sufficient numbers for statistical analysis. Practically, this gave enough room for the seedlings to grow without too much competition for resources and space, additionally allowing the growing roots to be clearly observed.

### 3.4.2 Results

Five batches of paired RGA were conducted, from which, several graphs could be produced, figure 3.10: A, average root length and figure 3.10: B, the average root growth rate. The root growth rate was calculated at the mid-point of each 24-hour period. Figure 3.10: A, *sk5* and *mur1* show significantly shorter and slower growing roots when compared to *col0* and *IDA*.

After the initial experiment, it became clear that only the growth of the first root produced from the seed should be measured. Some of the mutant genotypes were observed to produce additional roots and increased lateral root growth later during the experiment. As this growth was difficult to accurately measure, the frequency of its occurrence was noted but measurements were not taken.

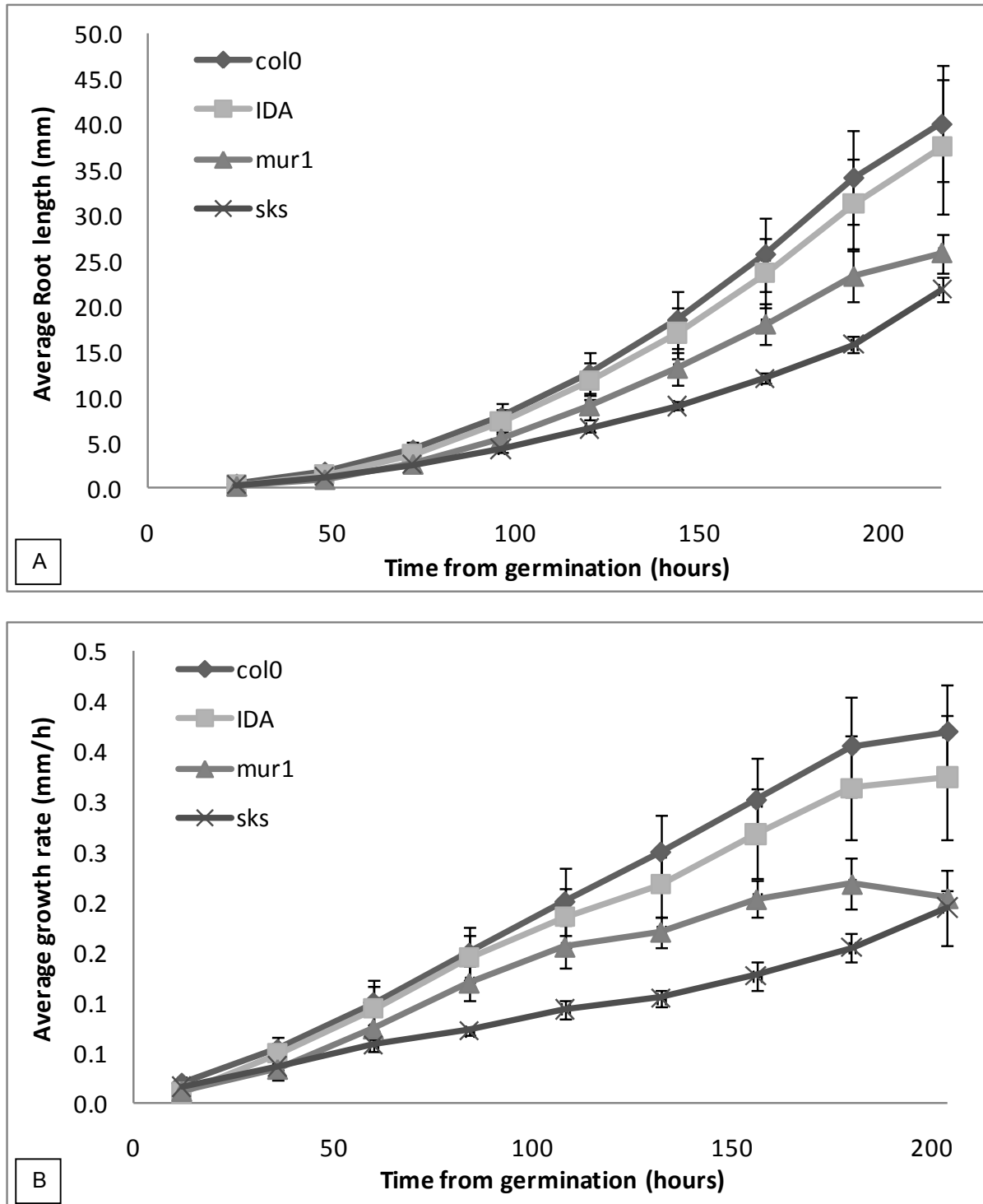
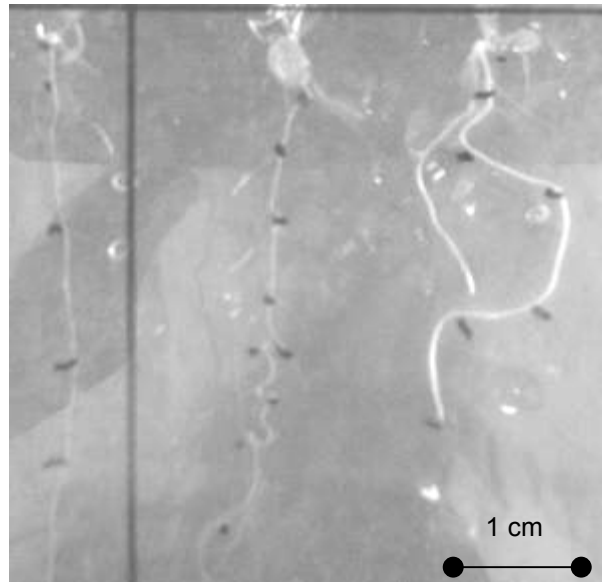


Figure 3.10: (A) shows the average root length of the four genotypes over the first 216 hours of growth. *sks* and *mur1* show statistically significant differences to *col0* from 120 hours and 216 hours respectively. (B) Shows the average root growth rate calculated at the mid-point of each of the 24-hour periods. The *sks* and *mur1* mutations show statistical significant differences to *col0* from 84 hours and 180 hours respectively ( $P > 0.05$ ). All error bars are the standard error. Results are taken from the averages of 5 sets of data 16 roots for each mutation paired with 16 *col0* (WT).



*Figure 3.11: shows an example of roots grown in the root growth assay. Three roots visible, the furthest left was a col0 root and the two right of the line were mur1. The second mur1 root to the right of the line demonstrates both root curved growth and adventitious root emergence, two additional growth processes that could not be accurately measured but may have affected the maximal root growth.*

### 3.4.3 Discussion

These findings support the data seen in section 3.2 concerning the growth of the shoots and roots, with the col0 and ida of comparable maximal growth of both root and shoot, followed by mur1 and finally sks. These results not only support the conclusion proposed in sections 3.2 and 3.3 but also enhances them. Despite the use of optimal growth conditions and the simplification of measurements using only one directional growth of the RGA showed similar results to those obtained in the investigation of plant growth characteristics (section 3.2). However, the RGA was more accurate and highlighted some additional differences. It showed that mur1 had significant shorter roots, unlike the PGC day 35 heights that show no significant differences. This evidence suggests that the mutations affect the entire organ not just local areas when concerning growth.

Speculating the causes of these results, it is possible that sks and mur1 have difficulty in maintaining turgor or during growth the walls react incorrectly to the increase in turgor pressure. The mur1 mutation affects the cross-linking of the cellulose fibrils in the primary wall. Changes in the ability of the fibres in the walls to be linked will affect the way in which it behaves during growth. In the case of the root system, the mutation causes a reduction in the maximal growth and growth rate significantly.

### Chapter 3: Characterising Phenotype

The *skt* mutation causes a reduction in total pectin present in the wall and its ability to crosslink, reducing the intercellular adhesion of the middle lamella. The results in figure 3.10 suggest that cell adhesion plays a prominent role in expansive growth. The changes in cell adhesion caused by the *skt* mutation may partially explain the differences seen in the growing roots (figure 3.11), which will be examined later.

With the addition of a time scale, the root growth assay allowed the acceleration of the root growth to be quantified as a rate. This rate was calculated for the mid-point of each 24-hour period. Figure 3.10: (B) shows the comparison of these rates, exhibiting a similar pattern to that seen in figure 3.10 (A). However, *ida* had a slightly lower growth rate than *col0*. It also showed *mur1* and *skt* to exhibit similar final rates. Towards the end of the experiment, the roots can be seen to reach a steady state growth rate, after approximately 150 h for all of the genotypes. This demonstrates that roots growth was no longer accelerating, but growing at a constant rate, ranging from approximately  $0.4\text{mmh}^{-1}$  for *col0* and  $0.2\text{mmh}^{-1}$  for *skt*.

As explained in section 2.9 primary plant growth is a combination of individual cell longitudinal expansion and the production of new cells from the apical meristem. Root growth rate is a combination of the two factors, but from the evidence from figure 3.10 alone it is not possible to suggest where the mutations were having the most effect. Cell expansion has been discussed earlier with the wall relaxing under the influence of turgor pressure to cause elongation. The weakness in the wall may cause the differences in growth due to the walls acting differently when the turgor pressure increases. The reduction in the pectin of *skt* may have an effect on cell adhesion. The pectin rich lamella will be severely affected by the *skt* mutation, reducing the strength of the cell-to-cell adhesion allowing the cells to move when under pressure of external forces. It has been shown that the epidermal cells of the 4-day-old roots detach (Mouille, et al 2007). This loss of cells and cell movement can explain the loss of overall length and slower growth rate.

The structure of the root systems was different between the genotypes. The *mur1* and *skt* produced tended to produce more adventitious roots when compared with the single primary root produced by *col0* and *IDA*. Adventitious growth occurs in nature as a method of taking advantage of an area of high concentration of desirable nutrients. To achieve this growth will be directed towards this area

in addition to the production of additional roots to maximise the uptake. Adventitious root emergence was approximately 40% for *sks* and 25% for *mur1* compared with 10%; figure 3.11 shows examples of normal *col0*, straight *mur1* and a curled root with adventitious root emergence. These adventitious roots are often all of shortened but equal lengths covering a large area of the media close to the zero line. This partially explains the differences in the overall lengths found in the root growth assay. Only the length of the primary root was recorded, any additional growth was omitted due to the changes in the method after the initial investigation. However the reason why the adventitious root emergence was so high in the mutants is the key to the reduction in root length. It is possible that this adventitious root emergence were analogous to the production of extra leaves seen in the PGCs. The plant may find it difficult to produce sufficiently long roots due to the effects of the mutations for adequate uptake. To counter this deficit, multiple roots are produced, which were individually shorter in length. The fact that this is purely advantageous feeding is possible, but this is unlikely. During the production of the media, it is stirred to aid in the dispersion of the nutrients evenly throughout. This homogeneity of the media will hopefully ensure the plants will not be influenced into adventitious feeding, as there will be no localisation in nutrient distribution. The *col0* and *ida* mutations do not produce large numbers of adventitious roots when grown on the same media, also suggesting that adventitious feeding is not the case.

The shape of the root systems of *mur1* and *sks* are different to the *col0* and *ida* pairing, as seen in the rosette leaves of the PGC in figures 3.1 and 3.2. Figure 3.11 shows an example of these curled non-straight roots. This too could have been explained by advantageous feeding, with the roots being directed to an area of the media with a high concentration of nutrients. However this is unlikely as figure 3.6 shows two roots of the same seedling next to one another, with one straight the other curved. It once again is likely to be a mutational effect, the *mur1* causing the weaker primary cell walls and *sks* due to the movement or loss of cells causing unequal expansion leading to curving.

### 3.4.4 Conclusions

From the evidence presented from the RGA it can be concluded that the mutations affect both root and shoot growth. This demonstrates that the *ida* mutation again has similarities to the *col0* in length, rate and root profiles. The *mur1* and *sks* however, show significantly shorter and slower growing

roots. The hemicellulose and pectin mutations appear to be causing the roots to develop at a slower rate and to a reduced maximum. This supports the evidence from section 3.2. It is possible that both may be responding to turgor pressure in different ways compared to the wild type. However the reason for this may affect the outcomes of future investigation. The *mur1* mutation affects hemicellulose, which is an essential component in the primary cell wall. It is this primary cell wall that is the major structural component of the cell wall. Therefore anything that would compromise its performance could be anticipated to cause a difference at the single cell level. The *sks* mutation affects pectin the main component in the middle lamella and therefore affects cell adhesion. The changes in growth profile seen to this point are caused by the reduction of cell adhesion. This region is not suspected of possessing any mechanical significance of the single cell wall. The reduction of pectin is therefore not anticipated to affect the intrinsic properties to be investigated (chapters 6 and 7) These two genotypes also had an increased tendency to form curved and/or adventitious roots. These changes to the root system only give a partial reason for the results presented in this section and therefore further investigation, as adventitious feeding must be discarded due to the homogeneity of the media and the frequency of occurrence.

### **3.5 Root Cell Length Profile (RCLP)**

As described in section 2.9, the process of plant cell expansion has two components, the production of new cells in the meristem and the elongation of these cells. The previous results in this chapter have demonstrated that mutations in the selected cell wall affecting genes had a variety of effects on the growing plant.

After highlighting the differences in root growth it was important to investigate the regions of the growing root. This was an effort to determine where the mutations were causing the differences seen in the growth measurements. By investigating the maximum longitudinal length of the cells along the root, it will be possible to separate influences of the two components of expansion. Through an approximation of the lengths of the zones (division, elongation and differentiation, (figure 2.8) enables the region in which the mutations have the greatest effect to be proposed.

### 3.5.1 Method

On the completion of the root growth assay experiments, the longest roots from each genotype of 20 plates was removed and placed in 70% ethanol. To measure cell length profiles, the root was first rehydrated and crushed by hand between a glass slide and a cover slip. The cell density in the tip required it to be further broken so that individual cells could be visualised (figure 3.12). The eyepiece graticule of a binocular microscope was calibrated with a 100  $\mu\text{m}$  slide graticule; this was then used to measure cell length away from the root tip. The first 250  $\mu\text{m}$  could not be measured due to the density of cells in the apical meristem. Initially measurements were taken every 125  $\mu\text{m}$  to allow for the rapid changes in cell length close to the meristem. The distance between measurements was increased to 250  $\mu\text{m}$  to allow for the rapidly expanding cells; this was to keep the areas measured defined as cell length increases as measuring every 125 was not possible as the cells expand. Towards the distal region of the elongation zone, the measurements were further extended to 500  $\mu\text{m}$ . Additionally, the length at which root hairs were first found was noted for each root. Figure 3.12 shows the region of measurement for the root cell length experiment, the cells in the root tip can be seen as it has been crushed to reveal them.

### 3.5.2 Results

From the raw data from the RCLP experiments the following graphs could be drawn, figure 3.12 the average root cell length at regular intervals moving away from the root tip, and the average distance to root hair emergence from the root tip, figure 3.13. The two figures represent the averages of three sets of 20 roots taken for the RGA plates.

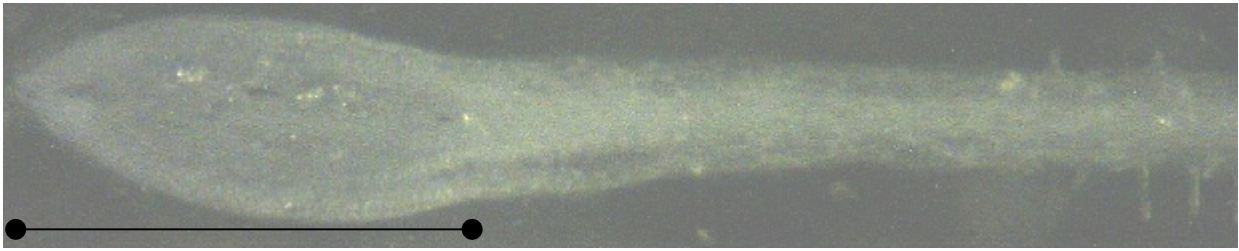


*Figure 3.12: The region over which the root cell lengths were measured. In the photograph, cells in the root tip can be seen (the area above the scale bar) as it had been crushed between the slide and coverslip to expose them. Root hairs can also be seen as they emerge towards the distal end of the root section shown. Scale bar is 1000 $\mu$ m.*

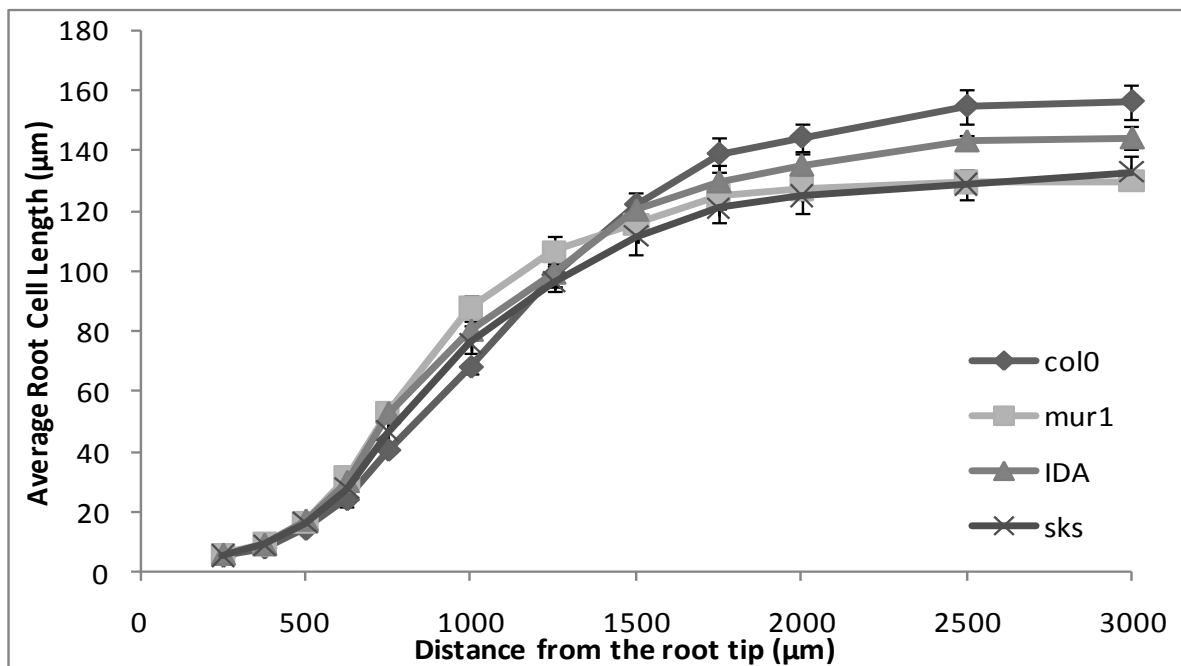


*Figure 3.13: the average root cell length moving away from the root tip. All error bars are shown as the standard error. Between 750 and 1000  $\mu$ m mur1, IDA and sks root cells are significantly longer than col0. After 1250  $\mu$ m col0 cells are significantly longer than sks and mur1, and from 1500  $\mu$ m significantly longer than IDA. From 2000  $\mu$ m IDA cells are significantly longer than mur1 and sks. ( $P > 0.05$ )*

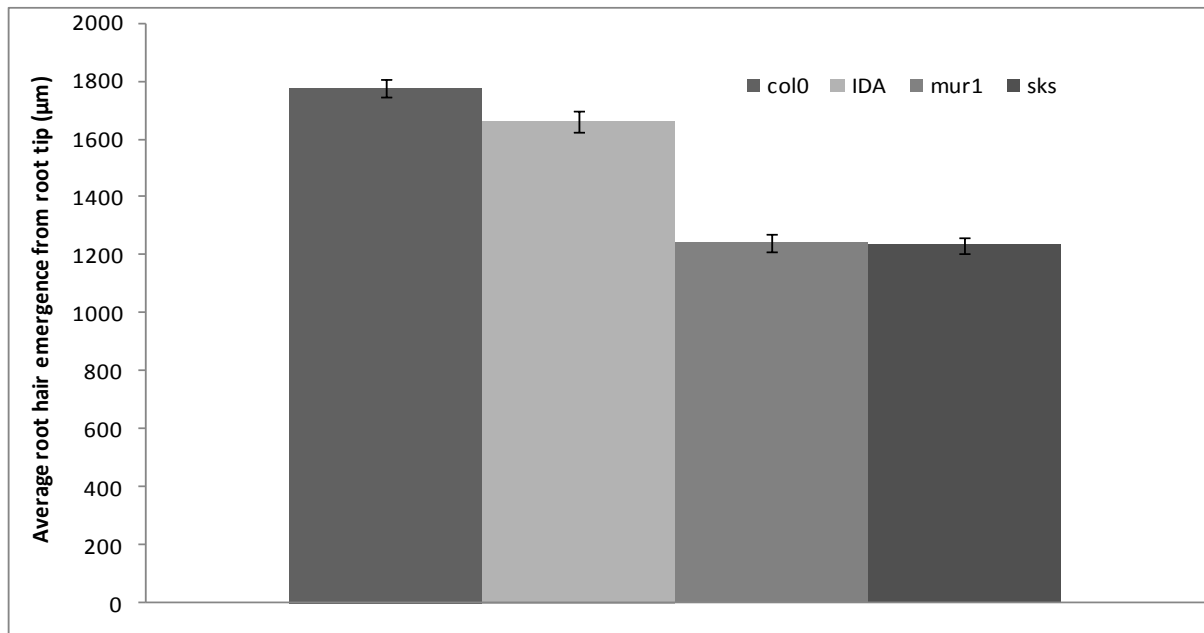


**Figure 3.14:** the average distance to the emergence of root hairs from the root tip. All error bars are shown as the standard error. Statistically *col0* and *IDA* show lateral root emergence further along the root than *sks* and *mur1*. ( $P > 0.05$ )

### 3.5.3 Discussion

From figure 3.13 the s-shaped curves for the four genotypes can be seen. Three distinct regions can be identified, cells exiting the zone of division and beginning to elongate, cells elongating and cells ceasing elongation and reaching a constant length. It is clear that there were differences between the four genotypes, with the mutant genotypes beginning to show deviation from the WT as early 500 µm. Statistically significant differences are not seen until 750 µm and 1000 µm for *ida* and *mur1*, with *sks* only at 1000 µm. This suggests that all mutant cells exiting the zone of division expand quicker, giving longer root cells in distal region of the root expansion zone of the mutants, in particular *mur1* when compared to *col0*. This could be due to the mutations allowing the cells to expand more easily and with less control when compared to the *col0*, where the cell walls show more control over the cell expansion. This regulation can be seen in the straight line that the *col0* exhibits between the initiation of elongation and the eventual deceleration. By 1250 µm there are no significant differences between the genotypes and 1500 µm the average cell length of *col0* has overtaken those of the mutants. By 1750 µm and onwards, the cell length of *sks* is significantly lower than *col0*, similarly, *ida* at 2500 µm and *mur1* after 2000 µm show significant differences. Cross-linking is much faster than fibre deposition, and from the RGA it was found that the growth rates of the genotypes varied greatly.

The *mur1* and *sks* mutations grew more slowly and the cells may spend more time elongating. It has been shown the elongation zone occurs between 500-2000  $\mu\text{m}$  behind the root tip, therefore *mur1* and *sks* cells may spend as much as twice as long in the elongation zone, giving significantly longer for these changes to happen. It is also possible that after this initial rapid expansion the increase in turgor pressure that causes the longitudinal expansion to occur at a faster rate than deposition. Overly extending the fibres in the wall before new fibres can be deposited which may result in the early deceleration (Boyer, 1988). Maintenance of turgor pressure is responsible for the continued elongation, with the *mur1* mutation affecting the primary cell wall possible may make the maintenance of turgor harder, the *sks* cells with reduced pectin therefore reduced cellular interactions not containing the cells and aiding in the maintenance of turgor.

By the end of the investigation, cells of all the genotypes have stopped elongating; therefore these cells must have moved in to the zone of differentiation. Figure 3.12 suggests that the mutations may have similar length elongation zones to *col0*, *mur1* stopping around 2000 $\mu\text{m}$ , and the others soon after. It would appear that factor that initiate elongation are positional not cellular, with the arresting of elongation similar regardless of genotype and therefore the size of cells that precede them. This sets the zone of elongation to the area between 500-2000  $\mu\text{m}$  after the root tip, giving the cells 1500  $\mu\text{m}$  to elongate before they are out of the region and no-longer influenced to do so.

The early cessation of expansion in the mutants may explain the results from the RGA. Each of the *col0* cells is approximately 25  $\mu\text{m}$  longer in length in the proximal region of the elongation zone than the root cells of *mur1* and *sks*. This significant difference explains the differences seen in root lengths when compared to *col0*, as the maximum length of the root cells is a major component in the overall length of the root itself. However the differences between *sks* and *mur1* in the RGA cannot be explained by the RCLP so other factors may be involved. The *ida* mutations show only small non-significant differences in the RGA, but after 2500  $\mu\text{m}$ , significant differences can be seen in the RCLP, confirming that other factors are involved.

One contributing factor is the transition into the zone of differentiation and the amount of energy being used. As described in previously in section 2.9, overlapping the proximal region of the zone of elongation is the zone of differentiation. This is where the root cell elongation slows and differentiation

begins, forming transport vessels, root hairs and lateral roots. To investigate the degree for which this overlap occurs, the emergence of root hairs was recorded. As an easily identifiable external marker, the root hair emergence was used to identify the start of this overlap. The cessation of elongation leading to cell of constant length seen in 3.12 taken to be the end of the elongation zone. Figure 3.13 shows that *mur1* and *sk5* begin to produce root hairs significantly earlier than *col0* and *ida*. However there are once again no differences between *col0* and *ida* or *mur1* and *sk5*, so this is not the extra factor causing the differences between RGA and RCLP results discussed previously in this section. The emergence of root hairs does however correspond approximately with the beginning of the cessation of root cell elongation seen in 3.12. Suggesting that the overlap between regions is large, thus reducing the total length devoted solely to elongation to as little as 1000µm in the case of *mur1*.

### 3.5.4 Conclusions

It can be concluded that the mutations caused a different elongation profile to that of *col0*, where the inability to respond to increases in turgor cause rapid expansion. This rapid expansion may cause a change in cell wall properties leading to a reduction in the maximum cell length and subsequently shorter overall root length. In addition to this, the emergence of root hairs identifies the region of deceleration in elongation as roots begin to differentiate reducing energy available for elongation and changes in the wall preventing elongation. The root cells therefore have approximately 1000 µm in which their sole purpose is to expand before they enter the zone of differentiation. Meaning that the time available for each cell to expand is limited, therefore altering the maximum length to which they can grow. The cause of the differences between the two pairs of *col0* and *ida*, and *mur1* and *sk5* can therefore be inferred, however this does not suggest a reason for the small differences between the pairs. The only other factor that could affect this is the rate of cellular production from the meristem.

## 3.6 Chapter Conclusion

Table 3.1 contains a summary of the main point from the chapter.

	col0	ida	mur1	sk5	general observations
PGC	Significant differences too many aspects of the investigation when compared to <i>mur1</i> and <i>sk5</i> , e.g. early to germination and flowering, much higher stems and wider rosettes.	Similar to col0 throughout the investigation, <i>ida</i> mutation appears to have little or no effect on aerial growth.	Between the col0/ <i>ida</i> results and <i>sk5</i> , although still shows significant differences.	Severe effects of plants growth, with stunted growth and morphological changes drastically. Interestingly plants produce additional rosette and cauline leaves.	Enables the genotypes to be grouped col0/ <i>ida</i> and <i>mur1/sk5</i> . Both groups exhibit similar phenotypes despite phenotypic differences.
FW:DW	Preliminary data suggests the mutations affect the amounts of polysaccharide present in the wall. Warrants a more sensitive investigation in an attempt to determine the effects on the presence of each component in the wall of each genotype.				Gradual reduction in moisture content on the plants evidence to suggest that the plant go through maturation process whereby more material is deposited.
RGA	Show significantly longer and faster growing roots compared with <i>mur1</i> and <i>sk5</i> .	Similar to col0 throughout the investigation, <i>ida</i> mutation appears to have a slight affect on the root growth however nothing significant.	Both <i>mur1</i> and <i>sk5</i> show significant reductions in growth rate and length. Adventitious root growth more prominent, similar to the additional leaves in PGC.		Results show the same pattern as seen in the PGC.
RCLP	Initially shows a reduced cell length compare with the other three genotypes in the proximal region of the elongation zone. Distal cells expand significantly longer than all three mutations. Root hairs emerge further from the root tip compared with <i>mur1</i> and <i>sk5</i> .	Mutation appears to cause the root cells in a manner between that of col0 and the other two mutations. Root hairs emerge at a similar distance to those of the col0	Show significantly faster expansion in proximal cells in the expansion zone. However by the time expansion had ceased, both col0 and <i>ida</i> show significantly longer root cells. Root hair emergence is much earlier than the other two genotypes.		Results suggest the zone of elongation of all genotypes is approximately 1000 $\mu\text{m}$
General Observations	As the control show the features by which the cell wall mutations are to be measured	<i>ida</i> is known to affect a small region of the plant, and therefore has little general affect.	Often exhibits reductions compared with col0/ <i>ida</i> , however not as severe as <i>sk5</i> .	The most severe reduction is the majority of the phenotypic tests.	As a preliminary investigation shows a variety of phenotypic differences are caused. Results suggest that the more sensitive investigation will yield interesting information.

## ***Chapter 4: Optimising Arabidopsis thaliana Cell Suspension Cultures for the Generation of Single Cells.***

---

To facilitate investigation of the mechanical properties of individual plant cells, suspension cultures were produced. Ideally, single spherical viable plant cells are required for use with the microcompression technique (chapter 6) and for the investigation of wall thickness (chapter 7). Suspension cultures are also required for the biochemical analysis (chapter 5) but the generation of single cells is not necessarily required. Previous studies have used tomato cells as a simple system to generate a large number of single cells. The limited genetic background for tomato plants necessitated changing to *Arabidopsis thaliana* as an experimental system. Section 2.13 discusses the benefits of the use of *Arabidopsis*.

There are many potential methods to generate single cells, however all have potential problems. Enzymatic treatments, mechanical grinding or physically pulling the cells apart would damage the walls, compromising the viability of the cells (Naill and Roberts, 2004). Therefore a more subtle approach was designed to minimise damage and maintaining cell integrity, whilst providing sufficient material for the investigation

Work done previously with tomato cells utilised a suspension culture technique (chapter 2.12) to facilitate the generation of the single cells (Blewett et al., 2000). This involved the growth of the cells in liquid media, which were perturbed by constant orbital agitation. Cells in suspension cultures have reduced packing density compared with plant cells due to the relatively large space in the experimental system. Increased movement by agitation may help reduce the cellular contact producing more single cells.

One major problem exists with the use of cultured cells. The investigation of the mechanical properties of these cells assumes that cultured cells, in particular the proportion that are seen to be

single are representative of the population of cells in the plant. Ensuring that relevance is maintained from plant cells to those in culture was paramount to the project.

#### **4.1 Initiation of Cellular Suspension Cultures**

The culturing of plant cells in an artificial system is a multi-stage process, starting with the seeds that were generated in chapter 3. The maintenance of the sterile environment was paramount for the success of the experiment. Using flow hoods, aseptic technique autoclaves etc. to minimize the risk of infection (Axelos *et. al.*, 1992).

##### **4.1.1 Seed Surface Sterilisation**

Seeds were first sterilized by two methods, Sodium hypochlorite and desiccation. For the methods see appendix 2.

##### **4.1.2 Investigation of Optimum Explant location**

In the literature, there are several methods of producing plant cell suspension cultures; all are multi-stage processes conducted on sterile solid and liquid media. However the composition of the media and the possible regions from which to take the tissue as donors for cells for the cultures were not consistent. The donor cells are known as the explant. Without a defined protocol no cultures can be produced with confidence. Before large volumes of cultured cells were produced, an investigation to optimise the process of producing *Arabidopsis* suspension cultures was conducted.

The investigation optimised explant source and media composition. Root, shoot and callus cell types were tested simultaneously. In addition to this, cell types regenerated from callus will be tested to ensure purity. Due to the near impossibility of isolating pure undifferentiated cells, the callus in this experiment will be grow directly from the roots and shoots of the seedlings. Calluses are regions of undifferentiated cells, created by influencing gene expression producing totipotent cells. This is called the acquisition of competence, with the reversal of previous differentiation to the totipotent state. This

means that given the correct combination of growth factors the callus cells can be committed to take on any cell fate.

### 4.1.3 Germination

The surface sterilized seeds were germinated under sterile conditions to produce seedling for the next stage of the process. The germination media used composed of: 4.33 gL<sup>-1</sup> MS medium with Gamborg's vitamins, 30 gL<sup>-1</sup> sucrose, 0.2 gL<sup>-1</sup> myoinositol, this solution is then adjusted to pH 5.7 (using 1M HCl or 1M KOH). 8 gL<sup>-1</sup> tissue culture grade agar was then added and then autoclaved. Myoinositol is a lipid compound added to media to maintain membrane integrity. Once cooled, in a flow hood the media was poured into sterile circular petri dishes and allowed to set. The surface sterilised seeds were sown on the media and the dishes sealed with para-film. These were placed in the growth room at 22<sup>o</sup>C with constant light and grown for 1-2 weeks (Encina, *et. al.*, 2001).

### 4.1.4 Media Compositions for Explant Investigation

This next stage of the process is where the seedlings from germination all transferred to fresh media specific for the cell type required. Unfortunately there was not an established protocol found in the literature. Three cell types are suggested for the generation of suspension cultures root, shoot and callus cells. To investigate the optimum cell type, large amounts of callus was grown. Samples of the callus tissue were transferred to growth media optimised for the specific for one of the three cell types. The aim of the cell specific media was to maximise the number of cells available and ensure the purity of cell type. Once sufficient callus material has been grown shoot and roots will then be regenerated this will guarantee the cells to be of the desired type. This method of tissue regeneration exploits the totipotency of the callus cells, allowing masses of terminally differentiated cells (root and shoot) to be generated that are required for the next stage in the process.

#### 4.1.5 Composition of the Root Induction Media (RIM)

To induce the differentiation of cells into root cells they required an increased level of auxin, see chapter 2.11.1. Thus the RIM was supplemented with an elevated level of hormones from the auxin family (Valvekens, *et. al.*, 1988) . RIM as germination media with:  $1 \text{ mgL}^{-1}$  Indole acetic acid (IAA),  $0.2 \text{ mgL}^{-1}$  Indole-3-butyric acid (IBA) and  $0.2 \text{ mgL}^{-1}$  Kinetin. The growth regulators (GRs) were added to the solution prior to pH adjustment.

#### 4.1.6 Composition of the Shoot Induction Media (SIM)

To induce the differentiation of cells into shoot cells they require an increased level of cytokinin chapter 2.11.2, thus the SIM will be supplemented with elevated levels of Cytokinin type hormones (Cary, *et. al.*, 2006). SIM as germination media with:  $2 \text{ mgL}^{-1}$  6-( $\gamma$ -dimethylallylamino)purine (IPAR) and  $0.2 \text{ mgL}^{-1}$  Napthalene Acetic Acid (NAA). The GRs were added to the solution prior to pH adjustment.

#### 4.1.7 Composition of the Callus Induction Media (CIM)

The third cell type that was investigated was callus. A callus is a region of viable undifferentiated cells, known as totipotent cells. This totipotency enables cells to take on any cell fate if given the correct chemical stimuli. Transferring the root cuttings to a CIM causes the cells to acquire competence, demonstrated as the ability of existing cells returning to an undifferentiated state, while nacent cells will remain totipotent, remaining undifferentiated

The potency and availability of the GRs needs to be closely controlled. To induce the sections to form calluses they require approximately equal amounts of both auxin and cytokinin. CIM as germination media with:  $0.5 \text{ mgL}^{-1}$  Benzylaminopurine (BAP),  $1 \text{ mgL}^{-1}$  NAA,  $1 \text{ mgL}^{-1}$  IAA and  $1 \text{ mgL}^{-1}$  2,4-Dichlorophenoxyacetic acid (2,4-D). The GRs were added to the solution prior to pH adjustment (Encina, *et. al.*,2001).

The seedlings were first grown for 1-2 weeks on a germination medium then transferred to CIM for another 1-2 weeks to further their development. Explants acquire competence during the first growth

period on the CIM. This allows the cells time to respond to the growth regulators which have been added to the media (Howell et al., 2003). After this period, the cell material was finely cut, and transferred to RIM, SIM or CIM. The samples are finely cut to invoke a wounding response that leads to rapid cytogenesis. This stage commits the undifferentiated cells to the desired cell fate. The samples were grown for 4 weeks (Che et al., 2006). This process is shown in Figure 4.1.

#### 4.1.8 Liquid Culture

After the final growth period on solid agar, the tissue that had been grown was used to initiate the suspension cultures. Approximately 1g of callus tissue was placed into a 250 ml conical flask containing 50 ml of liquid culture medium (LCM) (Encina, et al., 2001). LCM was identical to the solid versions with the exception of the agar, which was withheld. The cellular masses were finely cut; placed into LCM and rotated at 120 revolutions per minute (rpm) on an orbital shaker. The literature suggests speeds between 80-120 rpm. It was decided that the maximum speed of rotary motion would be used for several reasons; the rotation may aid the production of the single cells, the movement will gently aid the separation of any weak intercellular contact between the loosely aggregated cells; it is also necessary to allow adequate access to all the components in the media especially the GRs, as these maintain the callus growth and suppress any differentiation.

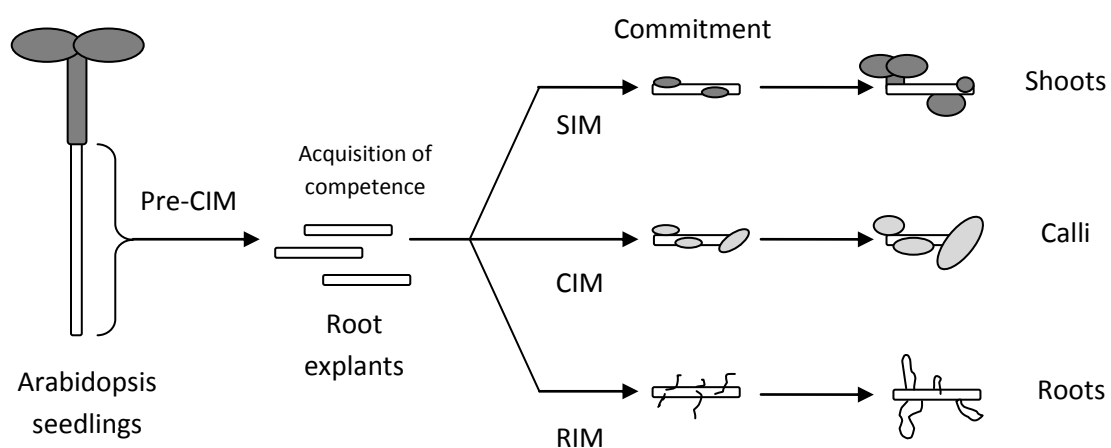


**Figure 4.1:** The protocol for producing the explant material by tissue regeneration. These regenerated tissues were tested to discover the optimum explant for the initiation of the suspension cultures. Liquid cultures were inoculated with similar amount of tissue and the numbers of single cells produced were scored. The results of this investigation can be seen in figure 4.3 (Adapted from Che et.al. 2006).

## **4.2 Maintenance**

Once the cultures had been initiated, constant maintenance was required. This was to ensure that the cultures remain viable. This involves daily monitoring checking for infection and monthly sub-culturing. This required taking a sample from the existing culture and combining it with an amount of fresh liquid (e.g. 25 ml existing culture and 25 ml fresh media). This procedure replenishes the cells with all the nutrients that they require as well as the growth regulators to continue to influence their differentiation and it also removes some of the toxins excreted by the cells that could be hazardous if allowed to accumulate.

## **4.3 Callus Reserve**

When initiating the liquid cultures, samples of callus cells were not transferred to the liquid medium. Instead were placed onto fresh solid CIM. This callus stock was maintained by monthly sub-culturing onto fresh media. Keeping a reserve of callus growing on solid media was beneficial in many ways. The convenience of not having to re-start the culture process from the beginning if a batch becomes infected or a new batch is required will be very beneficial. As the callus is sterile and grown under the same conditions as those before, it is ready to use immediately with as little variation as possible.

## **4.4 Quantifying Cell Culture Composition**

Quantifying the effect of varying the conditions on the cultures was essential to assessing the process. Cell culture is often quantified using flowcytometry, especially with yeast or bacterial cells (chapter 8.2.1). However, the large cellular aggregates in the *Arabidopsis* cultures would block the system rendering it useless. Therefore a more robust method was utilised. The haemocytometer is a microscope slide adapted for cell counting, containing a shallow well with a calibrated grid on the base of the well for cell counts. To calculate the quantity of each type of aggregation (single/aggregate) was contained within each ml of culture, an average of the four corner quadrants of the grid was taken then multiplied by 1000. This was completed in triplicate for each sample. This method was used to compare the cultures, allowing aggregates contained in these samples to also be measured and the

numbers of cells counted. This is the main advantage of this method over flowcytometry. Additionally, through the calibration of the eyepiece graticule the diameters of the cells in the cultures can be observed. These value can be used to estimate the total number of cells in the entire culture assuming that the samples are representative of the culture.

### **4.5 Cell Viability**

The cultures that have been produced contain many spherical bodies that may be single living cells. For the actual number of viable single cells the live cells must be distinguished from the dead.

Stains are often used to indicate the viability of cells in culture. Neutral Red (NR) is a viability stain that is taken up in to the vacuoles of viable cells; it does not bind to plant cell walls of both viable and non-viable cells (Dubrovvsky, *et.al.*, 2006. NR was added to each sample to a final concentration of  $1 \times 10^{-4}$  M, 2 hours prior to counting. This is sufficient stain to make the viable cells noticeable and low enough not to raise any toxicological issues.

### **4.6 Likely Problems to be Encountered**

Tissue culture is a very important area of biological sciences, but there are many inherent problems with the techniques. There was a high possibility of infection at every step of the process, due to the warm, humid and nutrient rich environments that the culture flasks and plates provide. For the investigations to be halted due to contamination as insufficient tissue was unavailable would be a costly error. Initially, this occurred with a high frequency with large numbers of the cultures that were initiated becoming infected. These had to be discarded as the relivance of the cells contain in the culture would be compromised. The use of antibiotic and antifungal agents were rejected, as whether they would affect the cell wall could not be confirmed. However as aseptic and culturing techniques were improved the infection rate was greatly reduced. Increasing the number of replicates to a minimum of three for each sample also It was these infection that caused the need for a reserve of callus cells on solid media.

## 4.7 Results

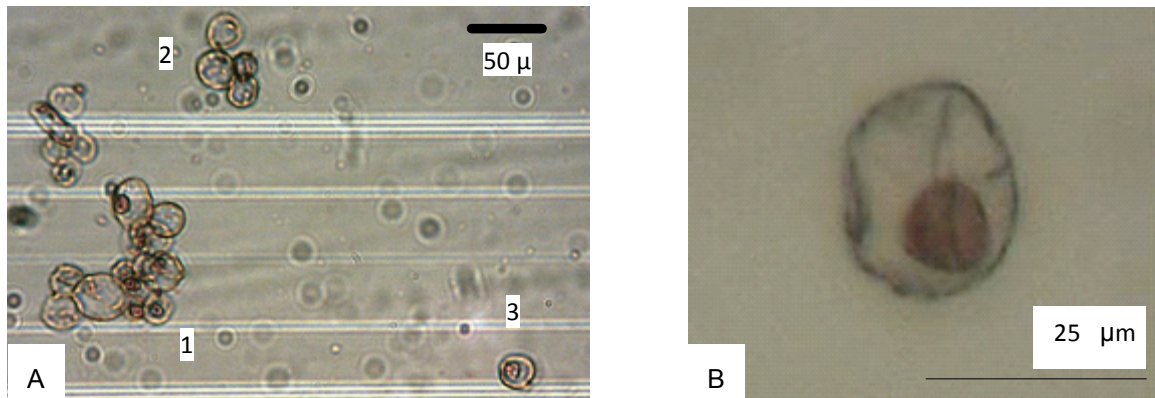


*Figure 4.2: samples cultured cells stained with NR protocol. (A) Examples of 3 different categories of cell class large cell aggregate (1); small cell aggregate (2) and single cell (3). Similar diameters of single cells and individual cells in the aggregates can be seen. (B) Gives an enlarged example of a single cell stained with NR. NR proves the cell is viable as only the vacuole is stained*

Using the quantitative analysis of the NR and haemocytometer, the culturing process was scored at each level. In addition to this, equal numbers of cultures were initially grown in dark conditions to investigate the effects of light on the growth of the cultures and therefore single cell production. Figure 4.2 shows examples of NR stained cells.

Using the haemocytometer the numbers of single cells, small aggregates (between 2 and 10 cells) and large aggregates (>10 cells), were counted. The total number of cells in the culture could be calculated. From this total an estimate of the percentage that were single cells was made. The diameters of the cells in these categories will also be compared, to ascertain the relevance of the single cells to the rest of the population.

### 4.7.1 Explant which Produces the Highest Number of Single Cells

The investigation into explant choice yielded some interesting results. Figure 4.3 shows the results of an investigation into the effects of single cell production by three different explants of the WT. In addition to this, the effects of the presence or absence of light during the growth period was also

investigated. To investigate the effects of the absence of light, flasks were wrapped in foil to allow them to be placed on the orbital shaker next to the light grown ones. It can be seen that the location of the explant has a significant effect on the number of single cells produced. However the explant showed little effect on the dark grown cultures, with callus; root and shoot cells produced similar numbers of single cells. It is possible that the absence of light affects the developmental state in which the cells, changing the gene activation profile when compared with the light grown samples.

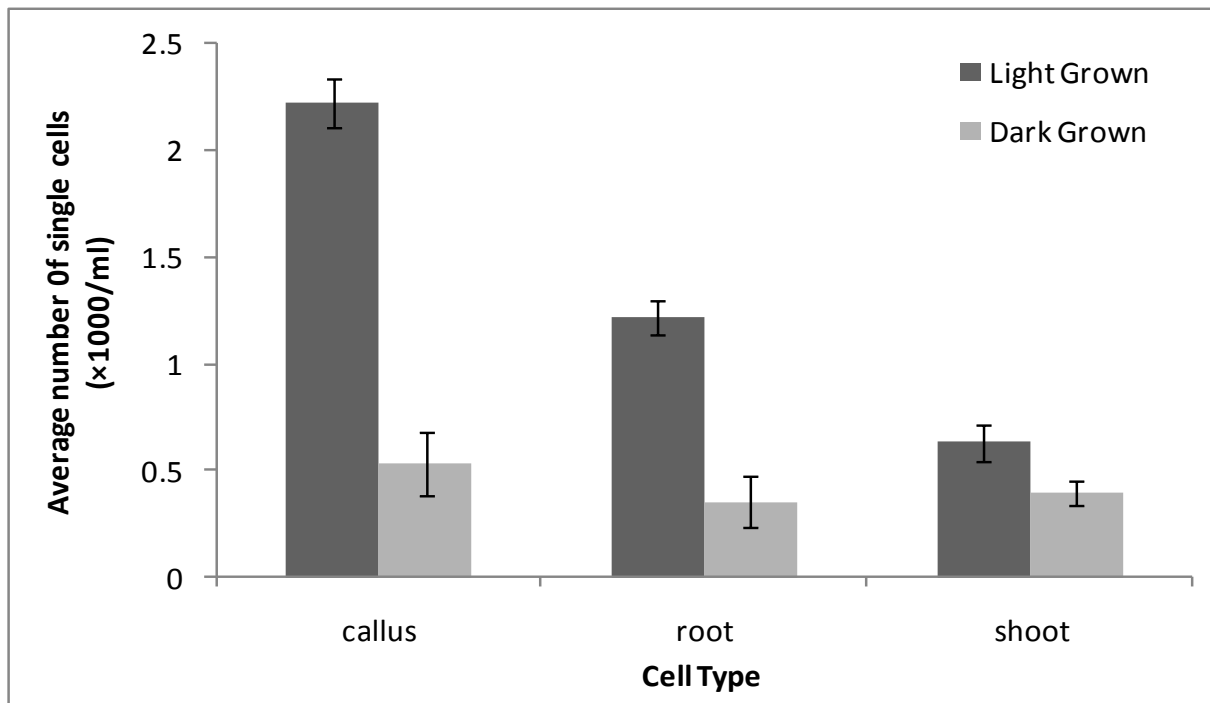


**Figure 4.3:** Shows the average number of single cells generated from different explants of two-week-old *col0* cultures. Also shown is the effect of absence of light. As the cells have been subjected to the same conditions throughout the growth phases, all other variables have been standardised allowing paired analysis. Callus cells generate significantly more single cells than either root or shoot cells, with root cells also showing a significant increase over shoot cells. All cell types show a significant difference when the dark and light grown samples were compared. ( $P > 0.05$ )

## Chapter 4: Suspension Cultures

When the two data sets are compared there are significant differences. The light grown cultures show a significantly higher level than the dark grown cultures. When the light grown cultures are compared to each other, callus cells show a significantly higher number of single cells than root and shoot type cells. Root cultures also show significantly higher levels of single cells compared with shoot samples. These data suggest that both the explant and light availability have an effect on the single cell production, with light grown callus the apparent optimum. It must be remembered that this is not a proportion of the total cell count however, but the objective of this investigation is to discover the optimum conditions for the production of single cells.

Figure 4.4 shows the pH profile of a set of cultures over the first three weeks. It can be seen that the pH of the culture is not affected little by its age, nor by the genotype of cells it contains. The external medium is set to pH 5.6 when the medium is made; this is to encourage the disassociation of the loosely bound callus cells by acidic creep in the walls (section 2.9.2.1). This paired with the motion of the orbital shaker will generate the single cells required. The profiles of the cultures shown in figure 4.4 suggest that despite minor fluctuations the pH stays around 5.6.

One of the main concerns of using single cells is how well they represent the population. If it cannot be said that the single cells are representative of the whole population, then it will not be as easy to justify them as a model system. Figure 4.5 shows that the percentage of single cells of the whole population. The *sks* cultures show the highest proportion of single cells produced, reaching a plateau of approximately 4.5% after 7 days. This increase in the number of single cells produced by the *sks* cultures is likely to have been caused by the reduction of pectin in the walls. This reduction of pectin caused reduced cell-to-cell adhesion between the cells in the aggregates resulting in the increased number of single cells.

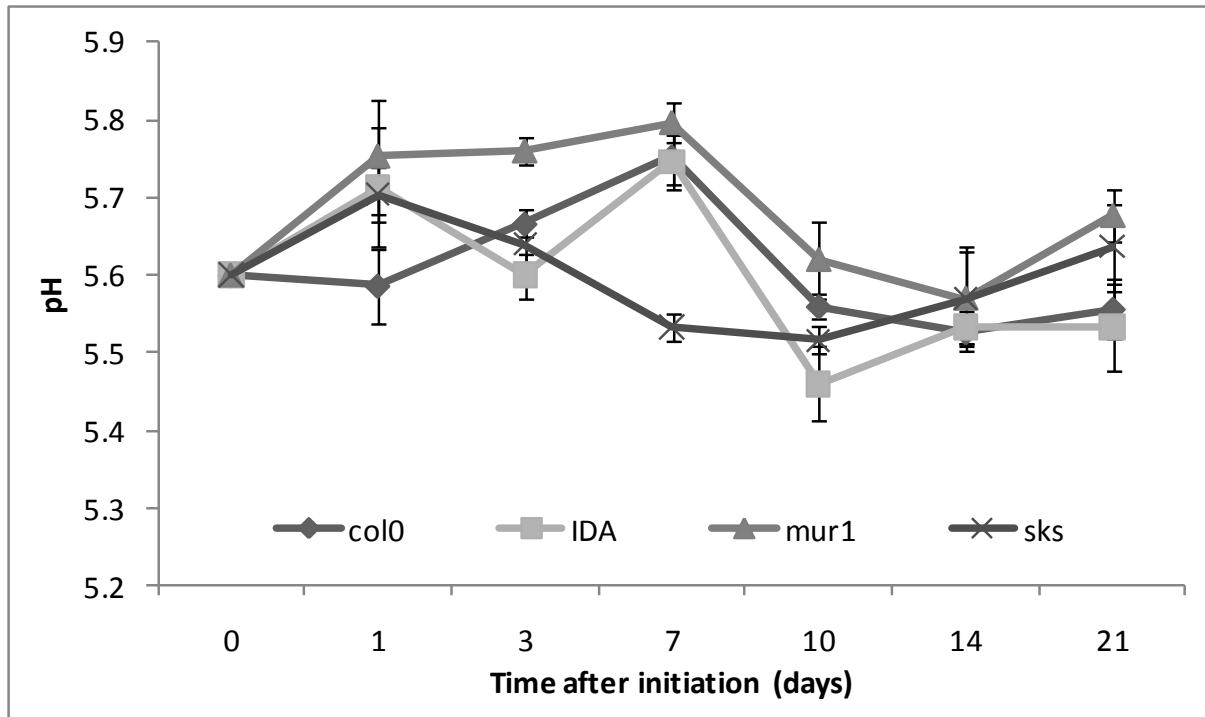


Figure 4.4: shows the fluctuations of pH of the suspension cultures for 21 days after initiation. This was seen as the life of a culture as sub-culturing was done at 28 days. Each genotype has error bars representing the standard error.

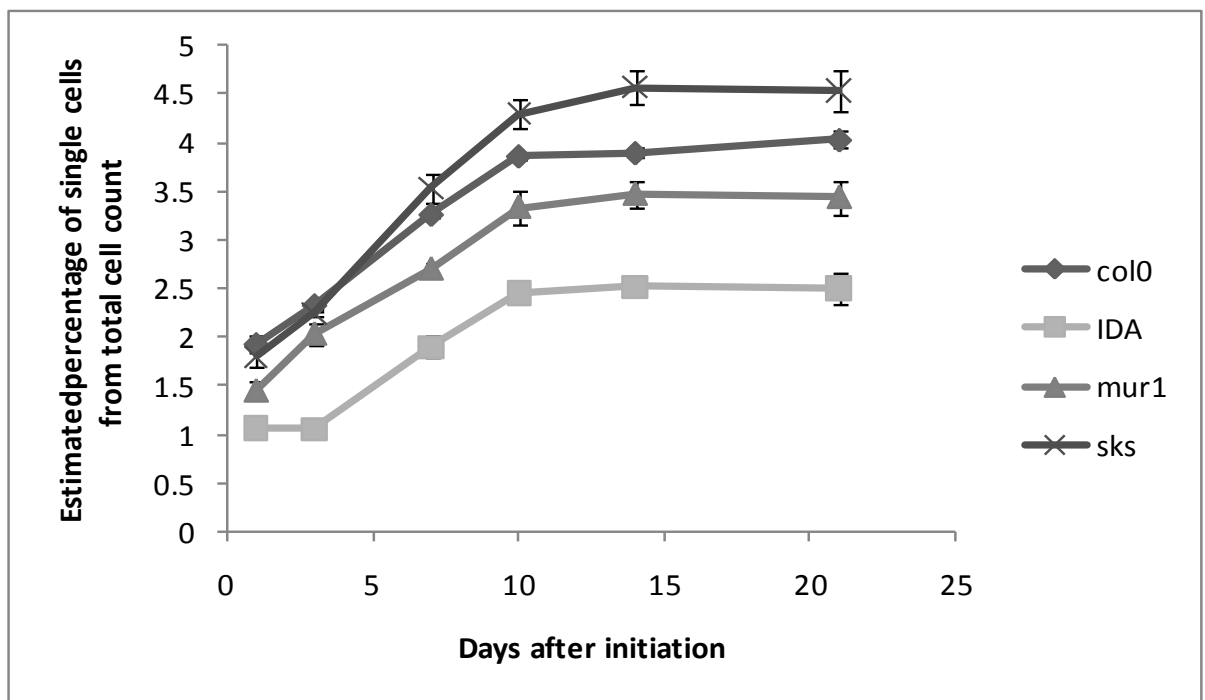
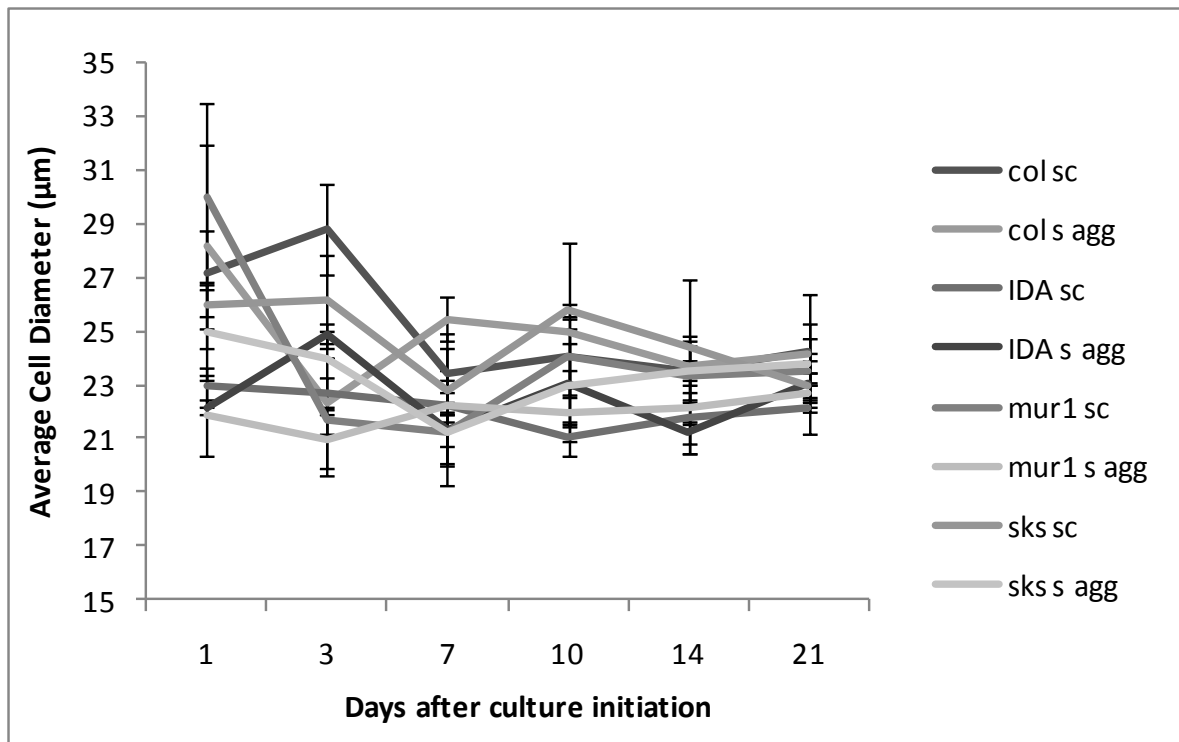


Figure 4.5: shows the number of viable single cells as a percentage of an estimated total cell count. The number of cells in the large aggregates was very difficult to measure correctly. Therefore an estimate for the cell number for each large aggregate was made based on size, shape and density. Error bars represent the standard error. The ida mutation shows significantly lower levels of all genotypes throughout the experiment. sks and col0 are significantly higher than mur1 from day 7. The sks mutation has a significantly higher percentage of single cells from day 10, presumably caused by the reduction of cell-to-cell adhesion as a result of the mutation ( $P > 0.05$ ).

A similar pattern is seen with the other genotypes but at a lower level. The *ida* mutation shows significantly lower percentage single cells when compared with all of the other genotypes throughout the experiment. Although this is a fairly low percentage compared to that found with the tomato cells used previously, as the percentage of single cells increases to over 10% between 21-28 days. Unlike the *Arabidopsis* cells which appear to plateau after 15 days. However, it must be remembered that these are estimated figures as viable whole cell counts of aggregated cells is near impossible.

It is possible to examine the sizes of the cells in the population to compare the single cells to those of the individual cells in the aggregates. Samples of each genotype were stained using NR at various time points during the first three weeks of growth. The diameters of the viable single cells and those in the small aggregates were measured.



**Figure 4.6:** shows the average diameters of the single cells and cells contained within the small aggregates. Each point has an error bar represented by the standard deviation. No significant differences can be seen between the either of the cell states or genotypes. Cell diameters for all genotypes and cell state appear to be converging at an average diameter of 25 µm. Error bars represent standard error.

Figure 4.6 shows a comparison of those measurements. No significant differences for the diameter of the single cells to those in the small aggregates can be seen at any point during of the investigation or for any of the genotypes. This means that the walls of the single cells may be affecting the spherical expansion in similar ways to those in the small aggregates. Over the course of the experiment there appears to be a convergence of all the cell diameters to approximately 25  $\mu\text{m}$ .

The figures for the large aggregates are not shown because it was difficult to measure the diameters due to cell density. Therefore an accurate average could not be determined. Observations of the cells on the exterior of the large aggregates show similarities to those in the small aggregates. This may be due to the lower cellular density, which is similar to the small aggregates, hence the similarity in size.

### 4.7.2 Media investigation

The callus media used for the previous investigations was chosen as it reflected the balance between Auxin and Cytokinin that is required for callus development. However it is important to test others, to prove it is optimum. A second callus media was chosen to be trialled against the first, using a different combination of growth regulators. The medium composed of MS medium 4.4  $\text{gL}^{-1}$ ; Sucrose 30  $\text{gL}^{-1}$ ; Kinetin 0.25  $\text{mgL}^{-1}$ ; NAA 2.0  $\text{mgL}^{-1}$ ; adjust to pH 5.7 Agar 8.0  $\text{gL}^{-1}$  and autoclave. The GR's in the second as mostly different compared to the first, allowing further comparison. However, when root sections were placed onto samples of each media, those on the second media took twice as long to reach a usable size. It was therefore decided that this media would not be suitable and the original would be used. This lack of growth can be attributed to the differences in the growth regulators, possibly not in the correct ratio, or weaker ones reducing the number of cellular divisions.

### 4.8 Discussion

Previous research into the mechanical properties of plant cell walls used suspension cultures cells derived from tomato tissue. (Blewett, *et. al.*, 2000) To apply these methods to the *Arabidopsis* cells it was important to provide samples of single, viable and spherical cells that are representative of the whole population. Ideally cells could be tested *in-situ* or fresh single cells removed from the plant,

## Chapter 4: Suspension Cultures

however this option was not available. To remove cells by mechanical or chemical means would reduce the relevance of the data due to wall damage. The use of suspension cultures is required to generate the single cells, as it is a gradual process, decreasing wall damage increasing the survivability of the single cells.

Over the course of this chapter, the methods of single cell generation by suspension culture techniques were optimised. It was important to establish a standardised protocol that will reliably generate a quantity of cells that can be used for compression. Using a standardised protocol allowed for more thorough statistical analysis. This enabled stronger conclusions to be drawn. Media composition, explant and light conditions were all investigated to determine the relative effect on single cell production. It was interesting to see the degree of variability caused by the different conditions. It was assumed that the changes would cause differences in the number of single cells produced, clearly demonstrated by investigating the affects of the presence or absence of light (figure 4.3)

Ideally the percentage of single cells in the population would have been much higher. A higher percentage would have automatically shown the relevance of the single cells produced to the *in-situ* cells. Initially the failure to produce a high percentage of single cells was disappointing. From figure 4.5, it can be observed the genotypes have an effect on single cell percentage. The *sk5* mutation produces the highest proportion of single cells and *ida* cells the lowest. The *sk5* mutation causes a reduction of total pectin and its ability of form cross-links. This reduction combined with the other factors affecting (e.g. motion and space) provided the perfect circumstance for single cell production. However, the *ida* mutation produces approximately half of the single cells when compared to *sk5*. The mutation appears to be able resist the culturing effects and produce a smaller number of single cells. This may be due to a change in the wall biochemistry. The mutation affects the abscission of the plant, usually attributed to the flowering regions. This is a highly specific mutation that may not be active in the cultured cells. In the opposite way to *sk5*, increased cross-linking or additional polysaccharide may reduce separation. This reduction limits the number of cells available for compression that may prove problematic.

When the diameters of SCs to those in the individual cells contained within the small aggregates of each genotype no differences could be seen (figure 4.6). The average size of the SCs was

approximately 25  $\mu\text{m}$ , which is comparable to the average size for a cell in the plant was around 30  $\mu\text{m}$ . This similarity in size, confirms the removal of any influences of growth, establishing the analysis of single cells from a suspension culture as a viable way to investigate the intrinsic mechanical properties of the plant cell wall. Additionally, single cell production by this protocol was reliable despite its low yield. It also proved sufficient material for regular compression testing,

The method established over the course of these investigations has been proven to produce the requisite material for compression testing. The process could have been continually refined, an increase in SC yield or reduce culture time would have been beneficial. However, establishing this protocol was a time consuming process. Alternatives and variation were tried and found to be sub-optimal. Therefore it was decided to use the method, rejecting further refinement, as benefits would not reflect the time invested.

### **4.9 Conclusions**

The objective was to produce a reproducible protocol for the generation of single *Arabidopsis* cells for compression analysis. It can be concluded from the evidence presented in this chapter that this objective has been achieved. Despite the low levels of the single cells produced the protocol reliably produces the desired cell types. The single cells appear to be representative of the cells contained in the aggregated cell clusters in dimension, and the average diameter is similar to an overall average for the plant cells. As the cells for the genotypes show no differences in cell diameter, the effects of growth may have been removed by culturing. Therefore the differences in the single cell production can be attributed to biochemical differences in the wall properties, which in turn are caused by the mutations. It is these changes in biochemical composition that have been investigated in chapter 5.

## ***Chapter 5: The Biochemical Analysis of the Polysaccharide Composition of the Arabidopsis thaliana Primary Cell Wall***

---

Evidence has been presented in chapter 3 to show the mutations in cell wall genes have an effect on growth. Differences in single cell production in chapter 4 suggest that the composition of the wall is causing the genotypes to separate in different proportions. Chapter 2.4 discussed the properties of the fibres that make up the plant cell wall (McCann *et al.*, 1992). The three main components of the *Arabidopsis* cell wall are pectin, hemicellulose and cellulose. The levels of these polysaccharides may be affected by the mutations, causing or contributing these growth differences. Col0 is the wild type, *sk5* has reduced pectin, *ida* affects the abscission regions and *mur1* affects the biosynthesis of a hemicellulose precursor. More specific information is required to compare the mutations, both in plants and culture (Zabackis, *et al.*, 1995). It is important to investigate the relationship between the two culture stages, as the relevance of the cells in culture must be maintained. In chapter 4 the dimension of the cells in cultured and plant were observed. These results proposed that the culturing process did not have an adverse effect on the sizes and shapes of the cells. This investigation must be continued, investigating the wall composition (Hoff and Castro, 1969) of the four genotypes at both culture stages.

As each mutant has a specific polymer that it affects, each of the three polysaccharides must be investigated as several differences can be hypothesised. From the knowledge acquired on the *sk5* mutation, an observed reduction of total pectin should be expected (Leboeuf *et al.*, 2005). The amount of cellulose present could also be lower in *mur1* and *sk5*, as growth was significantly reduced in the plants after 40 days (chapter 3). However these are not direct results of the mutations but as secondary developmental effects. The reduced growth will cause a reduction in cellulose of *sk5* and *mur1* when they are compared to col0 and *ida*. Hemicellulose may also be lower, in proportion to reduction in cellulose for the same reasons. However this is speculation, the only definite difference that should be observed is the reduction of total pectin in *sk5*.

To analyse cell wall composition there are two main methods, spectrophotometry and High performance liquid chromatography (HPLC). Both require the cell wall to be broken down and the components then analysed, this is not an in-situ analysis. HPLC uses a column of polysaccharide beads to separate the components and fractionate quantify with a detector. This is an accurate and well-known technique, however it is very expensive. This is due to the costs of the highly specific columns that were required. Spectrophotometry is cheaper but time consuming, as the components must be individually extracted from the total polysaccharide before they can be analysed. This is where HPLC has the advantage, by separating the total polysaccharide into fractions dependant on size or charge. However, for the purpose of this investigation spectrophotometry was chosen because of the lower cost.

### 5.1 Cellular Material

For the growth the whole plant samples there were several options. The above ground region was prepared with the same method of the PGC (chapter 3.2). The region will be removed from the roots and measured. For the roots it will be more complicated. Agar grown systems are too small to allow for approximately 40 days growth, soil and vermiculite systems are difficult to remove the complete root system without damage. The only other alternative is hydroponics, where the roots of growing plants are immersed in a liquid nutrient solution.

For hydroponics, *Arabidopsis* seedlings were germinated on pieces of Rockwool suspended above a tank of half strength liquid MS medium. The liquid was agitated using an air stone and a fish tank pump. For the first week, to allow for germination, this was housed in a growth cabinet and kept at 20°C and 85% humidity. However, after 1 week the germination rate for all genotypes was very low (between 25-50%), the survivability of those that germinated to week 2 was also low (50%). From the 86 seeds that were sown only two produced enough root material for investigation. There was insufficient time to optimise the method and it was therefore abandoned.

In Chapter 3, the above ground region was investigated requiring large numbers of plant to be grown. This method successfully produces large amounts of cellular tissue that could be used for this

investigation. Root material was therefore overlooked in favour of shoot material due to the ease of access to large amounts of material and the relatively low maintenance required.

Cultured cells were prepared using the protocol in chapter 4. For the purpose of this investigation, samples for each genotype and culture stage were prepared in triplicate, ensuring sufficient numbers for each sample for statistical analysis. More replicates would be beneficial however the number of samples that could be physically handled limited the experiment.

## **5.2 Method**

Spectrophotometric analysis requires the sequential extraction of the individual polysaccharides from a solution of total polysaccharide. These individual components are then analysed in a spectrophotometer to quantify the amounts present.

Native plant proteins must firstly be denatured to deactivate them preventing the degradation of the polysaccharides (appendix 3). Without this stage the proteins may continue to affect the polysaccharides product and therefore the results. De-proteination will allow the samples to be stored for much longer without degradation, allowing time to process all the samples.

To analyse fully the polysaccharides, they must first be extracted from the cell wall. The alcohol insoluble residue (Stevens and Selvendran, 1980) (appendix 4) is prepared for samples of approximately the same fresh weight, 17g for plants and 4g for cultures. These values were chosen as they were similar to the amounts of material available for earlier experiments (chapters 3 and 4). The organelles, plasma membrane and any other potential contaminants were removed as they may interfere with subsequent analysis. The polysaccharide components are insoluble in alcohol, however many of these contaminants are, allowing them to be removed easily.

Bulk extraction of the polysaccharides was not acceptable as the levels of each component were required. Gradual removal of wall components from the total polysaccharides by sequential extraction was the most applicable method (appendix 5). These samples must be de-salted, as this will affect

the spectrophotometer. This is achieved using dialysis (appendix 6). The content of the de-salted fractions can then be analysed using the spectrophotometer (appendix 7)

### 5.3 Results and Discussion

To analyse the levels of polysaccharides liberated during the extractions, calibrations were done using solutions of known polysaccharide concentration. The optical densities for these solutions were recorded and the values for the experimental solutions can be extrapolated from these calibrations. For further information refer to appendix 5. From this data the following figures were drawn. Figures 5.1-5.5 have been normalised to show the amounts of polysaccharide liberated from each gram of the initial fresh weight of cellular material.

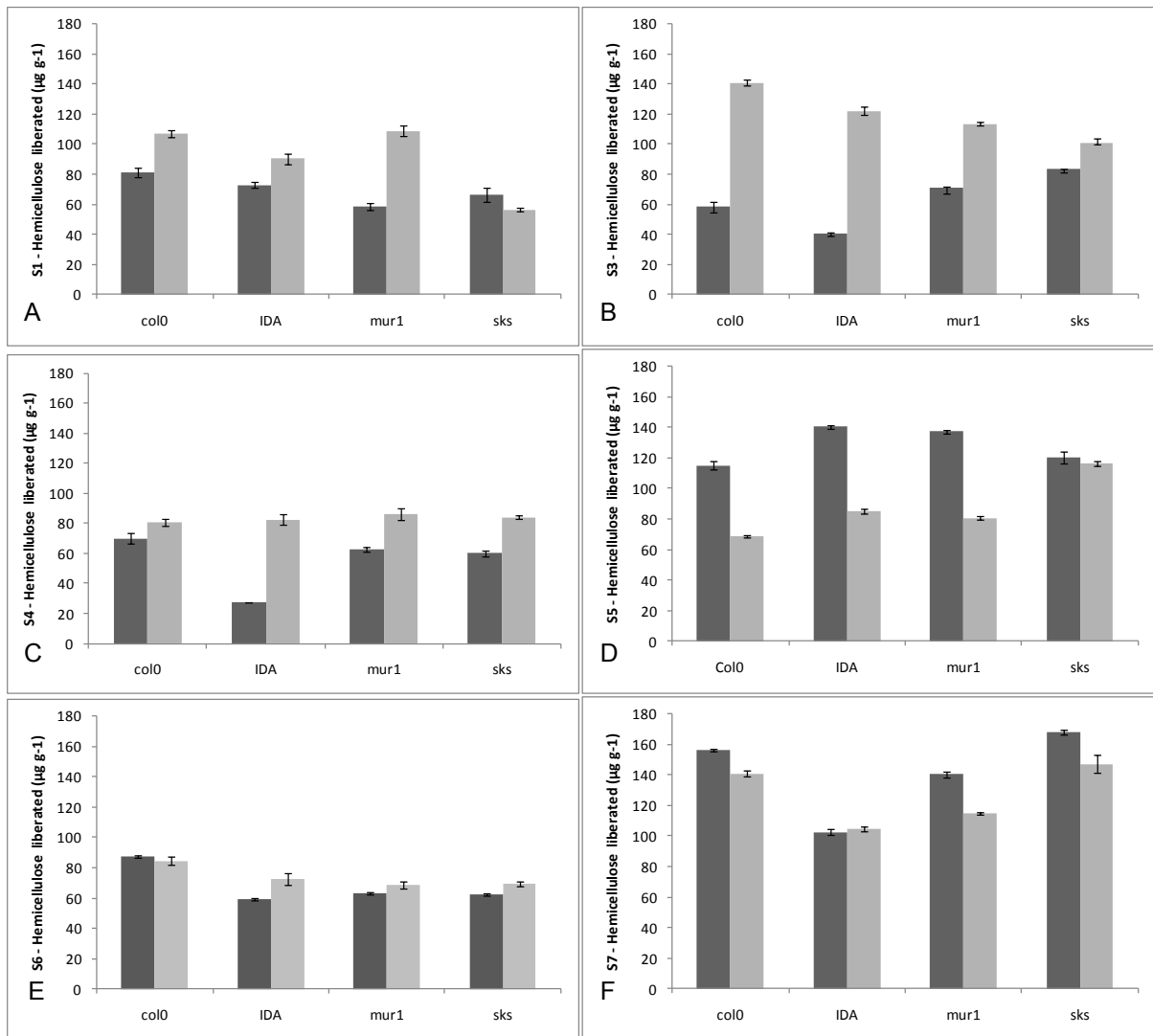
#### 5.3.1 Hemicellulose

Firstly the amount of hemicellulose liberated from the samples was analysed. From information on the mutations (section 2.13.2) gathered in the literature survey, it is possible that there will be no differences seen. The *mur1* was the most likely candidates to show significant differences to the *col0*, but due to the nature of the mutations it was unlikely to affect the amount present. Looking in detail at figure 5.1, there are several major differences in the graphs. Throughout the extractions, there are few significant differences of to be seen between the genotypes of the same cell culture stage.

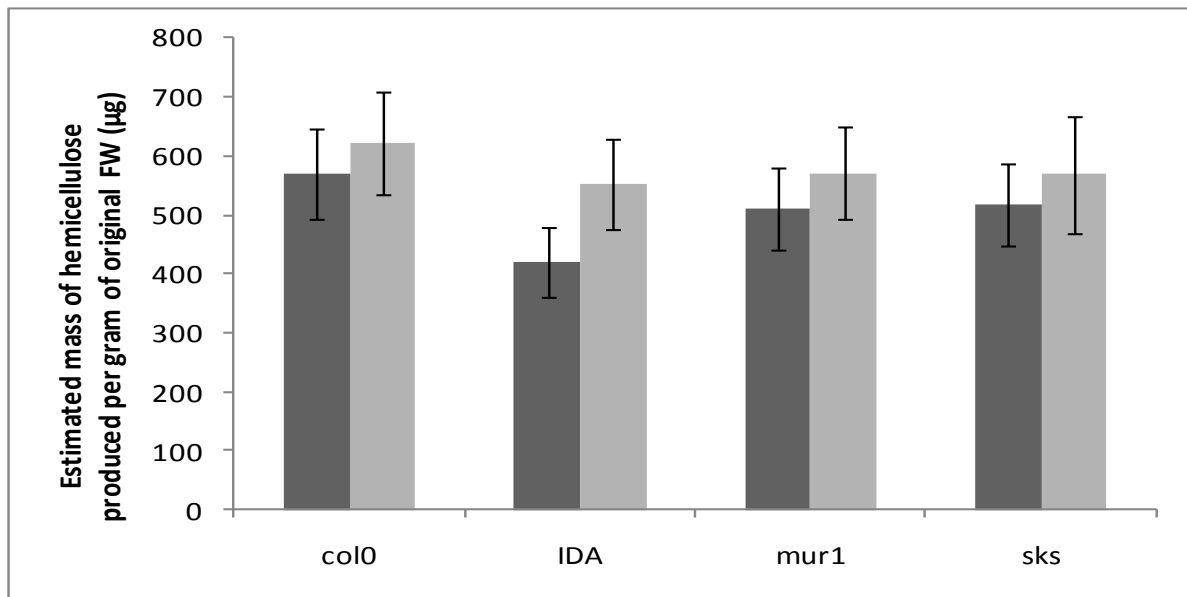
Between the cell types there are several differences of note. (A) And (B) show a higher level of native hemicellulose concentration of all genotypes in the plant tissue over the cultured tissue. (C) Highlights a similar pattern with the mannose rich hemicelluloses as found in (A) and (B). The majority of samples in (D) differ, showing the converse relationship to those seen previously, with more hemicellulose produced from the cultured tissue.

Figure 5.1 (E), highlights comparable levels of hemicellulose that are liberated from plant and cultured tissues. In (F) the levels of extracted polysaccharide are mostly higher again in the cultured tissue. These small differences suggest that the total amounts of hemicellulose extracted will be higher in the

plants, despite the cultured cells showing higher levels 2 of the 6 stages. These results were combined to get the total of hemicellulose extracted; this can be seen in figure 5.2.



**Figure 5.1:** Data from each stage where hemicellulose was extracted cultured tissue shown in light grey plant tissue shown in dark grey. (A) Stage 1 and (B) stage 3 contain a proportion of the native hemicellulose. (C) Stage 4 contains the mannose rich hemicellulose. (D) Stage 5, (E) stage 6 and (F) stage 7 all show a large proportion of the total hemicellulose, which has been de-acetylated due to the nature of the extraction. The error bars show the standard error. The differences are discussed at length in the results chapter 5.5.1.



*Figure 5.2: Amount of hemicellulose extracted per gram of fresh weight. Stages 1, 3, 4, 5, 6 and 7 extract a portion of the total hemicellulose present, a combination of the data shown in figure 5.1. Each data set contains three replicates with three measurements taken from each sample. The pooled data shows total hemicellulose liberated for plant and cultured tissue of each genotype. The total hemicellulose liberated is not influenced by either genotype or culture stage.*

Although there are differences, there are none of any statistical significance. The differences seen in figure 5.1 are lost when the sum is taken, resulting in no net difference. This was not to be unexpected as the amounts of plant tissue used were much higher. From the hemicellulose results, it can be determined that neither the culturing process nor genotypes have any overall effect on the levels of hemicellulose in the cell walls. From the information in the literature (section 2.13.2) given for the mutants, this is not unexpected. It is possible that *mur1* may have shown differences in hemicellulose production. The mutation does not affect the amount of hemicellulose present in the wall, but the role the fibres play in the wall. These results are encouraging, as the similarity shows that cultured cell walls show relevance to their plant equivalents, especially as no differences were expected.

## 5.3.2 Pectin

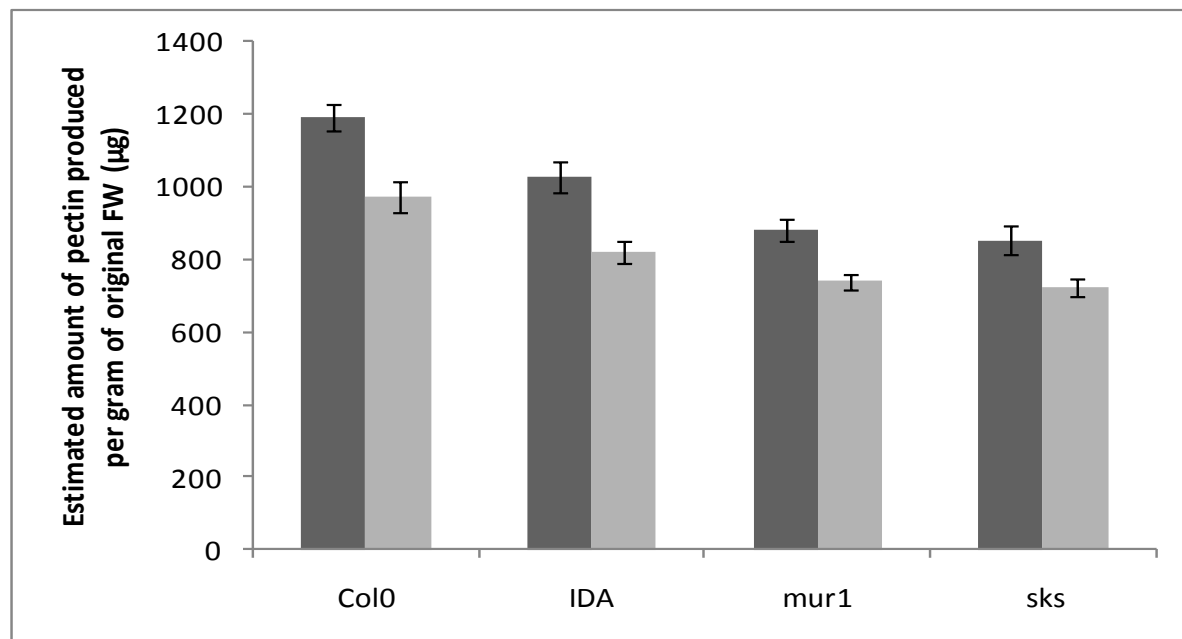


**Figure 5.3:** Estimated amount of pectin produced per gram of initial fresh weight for both cultured (dark grey) and plant (light grey) of tissue from each genotype. Error bars give the standard error. Statistically there is significantly more pectin produced by the *col0* and *ida* compared with *sks* and *mur1* in both cultured and plant tissue. The amount of pectin present in the cultured tissue is significantly higher than that produced by the plant tissue of *ida*, *mur1* and *sks* ( $P > 0.05$ ). *Col0* also shows this difference but at a non-significant level.

The next polysaccharide to be analysed was pectin. The results for pectin were very different from those seen the equivalent figure for the hemicellulose. The amount of pectin produced per gram of cultured tissue was higher when compared to the plant tissue (figure 5.2). These differences are significant ( $P > 0.05$ ) for *ida*, *sks* and *mur1* with *col0* showing a non-significant difference between the culture stages.

This was the first evidence to suggest that the culturing process has had a major effect on the biochemistry of the wall. The increase may have been an attempt to maintain cell-to-cell adhesion as the cells were separated by the agitation. Alternatively, the extra space afforded to the cells to move to allow for separation to single cells has caused the cells to over-produce pectin. Simply put, they produced more pectin because they could, especially with the primary cell wall expansion restricted by microtubules. With space and nutrients unlimited the cells continued to produce pectin when their plant counterparts would have been restricted. However, this is purely speculation.

To validate this, the differences between the cultured and plant tissue must be analysed. The *col0* and *ida* show significantly higher amounts of pectin than *mur1* and *sk5* for both plant and cultured cells. This pattern is reminiscent of the results of the growth experiments of chapter 3. It was expected that the *sk5* mutants would show a lower level compared to *col0*, because the literature suggests that *sk5* produces less pectin as a direct result of the mutation. The lower level levels of pectin in *mur1* are unexpected. Although not as low as *sk5*, it is possible that this is a developmental effect, as less pectin is required because there was less growth, as the plants are smaller. Unfortunately, this argument does not apply to the cultured cells as any growth variables are removed due to the homogeneity of the growth conditions.

In the subsequent investigations, the compression testing (chapter 6) and mathematical modelling (chapter 7), the effects of the increased pectin levels should be monitored. The thicker middle lamella should not affect mechanical properties determined by micromanipulation. The model uses only the thickness of the primary cell wall when calculating the initial thickness ratio for the input parameters. Pectin is also not thought to be of any mechanical significance, so an increase in the amount present should not cause any affect considering the relatively small increase. The observed diameters and measured diameters should be checked, as it is possible that this may differ. The pectin may be observed as part of the wall, but mechanically offering little resistance will discount it from the measurements.

### **5.3.3 Cellulose**

After the 6 extraction stages, the remaining residue of insoluble polysaccharide must be analysed. As most of the hemi-cellulose and pectin have been extracted the remaining residue consists mostly of cellulose. By nature it is insoluble; therefore all cellulose present in the samples will pass into the residue. It is therefore feasible to take the dry weight of the residue to correspond to the amount of cellulose present.

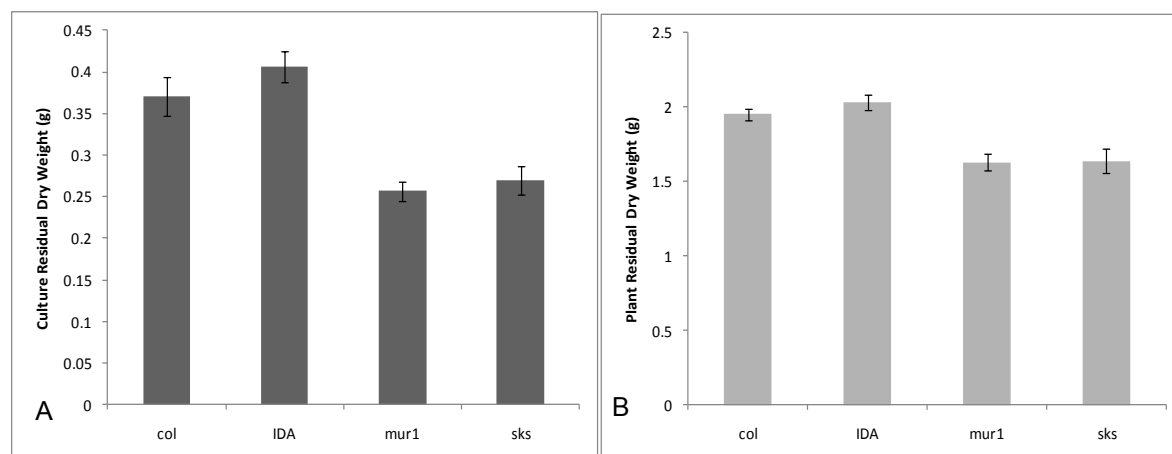


**Figure 5.4: Dry weight of the residue.** The residue contains remaining polysaccharides that remain insoluble from the extraction. (A) Cultured tissue (dark grey) and (B) plant tissue (light grey) error bars represent the standard error. Residue constitutes mostly of the cellulose present in the wall, as all other polysaccharides have been removed. The *mur1* mutation shows significantly lower levels of residue from the plant tissue that *col0* and *ida*. The *sks* mutation resulted in significantly lower amounts of residue than *ida* for both plant and cultured tissue ( $P > 0.05$ ) and non-significant differences to *col0* for both culture and plant. The *ida* mutation shows a slight increase in residue compared with *col0* (not significant) in both cultured and plant tissue.

The dry weights of the residues are shown in figure 5.4. From this it can be seen that the plants and culture residues have vastly different DW, but this was to be expected due to the initial weights. When the genotypes were compared, several interesting results were found. In figure 5.4 (A) the residual dry weights of the cultured samples are given. The *ida* mutation demonstrates a higher dry weight when compared to *col0*, although this difference is not significant. It also shows a higher residual dry weight to both *sks* and *mur1* but these differences are statistically significant. *Col0* has differences to *sks* and *mur1* however only the *mur1* value is significant. Figure 5.4 (B) gives the residual dry weight of the plant samples. The differences are exactly the same as those seen in the cultured cells.

To compare the cell types the data must be converted in to a comparable state. In chapter 3 this was done using the moisture weight as a percentage. Taking the converse will yield the percentage of the total that equates to the polysaccharide content. Figure 5.5 is a graphical representation of this calculation. In addition to the results from this chapter, the percentages from chapter 3 and chapter 4 are also shown for reference. (A) Comparing the culture weights from chapters 5 and 4 larger differences than the plants, however still do not give significant differences. (B) Comparing the chapter 5 to the chapter 3 data for the plants shows some small differences. With *ida* and *sks* are slightly higher and the *col0* and *mur1* lower. This (A) and (B) suggest that the chapter 5 samples are comparable to the previous data and therefore representative of the tissue. As the results from

chapters 3 and 4 have not undergone the same treatments they are being used as a method for justifying relevance.

Comparing the genotype residue from the extraction (figure 5.5 (C)), there is the same pattern previously in this chapter and chapter 3. With col0 and IDA of comparable level, and mur1 and sks significantly lower. When comparing the cell types, the differences seen are not significant.

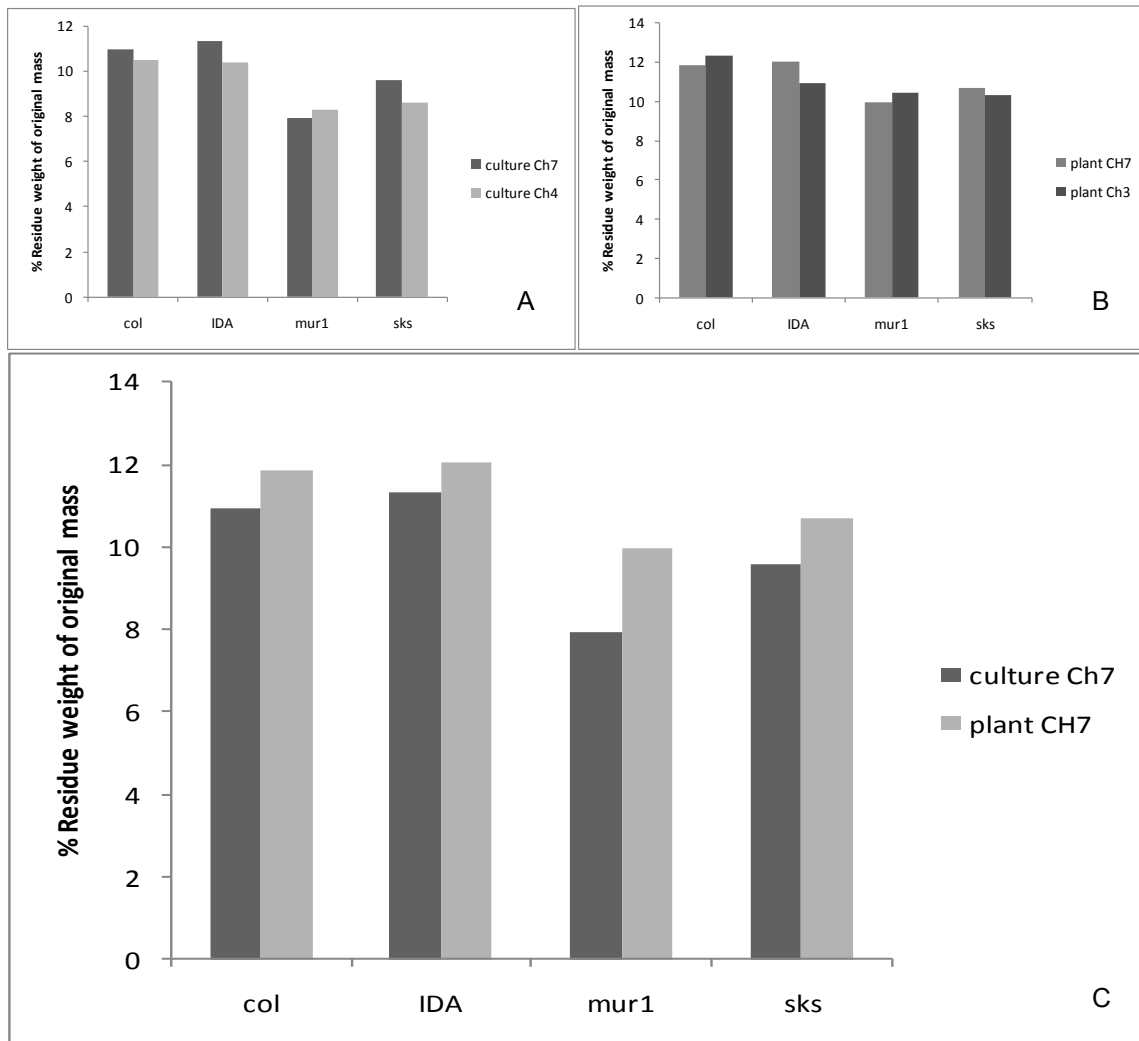


**Figure 5.5:** The percentage of the original fresh weights that corresponds to the dry weight residue. (A) Comparison between values for cultures from chapters 5 and 4. (B) Comparison between values for plants from chapters 5 and 3. (C) Comparison between the plant and culture values from chapter 5.

## 5.4 Conclusions

With the investigation of the biochemical composition complete, some of the major questions can now be addressed. The results in chapter 3 show that the phenotypic effects of the mutations have split the four genotypes into two groups. Col0 and *ida* showing similar growth profiles, and the *mur1* and *sks* mutations have profound effects on the growth characteristics. These results now have a partial explanation from the results of this chapter.

It was important to establish the relevance of the data, through comparison of the plant and cultured data in addition to previous results. Maintaining the relevance of the experimental results to the information that would be gained from the plants is fundamental to the investigation, hence the constant referral to these sources. Throughout chapter 4, cultured tissue was extensively referenced to the relevance to the native tissue. With measurements of the single and aggregated cells proving the culturing process produces cells that were of comparable diameter to those in the root, averaging approximately 25µm.

For the majority of the results there was a correlation between the cultured and plant tissue. The one example of statistical differences is in that of the pectin data. The results showed the culturing process has had a profound effect on pectin production. Comparing the hemicellulose and cellulose data, suggests that this result is confined to the pectic polysaccharides. There are two main possibilities for this. Due to the nature of the culture environment, the cells are provided a relatively infinite space to expand and unlimited nutrients. Without spatial regulation of the plant, the cells continually produce pectin, resulting in the increase observed. Alternatively, the constant perturbation of the liquid causes the loosely adhered callus cells to gradually apart as was intended to produce single cells. It is possible that due to the gradual nature of this release, the cells produce additional enlarged middle lamella in an attempt to maintain adhesion.

To investigate whether either of these theories is correct the middle lamella region of the cultured cells was analysed when the primary wall thicknesses were analysed using TEM for the modelling chapter (chapter 7). It is possibly this overproduction of pectin may have an effect on the measurement of the cellular diameter. The observed cell diameters taken in chapter 4 and 6 must be accurate as they play

a vital role in many subsequent calculations. The diameters taken from the TEM are not applicable as they were from dehydrated cells. It was possible to compare the observed diameters with those taken from the compression data and the modelling data. Chapter 6 covers the microcompression in great detail and it is possible that this over production of pectin may explain some of the results. As for explaining the questions asked in chapter 3 of the causes of the differences in growth rate and total root length. It is possible to suggest biochemical reasons for these results.

Hemicellulose, the fibres responsible for cross-linking cellulose polysaccharides showed no differences between either genotype or cell type. As the *mur1* mutation is known to affect hemicellulose, it can be concluded that the mutation does not affect the amount of hemicellulose produced, and more likely causes a reduction in the effectiveness of the polysaccharide to form crosslinks. Theoretically this will manifest itself as a reduction of the mechanical properties of the single cells to be analysed by micro-compression. Additionally, the lower levels of pectin and cellulose seen between *col0* and *mur1* will have an effect on the growth properties. However to definitively suggest the major cause is highly unlikely and more likely that there is a combination of factors.

For *sks* the severe reduction in pectin is increasing likely to have caused the growth differences. It is now possible to place a figure on the reduction, approximately 30% for the cultured tissue and 25% in plant tissue when compared with the WT. This is reassuring as these values correlate with those quoted in the literature. Combined with the lack of a significant difference in the quantity of cellulose present, this suggests that the reduced adhesion of the cells plays a large role in the growth differences seen *in-planta* (chapters 3 and 4). However the role of the reduction in pectin on the mechanical properties of the primary wall is yet to be determined (chapter 6 and 7).

The *ida* mutation remains similar to *col0* as results in previous chapters have suggested. This evidence is supported by the results in this chapter. To predict that the mechanical properties of the single cell walls of these cells would not be dissimilar to those of the *col0* on the evidence presented would not be unexpected. To confirm these hypotheses, the Microcompression of samples of single cell from suspension culture was conducted in chapter 6.

## *Chapter 6: Compression Testing by Micromanipulation*

---

### **6.1 An Introduction to Compression Testing by Micromanipulation**

Micro-compression has been used to measure the mechanical properties of many biological materials as described in section 2.14.2. During its evolution, micro-compression has been through many iterations (Zhang et al., 2009).

The current techniques use a 'stamping' action known as compression testing by micromanipulation (Zhang et al., 1991). This technique was the most applicable to this investigation, having previously been used to compress single tomato cells (Wang et al., 2004). It involves compressing a single cell between a large flat glass probe and glass base (Blewett et al., 2000). The sample is placed in a glass chamber and the cells allowed time to settle onto the base. A probe attached to a force transducer is positioned over the sample and moved downwards to compress the cell. Figure 6.1 gives a schematic of this process.

The force being imposed on the cell is found as a function of the probe displacement, e.g. the gap between the probe and chamber base. From these data the elastic modulus and the initial stretch ratio can be found by mathematical modelling (chapter 7). Elastic modulus ( $E$ ) is a mathematical description of tendency of the wall to be deformed elastically, assuming the cell wall material can be describes as elastic.  $E$  is taken to be the ratio of stress over stain, in this case generated by the compression of the cells. The initial stretch ratio ( $\lambda_s$ ) is the difference in the cell radius at some positive turgor pressure to the radius at zero turgor pressure (Zhang et al., 2009) and is an important determinant of the force required for a given deformation.

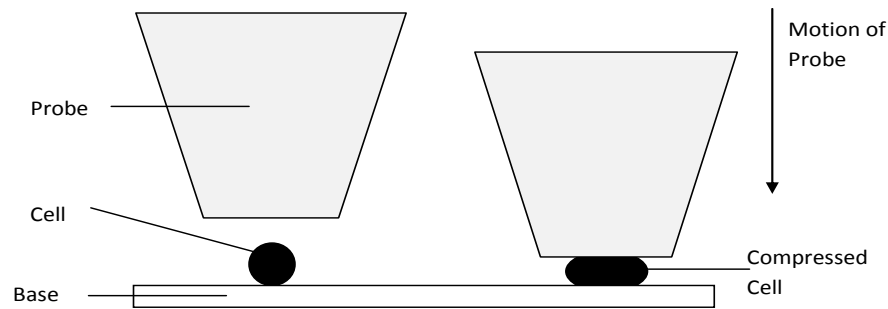


**Figure 6.1:** schematic diagram of the compression of an individual cell between a large flat probe and a glass slide. (Not to scale).

## 6.2 Probe Manufacture and Transducer calibration

Glass probes must be made that are suitable for the particular cells being compressed. For information on probe manufacture see appendix 7. The probe is mounted onto a force transducer (appendix 8) chosen for the suitability to the nature of the cells to be compressed. The force transducer converts the forces of compression into a voltage that is acquired by a data acquisition card in a computer. The 400A force transducer (Aurora Scientific, Canada) was chosen. This was the same as that used for yeast (Stenson et al., 2009) and tomato cell (Wang et al., 2004) compression. Its maximum scale of 50 mN was predicted to be sufficient for *Arabidopsis* cells. The transducer was calibrated to ascertain the sensitivity (appendix 9) and compliance (appendix 10) and was found to comply with the manufacturer's specifications.

## 6.2 Current Techniques

Tomato cells have been compressed using two different micro-compression rigs, a Low Strain Rate micro-compression Tester (LSRT) (Blewett et al., 2000) and a High Strain Rate micro-compression Tester (HSRT) (Wang et al., 2004). Both were built in conjunction with Micro Industries Ltd (Oxon, UK) and use compression testing to obtain voltage/time data. The two rigs have many similarities but have key differences that give specific properties and therefore affect their use.

### 6.2.1 Low Strain Rate Tester (LSRT)

The LSRT (Shiu et al., 1999) apparatus can be seen in figure 6.2. The samples containing single cells from suspension cultures (chapter 4) are held in a glass chamber mounted on a microscope stage. This can be visualised from the side using a high performance CCD camera (4910 Series, COHU Inc., San Diego, USA) and from below using an inverted microscope with 20× objective lens (Leica Imaging Systems Ltd, Cambridge, UK) attached to Norbain Vista CCTV camera (Norbain SD Ltd, UK). These in turn are connected to monitors allowing the cells to be easily visualised from both angles whilst still allowing fine adjustment in the horizontal plane. This is essential for several reasons, e.g. positioning of the probe above the cell, for calculating cellular diameter and the distance from probe face to cell. The stage is illuminated using fibre optic light sources (MFO – 90, Mircotec fibre optics), ensuring there is sufficient light to allow the cells to be viewed clearly.

The transducer (with probe attached) was mounted on an arm connected to a stepping motor. The stepping motor system (Prior-Martok Ltd., Cambridge, UK) was controlled through a PC and Hyperterminal program (Hilgrave Inc. Monroe, MI, USA), which varies the speed and distance of the motion (See appendix 10 for list of full controls). The step distance was calculated as 0.012  $\mu\text{m}$  the same as that stated by the manufacturer and the maximum speed was calculated to be  $66\mu\text{ms}^{-1}$ . A detailed method for calculating the stepping distance and motor speed can be found in appendix 11.

A single cell was selected using the inverted microscope view, allowing the probe to be positioned above the cell ensuring that it is in the centre of the probe and the side view microscope allows the height of the probe above the cell to be seen. The probe is then lowered so that the probe is just above the cell; it is then moved towards the base compressing the cell whilst recording the voltage trace using the PC software.

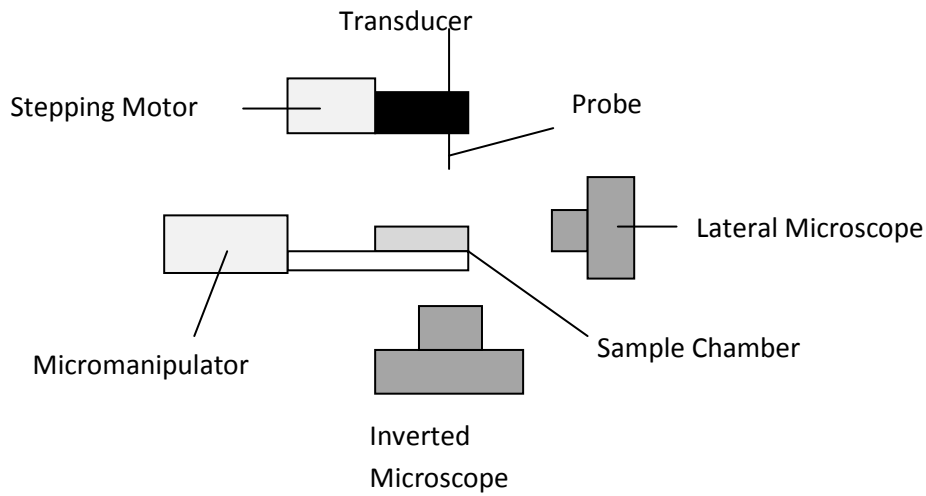


**Figure 6.2: Schematic of the low strain Rate Compression Testing Apparatus (LSRT). The main components can be seen, the probe mounted on the force transducer, which is attached to a stepping motor. This is positioned above the sample chamber, which is held in a stage attached to a micromanipulator. Two microscopes are used for lateral and inverted views of the sample chamber.**

There are two major problems with the LSRT, motor lag and backlash. Motor lag occurs when the motor is initiated to move but does not respond immediately to the assigned speed. Although the time to reach the speed is small it can still have a significant effect on the calculated displacement of the probe. Backlash occurs from looseness within the gearing apparatus that prevent the motor from returning accurately to the initial position. This can lead to a small error when calculating the probe displacement.

Leaving a gap between the probe tip and cell was intended to counter these problems, allowing the system to reach full speed before contacting the cell. However this can lead to errors calculating the point of contact between the probe and the cell, this will be discussed later.

### 6.2.2 High Strain Rate Tester (HSRT)

The HSRT is a fairly recent development, allowing the same experiments to be run at greatly increased speeds compared to that of the LSRT (Stenson et al., 2009). A schematic of the HSRT can be seen in figure 6.3.

The HSRT has two motors capable of providing the motion for compression, a stepping motor (Prior-Martok Ltd). This is also a piezo electric stack (Model P-841.60, Physik Instrumente (PI) GmbH & Co. KG, Germany), which utilises the piezo electric effect to induce deformation in certain ceramics. The stepping motor is similar to the one used in the LSRT, but is capable of speeds of approximately  $200\mu\text{s}^{-1}$ . It is controlled using a Prior control box (Prior-Martok Ltd., Cambridge, UK), which controls the speed by varying the percentage of the maximum used. The motion of the probe is controlled using the Hyperterminal program (Hilgrave Inc. Monroe, MI, USA) in a similar manner to the LSRT.

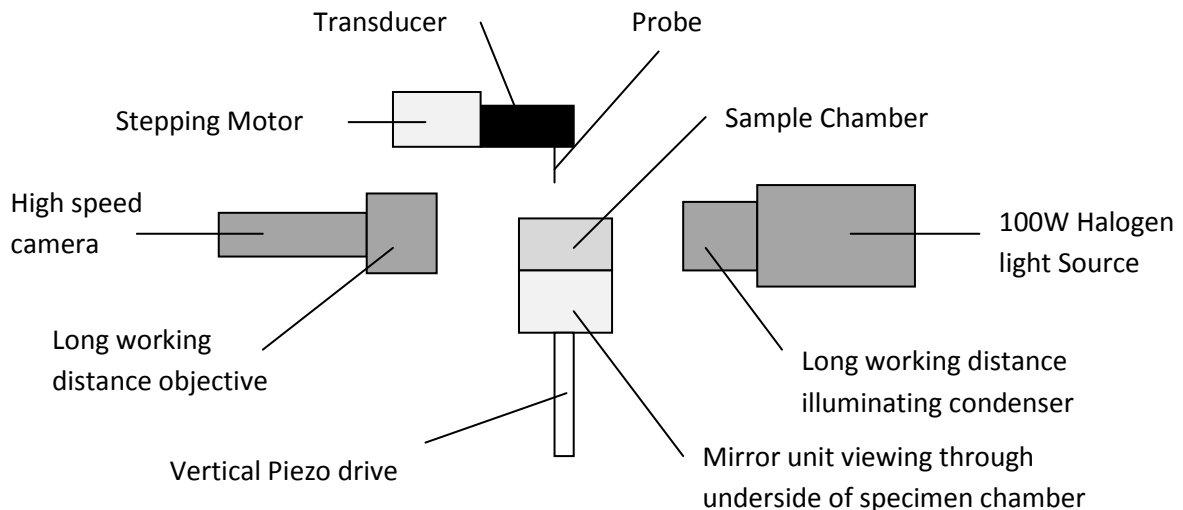


*Figure 6.3: Schematic of the High Strain Rate compression testing apparatus (HSRT). The transducer mounted probe is positioned above the sample chamber and attached to a stepping motor in a similar manner of the LSRT. Additions include the high power light source and condenser, to improve illumination for the high-speed camera. The inverted microscope has been removed for piezo electric drive below the sample chamber. A mirror unit and camera allow an inverted view.*

## Chapter 6: Compression Testing

However the piezostack is capable of speeds of at least  $1500 \mu\text{ms}^{-1}$  (Wang et al., 2004), although the maximum speed is yet to be determined, as it was not required for current uses. The piezostack utilises the piezoelectric effect to generate the method of motion. This requires the probe to be positioned above the cell and then the stage is moved towards the tip, unlike when using the stepping motors where the probe is moved down towards the cell. The distance for piezo stack motion is limited to  $80 \mu\text{m}$  but this is not an issue for *Arabidopsis* cells as the average diameters are approximately  $25 \mu\text{m}$ , as can be seen in figure 4.6.

Like the LSRT the samples can be view from the side and from below, the side view is attached to a high-speed camera (HSC) (MEMRECAM ci/RX-2, NAC Image Technology Incorporated, Japan). This enables the capture of video at 500 frames per second, meaning that the full motion of the compression can be viewed. This would not be possible with a normal camera due to the high speed of motion. To magnify the view, a  $20\times$  (scanning) lens and a  $35\times$  (high power) objective lens were used in addition to a  $7\times$  auxiliary objective giving a total magnification of  $245\times$ .

To gain an inverted view is not as simple on the HSRT compared with the LSRT. This is due to the inclusion of the piezostack beneath the stage, meaning that there is no room for an inverted microscope. A mirror at a  $45^\circ$  is positioned between the stage and the piezostack (Wang et al., 2004) allowing the sample to be viewed using another horizontal microscope attached to a Norbain Vista CCTV camera (Norbain SD Ltd, UK). Both views were shown on separate monitors allowing for ease of use. Illumination of the sample is achieved using a long working illuminating condenser positioned in line with the side view microscope focussing the light through the sample chamber in addition to a fibre optic light source.

However the HSRT was originally built to use with slightly larger samples, e.g. single tomato cells that are at least  $80 \mu\text{m}$  in diameter. This means that the system was not optimised to visualise the small *A. thaliana* cells that average only  $20\text{-}40 \mu\text{m}$  in diameter. The inverted view was limited to  $4.5\times$  magnification due to the lack of space for a larger lens. The inclusion of the high-speed camera also reduces the maximum magnification possible for the side view, as the light collection time for the image is reduced. Due to the low exposure time of the frames of the high-speed camera, low light levels may affect the quality of the videos.

### 6.4 Interpreting the Data

From the compression event, a voltage/time trace is produced; an example can be seen in figure 6.4. Using this raw voltage/time data from the compression and the corresponding baseline reading, various values can be calculated. A baseline is recorded when the probe is not in contact with anything, to acquire the background voltage in the system. It is possible to adjust the baseline to a required level on the transducer power box.

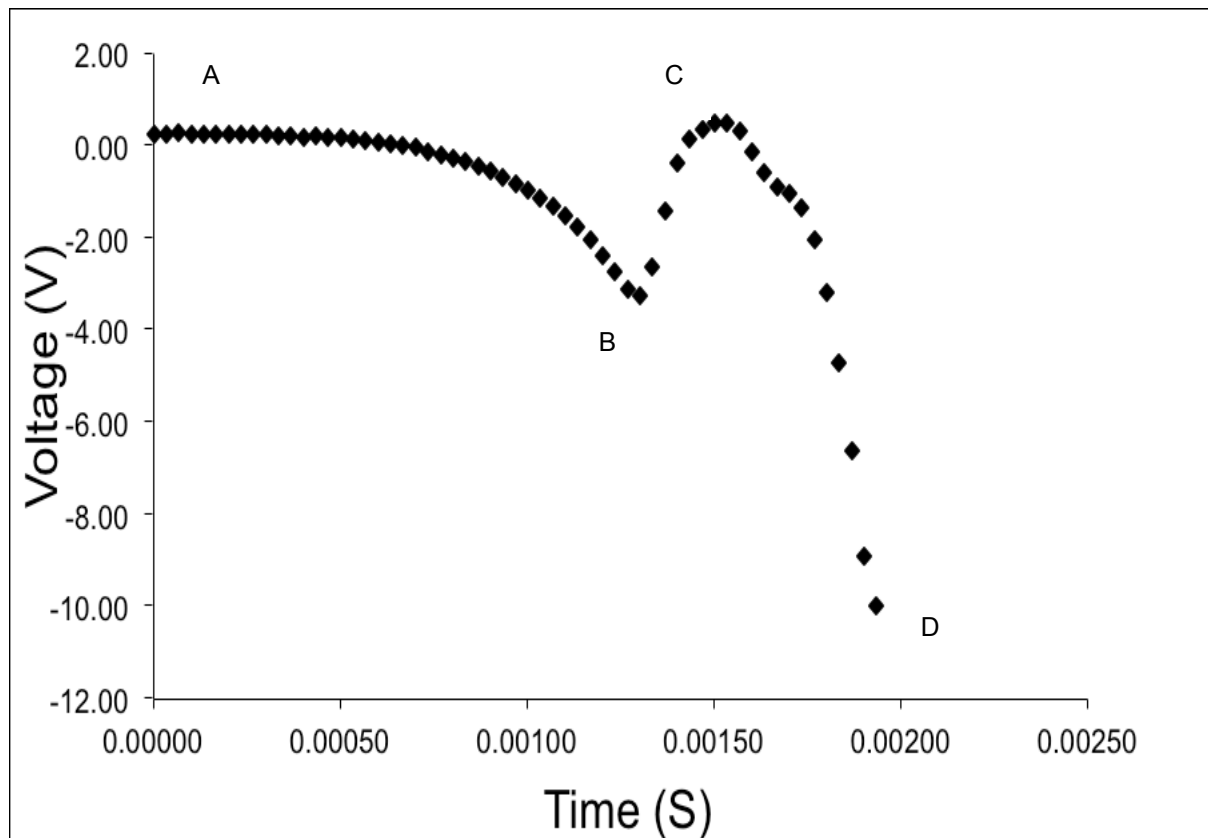


*Figure 6.4: an example of a voltage/time graph from a compression of a single Arabidopsis cell using the HRST at  $3000 \mu\text{ms}^{-1}$ . (A) Gives the point of initial contact between the probe and the cell. Cell rupture occurs at (B). (C) Shows the initial point of contact with the base/debris, compression then continues until the probe rests on the chamber base (D). This figure is the opposite to all other figures in this chapter as the voltage is recorded negatively away from zero. The calculations made from this data express the values positively*

## Chapter 6: Compression Testing

The compressive force (mN) acting upon the cell at any time is determined from the voltage – time traces by the difference between the output voltage (V) ( $W$ ) and the baseline voltage (V) ( $W_0$ ):

$$(1) F = K (W_0 - W)$$

Where  $K$  represents the sensitivity of the transducer ( $\text{mNV}^{-1}$ )

The displacement of the probe was determined from the same voltage time trace. Displacement ( $\mu\text{m}$ ) is dependent on the speed of compression and the compliance of the system:

$$(2) D = v (t - t_0) - S.K. (W_0 - W)$$

Where  $v$  is the speed of compression ( $\mu\text{ms}^{-1}$ ),  $S$  is the compliance of the system ( $\mu\text{m mN}^{-1}$ ) and  $t$  is the sampling time ( $\text{s}^{-1}$ )

From the raw voltage/time data, force-displacement values can now be determined; an example of this is represented graphically in figure 6.8. From these graphs several values can be interpreted for each cell, the cell diameter ( $\mu\text{m}$ ), rupture force (mN) and displacement at rupture ( $\mu\text{m}$ ). The cell diameter is determined as the distance between the initial point of contact of the probe with the cell and the point at which the probe can move no further. Figure 6.5 shows an example of this; the distance between points A and D is taken to be the diameter of the cell

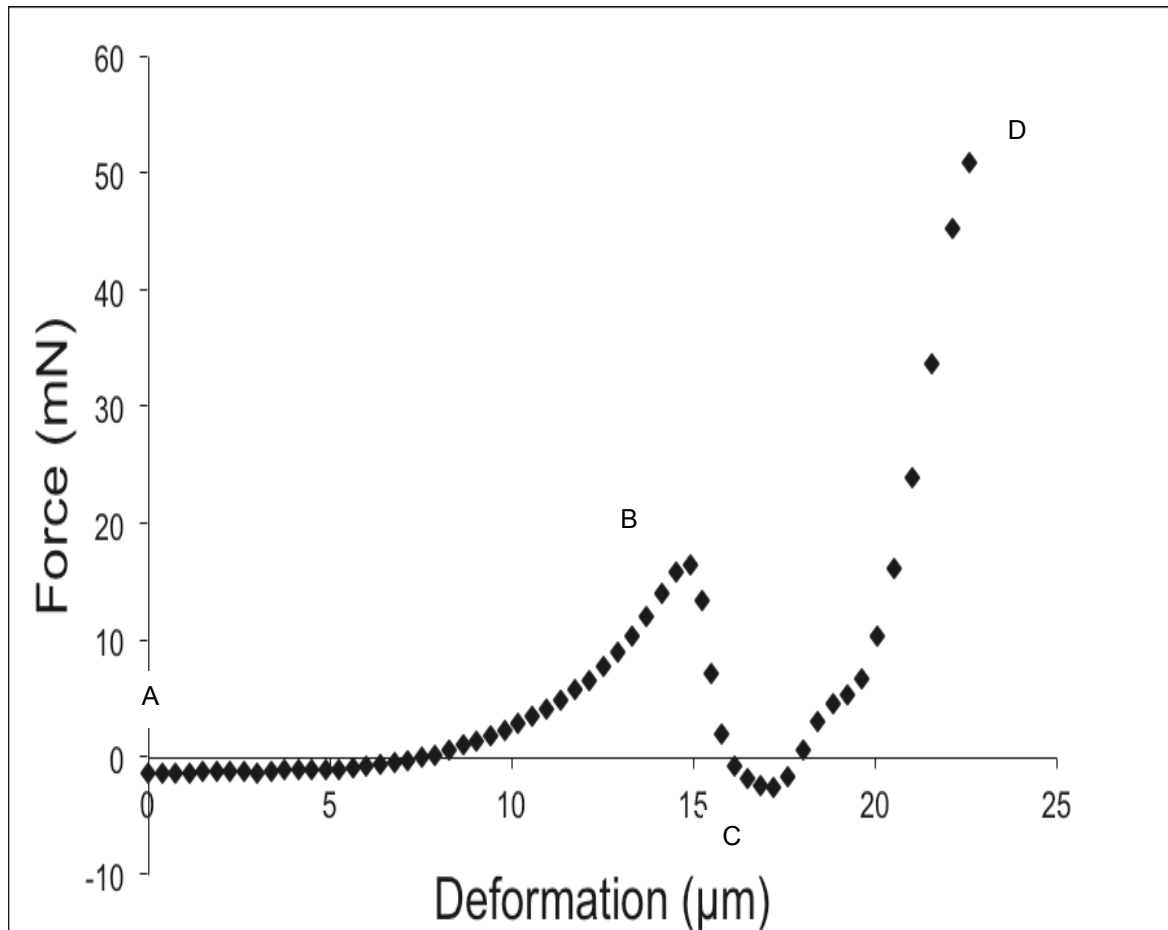


**Figure 6.5:** an example force/displacement graph generated from raw voltage/time data. (A) The initial point of contact of the probe with the cell. (B) The rupture point. (C) The point of contact with the base/ debris. (D) The point at which the probe rest on the chamber. From this example the diameter of the sample can be taken as approximately 25µm, the distance between (A) and (D).

### 6.5 Adapting the current techniques for single *A. thaliana* cells

Previously, tomato cells have been compressed using the LSRT (Blewett et al., 2000) and HSRT (Wang et al., 2004). Tomato cells (*Lycopersicon esculentum*) are much easier to isolate as discussed in chapter 4.1 and are significantly bigger than single *A. thaliana* cells that were produced in section 4.7. The tomato cells are approximately 80 µm compared with the 20-30 µm for *Arabidopsis*. However, even allowing for the size difference it may be anticipated that the *Arabidopsis* cells may behave in a similar manner to the tomato cells during compression. This is because both species have walls made of the same components (cellulose; hemi-cellulose and pectin, see chapter 2.4.) that should have similar mechanical properties. As the mutations chosen (section 3.1) are in the same genetic background (col0) the effects of differences in this composition are the variables that were being investigated.

## Chapter 6: Compression Testing

It was decided that repeating the initial work that yielded data from tomato cells should be the initial starting point for the *A. thaliana* cells. Therefore the LSRT was used with at a compression speed of  $23 \mu\text{ms}^{-1}$  (Blewett et al., 2000). A sample of cells from suspension was placed into the chamber. Single cells were positioned under the probe and compressed to 100% deformation. It was important that only one cell was positioned beneath the probe during compression. As the model stipulates that the force/deformation traces used relate to a single spherical cells. Therefore any debris or additional cells within the area of the probe would affect the data. Any single cell that was found without a clear area for compression was ignored. Care was also taken to clear the tip of the probe of any cellular material that may have become attached during the previous compression. This was achieved by slowly moving the probe along the surface of the chamber. Temperature was monitored throughout each experiment and fluctuated around  $25 \pm 2$  °C.

The time voltage traces that were gained for a speed of  $23 \mu\text{ms}^{-1}$  were unusable, as no response was seen from the cells. The probe touching the base of the chamber caused the only voltage changes observed. Unfortunately it was not possible to distinguish viable and non-viable cells in the preliminary experiments but it seemed unlikely that all the cells in three batches of twenty that were compressed were non-viable. Subsequently, cells were stained with Neutral Red (NR) prior to compression. The protocol for this can be found in section 4.5. NR stains the vacuoles of cells with intact membranes red. Therefore any cells not stained were ignored, and cells with stained vacuoles were chosen for compressed.

It was believed that the inability to generate a voltage response was potentially caused by the cells leaking water as they were put under pressure from the probe. It was believed that the hydraulic conductivity ( $L_p$ ) of *Arabidopsis* cells must be higher than that of the tomato cells, mainly due to the higher surface area to volume ratio of the smaller *Arabidopsis* cells. It has been reported that  $L_p$  values of different plant cell types range from  $2 \times 10^{-8}$  to  $10^{-5} \text{ms}^{-1} \text{MPa}^{-1}$  (Maurel, 1997). For the single tomato cells it was found that the  $L_p$  was approximately  $10^{-7} \text{ms}^{-1} \text{MPa}^{-1}$  (Hukin, 2002). For these investigations it was presumed that the relatively high rate of compression would negate the water loss. It must therefore be anticipated that the rate of compression for the *Arabidopsis* cells to negate water loss will be higher.

## Chapter 6: Compression Testing

For the *Arabidopsis* cells, the neutral red staining protocol was utilised in order to prove the membranes of the vacuoles were intact. This staining could be seen under the microscope, these were the cells were chosen to be compressed. It could therefore be presumed that at the current speed, water was being 'squeezed out' as the cells were compressed. Therefore the speed was not fast enough for the water loss to be negligible, which is essential for modelling purposes (chapter 7). It therefore seemed that tomato cells could only be used as a guide for *Arabidopsis* cells in relation to water loss. *Arabidopsis* cells are significantly smaller, giving a much higher surface area to volume ratio, making water loss much easier.

To negate the water loss, the time taken to complete the compression was reduced, requiring an increase in the speed of the probe movement. LSRT was used at its maximum speed of  $68 \mu\text{ms}^{-1}$  in order that time allowed for the compression was reduced, attempting to induce a force to build and not be lost as water was squeezed out. The first trace (triangles) in figure 6.6 shows an example of a force/deformation trace from a cell compressed at  $68 \mu\text{ms}^{-1}$ . However, force/displacement traces showed little difference from the cells compressed at  $23 \mu\text{ms}^{-1}$  and so the data were still unusable. To check the procedure, microcapsules were compressed to check the transducer and found to be working correctly. To check the cells, single mutant cells (*sks* and *ida*) were compressed at both speed, but still no voltage changes observed at either speed.

To continue working with the *Arabidopsis* cells, the speed had to be increased beyond the working range of the LRST, requiring the use of the HSRT. The stepping motor on the HSRT has a maximum speed of  $200 \mu\text{ms}^{-1}$  a near 3-fold increase from the LSRT. Col0 cells were again compressed and showed an increase in voltage response. However, this was only for approximately half of the range of the cells diameter measured from the video. In figure 6.6, the circles show force/deformation data of a cell of approximately  $25 \mu\text{m}$  in diameter compressed at  $200 \mu\text{ms}^{-1}$ .

Although the force did begin to increase this only occurred after the probe had moved approximately  $10 \mu\text{m}$ , suggesting that water was initially squeezed out of the cell but the force was eventually sufficient to negate the water loss. In addition to not representing the correct cellular dimensions which would affect the modelling, the force was not sufficient to rupture the cells, meaning that no

useful information can be taken from this data. However, the results were promising and showed an advance in the technique.

To further the protocol, it was necessary to use the second motor on the HSRT, the piezo-electric stack. Using the piezo stack required an alteration of the technique, as the motor is positioned below the chamber, which is then pushed upwards towards the probe during compression. The stack must be reset after every motion to ensure the upper limit of  $80\ \mu\text{m}$  was not breached. The maximum speed of the piezo stack is unknown, but it was considered unwise to use any more than necessary. A sample of col0 was compressed at  $1500\ \mu\text{m s}^{-1}$ . This was the maximum speed at which the tomato cells had been compressed. Force-deformation data for these compressions showed increased response in the force trace but still no evidence of force sufficient to rupture the cells. It was possible that the rupture forces were very small and had gone unnoticed. To see if this is the case, a signal amplifier was used, to amplify the voltage signal from the transducer by 10 fold.

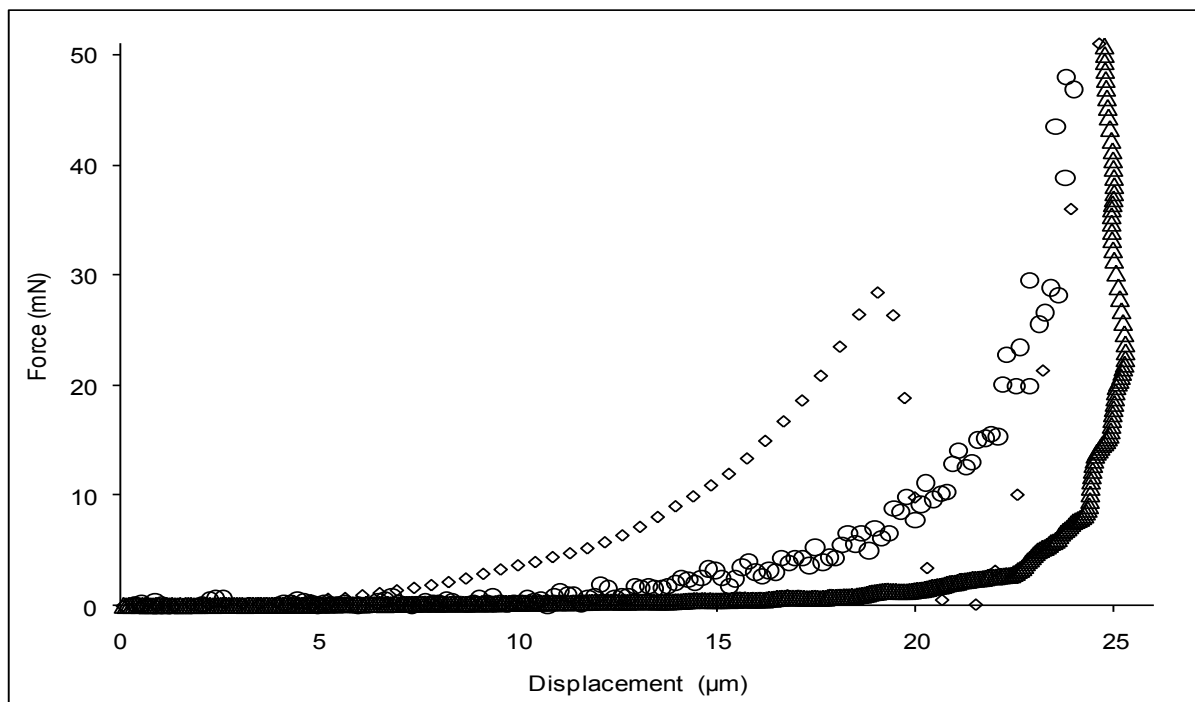


**Figure 6.6:** shows the stages in development of the compression of *Arabidopsis thaliana* single cells. Each curve demonstrates a typical example of a force/deformation curve calculated from the data at each stage. The triangle curve represents cells compressed at  $68\ \mu\text{m s}^{-1}$  using the LSRT. The circles represent cells compressed at  $200\ \mu\text{m s}^{-1}$  using the stepping motor on the HSRT. The diamonds represent cells compressed at  $3000\ \mu\text{m s}^{-1}$  using the piezo-electric stack on the HSRT with the output voltage from the transducer amplified  $10\times$ . The diamond curve follows the pattern seen in figure 5.9, typical of what is expected of a cell rupture.

## Chapter 6: Compression Testing

The cells compressed using the amplifier showed increased information in the low strain area, with the first bursts seen. However this was rare, raising concerns over the protocol being used. To investigate the hydraulic conductivity, a series of TIF images from a video of cell compression were manually analysed by image analysis by Professor C.R. Thomas to investigate the volume changes involved during compression, enabling an estimation of the  $L_p$ . The cells were stained with neutral red so therefore were seen to be viable. If the water loss was negligible, the volume should remain constant until rupture. Through this manual image analysis, a rough estimate of  $L_p$  was calculated of  $30 \times 10^{-6} \text{ ms}^{-1} \text{ MPa}^{-1}$  for this cell (Wang et al., 2006). Compared with the values above stated for the range of water loss that is acceptable for viable cells, this value is at the lower of the viable scale and a factor of 10 greater than that of the tomato cells.

The value calculated for the hydraulic conductivity suggested that even at  $1500 \mu\text{ms}^{-1}$  the hydraulic conductivity was too high for the water loss during compression to be considered negligible. It is possible that single *Arabidopsis* cells have very porous membranes and a very high hydraulic conductivity. This appears that this high hydraulic conductivity is related to the cells in suspension, as the hydraulic conductivity of *Arabidopsis* cells *in planta* is much lower. The  $L_p$  of cells *in planta* is in the region of  $1 \times 10^{-8} \text{ ms}^{-1} \text{ MPa}^{-1}$ , this is significantly lower than that of the cultured cells (Ranathunge and Schreibe, 2011).

In a final attempt to gain the force/deformation data required, it was decided to double the rate of compression to  $3000 \mu\text{ms}^{-1}$ , far beyond any speed that had been used previously. A sample of col0 cells was tested at this speed; the signal amplifier was also used to ensure any ruptures were identifiable. The maximum data acquisition rate of 10000 samples a second was used, increasing the total number of data points. With these values, an average cell of  $25 \mu\text{m}$  would return a complete compression with 85 points. In comparison, the same cell compressed at  $68 \mu\text{ms}^{-1}$  with a sample rate of 1000 samples per second would give 380 data points. This severely limits the amount of data that is available for analysis but was unavoidable.

This speed was finally sufficient to allow water loss to be negated and to rupture the cells. A sample of col0 cells was compressed at  $4000 \mu\text{ms}^{-1}$  to ensure  $3000 \mu\text{ms}^{-1}$  was sufficient. No differences were

seen between these two sets, however this may have been limited by the maximum rate of data acquisition.

Cells of each genotype were compressed using the same protocol and yielded similar force/displacement curves. Thus establishing a reliable protocol for the generation of the force deformation required. The final curve of figure 6.6 depicted by diamonds demonstrates an example of this, however this is amplified so the actual rupture force was 10× lower.

Samples of all four genotypes were compressed with this protocol at one and two weeks after initiation of the culture. The evidence in section 4.7.1 suggests that this was when the most single cells were available for compression. This enabled an investigation into the maturation of the cell wall and whether it has any effect on the cell wall properties. Samples for compression were generated using the protocol established in chapter 4 allowing paired analysis of each genotype after 1 and 2 weeks post culture initiation.

### **6.6 Results**

From the force/deformation data generated from the compressions of the four genotypes after 1 and 2 weeks in culture allow three parameters to be extracted. The diameter of the cell, the force required for membrane rupture the cell and the deformation at which the rupture occurred. The averages for each of these parameters for the four genotypes at one and two week after initiation can be seen in table 6.1. Analysis of variance shows no significant difference due to cell age allowing all the results to be pooled into one group for each genotype, which allowed more accurate statistical analysis.

As the cells in plant grow, a process of maturation occurs. This entails additional polysaccharide deposition and fibre cross-linking. As there is no effect of age on the rupture properties of the cells, it is possible that the maturation of the cells in culture may be different to the maturation of those in the plant. As if normal maturation were to occur, a difference in mechanical properties would be expected as the additional deposition and crosslinking occurs.

Genotype	Week	Cell Diameter ( $\mu\text{m}$ )	Rupture Force (mN)	Displacement at Rupture (%)
Col0	1	26.8 $\pm$ 2.6	1.1 $\pm$ 0.3	59.6 $\pm$ 8.3
	2	24.6 $\pm$ 1.7	1.6 $\pm$ 0.5	55.0 $\pm$ 6.0
<i>ida</i>	1	23.0 $\pm$ 1.2	0.8 $\pm$ 0.2	52.2 $\pm$ 5.8
	2	22.7 $\pm$ 0.4	0.8 $\pm$ 0.1	56.2 $\pm$ 5.2
<i>mur1</i>	1	26.8 $\pm$ 1.4	2.0 $\pm$ 0.6	53.0 $\pm$ 6.0
	2	24.2 $\pm$ 3.1	1.8 $\pm$ 0.5	47.4 $\pm$ 7.2
<i>sks</i>	1	25.4 $\pm$ 3.4	1.4 $\pm$ 0.5	63.3 $\pm$ 6.3
	2	28.4 $\pm$ 3.5	1.4 $\pm$ 0.4	60.0 $\pm$ 7.1

**Table 6.1:** Shows the average cell diameter, the average rupture forces and the percentage deformation at rupture for 1 and 2 week old suspension cultures of the four genotypes analysed. Error is equal to the standard error. There is no significant effect of age, enabling the pooling of the data sets ( $P < 0.05$ )

Figure 4.6 suggests that the cells in culture reach a maximum average cellular diameter during this period, which also implies that growth was not affecting the compression data (table 6.1). Figure 6.7 (A) shows the average cell diameters determined from the compression testing, these averages agree with those found in figure 4.6, approximately 25  $\mu\text{m}$ .

Comparing the forces at rupture of the single cells can give a preliminary insight into the mechanical properties; this comparison can be found in Figure 6.7 (B). From these data it can be determined that the *ida* mutation shows significantly lower forces at rupture compared with the *sks* and *mur1* cells, this is supported by analysis of variance. Col0 shows no differences to any of the other genotypes.

In Figure 6.7 (C) a comparison of the average percentage displacements at rupture can be seen. This can be seen as a measure of the flexibility of the wall and is taken to be the point at which the force applied to the cell is sufficient to cause membrane rupture as the inherent flexibility in the wall has been mechanically compromised. From the graph, no differences between the genotype were found suggesting that the mutations do not affect the flexibility of the wall.

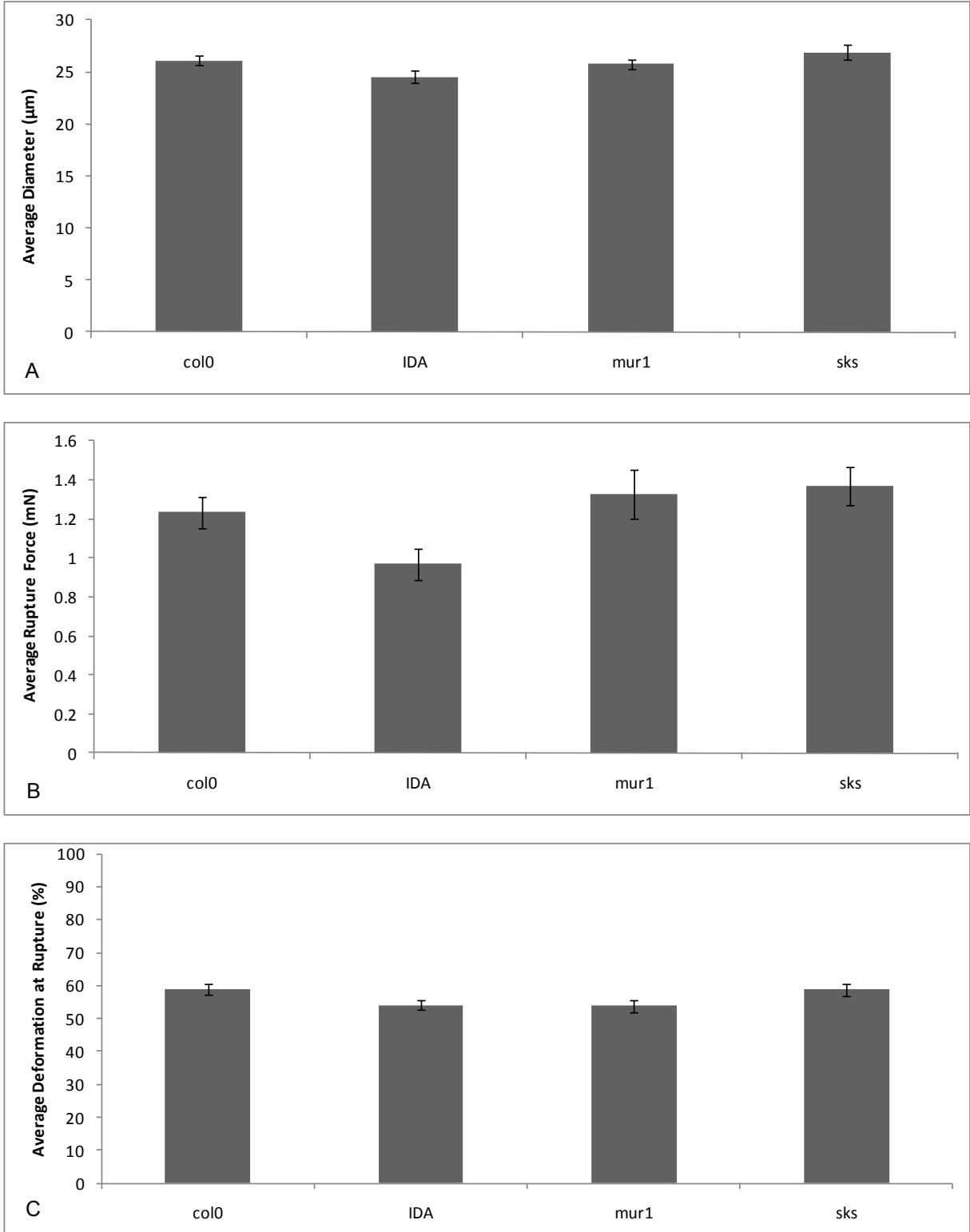


**Figure 6.7:** (A) Average diameter of the cells from the compression data for each genotype; (B) average force required for rupture for each of the genotypes; (C) the average percentage deformation at rupture for each of the genotypes. The error bars show the standard error. The mur1 and sks mutations show a statistically higher ( $p>0.05$ ) force required to rupture the cells when compared to the IDA mutation.

## 6.6.1 The relationship between cell diameter and rupture force

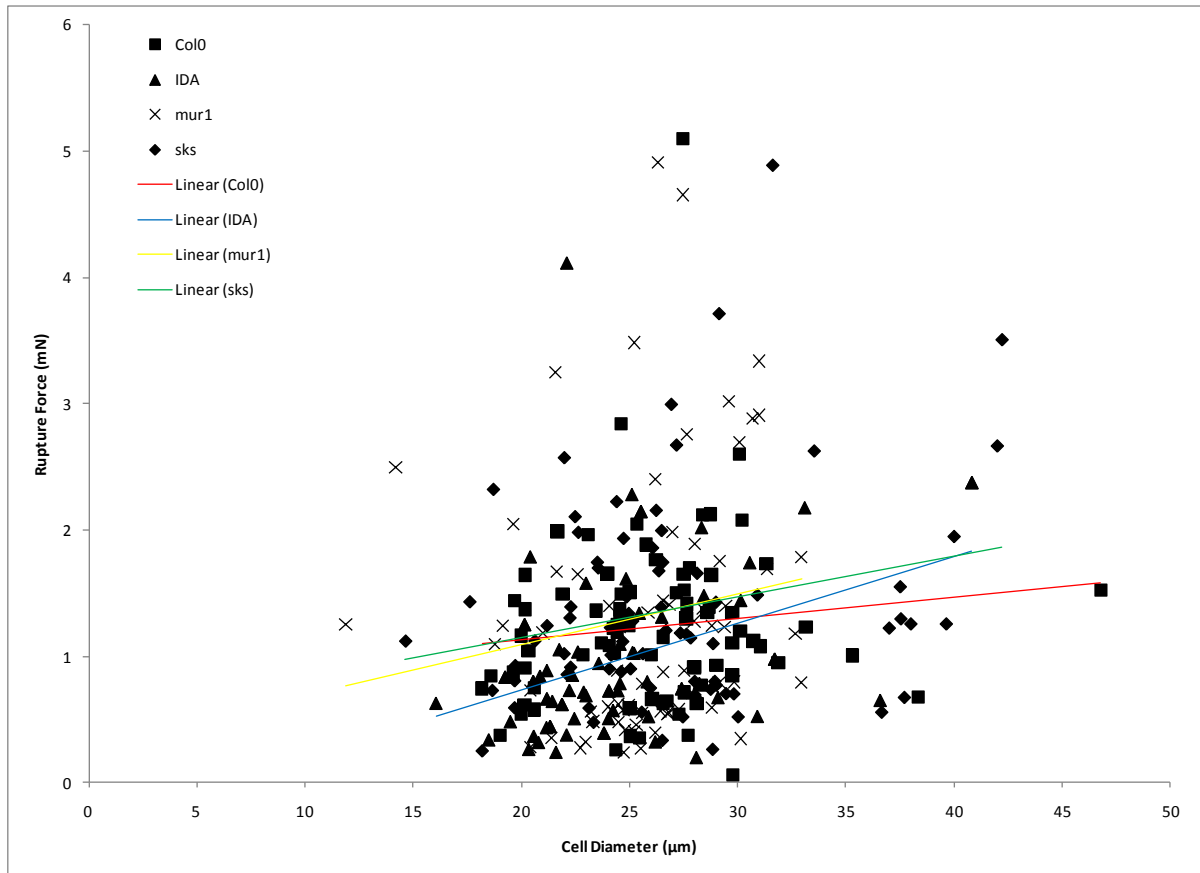


*Figure 6.8 shows the relationship between cell diameter and the rupture force for each of the genotypes. For each a linear trend line represents the general trend for the cells compressed. All trend lines show a positive agreement for this relationship.*

Figure 6.8 shows the relationship between the cell diameter and the rupture force of each cell of all genotypes compressed. It can be seen that the majority of the cells compressed appear in a 10 μm range (20-30 μm) and clearly show a great level of variation of rupture force. An example of two col0 cells highlights this; both are approximately 30 μm in diameter, but one ruptures with nearly no imposed force the other closer to 5 mN; however these are extremes with the majority of the forces falling between the 0.5 mN and 2 mN.

Even with this biological variability, the trend lines for each show agreement for the relationship. As discussed previously, maturity of the wall affects the amount of material present and the number level of cross-links. When the diameters of the cells for each genotype (figure 6.7 (C)) were compared, no statistical differences were seen between the diameters. This suggests that these differences seen in

the linear relationships are due to genotypic differences, either in wall thickness or the mechanical strength of the materials present.

### 6.6.2 The relationship between the cell diameter and the percentage deformation at rupture

Comparing the relationship between the percentage deformation at rupture and cell diameter has shown some interesting results. This relationship in yeast cells shows a negative trend. This relationship is also seen in three of the four genotypes. The linear relationship of the Col0 shows a much steeper gradient when compared to IDA and Sks, which exhibit near parallel lines. However mur1 shows an agreement, opposite to the other genotypes.

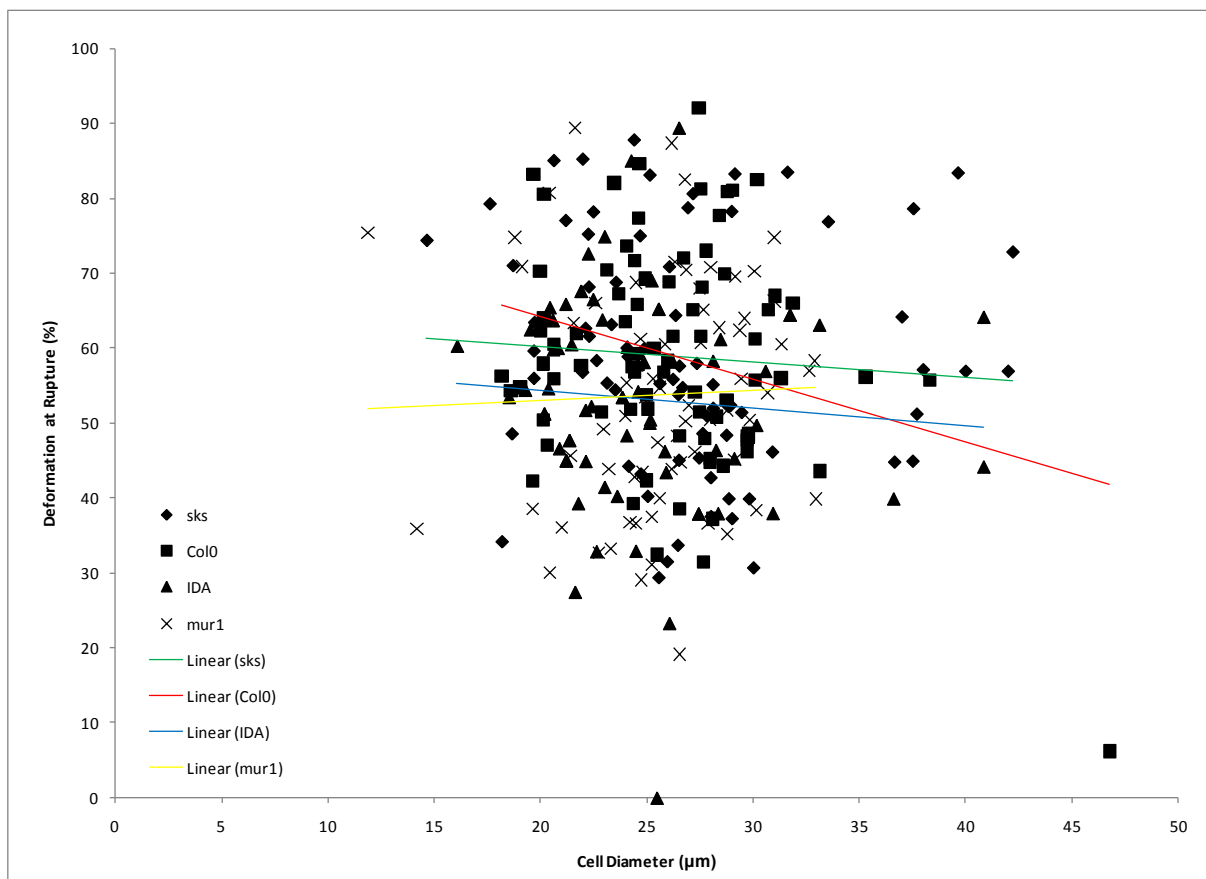


**Figure 6.9:** shows the relationship between cell diameter and the percentage deformation at rupture. Each genotype has a general line demonstrating a general relationship between the points. For all but mur1, a negative trend was seen.

## 6.6.3 The relationship between the percentage deformation at rupture and the rupture force

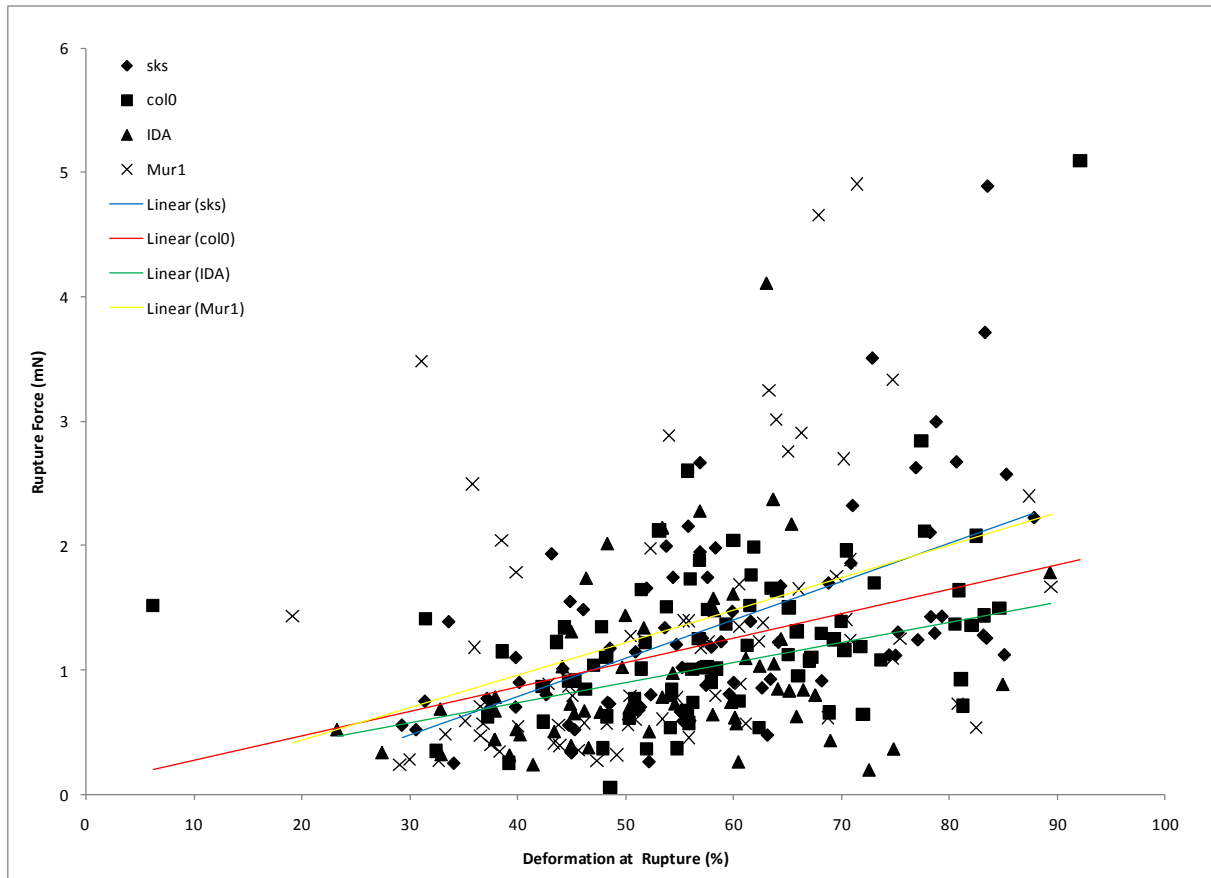


**Figure 6.10:** the relationship between the percentage deformation at rupture and the rupture force. Each genotype has a linear trend line, all of which show a positive trend.

The relationship between the percentage deformation at rupture and rupture force show positive trend for all of the genotypes. These data are representative of previous comparisons of the data from other organisms, e.g. yeast, which showed positive correlation. From this comparison, the stiffness of the walls can be inferred. A stiff, in-flexible wall will likely rupture at lower forces and at lower deformations. The data for the *A. thaliana* cells suggests that the majority of the cells show an intermediate % deformation with low rupture forces, suggesting a certain degree of flexibility.

#### 6.6.4 Non-bursting cells

Each population had a number of cells that did not rupture, even if the NR had stained the vacuole. The force/deformation curves for these cells resembled those compressed at lower speeds, see figure 6.6 using the curve for  $68 \mu\text{ms}^{-1}$  as an example. The walls or membranes of these cells may have been damaged but still intact. When the force was applied the membranes/walls failed and no ruptures were recorded. Therefore these compressions could not be analysed, nor carried forward for mathematical modelling, as there was insufficient data and this would have wasted time. This accounted for approximately 30% of the cells compressed. It is possible that even at  $3000 \mu\text{ms}^{-1}$  the hydraulic conductivity of some cells was still too high to allow a force to be generated.

#### 6.6.5 Elastic limit

When tomato cells were compressed they were found not to be linear elastic up to failure (Wang et al., 2004). Instead they reached an elastic limit, after which they no longer behaved elastically. This behaviour was also found for the *Arabidopsis* cells. The wall itself will have a limit to which it will be able to recover from exhibiting elastic behaviour. This is called the elastic limit, beyond which the wall will suffer permanent deformation, which is a visible when the cell does not recover its original shape.

To determine the elastic limit, cells were compressed to increasing increments of a percentage of the maximum diameter. This was done in 5% increments, replicating the protocol for tomato cells (Wang et al., 2004). Video footage was analysed to ensure cells returned to the original dimensions after the compression, demonstrating elastic behaviour. Once the cells did not return to the original dimensions, plastic deformation had occurred and the cell had reached or exceeded the elastic limit. This was found to be comparable with tomato cells, at between 30-35% for all genotypes. The percentage deformation refers to the diastral compression (e.g. the displacement of the probe) of the cell, not the deformation of the material is discussed in more detail in section 7.4.3.

## 6.7 Discussion

During the course of the compression testing many problems arose. Although section 4.7.1 suggested that there would be sufficient cells to complete the investigation this was not the case in practice. As only a small volume of the sample could be analysed at a time, only a portion of these single cells were available.

Visualisation of these cells by the horizontal camera was often difficult, as single cells were obscured by larger aggregates of cells. These had to be ignored as the diameter of the cell and distance from cell to probe could not be accurately measured. Using the inverted camera to locate cells suitable for compression was not always reliable, as debris might appear spherical, but were shown to be flat with the horizontal camera, or alternatively within the circumference of the probe blocking complete compression of a spherical cell. Time was lost locating spherical cells that were seen using both cameras, reducing the potential number of cells that were compressed.

The micro-compression rigs have utilised the same principles for several iterations of the design. It was initially anticipated that the *Arabidopsis* cells would behave in a similar manner to the tomato cells. Unfortunately, this was not the case. The hydraulic conductivity of the *Arabidopsis* single cells proved too high for data to be collected at low speeds. Several, smaller speed increments were trialled, all of which shown gradual improvements in the responses seen in voltage trace, but were ultimately seen as method development in the process of optimising the technique. The speeds of compression available range from as low as  $23 \mu\text{ms}^{-1}$  to the newly established maximum of  $3000 \mu\text{ms}^{-1}$ . However as a development of the method it was important that a protocol be established for the generation of data from the *Arabidopsis* cells. The acquisition of the compression data pushed the current equipment to the limit of the capabilities. Faster speeds of compression could not have been realistically used as the sample rate was at a maximum. The compression of an average cell only yielded 85 data points, this number would have been significantly reduced if the speed were increased. However, if the speed of  $3000 \mu\text{ms}^{-1}$  was insufficient it is possible that any increase would have been ineffectual.

## Chapter 6: Compression Testing

Initially, it was theorised that the cells might show some degree of maturation. Maturation would involve biochemical modification that would alter the properties of the wall, mirroring changes that are occur in the plant, for example cells moving through the developmental zones of the root, leading to polysaccharide deposition and additional cross-linking (chapter 2.9). These differences were not found. However the results enabled the elimination of cell age as a factor. The environment in culture appears to have been conducive to division, but has prevented maturation in addition to cessation of differentiation that was required (chapter 4).

As it was found that the ages of the cultures had no effect on the physical properties of the cells, it enabled the data to be analysed as one data set rather than two smaller ones. This allows for greater statistical certainty of any conclusions with a larger number of repetitions for each to compare, with approximately 70 cells for each genotype. With this greater pool of data to draw upon, these initial measurements were analysed and compared. Through analysis of variance of the effect of genotype on rupture force, IDA was shown to be statistically lower than *sk5* and *mur1*. The initial aim of the investigation was to prove that through the use of micro-compression those differences in the mechanical properties of single *Arabidopsis* cells could be seen. Although the rupture force is not an intrinsic property, it does demonstrate a statistical difference suggesting that further investigation through mathematical modelling would be beneficial. More information will be extracted through the modelling and allow the genotypes to be compared on an intrinsic level, which was the other initial aim of the project.

Cells dimension from the compression testing reaffirm those observed in chapter 4. These measurements in chapter 4 were conducted as a preliminary investigation into the relevance of the cells in culture to those of the aggregates and therefore the population. Having the figures from this chapter mirror those, reiterates the representative nature of the single cells.

## 6.8 Conclusions

To generate the required force/deformation data the current equipment was pushed to the limits of its operating potential. The elevated hydraulic conductivity was potentially caused may have been caused by the high surface area to volume ratio and/or a highly porous membrane. Despite this obstacle, modifications to the technique allowed the data to be generated. However the causes of this increased hydraulic conductivity would make an interesting investigation in the future (section 8.3)

The data presented in this chapter proves that differences can be detected in the properties of single *Arabidopsis* cells. Through biochemical analysis in chapter 5, the levels of cellulose were found to be lower in *sks* and *mur1* when compared to *col0* and *IDA*. It would have been presumed that this change in biochemistry would have reduced the mechanical properties of these two genotypes. However this is not the case; and the rupture forces are found to be higher. Results from chapter 3 suggest that at the plant level, the *mur1* and *sks* mutations severely affect the growth of the plants and that lower mechanical properties would have been anticipated.

The occurrence of an elastic limit at approximately 30% means that this rupture force many not is taken as a figure for direct comparison. This limit means that only the first 30% of the compression information relates to the elastic behaviour and therefore the point at which the current model is applicable (chapter 7). This apparent rupture point occurs beyond this limit so allows only tentative conclusions towards the ultimate effects of the mutation.

The rupture force is not an intrinsic mechanical property. Therefore they have values that are dependant on the method of measurement and therefore can only be used as a preliminary indicator of the underlying mechanical properties. Through the more detailed analysis of the mathematical modelling, the intrinsic parameter of the elastic modulus can be determined from the force/deformation data. This value giving a figure on which the affects of the biochemical changes on wall properties can be compared. This analysis can be seen in chapter 7. With culture conditions standardised (figure 4.4); and with age and growth negligible, any differences seen can be attributed to the mutations and the biochemical changes (chapter 5) they have on the wall.

## Chapter 6: Compression Testing

From an engineer's perspective, the data received at these speeds is necessary to discover the true mechanical properties. However, biologists are more concerned with the time dependant effects of growth. As growth is not an instantaneous, but rather a dynamic process that is as proactive as it is reactive. A plant physiologist may be cautious of measurements of biological materials at such high speeds, as any results may not be relevant to the biological processes that are occurring. However it should be remembered that the mechanical properties of the wall have bearing on growth, regardless of the time scale. This was addressed in the selection of the mutations (section 3.2), taking those directly affecting polysaccharides present in the wall. Changes that would occur in the wall of each cell in the plant, therefore the affect time dependant nature of biological investigations and a distinct relevance to these investigations.

Despite the current limitations of the raw compression data, it has shown that difference in the cell wall composition cause detectable differences in the single cells. Not only this but differences were found at this level and it is anticipated that the application of more refined data analysis through mathematic modelling will extract the intrinsic info that was sought at the outset of this investigation.

## ***Chapter 7: Determining Mechanical Properties by Mathematical Modelling***

---

In order to investigate mutational effects on cell wall mechanical properties, more information about these properties must be ascertained. Preliminary interpretation of the compression data (chapter 6), must be consolidated with further analysis enabling more comprehensive conclusions to be drawn. Through computer modelling, it is possible to determine intrinsic mechanical properties (section 2.14.2). An intrinsic property is one where the result remains the same regardless of how it is measured. This method has been used for this purpose for single tomato cells (*Lycopersicon esculentum* vf36) (Blewett et al., 2000); yeast (*Saccharomyces cerevisiae*) (Stenson et al., 2009) and many other microscopic particles (Zhang et al., 2009). The following chapter introduces the modelling procedure and its optimisation for single *Arabidopsis* cells. The results of the modelling allowed direct comparison of the effects of the mutations on cell mechanical properties. With this information, conclusions were drawn about the relationships between plant growth data and single cell compression data.

### **7.1 Using a Mechanical Model to Determine Intrinsic Mechanical Properties**

An analytical model of single cell compression provides a means of interpreting experimental force/deformation data to quantify the elastic behaviour and failure of the wall. Simulation using implementations of the model for tomato and yeast have yielded elastic moduli and stresses and strains at failure (Thomas et al., 2000). It was hoped that similar information could be obtained for *Arabidopsis*. This was not self-evident as *Arabidopsis* cells from culture are generally smaller than either cultured tomato cells or directly recovered tomato fruit cells.

The most recent model, 'the Stenson yeast model' was created to investigate the mechanical properties of baker's yeast (*Saccharomyces cerevisiae*) It incorporated a revision of the stress-strain

model of previous work, thereby affecting the simulated cell wall behaviour (Stenson *et al.*, 2009). It was a development of a previous model used on tomato cells (Wang *et al.*, 2004) and this was the model that was initially applied to *Arabidopsis* cells. Both of these models built on work on sea urchin eggs of Feng and Yang (Feng and Yang, 1973) and Lardner and Puraja (Pujara and Lardner, 1979). Both assumed the cell is filled with incompressible liquid and water loss is negligible, but did not assume that the cell wall tensions are isotropic (uniform in all directions) as in earlier work. The models are based on a choice of cell wall material constitutive relationships. The governing equations relate the stresses and strains to the geometry during compression (Zhang *et al.*, 2009). The geometry is expressed in terms of the stretch ratios, the length of a section in a given direction following deformation divided by its original length.

The key parameters that are to be determined are the initial stretch ratio, a measure of cellular level of cellular inflation due to turgor and the cell wall elastic modulus. The simulations fit model predictions using values of the initial stretch ratio to the experimental data to enable the derivation of the of the elastic modulus (Stenson *et al.*, 2009). The software developed by J.D. Stenson and C.R. Thomas incorporates this model adding user-friendly input and output functions, including identification of the baseline calculation, the start of compression and the bursting point (if any) and the cell size. Manual intervention is permitted if the user does not agree with interpretation of the data by the software.

### **7.2 Adapting the existing software for *Arabidopsis thaliana* cells**

The Stenson yeast model was applied to a test set of col0 compression data using the associated software. The cells had been stained with NR by the method described in section 6.5. The vacuoles of these cells were seen to be red, indicating viable cells with intact membranes (section 4.5). Of the 10 cells tested, all were returned as dead by the program; the software was designed to identify and ignore dead cells so they would not be unnecessarily processed. With the NR proving the cells to be viable, there must be aspects of the data that the software could not handle that caused it to stop processing that cell.

### 7.2.1 Number of Data Points

Upon investigation it was found that the number of data points available for many of these cells was below the minimum set in the software for reliable processing, e.g. 300. This was due to the speed of compression required to make it possible to assume negligible water loss during compression (section 6.5). The high speeds and relatively small size of the cultured *Arabidopsis* cells limited the time for data acquisition. Despite the rate of acquisition being increased to the maximum possible, (10000 samples a second) it was calculated that an average cell of 25  $\mu\text{m}$  would only return 85 data points (section 6.5). Professor C.R Thomas therefore amended the minimum amount of data points for a cell to be considered viable to 125. This was taken from the average number of data points per compression as 85 plus (reduced slightly to allow for smaller cells) the 50 that are required for the baseline calculation (section 7.2.2). The test set was processed again, resulting in 5/10 fulfilling the criteria for to be considered viable. All the cells had passed the minimum data required, but had failed a subsequent level. This was still considered inadequate given all the cells were shown to be viable by NR staining

### 7.2.2 Baseline Identification

Identification of the baseline by the software is used to obtain a measure of the background voltage, e.g. when the probe is not touching the cell. This must be subtracted from the experimental data. As a function of the software, the baseline was found from the force-deformation data. It was found that this baseline identification was responsible for flagging the other cells as dead. The model divides the area prior to the compression into blocks of 25 data points. In the yeast model, the baseline was determined as the most frequent voltage in the 2 blocks prior to the initial point of contact. The most frequent voltages for these blocks were compared, and if the difference was outside of a user set tolerance the cell was classed as dead. For *Arabidopsis* the software was unable to determine the median values reliably due to the fluctuations in this region caused by the greater noise in the data. The noise is presumably caused by the speed of compression and the addition of the signal amplifier.

Professor C.R. Thomas replaced the frequency derived baseline with an earlier version of the baseline calculation (Wang et al., 2004) which utilised the averages of the first two blocks to calculate the

baseline. The data was re-analysed and 7/10 cells from the test set were processed as live. Cells where the averages of the two blocks were not within a user set tolerance were counted as dead. In a final attempt to calculate the baseline, the number of data points was reduced to only the first block of data points. This reduction resulted in 9/10 cells from the test set being processed as they were seen to be viable by the constraints of the model. Figure 7.1 represents this. The black and grey points prior to the rupture peak are the two blocks, to allow 9/10 through; only the black points were taken to calculate the baseline.

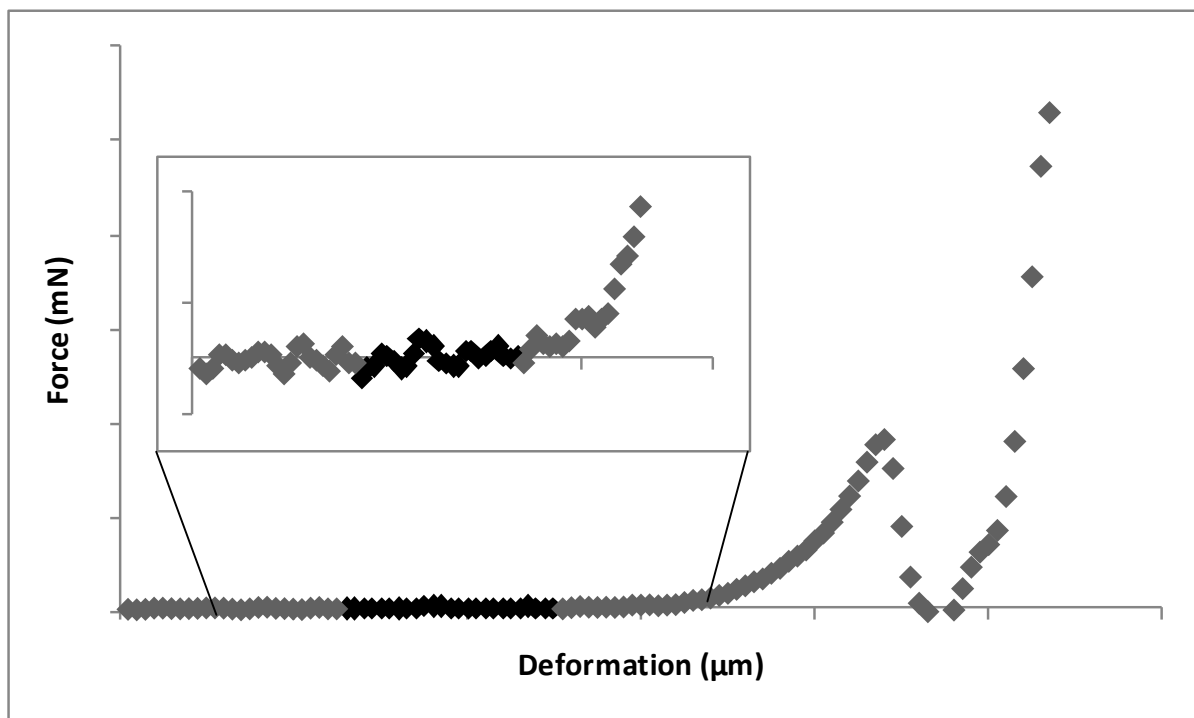


**Figure 7.1:** Highlights the change in baseline calculation for *Arabidopsis thaliana*. The data are force/displacement information from the compression of a single *Arabidopsis* cell approximately  $25\mu\text{m}$  in diameter. Before this modification any cells where the average of the first two blocks (1 block = 25 data points) was not within a user set tolerance the cell was dismissed as dead and not processed. Due to the noise of the baseline this meant that the majority of the cells were initially classed as dead, which NR staining (section 4.5) had suggested these cells were viable. Therefore, the software was modified to calculate the baseline as the average of the first block. In the figure the points in black (block 1) demonstrates this region.

### 7.2.3 The Initial Point of Contact

Adjustments to the software had enabled 9/10 cells from the test set to be process as live. The final cell from this set was found to have failed because the initial point of contact between the cell and the probe was incorrectly assigned. The software takes the initial point of contact as the first point after which the voltage does not return to the baseline until the bursting criteria have been satisfied. These are used to identify a burst, by a series of consecutive points with a drop in force. Such a series of points can be seen in figure 7.2 just after the burst.

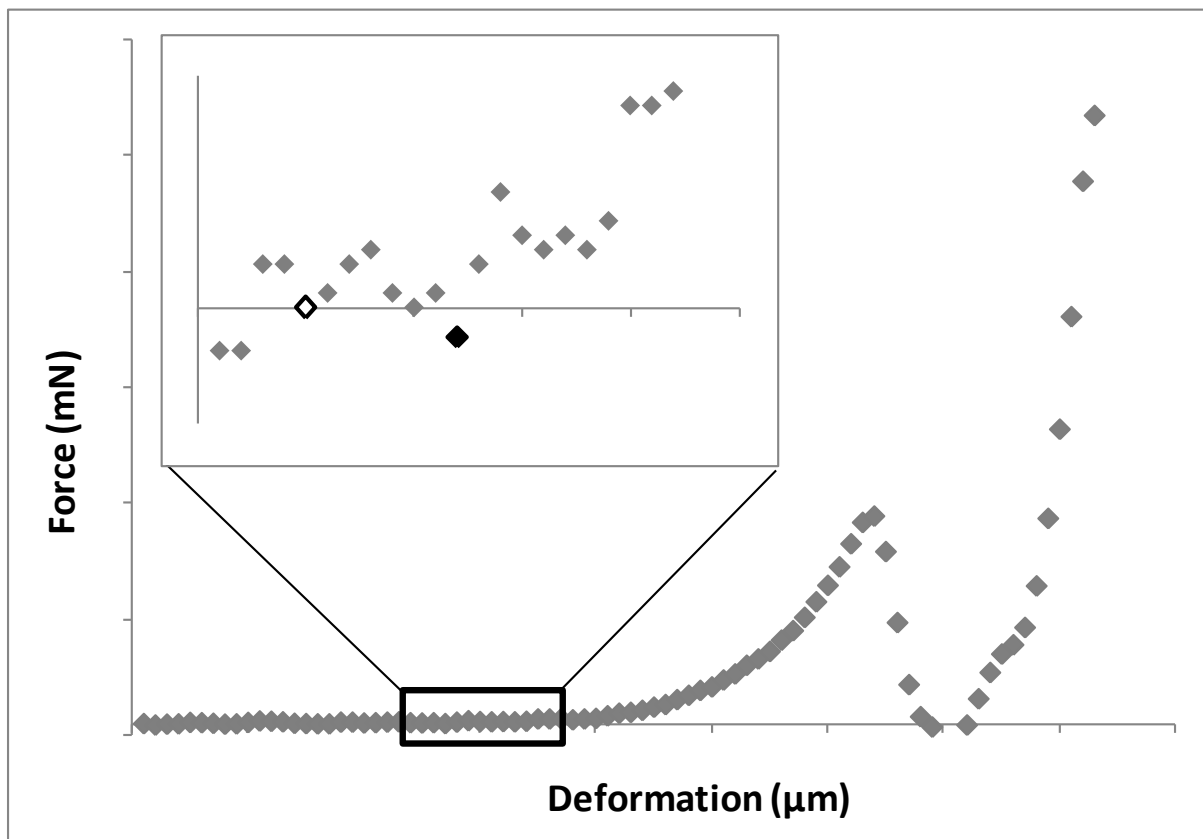


*Figure 7.2: gives an example of the selection of the initial point of the compression using the manual intervention function. The data are the force/displacement data for the compression of an Arabidopsis single cell approximately 25  $\mu\text{m}$  in diameter. The model would have selected the white point as the initial point of contact however the cell would therefore fail on other criteria. Therefore manual intervention was utilised to select the black point as the initial point of contact as this is the point from which the data does not return to the base line before rupture.*

To allow for problems in identification of the correct baseline or the initial point, a manual intervention routine of the software was utilised; demonstrated by figure 7.2. In this example the initial point would have been taken to be the white point as it was the first point to fulfil the criteria. Manually selecting the black point (fig 7.2) as the initial point of contact allowed the bursting criteria to be fulfilled allowing the cell to be processed as live. The software automatically recalculates the baseline from the new initial point, using the modification established in section 7.2.2.

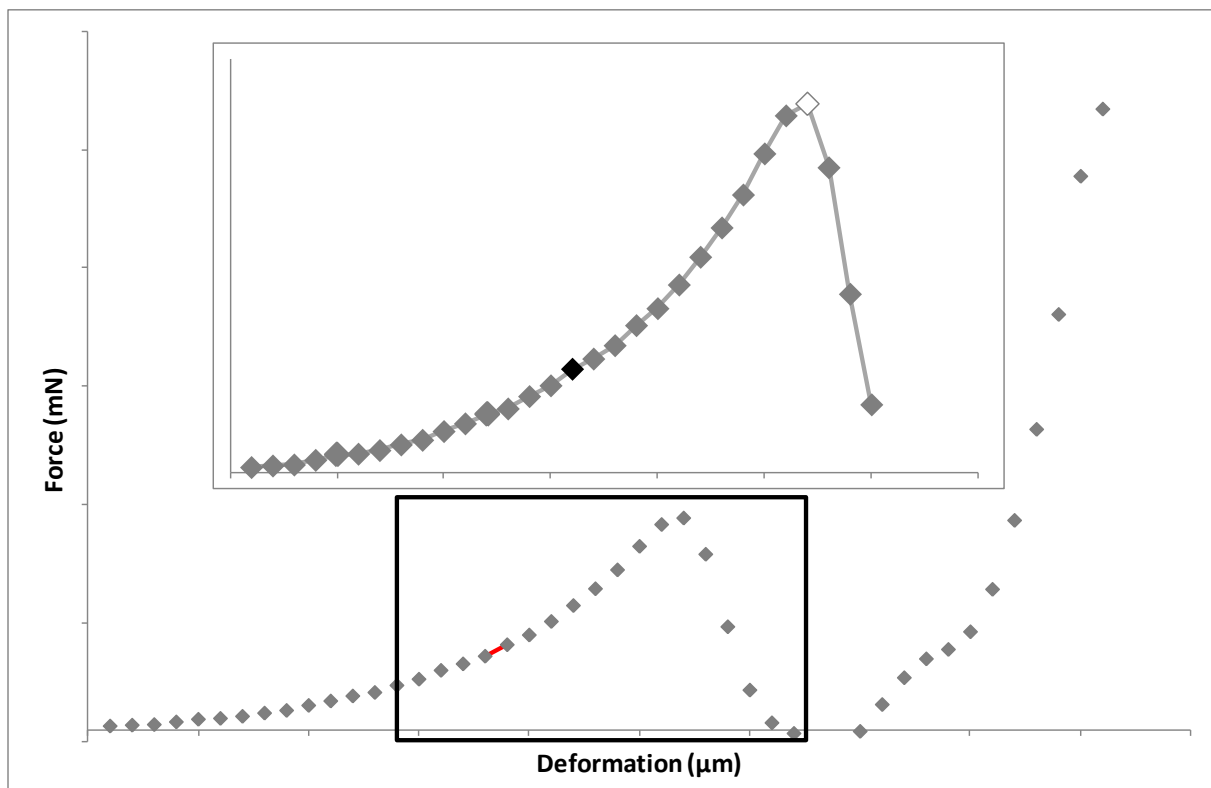


**Figure 7.3:** *The selection of the elastic limit using the manual intervention. The cell no longer behaves elastically after approximately 30% dimetral deformation. This required the selection of the data between the initial point of contact of probe and cell and elastic limit. The manual intervention function was utilised to select the elastic limit as the rupture point ensuring the model was fitted the desired range. The white point is the point at which the cell ruptures and was chosen by the software as the bursting point. The black point is the elastic limit; this was manually selected as the rupture point to omit the plastic region from the fitting procedure. Although the elastic modulus was found from a reduced set of data points, the bursting force was still identified correctly (as the white point in this illustration)*

From the compression data (chapter 6), it became clear that the *Arabidopsis* cells were not elastic up to failure. The cells demonstrated an elastic limit of approximately 30-35% deformation. Evidence from tomato cells (Wang et al., 2004) showed a similar voltage profile, and it was suggested that the walls are elastic until reaching an elastic limit at approximately 30% deformation after which the walls exhibit plastic behaviour until failure.

Due to the similarities of elastic limit and force/deformation profiles between the *Arabidopsis* and tomato cells, it was presumed that the *Arabidopsis* also behave plastically after the elastic limit. This therefore limited the amount of usable data that can be modelled from the compressions. As only those points up to the elastic limit can be usable, the model is not currently able to process this plastic region. Therefore the calculation of the elastic modulus at rupture was not possible. Using the manual intervention function of the software, similar to that used to identify the initial point of contact outlined above, allowed the elastic limit to be chosen as the bursting point. By selecting the elastic limit as the bursting point the range of data available for the model to fit the simulations to will be limited to the elastic data. Truncating the data in this way allowed the region of plastic deformation to be ignored as this was not applicable to this model. Therefore, the model will output a 'low strain' elastic modulus ( $E$ ) for the cells (Wang et al., 2004).

These amendments to the software allowed 98% of the cells producing force-deformation data to be processed. In addition to  $E$ , the model will output several parameters: the diameter of the cell; elastic limit; stretch ratios ( $\lambda$  -s) and the correlation coefficient.

### 7.2.1 Input Parameters

Table 7.1 gives the input parameters required and the values used. Compression speed was the speed of motion used; data capture interval was the sample rate used; volt-force and compliance were calculated with the transducer calibration (appendix 3). The initial thickness ratio, the ratio of the uninfected cellular diameter and the primary cell wall thickness, was calculated from the transmission electron microscopy (TEM) (Leboeuf et al., 2005), as described in section 7.3.

Input Parameter	Value
Compression speed (microns $s^{-1}$ )	3000
Data capture interval (s)	0.0001
Volts to force conversion ( $mN V^{-1}$ )	51.8
Compliance factor ( $\mu m mN^{-1}$ )	0.00044
Initial thickness ratio	0.077

**Table 7.1:** *The initial input parameters required by the model. These values are used in the constitutive equations of the model, and are values that must be specific for the specimen. Compression speed and data capture are parameters chosen during the compression development (chapter 6.5). Volts and compliance are parameters of the transducer and were determined during calibration (appendices 8-10). The initial thickness ratio, is calculated from the initial diameters and the wall thicknesses (section 7.3)*

### 7.3 The Cell Wall Thickness

The thickness of the wall is presumed to have an effect on the mechanical properties. In the calculation of E it is necessary for an average wall thickness to be determined as this value cannot be calculated for each individual cell compressed. It is important to determine the effect that the wall thickness of the mutant genotypes has as the three mutations may have differing effects on the wall. In the roots the cell lengths were measured using light microscopy (section 3.5). Using visible light with its long wavelengths limits the maximum magnification, reducing the resolution at high magnifications. A high level of magnification and very high-resolution images were required for this investigation therefore a more powerful technique was required. Electron Microscopy replaces visible light with a beam of electrons. These have a shorter wavelength allowing for the high magnification required. The thickness of the cell wall is needed with the dehydrated diameter to calculate the initial stretch ratio, which is a parameter used in the model.

Samples of cell culture tissue were created using the method established in chapter 4, were prepared by the protocol in appendix 12. Ultrafine sections between 800-1000Å (SAKAI, 1980) were cut and stained in preparation for use in the transmission electron microscope (TEM)(Williams et al., 2009)

## 7.4 Results and Discussion

Output Parameters	col0	ida	mur1	sk5
Cell diameter (microns)	20.5 ±0.7	19.0 ±0.8	21.1 ±0.6	23.0 ±0.7
Deformation at elastic limit (microns)	6.3 ±0.2	6.6 ±0.3	7.5 ±0.3	7.5 ±0.2
% Deformation of the wall at elastic limit	31.7 ±1.3	35.4 ±1.1	35.9 ±1.2	34.0 ±1.1
Low strain elastic modulus (MPa)	23.3 ±2.2	24.7 ±2.1	16.6 ±1.4	20.0 ±1.6
Lambda-s	1.0 ±0.0	1.0 ±0.0	1.0 ±0.0	1.0 ±0.0

*Table 7.2: output values from the parameters calculated by the model. Values are averages of those output by the software and are shown with the standard errors.*

The information extracted by the model can be found in table 7.2. These results will be discussed in section 7.4.2

### 7.4.1 Transmission Electron Microscopy (TEM)

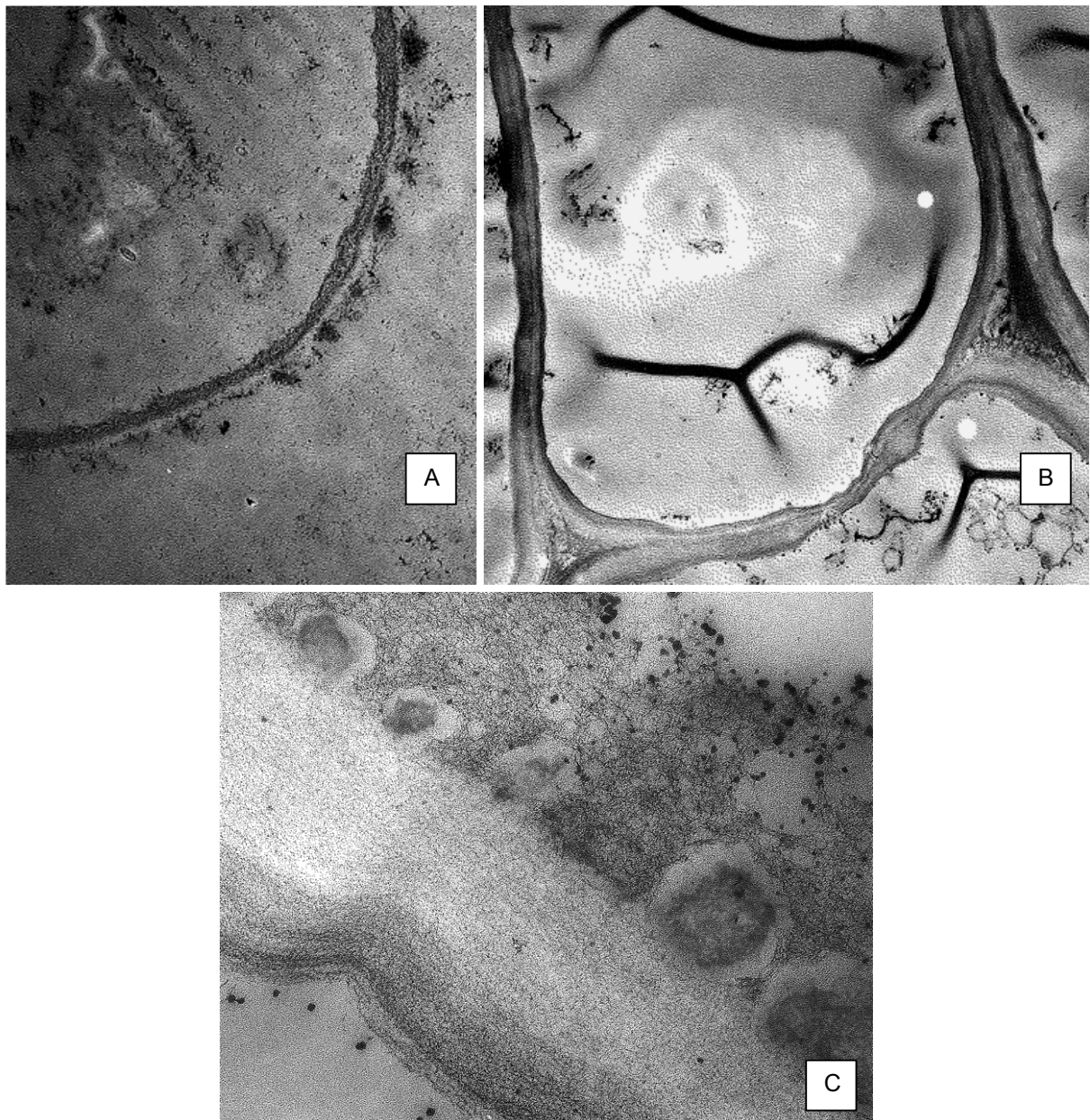


**Figure 7.4:** a selection of transmission electron microscopy micrographs. (A) Cross section of a single col0 cell at 5000 $\times$  magnification, the primary wall can be seen as the black band. On the outer edge an area of what is presumed to be pectin can be observed. (B) IDA cell contained within a cellular aggregate, 5000 $\times$  magnification. The primary walls of the adjoining cells are clearly visible, separated by a thin middle lamella. The triangular regions at the corners of the cells were also observed. (C) A cross-section of an sks wall from a single cell at 40,000 $\times$  magnification. The two regions of the wall, primary wall and the pectin rich region are clearly distinguishable. From this micrograph it can be seen that the two regions are of comparable thickness of approximately 300 nm. From the TEM micrographs (not all shown) the initial diameters were measured, to determine the initial thickness ratio for the input parameters.

From the TEM (Lebouff et al 2002), several micrographs were taken of each genotype. The wall thicknesses were calculated for the primary cell walls of each genotype. Figure 7.4 gives three examples of these photographs. These photographs were calibrated using photos of grids of known dimensions.

7.4 (A) give an example of a cross section through a single *col0* cell. Two regions are visible in the wall, the primary wall as the black band and beyond that a fuzzy region that is presumed to be a pectin rich region that would constitute the middle lamella of comparable thicknesses. The thickness of the primary wall varies little across the section, remaining around 300 nm.

Figure 7.4 (B) shows an aggregate of IDA cells, showing similarities to those in the plant, thick primary walls; thin middle lamella except at the triangular junctions. The primary walls appear to fluctuate in thickness ranging from approximately 80 nm to 600 nm at the corners. 7.4 (C) shows a cross section of an *sks* single cell. This highlights the two layers seen in 7.4 (A) at lower magnification. The two layers are of comparable thicknesses of approximately 300nm.

From the photographs, 25 measurements of single primary wall thickness were made for each genotype. The averages are shown in figure 7.5, these values suggested the thicknesses of single *Arabidopsis* primary cell walls range from 300 – 400 nm. When a sample of tomato cell walls were measured in the same manner, average thickness was found to be 685 nm. This makes them significantly thicker than the *Arabidopsis* walls. However these were much larger cells so comparatively these values are in agreement. When the *Arabidopsis* genotypes were compared, *sks* was found to produce significantly thinner primary walls than *col0*. Chapter 5 suggests that the amount of material present in the wall of cultured *sks* cells is significantly lower than that of *col0*. It is also known that the *sks* mutation causes a reduction in pectin in the primary cell wall. The *mur1* mutation was also shown to have reduced polysaccharide in the wall, which is not reflected in the wall thickness. There is a difference but it is not significant.

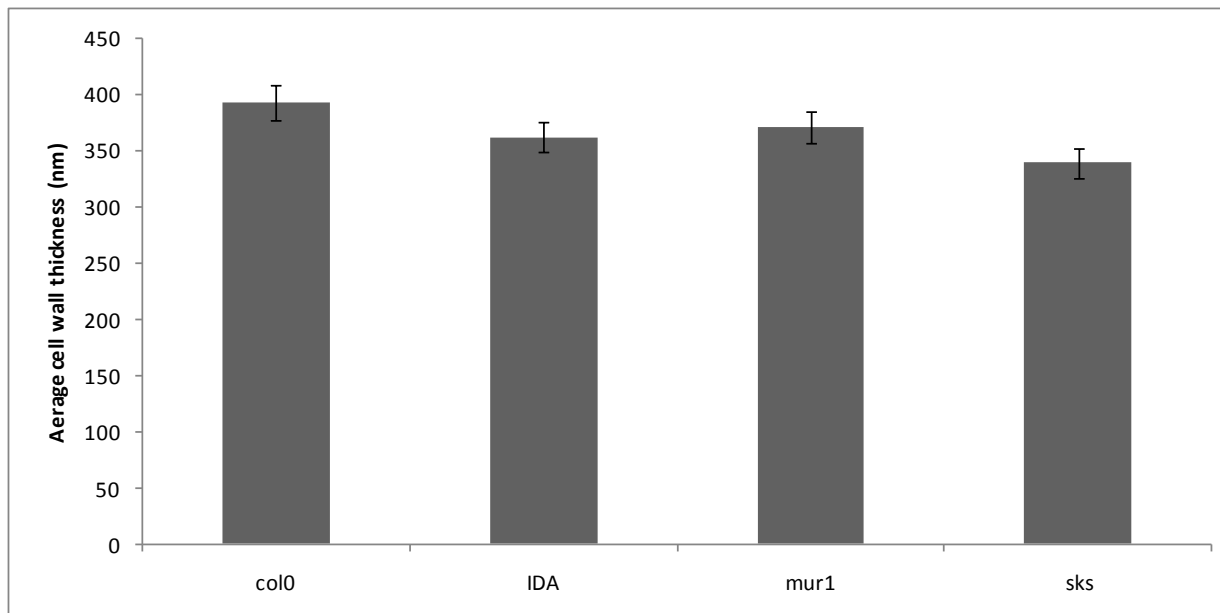


**Figure 7.5:** The average primary cell wall thickness of the four *Arabidopsis thaliana* genotypes, for samples of the cultured cells. Error bars represent standard error. 25 measurements were taken for each of the genotypes. *Sks* has significantly thinner primary walls than *col0*.

From figure 7.4 (A) and (C) it can be seen that the single cells reach an apparent homogeneity in the walls, having comparable thicknesses through the circumference. On the contrary, the walls of the aggregated cells are found to show large variations in the wall thickness, in particularly at the corners of cells where the wall is much thicker.

An additional difference is the amount of pectin seen. In 7.4 (B) the middle lamella is present as a thin layer between the walls with the exception of the corners. This is the traditional distribution for pectin in the cell wall. However, 7.4 (A) and (C) do not replicate this distribution. The primary walls of the single cells appear to be encompassed in a layer of pectin of comparable thickness. In Chapter 5, the biochemical analysis suggested that the cultured cells produced extra pectin compared with the plant growth cells, and speculated in reasons for this increase. This increase can be seen in figure 5.3. It was speculated that the cultured cells might have produced excess pectin because they are attempting to re-establish or maintain intracellular adhesion as the culturing causes them to separate. However the polysaccharide deposition is not directed, as no thickening can be seen at these points, but rather a standard thickness.

The initial diameters of the cells were taken from the TEM pictures, and used with the wall thicknesses to calculate the initial thickness ratio. An initial parameter required by the model, table 7.1, the value was determined to be 0.077.

8 images were taken for each genotype; this was limited due to time and expense. A profile of a single cell would show the thicknesses at different positions allowing the theory the wall adopts a standardised thickness.

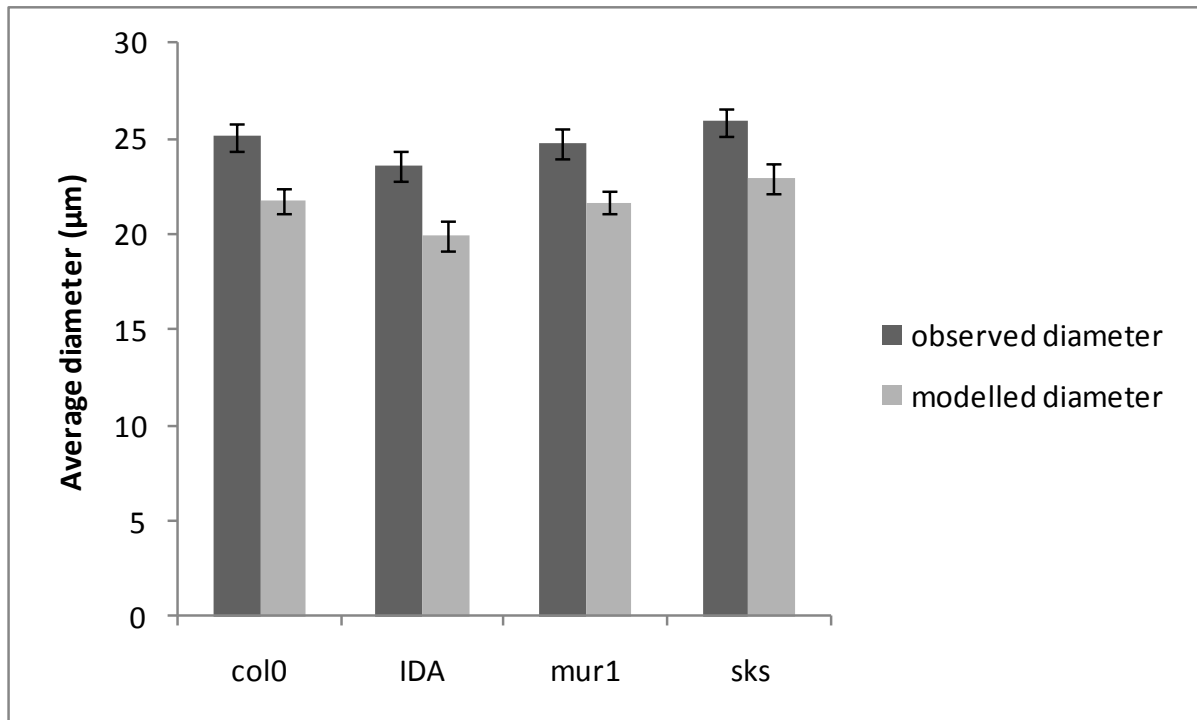


**Figure 7.6:** the average diameters of the cells, observed during the microcompression and those determined by the modelling. The pattern of the diameters is the same between the two data sets; however the observed diameters are significantly higher than those given by the model ( $P>0.05$ ).

It is possible that this additional pectin may affect the dimensions of the cells when compressed. When compared, the diameters observed under during compression were found to be significantly higher than those in calculated by the model. This can be seen in figure 7.6. No differences of any significance were found between the genotypes from the same measurement. They do appear to follow the same pattern, but with the modelled diameters lower. Physically, the differences account to approximately 3  $\mu\text{m}$ . This may be in part due to human error in measuring the cells and the accuracy of the equipment. At the magnification used on the compression rig and light microscope the two layers were indistinguishable, only the high magnification of the TEM was able to show this.

Figures 7.4 (A) and (C) give evidence for this increased pectin deposition. Unfortunately, this additional layer can only account for approximately 300nm, which still cannot solely account for the differences observed but combined with the observational errors could explain a large portion of the difference.

### **7.4.2 Low Strain Elastic Modulus (E)**

The force-deformation data collected in the plastic region cannot currently be modelled, limiting analysis of the compression data to a (relatively) low strain elastic modulus rather than the modulus to failure. This was expected, as tomato cell compression had met with similar complications. The elastic limit of the plant walls limits the amount of data points usable for determining E to the low strain region. This ensures that any plastic deformation data is omitted from the analysis.

The genotype averages taken from the model for the calculation of E can be seen in figure 7.7. From this figure it can be seen that differences can be detected in the low strain elastic modulus. These results suggest that the mutations do have an effect on the intrinsic mechanic properties of the cell wall. IDA and col0 show a significantly higher modulus than that of the mur1 mutation.

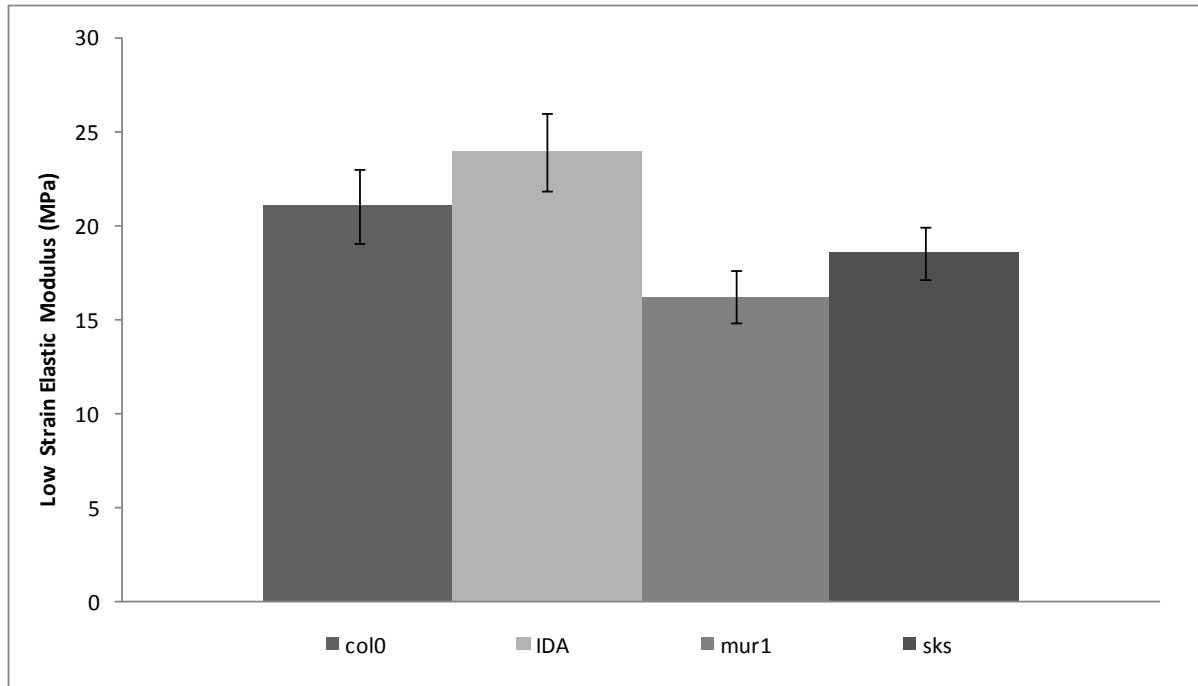


**Figure 7.7:** *The average low strain elastic moduli for the four genotypes. Error bars represent the standard error. T test analysis shows that col0 and IDA have a significantly higher low strain elastic modulus than mur1 (P.0.05). IDA also shows a non-significant difference to sks. Number of samples, col0=66; IDA=56; mur1=65 and sks = 86.*

This means that mechanically, the walls of the mur1 are intrinsically more flexible having a higher tendency to deform elastically. The mur1 mutations affect the hemicellulose of the primary cell wall. As hemicellulose is responsible for cross-linking the cellulose microfibrils it is possible that the mutation has affected this cross-linking, resulting in the reduction in the modulus found. An interesting result is that at the single cell level, the sks mutation has no significant differences to the other genotypes. This is contrary to the results from the whole plants where sks showed severe growth deficiencies.

As the sks mutation causes a reduction in pectin, the main component of the middle lamella, it is possible that the primary walls of the sks cells remain largely unaffected and as such display similarities to the col0. TEM analysis suggests that sks primary walls were thinner (figure 7.5) due to the reduction of pectin but show no affect on the mechanical properties. This has further implications in that it suggests the middle lamella has little mechanical significance to individual cells. However the developmental effects are obvious with the whole organism (chapter 3).

### 7.4.3 Elastic limit

When the preliminary results were collated in chapter 6, the results were analysed in the basis of the data at rupture. This encompasses both elastic and plastic regions. From figure 6.10 (B) suggested that the IDA was the weakest and mur1 the strongest. This is a somewhat unexpected conclusion given the results in chapters 3, 4, and 6 would have suggested the opposite outcome. As discussed this is not an intrinsic measurement and was only used as an initial guide. As is transpired, the intrinsic measurements revealed the opposite result.

The elastic limit was initially investigated in chapter 6, as a comparison to the tomato compression that had been done previously by Wang (Wang et al., 2004), this can be found in section 6.5. From this investigation it was determined that the elastic limit to lie between 30 and 35% displacement of the cellular diameter. Figure 7.8 gives the elastic limits from the modelling shown in table 7.2.

These more accurate measurements show that the elastic limits are of comparable levels to those observed in chapter 6.5. As the measurements made in chapter 6 acts as preliminary data, establishing the range in which the modelling results should be expected. This has validated the results seen in seen 7.8. There is one difference of significance; col0 shows a lower limit than mur1 and IDA. The elastic limit is the point at which the walls are no-longer behaving elastically. The point occurs at a reduced displacement, suggesting the mur1 and IDA mutations cause the walls to be more deformable.

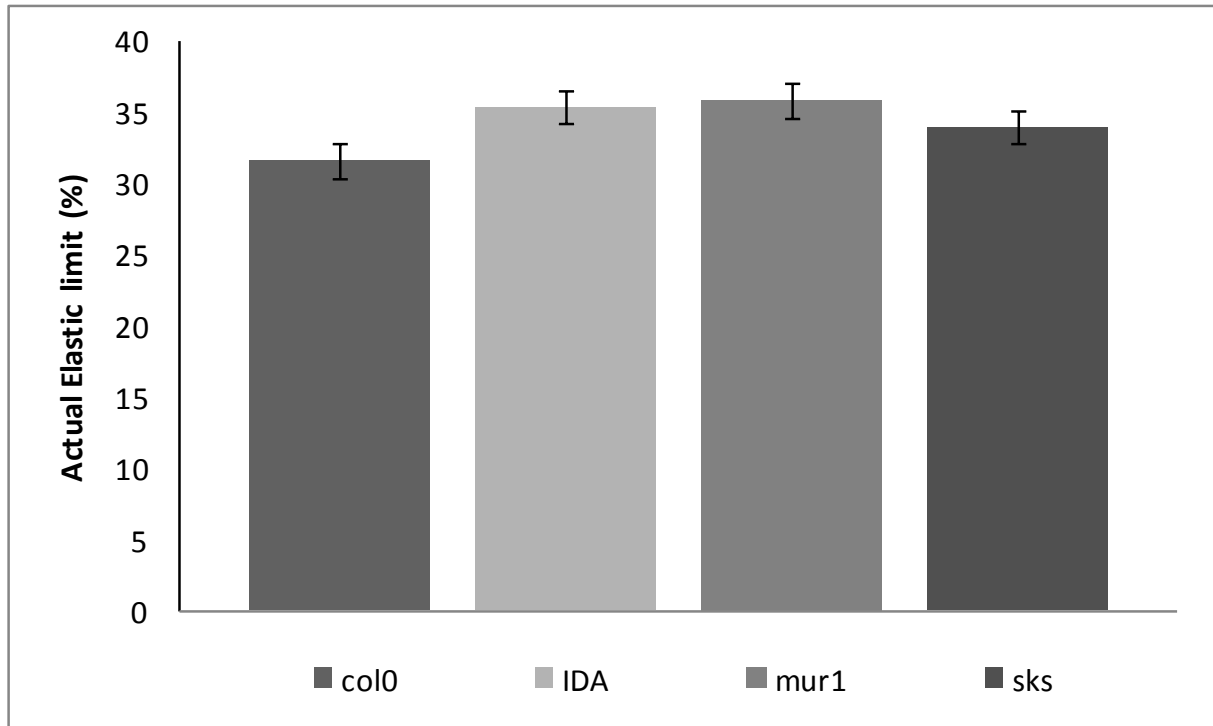


Figure 7.8: the average value for the elastic limits of the genotypes. This is the point at which the wall no longer behaved in an elastic manner and took on plastic traits. This is the point to which the data was used for the calculation of the low strain elastic modulus. The results show that the col0 cells had a significantly lower elastic limit than ida and mu1 ( $P > 0.05$ ).

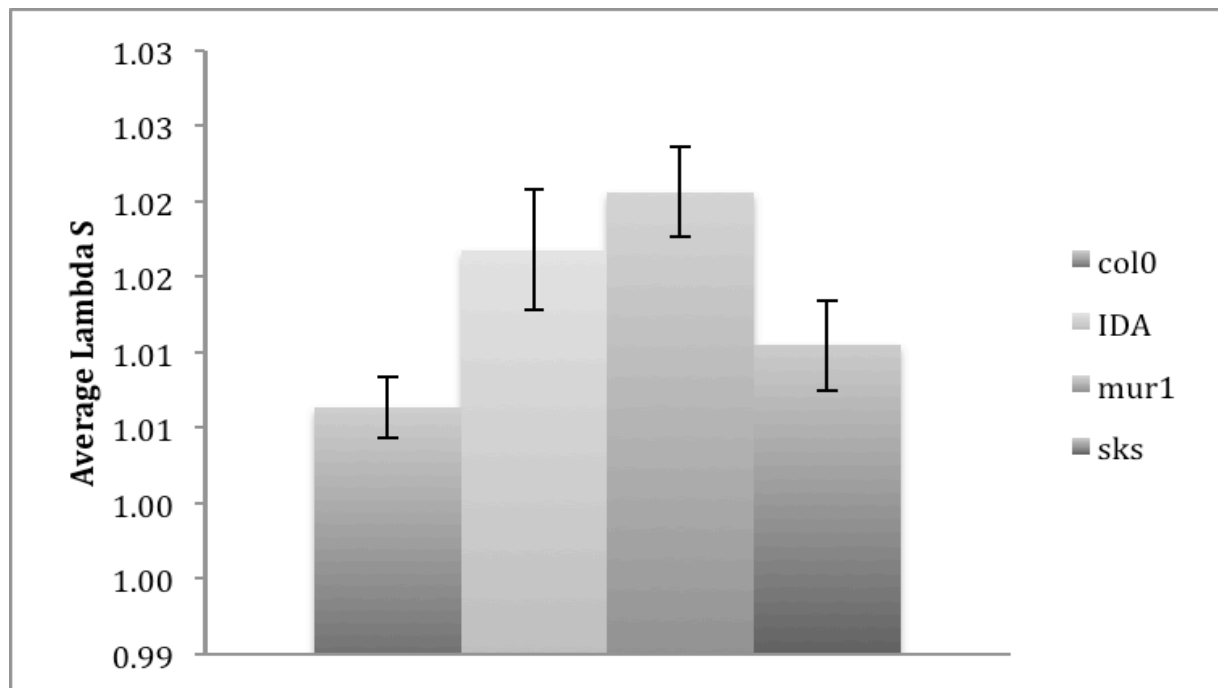


Figure 7.9: the average initial stretch ratio ( $\lambda_s$ ) for each genotype. The error bars represent the standard error. Significant differences can be seen, mur1 is higher than sks and col0; ida is higher than col0.

#### 7.4.4 Initial Stretch Ratio ( $\lambda_s$ )

One of the parameters calculated by the model is the initial stretch ratio ( $\lambda_s$ ) for the cells. This is a measure of the level of inflation, e.g. the turgor pressure at the start of the compression. Figure 7.9 is a representation of these values. It can be seen that the values are very low, as a value of 1 would indicate a cell with no turgor. Col0 cells demonstrate the lowest of all the genotypes, suggesting that they had the lowest average turgor.

The turgor is responsible for the expansion of the cells, however in figure 4.6 the diameters of the cells in culture both single and aggregated had not changed for several days. It was suggested that the cells were no longer growing and therefore would not require the maintenance of a high turgor required for expansion. If the cells were growing, a higher turgor would be expected. It is also possible that the changes in the wall are having some effect; however,  $\lambda_s$  is not an intrinsic mechanical property unlike  $E$ .  $\lambda_s$  is a derived value, where the calculated value is dependent on several functions.  $E$  is an established parameter that is well understood. Therefore,  $\lambda_s$  was not chosen as a useful measure of effects of mutations on the properties of the cell wall.

#### 7.5 Conclusions

To investigate the link between biochemical composition and mechanical properties was the original goal of the project. Through mathematical modelling of the compression data this has been achieved. It has been shown that the *Arabidopsis* cells exhibit similar properties to those of the tomato cells, e.g. elastic up to a limit of approximately 30%, after which they behave in a manner that is presumed to be plastic, allowing the calculation an intrinsic mechanical property, the low strain elastic modulus.

The evidence shows that the *mur1* mutation affected the biochemical composition of the wall, a change that is consistent with its lower elastic modulus compared to the wild type. The *mur1* mutation affects hemicellulose in the primary wall. This polymer is thought to cross-link the cellulose fibres adding the integrity of the structure (section 2.4.2). Although in section 5.5.1 no differences were found in the amount of hemicellulose present it was presumed the mutation would affect function. This is supported by the results in this chapter suggesting that by modifying the hemicellulose the

*mur1* mutation has lowered the elastic modulus. This supports the results seen in plant growth in chapter 3, where the roots and shoots of the *mur1* plant consistently showed altered growth.

It was known that the *sks* mutation affects pectin in the cell wall. Pectin is predominantly contained within the middle lamella and was speculated that this holds little or no mechanical significance for the individual cell. Therefore it can be stated that the reduction in pectin and the reduction of intracellular adhesion the *sks* mutation causes is therefore the major cause of the growth differences seen in chapters 3, 4 and 5 not a weakening in the primary cell wall.

This evidence suggests that any pectin present in the primary wall also holds little mechanical significance. Evidence from TEM images (section 7.4.1) showed *sks* primary walls have a reduced thickness compared with other genotypes, which is a result of the *sks* mutation. Despite a reduction in primary wall thickness caused by the *sks* mutation, no significant reduction seen in the values for the low strain elastic modulus between *col0* and *sks*.

The *ida* mutation shows a similarity to *col0* again, this justifies the results seen in chapters 3, 5 and 6. The affects of the mutation must be conditional, only noticeable in the abscission regions. Therefore, it does not affect the general wall properties, as shown by the wild type characteristics throughout.

## ***Chapter 8: Further Work and Discussion***

---

Through analysis and discussion of the data several areas of potential improvement or additional analysis became apparent. In this chapter, these are discussed in relation to the data presented, and speculations on potential results are presented.

### **8.1 Chapter 3**

In Chapter 3 an investigation is described into the effects of the mutations on shoots and roots is described. Analysing the shoots and root systems in parallel showed that the mutations caused many differences in the growth patterns of these regions. As a general rule, the *ida* mutation showed similarity to the wild type throughout the investigation. This mutation may have been a very specific mutation, potentially affecting only a small proportion of the aerial region. Therefore the differences seen were insignificant. The *sk5* mutations showed a large number of severe mutational effects. Stunted growth showed the apparent effects of the reduction of cell-to-cell adhesion. The *mur1* mutation can be seen as a middle point between the *col0/ida* phenotypes and the severely altered *sk5*. For a full summary of the chapter refer to section 3.6.

#### **8.1.1 Root Growth Assay**

The root growth assay (RGA) was a successful investigation into the maximal growth of the roots in a controlled system (section 3.4). This built on the results presented by the plant growth characteristics investigation (section 3.2). However, there are two additional investigations that could be conducted using this system. Experimental duration was limited by the physical length of the plates; plates of greater length would increase the time available. The results in figure 3.9 (B) show the roots growing at what appears to be a steady state growth rate by the end of the investigation. The use of longer plates would allow this to be confirmed. With the time increased using longer plates, the inclusion of sucrose into the media would be unnecessary. As the sucrose was initially added to remove the

energy production lag associated with germination, the results were taken to be the maximal growth properties not the native growth properties. It could be anticipated that any results gained in this manner would show a correlation with the maximum rates to those gained with sucrose. This would be representative of natural growth (section 2.9)

### **8.1.2 Root Cell Length Profiling**

The root cell length profile (section 3.5) highlighted a differential growth profile along the elongation zone of roots taken from the RGA. There are two techniques that may add an additional level of analysis

#### **8.1.2.1 Zones of the Growing Root**

The cell density in the root tip and the elongated cells length in the distal regions made it difficult to accurately measure the lengths of the zones in the root (section 2.9). A method of video analysis has been used to measure growth velocities and the expansion rates of the roots using time lapse photography (Wiese et al., 2007). The technique can track artifacts on the surface of the root and measure to the relative distance as the root grows. From this, the growth rates can be determined. Through image analysis (Thomas and Paul, 1996) these techniques are sensitive enough to analyse to measure the dense root tip and meristem (van der Weele et al., 2003). Applying this technique could help further define the zones on the root and provide information on cell production rates of the meristem.

#### **8.1.2.2 Fluorescent Staining**

The use of fluorescent stains is widely used in study of plant genetics (Laloue et al., 1980); biochemistry to ascertain viability (Widholm, 1972) and physiology to investigate growth (Martin, 1959) function (Hoson, 1991). It is also possible to stain specifically, for example looking at cytoskeleton (Lloyd, 1987) and polysaccharides (Barry et al., 1991; Smith and McCully, 1978). The main protocol for this is the generation of a fluorescently tagged antibody marker that attaches to the specific target.

## Chapter 8: Further Work

These can be seen with a fluorescent microscope. Generating specific tags to suit the wall mutations is possible and so will highlight the differences in the wall architecture and composition. Combining this with the roots that have been grown in the RGA and RCLP additional mutational effects may be discovered.

### 8.2 Chapter 4

This chapter presented the optimisation of the suspension culturing process for the development of single cells. The results show that thousands of single cells were found in each ml of culture. With the production of this many cells, potentially allows additional investigations to be conducted into the transcriptomics of the cells.

#### 8.2.1 Flowcytometry

Flowcytometry uses a laser to measure cellular flux (Dopolezel, 1991). This will only works with single cells as aggregates may block the apparatus. However, it may be possible to separate the cultures into fractions thus making the possibility of using the flowcytometer feasible.

Combined with the flowcytometer is to assess the activity of certain genes that are being expressed by the cell (Dpoolezel et al., 1989). This is done by fluorescently labeling their gene products with molecules that are specific to that product, e.g. labeling the product of a cell wall component gene. Labelling would be done using *in-situ* hybridisation (Meyerowitz, 1987). This would show the amount of these molecules being produced by measuring the levels of fluorescence by a fluorimeter contained in the flowcytometer. This could be useful in measuring the changes in the cell wall composition due to the cell wall mutations by measuring there gene products.

## 8.2 Chapter 5

### 8.2.1 Alternative Methods for Analysis of Cell Wall Biochemical Composition

In chapter 5, an investigation using spectrometry and biochemical assays was used to determine the composition of the walls. In particular the varying amount of the three major polysaccharides contained within the walls of the plant and cultured tissues. There are several alternative techniques that can be applied to further this investigation.

### 8.2.2 Confocal Raman Microscopy

Recent advances in microscopy and laser excitation have enabled the combination of the analysis of raman spectra (Petry et al., 2003) in the same plane as confocal images. A Raman spectrum (De Gelder et al., 2007) shows the energy shift of the excitation laser as a result of inelastic scattering by the molecules. The excitation light induces vibrations of the chemical bonds within the molecules, so each molecule can be identified by its individual Raman spectrum (Kneipp et al., 1999). The spectra are collected with a high sensitive confocal microscope connected to a high-throughput spectrometer equipped with a CCD camera. This technique has the potential to distinguish the chemical composition of materials by the spectra generated. Raman spectra have been generated for many biological materials (Choo-Smith et al., 2002) including several plant species black spruce (Agarwal, 2006); poplar (Gierlinger and Schwanninger, 2006) and *Equisetum hyemale* (Gierlinger et al., 2008). The walls of these cells usually contain large quantities of lignin that is not found in the *Arabidopsis* primary cell wall. However, the results of the technique are not dependant on wall composition so the technique should be applicable to the *Arabidopsis* cells.

The combination of the confocal microscopy and the raman spectra allow the relation of the relative spectra produced to the on the cell it was produced. For example, this pairing will allow the comparison of middle lamella spectra and primary wall spectra. Figure 8.1 shows an example of some preliminary data from confocal raman microscopy for the *Arabidopsis* col0 and sks genotypes.

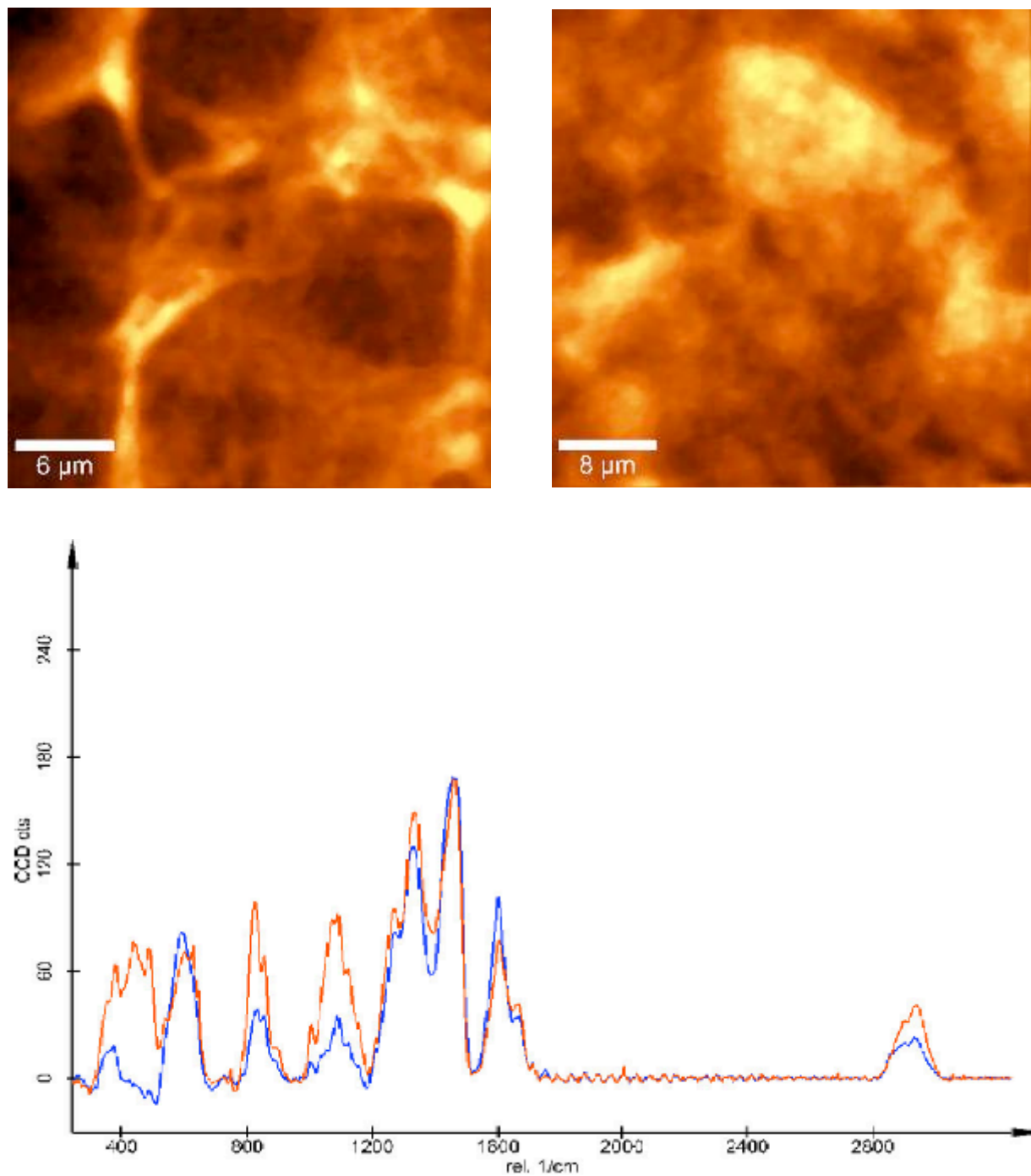


**Figure 8.1:** Results from a preliminary investigation into the raman spectra of *Arabidopsis thaliana* cell wall mutations. (A) A confocal image of a sample of *sks* suspension cultured cells. (B) A confocal image of a sample of *col0* suspension cultured cells. Both (A) and (B) are coloured to represent the raman spectra generated at that point. (C) Raman spectra recorded on snake skin (red) and sample C019 (blue). The spectra presented, are average spectra from the image scans (16384 spectra each). Both spectra show Raman bands at the same wave numbers, with variations of peak intensities. To compare peak intensities, both spectra were normalized to the peak at 1458/cm.

To investigate the potential application of the technique to the *Arabidopsis thaliana* cells, samples of the col0 and *sk5* were sent to WiTec, Germany. Samples were analysed and the resulting spectra presented in 8.1. Col0 and *sk5* were used as the results from chapter 3 had shown that they had shown the biggest growth differences. The literature (section 2.13) had suggested *sk5* had a reduction of pectin. It was hoped these differences would be detectable by the raman spectra. (A) *sk5* and (B) col0, show confocal images of the samples coloured to represent the spectrum gained at that point. The average of these spectra are shown in figure 8.1 (C), normalised to the highest peak (1458/cm). These data show

An advantage of the WiTec system is the option of a combined atomic force microscope (AFM) (Binnig et al., 1986). AFM (Meyer, 1992) can be used to image the topography of a surface (Kasas et al., 1993). A cantilever arm is moved across the surface and the deflection of the arm is recorded. AFM has been used to image the surfaces of biological material (Hansma and Hoh, 1994) cells (Butt et al., 2010) and to profile the plant cell wall (Kirby et al., 1996). There are also protocols for the immobilisation of spherical bodies for use with AFM (Kasas and Ikai, 1995). In addition to the surface topography, AFM can be used to determine some mechanical properties (Butt et al., 2005). This has been applied to many materials including the cell organelles (Yamada et al., 2002) and the cell wall (Ding and Himmel, 2006). AFM could be used as a standalone technique; however the combination of the confocal raman spectra, surface topography and mechanical properties from AFM of the same sample would enable a superior level of comparison of the wall.

### 8.3.3 High Performance Liquid Chromatography (HPLC)

As discussed in chapter 5, a possible alternative to the biochemical analysis was the HPLC (Kaar et al., 1991). Unfortunately, the process was too costly as the columns necessary were unavailable and the spectrophotometric option was chosen. The technique has been used to investigate many aspects of *Arabidopsis* physiology (Bloor and Abrahams, 2002). The HPLC is more sensitive than the spectrophotometer, and with the appropriate equipment could provide additional information on the wall composition (Zabackis et al., 1995) and further investigate the differences caused by the mutations (Gardner et al., 2002).

### 8.3 Chapter 6

Chapter 6 detailed the development of the compression testing technique to generate force/deformation data from the single *Arabidopsis* cells. It is possible that with additional development that the process could be further refined, however this was not possible at the time but may be beneficial for future investigations. Improvements could be made to the rigs themselves to increase the versatility and increase the accuracy of the measurements. The main issue was with the quality of the optics on the system. The use of a confocal microscope would aid the visualisation and the video capture of the cells during compression.

There are two additional experiments that could be done using compression testing. Firstly, blocking the water channels will allow testing the effect they have on compressibility of the cells. It was suggested section 6.4 that the hydraulic conductivity of the cells was very high. Aquaporins, water channels in the plasma membrane are known to be readily blocked using heavy metals, for example Mercury (Savage and Stroud, 2007). Secondly, relaxation of the wall after the compression can be measured. Using a squeeze-hold experiment, the changes in the wall responding to the compression can be assessed in addition to hydrodynamics.

The negative water loss during compression, the speed had to be increased to 3000 $\mu\text{m}\cdot\text{s}^{-1}$ . When a series of TIF images was analysed through manual image analysis, the  $L_p$  was found to be at the lowest end of the scale. It was found that this did not occur in the tomato cells, so it would be interesting to investigate whether it was caused by the change in species or as a result of the culturing process. To investigate the cells it would be possible to analyse the video footage many compressions of different genotypes from this investigation. This would allow the derivation of the  $L_p$  by measuring the change in volume of the cell during compression.

## 8.4 Chapter 7

### 8.4.1 Improvements to the Software/Model

Through mathematical modelling of the compression data from chapter 6, intrinsic parameters of the mechanical properties of the single cell wall were determined. A version of the model tailored to the *Arabidopsis* compression data was created to cope with the noisy data, allowing the low strain elastic modulus for the single cells was determined. However, the model was unable to process the data beyond the elastic limit. This plastic region that continues to failure contains further information on the mechanical properties. The development of an elastic/plastic model would allow the complete data to be analysed.

## 8.5 General Observations

The results in chapter 5 suggest that there are differences between the plant and cultured wall composition, in particular figure 5.3. This shows that the amount of pectin the walls of the cultured cells is significantly high than the amount contained in the plant walls. Possible reasons for this were suggested section 5.5.2. However a definitive cause for this should be investigated. It was suggested that the cells are either actively up regulating pectin gene expression to increase production or are undergoing a reactive process of producing more pectin because the cells are attempting to maintain intracellular adhesion. This result also raises the question of whether this is the only difference between plant and cultured cells, or simply the most obvious. Transcriptomics of the *Arabidopsis* genome is possible to determine the activity of every gene, allowing comparison between the culture stages (Ramonell et al., 2002). This is possible as *Arabidopsis* has been the target of a genomic sequencing project (section 2.13.1). Microarrays (Zimmermann et al., 2004) allow the levels of gene products for each gene of the genome to be quantified (Goda et al., 2002). The transcriptome of samples of plant and tissue cultured cells would be extracted hybridised to a microarray chip (Breyne et al., 2002). A plate reader detects the relative intensities of the gene products. This allows quantitative comparison of differences in gene expression throughout the entire transcriptome. This technique has been used to investigate the differences between root and shoot cells (Horvath et al., 2003) and between cultured and plant cells (Menges et al., 2003).

To determine the genetic cause of the differences observed throughout the investigation would be of particular interest. Whether the altered gene expression has any subsequent effects causing the regulation of additional genes other than the named mutation to be affected. Some examples of this can be found earlier in the investigation. Section 3.2 showed the leaves of the *sk*s plants were observed to curl, greatly reducing the total surface area. Additional cauline and rosette leaves are produced during the same period. Throughout the root growth assay, many *sk*s and *mur1* seedlings produce curled primary roots or multiple 'adventitious roots'. Sadly there was no direct way to measure these differences during the investigation, merely to highlight the occurrence. The use of microarray analysis may highlight genes that could potentially be attributed to these changes seen.

### 8.6 Final Conclusions

The ultimate goal of this project was to investigate the mechanical properties of the primary plant cell wall, specifically how changes in the composition of the wall would affect these properties. Three separate genotypes each containing a mutation in a gene involved in the production of the cell wall were chosen. This allowed an investigation of the regions of the *Arabidopsis* cell wall and the different fibers they contain. The literature profiling the effects of the mutations at the molecular level is contained within chapter 2.

It was found through extensive phenotyping of these mutations in chapter 3, that the mutations had a variety of effects on plant growth. Height/length and growth rate of the roots and shoots showed a wide range of results between the genotypes. In addition to this several developmental observations were made with respect to leaf and lateral/advantageous root emergence and the shape these took. These observations are resultant from the mechanical properties of the wall and the effect of turgor pressure. But how do these observations relate to the results presented in the later chapters?

Chapter 4 profiles the culturing process used to generate the single cells required for the later investigations. It also presented an opportunity to assess the behavior of the different genotypes in culture and whether the mutations in the cell wall genes cause any obvious differences. From the literature and the results from chapter 3 several differences were anticipated. The *sk*s mutation would

cause the production of loosely aggregated cell clusters, potentially resulting in an increase level of single cell generation. This was due to the mutation affecting the ability of the pectin molecules crosslinking and the overall of reduction of pectin present in the wall. With regard to the other mutations should behave in a similar manner to *col0*, as the other genotypes are not expressly concerned with cell adhesion. However this was not the case. The *sk5* mutation behaved as expected producing the highest numbers of single cells of any genotype. It was also found that *ida* cells produced significantly lower numbers of single cells (figure 4.5). This suggests that either the cells are more strongly adhered than the other genotypes. The similarities between *col0* and *ida* were common throughout chapter 3 during the plant phenotyping, this reduction in single cell production being the first major different between these two genotypes during the investigation. The *ida* is specific to abscission regions and it is therefore possible that these gene is not being expressed in the cultures as it is not constitutive nor may not be required. Through monitoring of the cultures during the 4 weeks between initiation and sub-culturing it was found that the diameters of the cells of all the genotypes became increasingly consistent, eventually leading to an average diameter of approximately 25  $\mu\text{m}$ . Which corresponds to the average size of a cell in the plant.

It was clear from the results in chapters 3 and 4 that there were differences in the cells in culture and in plants. In chapter 5 the amounts of each of the three major polysaccharide groups in the walls of the plant and cultured cells was measured. From the results in chapter 3, it was expected that the amounts of pectin present in the *sk5* cultured and plant cells to be greatly reduced compared to *col0*. The *ida* and *mur1* may have little to no effect on the amount of polysaccharide in the wall compared to *col0*, due to the nature of the mutations. It was also anticipated that the amounts of polysaccharide would remain consistent between the cultured and plant cells. These predictions were mostly correct, save for one unexpected result, as the amount of pectin produced by the cultured cells was much higher than the plant cells. It has been discussed that the cells may be trying to maintain cell-to-cell adhesion in the loosely packed cell aggregates requiring the production of more pectin.

Samples of these cultured cells were used to investigate the properties of the walls of individual cells in chapter 6 and these results were modeled to determine the mechanical properties in chapter 7. To generate the forces sufficient to negate water loss for the cell during compression, the speed of the probe had to be greatly increased from any prior investigation using this technique. 3000  $\mu\text{m s}^{-1}$  was

found to be a sufficient speed to negate the water loss. At this speed the number of data points taken for each compression was greatly reduced, this was due to the data collection software was running at the maximum sample rate of 10000 samples per second. It can therefore be presumed that the hydraulic conductivity ( $L_p$ ) of the single cells in culture is very high, preliminary investigation proved this placing these cells at the high end of the range of viable cells. It has been suggested that a possible cause for this would be the high surface area to volume ratio of the single cells, especially when compared to the tomato cells. When compared with values taken from literature concerning the  $L_p$  of cells contained within the plant, the cultured cells were significantly higher. However the reduction is similar when compared with that of the tomato fruit and tomato culture cells. Thus returning to the surface area: volume ratio of the single cells as the causes. It is possible that the culturing process has additional affects on gene transcription that could cause the increased  $L_p$ . An investigation into the transcriptomics of the plant and cultured cells would have added great depth to the investigation and would have been conducted if time and budget had allowed.

From the initial results taken from the force compression data (chapter 6) some unexpected differences were seen. From chapter 3 it was predicted that the *mur1* mutation would cause a significant difference in the walls in the single cells. The reduction in the amount of cross linking of the cellulose fibers in the primary wall caused significant differences in shoot and root growth, potentially causing a weakness in the individual cell walls. The *sks* mutation causes significant differences in the plant growth, however it was possible that this may not transfer to the single cells. As the *sks* mutation causes a reduction in pectin and it is thought that pectin does not have any structural significance in the primary wall. It was suggested that the differences seen in chapter 3 were caused by the reduction in cell-to-cell adhesion attributed to the decrease in pectin present in the middle lamella rather than any intrinsic mechanical weakening of the primary wall.

Firstly, the cells in culture appear to forego the maturation process that cells would normally undergo in the plant. Table 6.1 shows that there are no differences between cells from one or two week old cultures, except for the convergence of cellular diameter seen in chapter 4. A cell in the plant would have had additional fibre deposition and cross-link formation over the same time scale. However this is due to the influences of changing concentrations of the growth regulators as the plant grows.

From figure 6.7 the bursting force was used as an initial point of comparison of the physical properties of the single cells. The averages shown here indicate that the *mur1* and *sk5* have a high bursting point compared with *col0* and *ida*. These results are the complete opposite to what was expected. There are two possible causes for this, as the bursting point is not an intrinsic property and the apparent elastic/plastic behavior of the wall under compression. As the bursting point is not an intrinsic property, no firm conclusions can be taken from this. Although, the detectable differences are encouraging suggesting that the more detailed analysis will enable more accurate conclusions. The elastic/plastic behavior of the wall may cause some differences in the way the wall compresses. Even though this is the point at which the membrane fails resulting in the rupture it falls outside of the range of the data that was analysed by the model. The amount of data from each compression that was usable by the model was limited to that found between the elastic limit and the initial point of contact.

The force/deformation data from the elastic region of compression was fitted using the simulations of the model, enabling the calculation of the low strain elastic modulus for each cell. The direct comparison of the values for each genotype highlighted two major results. Firstly, the *ida* and *col0* genotypes were found to have higher moduli than the *mur1* genotype. This is closer to the vast majority of the results from chapters 3 where *mur1* showed reductions in growth but showed little reduction in the quantity of polysaccharide in the wall (chapter 5). It can be concluded that the deformability of the wall resultant from the reduction in cellulose cross-linking is responsible for the differences in growth observed during the phenotyping experiments.

The most interesting result was that of the *sk5* mutation, as it was found to have no differences in low strain elastic modulus when compared to *col0* at the single cell level. This is a dramatic change, considering the differences in growth seen in chapter 3. This result suggests that the single cells of the *sk5* genotype are no more deformable than the wild type and therefore all the phenotypic differences in chapter 3, therefore must be caused by the reduction of cell-to-cell adhesion in the middle lamella. This result allows further insight into the role of pectin with regards to the relationship of the cell wall properties of the single cells and growth characteristics of the plant. For the dramatic differences in growth seen in chapter 3 caused by the *sk5* mutation, some differences in the wall properties of the single cells would have been expected. With the *sk5* mutation causing a reduction in the total amount of pectin in the cell wall proved by the investigations in chapter 5 not transferring into

any detectable differences in the wall properties. It can therefore be concluded that the pectin does not hold any mechanical significance in the cell wall, but plays a huge role in the behavior of the growth plant that requires the adhesion of cells to be maintained.

Following the logical process from plant through to single cells and back again has shown the validity of the conclusions drawn. This study has taken a novel approach to allow fresh insight in to an area of plant physiology that has been the subject of much debate. The investigation has enabled a direct relationship between the mechanical properties of the single cells and the composition of the primary cell wall, which was the ultimate objective of this project. Revealing that even at the single cell level differences in the mechanical properties can be found. These differences were caused by mutations in cell wall genes and were predicted from a whole plant phenotype at the beginning of the investigation.

## *References*

---

- Agarwal,U. (2006). Raman imaging to investigate ultrastructure and composition of plant cell walls: distribution of lignin and cellulose in black spruce wood (*Picea mariana*). *Planta* 224, 1141-1153.
- Allen, C. E. On the Origin and Nature of the Middle Lamella. *Botanical Gazette* 32[1], 1-34. 1901.
- Alonso, J.M., Stepanova, A.N., Leisse, T.J., Kim, C.J., Chen, H., Shinn, P., Stevenson, D.K., Zimmerman, J., Barajas, P., Cheuk, R., Gadrinab, C., Heller, C., Jeske, A., Koesema, E., Meyers, C.C., Parker, H., Prednis, L., Ansari, Y., Choy, N., Deen, H., Geralt, M., Hazari, N., Hom, E., Karnes, M., Mulholland, C., Ndubaku, R., Schmidt, I., Guzman, P., Aguilar-Henonin, L., Schmid, M., Weigel, D., Carter, D.E., Marchand, T., Risseeuw, E., Brogden, D., Zeko, A., Crosby, W.L., C. Berry, C.C. and Ecker J.R. (2003). Genome-Wide Insertional Mutagenesis of *Arabidopsis thaliana*. *Science* 1: 301 (5633), 653-657.
- Arathoon,W.R. and Birch,J. (1986). Large-scale cell culture in biotechnology. *Science* 232, 1390-1395.
- Arioli,T., Peng,L., Betzner,A.S., Burn,J., Wittke,W., Herth,W., Camilleri,C., fte,H., Plazinski,J., Birch,R., Cork,A., Glover,J., Redmond,J., and Williamson,R.E. (1998). Molecular Analysis of Cellulose Biosynthesis in *Arabidopsis*. *Science* 279, 717-720.
- Axelos M, Curie C, Mazzolini L, Bardet C, Lescure B. (1992). A protocol for transient gene expression in *Arabidopsis thaliana* protoplasts isolated from cell suspension cultures. *Plant Physiology and Biochemistry* 30, 123–128.
- Bacic, A., Harris, P.J. and Stone, B.A. (1988) Structure and function of plant cell walls. In *The Biochemistry of Plants*, Volume 14 (Priess, J., ed.). New York: Academic Press, pp. 297-471.
- Bacic,A. (2006). Breaking an impasse in pectin biosynthesis. *103*, 5639-5640.
- Barry,P., Prensier,G., and Grenet,E. (1991). Immunogold labelling of arabinoxylans in the plant cell walls of normal and bm3 mutant maize. *Biology of the Cell* 71, 307-311.
- Baskin,T.I. (2000). On the constancy of cell division rate in the root meristem. *Plant Molecular Biology* 43, 545-554.
- Beebo,A., Thomas,D., Der,C., Sanchez,L., Leborgne-Castel,N., Marty,F., Schoefs,B.t., and Bouhidel,K. (2009). Life with and without AtTIP1;1, an *Arabidopsis* aquaporin preferentially localized in the apposing tonoplasts of adjacent vacuoles. *Plant Molecular Biology* 70, 193-209.

## References

- Beemster, G.T.S. and Baskin, T.I. (1998). Analysis of Cell Division and Elongation Underlying the Developmental Acceleration of Root Growth in *Arabidopsis thaliana*. *Plant Physiol.* *116*, 1515-1526.
- Benfey, P.N., Bennett, M. and Schiefelbein, J. (2010) Getting to the root of plant biology: impact of the Arabidopsis genome sequence on root research. *The Plant Journal*: *6*, 1992-1000.
- Benjamins, R. and Scheres, B. (2008). Auxin: The Looping Star in Plant Development. *Annual Review of Plant Biology* *59*, 443-465.
- Berger, F., Hung, C.Y., Dolan, L., and Schiefelbein, J. (1998). Control of Cell Division in the Root Epidermis of *Arabidopsis thaliana*. *Developmental Biology* *194*, 235-245.
- Bevan, M. and Walsh, S. (2005) The Arabidopsis genome: A foundation for plant research. *Genome Res.* *15*: 1632-1642
- Binnig, G., Quate, C.F., and Gerber, C. (1986). Atomic Force Microscope. *Phys. Rev. Lett.* *56*, 930.
- Blancaflor, E.B. and Masson, P.H. (2003) Plant Gravitropism. Unraveling the Ups and Downs of a Complex Process. *Plant Physiol.* *133*: 1677-1690.
- Blewett, J., Burrows, K., and Thomas, C. (2000). A micromanipulation method to measure the mechanical properties of single tomato suspension cells. *Biotechnology Letters* *22*, 1877-1883.
- Bloor, S.J. and Abrahams, S. (2002). The structure of the major anthocyanin in *Arabidopsis thaliana*. *Phytochemistry* *59*, 343-346.
- Bonati, A. (1980). Medicinal plants and industry. *Journal of Ethnopharmacology* *2*, 167-171.
- Bonin, C.P., Potter, I., Vanzin, G.F., and Reiter, W.D. (1997). The MUR1 gene of *Arabidopsis thaliana* encodes an isoform of GDP-D-mannose-4,6-dehydratase, catalyzing the first step in the de novo synthesis of GDP-L-fucose. *PNAS* *94*, 2085-2090.
- Borstlap, A.C. (2002). Early diversification of plant aquaporins. *Trends Plant Sci.* *7*, 529-530.
- Bouton, S., Leboeuf, E., Mouille, G., Leydecker, M.T., Talbotec, J., Granier, F., Lahaye, M., Hofte, H., and Truong, H.N. (2002). QUASIMODO1 Encodes a Putative Membrane-Bound Glycosyltransferase Required for Normal Pectin Synthesis and Cell Adhesion in *Arabidopsis*. *Plant Cell* *14*, 2577-2590.
- Boyer, J.S. (1988). Cell enlargement and growth-induced water potentials. *Physiologia Plantarum* *73*, 311-316.
- Brady, C.J. (2003). Fruit Ripening. *Annual Review of Plant Physiology* *38*, 155-178.
- Brett, C.T. (2000). Cellulose microfibrils in plants: Biosynthesis, deposition, and integration into the cell wall. In *International Review of Cytology*, Academic Press), pp. 161-199.

## References

- Breyne,P., Dreesen,R., Vandepoele,K., De Veylder,L., Van Breusegem,F., Callewaert,L., Rombauts,S., Raes,J., Cannoot,B., Engler,G., Inz+®,D., and Zabeau,M. (2002). Transcriptome analysis during cell division in plants. *Proceedings of the National Academy of Sciences of the United States of America* 99, 14825-14830.
- Burg,S.P. and Burg,E.A. (1965). Ethylene Action and the Ripening of Fruits: Ethylene influences the growth and development of plants and is the hormone which initiates fruit ripening. *Science* 148, 1190-1196.
- Burget,E.G. and Reiter,W.D. (1999). The mur4 Mutant of Arabidopsis Is Partially Defective in the de Novo Synthesis of Uridine Diphospho L-Arabinose. *Plant Physiol.* 121, 383-390.
- Butt,H.-J., Wolff,E.K., Gould,S.A.C., xon Northern,B., Peterson,C.M., and Hansma,P.K. (2010). Imaging cells with the atomic force microscope. *Journal of Structural Biology* 105, 54-61.
- Butt,H.J., Cappella,B., and Kappl,M. (2005). Force measurements with the atomic force microscope: Technique, interpretation and applications. *Surface Science Reports* 59, 1-152.
- Carpita,N.C. and Gibeaut,D.M. (1993). Structural models of primary cell walls in flowering plants: consistency of molecular structure with the physical properties of the walls during growth. *The Plant Journal* 3, 1-30.
- Cary A.J., Che P. and Howell, S.H. (2002) Developmental events and shoot meristem gene expression patterns during shoot development in Arabidopsis thaliana. *Plant J.* 32: 867–87
- Casimiro,I., Beeckman,T., Graham,N., Bhalerao,R., Zhang,H., Casero,P., Sandberg,G., and Bennett,M.J. (2003). Dissecting Arabidopsis lateral root development. *Trends in Plant Science* 8, 165-171.
- Cassab,G.I. and Varner,J.E. (1988). Cell Wall Proteins. *Annual Review of Plant Physiology and Plant Molecular Biology* 39, 321-353.
- Chakrabarti,N., Tajkhorshid,E., Roux,B., and Pomes,R. (2004). Molecular basis of proton blockage in aquaporins. *Structure* 12, 65-74.
- Che,P., Lall,S., Nettleton,D., and Howell,S.H. (2006). Gene Expression Programs during Shoot, Root, and Callus Development in Arabidopsis Tissue Culture. *Plant Physiol.* 141, 620-637.
- Chivasa,S., Ndimba,B.K., Simon,W.J., Robertson,D., Yu,X.L., Knox,J.P., Bolwell,P., and Slabas,A.R. (2002). Proteomic analysis of the Arabidopsis thaliana cell wall. *ELECTROPHORESIS* 23, 1754-1765.
- Choo-Smith,L.P., Edwards,H.G.M., Endtz,H.P., Kros,J.M., Heule,F., Barr,H., Robinson,J.S., Bruining,H.A., and Puppels,G.J. (2002). Medical applications of Raman spectroscopy: From proof of principle to clinical implementation. *Biopolymers* 67, 1-9.
- Clowes,F.A.L. (1958). Development of quiescent centres in root meristems. *New Phytologist* 57, 85-88.

## References

- Cole, K.S. (1933). Surface forces of the *Arbacia* egg. *Protoplasma* 17, 480.
- Cosgrove, D. J. Cell Wall Loosening by Expansins. *Plant physiology* 118, 333-339. 1998.  
Ref Type: Generic
- Cosgrove, D.J. (1999). Enzymes and other agents that enhance cell wall extensibility. *Annual Review of Plant Physiology and Plant Molecular Biology* 50, 391-417.
- Cosgrove, D.J. (2000b). Expansive growth of plant cell walls. *Plant Physiology and Biochemistry* 38, 109-124.
- Cosgrove, D.J. (2000a). Loosening of plant cell walls by expansins. *Nature* 407, 321-326.
- Cumming, C.M., Rizkallah, H., McKendrick, K.A., Abdel-Massih, R.A., Baydoun, L., and Brett, C.T. (2005b). Biosynthesis and cell-wall deposition of a pectin xyloglucan complex in pea. *Planta* 222, 546-555.
- Cumming, C.M., Rizkallah, H., McKendrick, K.A., Abdel-Massih, R.A., Baydoun, L., and Brett, C.T. (2005a). Biosynthesis and cell-wall deposition of a pectin xyloglucan complex in pea. *Planta* 222, 546-555.
- De Gelder, J., De Gussem, K., Vandenabeele, P., and Moens, L. (2007). Reference database of Raman spectra of biological molecules. *J. Raman Spectrosc.* 38, 1133-1147.
- De Smet, I., Vanneste, S., Inzé, D., and Beeckman, T. (2006). Lateral Root Initiation or the Birth of a New Meristem. *Plant Molecular Biology* 60, 871-887.
- Decker, E.L. and Reski, R. (2004). The moss bioreactor. *Current Opinion in Plant Biology* 7, 166-170.
- Demirbas, A. (2007). Progress and recent trends in biofuels. *Progress in Energy and Combustion Science* 33, 1-18.
- Dewitte, W. and Murray, J.A.H. (2003). The plant cell cycle. *Annual Review of Plant Biology* 54, 235-264.
- Ding, S.Y. and Himmel, M.E. (2006). The Maize Primary Cell Wall Microfibril: A New Model Derived from Direct Visualization. *Journal of Agricultural and Food Chemistry* 54, 597-606.
- Doležel, J. (1991). Flow cytometric analysis of nuclear DNA content in higher plants. *Phytochem. Anal.* 2, 143-154.
- Doonan, J. and Fobert, P. (1997). Conserved and novel regulators of the plant cell cycle. *Current Opinion in Cell Biology* 9, 824-830.
- Dpoole, J., Binarov, P., and Lcretti, S. (1989). Analysis of Nuclear DNA content in plant cells by Flow cytometry. *Biologia Plantarum* 31, 113-120.
- Dubel, S. and Little, M. (1988). Microtubule-dependent cell cycle regulation is implicated in the G2 phase of *Hydra* cells. *J Cell Sci* 91, 347-359.
- Dubrovsky, J.G., Guttenberg, M., Saralegui, A., Napsucialy-Mendivil, S., Voigt, B., Balus, F and Menzel, D. (2006). Neutral Red as a Probe for Confocal Laser Scanning Microscopy

## References

Studies of Plant Roots. *Annals of Botany* 97: 1127–1138

Dunlop, E.H., Namdev, P.K., and Rosenberg, M.Z. (1994). Effect of fluid shear forces on plant cell suspensions. *Chemical Engineering Science* 49, 2263-2276.

Ebringerova, A. (2005). Structural Diversity and Application Potential of Hemicelluloses. *Macromol. Symp.* 232, 1-12.

Edouard, L., Sève, T., and Marc, L. (2004). Physico-chemical characteristics of cell walls from *Arabidopsis thaliana* microcalli showing different adhesion strengths. *Journal of Experimental Botany* 55, 2087-2097.

Emons, A.M. and Mulder, B.M. (1998). The making of the architecture of the plant cell wall: How cells exploit geometry. *Proceedings of the National Academy of Sciences of the United States of America* 95, 7215-7219.

Emons, A.M. and Mulder, B.M. (2000). How the deposition of cellulose microfibrils builds cell wall architecture. *Trends in Plant Science* 5, 35-40.

Encina, C.L., Constantin, M., and Botella, J. (2001). An easy and reliable method for establishment and maintenance of leaf and root cell cultures of *Arabidopsis thaliana*. *Plant Molecular Biology Reporter* 19, 245-248.

European, U.C., The Institute for Genomic Research, and Kazusa DNA Research Institute (2000). Sequence and analysis of chromosome 3 of the plant *Arabidopsis thaliana*. *Nature* 408, 820-823.

Evans, G.C. and Hughes, A.P. (1962). Plant growth and the aerial environment. *New Phytologist* 61, 322-327.

Fagard, M., Hofte, H., and Vernhettes, S. (2000). Cell wall mutants. *Plant Physiology and Biochemistry* 38, 15-25.

Fearnside, P.M. (1996). Amazonian deforestation and global warming: carbon stocks in vegetation replacing Brazil's Amazon forest. *Forest Ecology and Management* 80, 21-34.

Feng, W.W. and Yang, W.H. (1973). On the Contact Problem of an Inflated Spherical Nonlinear Membrane. *Journal of Applied Mechanics* 40, 209-214.

Fischer, R., Emans, N., Schuster, F., Hellwig, S., and Drossard, J. (1999). Towards molecular farming in the future: using plant-cell-suspension cultures as bioreactors. *Biotechnology and applied Biochemistry* 30 ( Pt 2), 109-112.

Fischer, R., Schillberg, S., and Emans, N. (2000). Toward molecular farming of therapeutic in plants. In *Developments in Plant Genetics and Breeding Plant Genetic Engineering Towards the Third Millennium*, Proceedings of the International Symposium on Plant Genetic Engineering, D.A.PhD Ariel, ed. Elsevier), pp. 229-238.

Fischer, R., Stoger, E., Schillberg, S., Christou, P., and Twyman, R.M. (2004). Plant-based production of biopharmaceuticals. *Current Opinion in Plant Biology* 7, 152-158.

Fry, S.C. (1986). Cross-Linking of Matrix Polymers in the Growing Cell Walls of Angiosperms. *Annual Review of Plant Physiology* 37, 165-186.

## References

- Fry, S.C. (1995). Polysaccharide-Modifying Enzymes in the Plant Cell Wall. *Annual Review of Plant Physiology and Plant Molecular Biology* 46, 497-520.
- Fu, X. and Harberd, N.P. (2003). Auxin promotes Arabidopsis root growth by modulating gibberellin response. *Nature* 421, 740-743.
- Gardner, S.L., Burrell, M.M., and Fry, S.C. (2002). Screening of Arabidopsis thaliana stems for variation in cell wall polysaccharides. *Phytochemistry* 60, 241-254.
- Gendreau, E., Traas, J., Desnos, T., Grandjean, O., Caboche, M., and Hofte, H. (1997). Cellular Basis of Hypocotyl Growth in Arabidopsis thaliana. *Plant Physiol.* 114, 295-305.
- Genschik, P. (2001). The Plant Cell Cycle, by D. Inzé, a special issue of *Plant Molecular Biology* 43, No. 5/6 (2000), Kluwer Academic Publishers, Dordrecht, The Netherlands, 2000. ISBN-0792366786 (Price: NLG 225, USD 110, GBP 69). *Plant Science* 160, 1081.
- Gierlinger, N., Sapei, L., and Paris, O. (2008). Insights into the chemical composition of *Equisetum hyemale*; by high resolution Raman imaging. *Planta* 227, 969-980.
- Gierlinger, N. and Schwanninger, M. (2006). Chemical Imaging of Poplar Wood Cell Walls by Confocal Raman Microscopy. *Plant Physiol.* 140, 1246-1254.
- Goda, H., Shimada, Y., Asami, T., Fujioka, S., and Yoshida, S. (2002). Microarray Analysis of Brassinosteroid-Regulated Genes in Arabidopsis. *Plant Physiol.* 130, 1319-1334.
- Godfray, H.C., Beddington, J.R., Crute, I.R., Haddad, L., Lawrence, D., Muir, J.F., Pretty, J., Robinson, S., Thomas, S.M., and Toulmin, C. (2010). Food Security: The Challenge of Feeding 9 Billion People. *Science* 327, 812-818.
- Green, P.B. and Bauer, K. (1977). Analysing the changing cell cycle. *Journal of Theoretical Biology* 68, 299-315.
- Guda, C., Lee, S.B., and Daniell, H. (2000). Stable expression of a biodegradable protein-based polymer in tobacco chloroplasts. *Plant Cell Reports* 19, 257-262.
- Hansma, H.G. and Hoh, J.H. (1994). Biomolecular Imaging with the Atomic Force Microscope. *Annual Review of Biophysics and Biomolecular Structure* 23, 115-140.
- Hayashi, T. (1989). Xyloglucans in the Primary Cell Wall. *Annual Review of Plant Physiology and Plant Molecular Biology* 40, 139-168.
- Hellwig, S., Drossard, J., Twyman, R.M., and Fischer, R. (2004). Plant cell cultures for the production of recombinant proteins. *Nat Biotech* 22, 1415-1422.
- Himmel, M.E., Ding, S.Y., Johnson, D.K., Adney, W.S., Nimlos, M.R., Brady, J.W., and Foust, T.D. (2007). Biomass Recalcitrance: Engineering Plants and Enzymes for Biofuels Production. *Science* 315, 804-807.
- Hiramoto, Y. (1963). Mechanical properties of sea urchin eggs : I. Surface force and elastic modulus of the cell membrane. *Experimental Cell Research* 32, 59-75.
- Hoff, J.E. and Castro, M.D. (1969). Chemical composition of potato cell wall. *Journal of Agricultural and Food Chemistry* 17, 1328-1331.

## References

- Hooke, Robert. *Micrographia*. Royal Society London. 1664.  
Ref Type: Generic
- Horvath,D.P., Schaffer,R., West,M., and Wisman,E. (2003). Arabidopsis microarrays identify conserved and differentially expressed genes involved in shoot growth and development from distantly related plant species. *The Plant Journal* 34, 125-134.
- Hoson,T. (1991). Structure and Function of Plant Cell Walls: Immunological Approaches. In *International Review of Cytology*, W.J.a.M.Kwang, ed. Academic Press), pp. 233-268.
- Howell,S.H., Lall,S., and Che,P. (2003). Cytokinins and shoot development. *Trends in Plant Science* 8, 453-459.
- Husken,D., Steudle,E., and Zimmermann,U. (1978). Pressure Probe Technique for Measuring Water Relations of Cells in Higher Plants. *Plant Physiol.* 61, 158-163.
- Ishii,T. and Matsunaga,T. (2001). Pectic polysaccharide rhamnogalacturonan II is covalently linked to homogalacturonan. *Phytochemistry* 57, 969-974.
- Jacobs,T. (1992). Control of the cell cycle. *Developmental Biology* 153, 1-15.
- Jaquinod,M., Villiers,F., Kieffer-Jaquinod,S., Hugouvieux,V.+, Bruley,C., Garin,J.+, and Bourguignon,J. (2007). A Proteomics Dissection of Arabidopsis thaliana Vacuoles Isolated from Cell Culture. *Molecular & Cellular Proteomics* 6, 394-412.
- Jarvis,M. (1984). Structure and properties of pectin gels in plant cell walls. *Plant, Cell & Environment* 7, 153-164.
- Jarvis,M. (1998). Intercellular separation forces generated by intracellular pressure. *Plant, Cell & Environment* 21, 1307-1310.
- Jarvis,M., Briggs,S.P., and Knox,J.P. (2003). Intercellular adhesion and cell separation in plants. *Plant, Cell & Environment* 26, 977-989.
- Johansson,I. (1998). Water transport activity of the plasma membrane aquaporin PM28A is regulated by phosphorylation. *Plant Cell* 10, 451-459.
- Johansson,I., Karlsson,M., Johanson,U., Larsson,C., and Kjellbom,P. (2000). The role of aquaporins in cellular and whole plant water balance. *Biochim. Biophys. Acta* 1465, 324-342.
- Kaar,W.E., Cool,L.G., Merriman,M.M., and Brink,D.L. (1991). The Complete Analysis of Wood Polysaccharides Using HPLC. *Journal of Wood Chemistry and Technology* 11, 447-463.
- Kasas,S., Gotzos,V., and Celio,M.R. (1993). Observation of living cells using the atomic force microscope. *Biophysical Journal* 64, 539-544.
- Kasas,S. and Ikai,A. (1995). A method for anchoring round shaped cells for atomic force microscope imaging. *Biophysical Journal* 68, 1678-1680.
- Kazusa DNA Research Institute, The Cold Spring Harbor and Washington University Sequencing Consortium, The European Union Arabidopsis Genome Sequencing Consortium,

## References

- and Institute of Plant Genetics and Crop Plant Research (IPK) (2000). Sequence and analysis of chromosome 5 of the plant *Arabidopsis thaliana*. *Nature* *408*, 823-826.
- Keegstra, K., Talmadge, K.W., Bauer, W.D. and Albersheim, P. (1973) Structure of plant cell walls. III. A model of the walls of suspension-cultured sycamore cells based on the interconnections of the macromolecular components. *Plant Physiol.* *5*, 8-97.
- Kirby, A.R., Gunning, A.P., Waldron, K.W., Morris, V.J., and Ng, A. (1996). Visualization of plant cell walls by atomic force microscopy. *Biophysical Journal* *70*, 1138-1143.
- Kneipp, K., Kneipp, H., Itzkan, I., Dasari, R.R., and Feld, M.S. (1999). Ultrasensitive Chemical Analysis by Raman Spectroscopy. *Chemical Reviews* *99*, 2957-2976.
- Krause, G.H. and Weis, E. (1991). Chlorophyll Fluorescence and Photosynthesis: The Basics. *Annual Review of Plant Physiology and Plant Molecular Biology* *42*, 313-349.
- Kropf, D.L., Bisgrove, S.R., and Hable, W.E. (1998). Cytoskeletal control of polar growth in plant cells. *Current Opinion in Cell Biology* *10*, 117-122.
- Laloue, M., Courtois, D., and Manigault, P. (1980). Convenient and rapid fluorescent staining of plant cell nuclei with [<sup>3</sup>H]33258' Hoechst. *Plant Science Letters* *17*, 175-179.
- Leboeuf, E., Guillon, F., Thoirion, S., Verine, and Lahaye, M. (2005). Biochemical and immunohistochemical analysis of pectic polysaccharides in the cell walls of *Arabidopsis* mutant *quasimodo 1* suspension-cultured cells: implications for cell adhesion. *Journal of Experimental Botany* *56*, 3171-3182.
- Lee, Y., Choi, D., and Kende, H. (2001). Expansins: ever-expanding numbers and functions. *Current Opinion in Plant Biology* *4*, 527-532.
- Lee, Y., Choi, D. and Cho, H. (2006) Expansins: expanding importance in plant growth and development. *Physiologia Plantarum*, *126*: 511-518
- Lee, Y.J. and Yang, Z. (2008). Tip growth: signaling in the apical dome. *Current Opinion in Plant Biology* *11*, 662-671.
- Levine, L.H., Heyenga, A.G., Levine, H.G., Choi, J.W., Davin, L.B., Krikorian, A.D., and Lewis, N.G. (2001). Cell-wall architecture and lignin composition of wheat developed in a microgravity environment. *Phytochemistry* *57*, 835-846.
- Lewis, N.G. and Yamamoto, E. (1990). Lignin: Occurrence, Biogenesis and Biodegradation. *Annual Review of Plant Physiology and Plant Molecular Biology* *41*, 455-496.
- Li, Y., Darley, C.P., Ongaro, V., Fleming, A., Schipper, O., Baldauf, S.L., and Queen-Mason, S.J. (2002). Plant Expansins Are a Complex Multigene Family with an Ancient Evolutionary Origin. *Plant Physiol.* *128*, 854-864.
- Li, Y., Jones, L., and Queen-Mason, S. (2003). Expansins and cell growth. *Current Opinion in Plant Biology* *6*, 603-610.
- Lin, X., Kaul, S., Rounsley, S., Shea, T.P., Benito, M.I., Town, C.D., Fujii, C.Y., Mason, T., Bowman, C.L., Barnstead, M., Feldblyum, T.V., Buell, C.R., Ketchum, K.A., Lee, J.,

## References

- Ronning,C.M., Koo,H.L., Moffat,K.S., Cronin,L.A., Shen,M., Pai,G., Van Aken,S., Umayam,L., Tallon,L.J., Gill,J.E., Adams,M.D., Carrera,A.J., Creasy,T.H., Goodman,H.M., Somerville,C.R., Copenhaver,G.P., Preuss,D., Nierman,W.C., White,O., Eisen,J.A., Salzberg,S.L., Fraser,C.M., and Venter,J.C. (1999). Sequence and analysis of chromosome 2 of the plant *Arabidopsis thaliana*. *Nature* 402, 761-768.
- Lloyd,C.W. (1987). The Plant Cytoskeleton: The Impact of Fluorescence Microscopy. *Annual Review of Plant Physiology* 38, 119-137.
- Ma,J.K.C., Drake,P.M.W., and Christou,P. (2003). The production of recombinant pharmaceutical proteins in plants. *Nat Rev Genet* 4, 794-805.
- McCann, M.C., Wells, B. and Roberts, K. (1990) Direct visualization of cross-links in the primary plant cell wall. *J. Cell Sci.* 96,323-334.
- McCann, M.C. and Roberts, K. (1992) Architecture of the primary cell wall. In *The Cytoskeletal Basis of Plant Growth and Form* (Lloyd,C.W.,ed.). London:Academic Press, 109-129.
- McCann, M.C., Wells, B. and Roberts, K. (1992) Complexity in the spatial localisation and length distribution of plant cell wall matrix polysaccharides. *J. Microscopy*, 166, 123-136.
- Madson,M., Dunand,C., Li,X., Verma,R., Vanzin,G.F., Caplan,J., Shoue,D.A., Carpita,N.C., and Reiter,W.D. (2003). The MUR3 Gene of *Arabidopsis* Encodes a Xyloglucan Galactosyltransferase That Is Evolutionarily Related to Animal Exostosins. *Plant Cell* 15, 1662-1670.
- Martin,F.W. (1959). Staining and Observing Pollen Tubes in the Style by Means of Fluorescence. *Biotechnic & Histochemistry* 34, 125-128.
- Marty,F. (1999). Plant Vacuoles. *Plant Cell* 11, 587-600.
- Mashmouhy,H., Zhang,Z., and Thomas,C.R. (1998). Micromanipulation measurement of the mechanical properties of baker's yeast cells. *Biotechnology Techniques* 12, 925-929.
- Mathur,J. (2004). Cell shape development in plants. *Trends in Plant Science* 9, 583-590.
- Maurel,C., Verdoucq,L., Luu,D.T., and Santoni,V.+. (2008). Plant Aquaporins: Membrane Channels with Multiple Integrated Functions. *Annual Review of Plant Biology* 59, 595-624.
- Maurel C. (1997). Aquaporins and water permeability of plant membranes. *Annual Review of Plant Physiology and Plant Molecular Biology* 48: 399-429.
- Mayer,K., Schuller,C., Wambutt,R., Murphy,G., Volckaert,G., Pohl,T., Dusterhoft,A., Stiekema,W., Entian,K.D., Terry,N., Harris,B., Ansorge,W., Brandt,P., Grivell,L., Rieger,M., Weichselgartner,M., de Simone,V., Obermaier,B., Mache,R., Muller,M., Kreis,M., Delseny,M., Puigdomenech,P., Watson,M., Schmidtheini,T., Reichert,B., Portatelle,D., Perez-Alonso,M., Boutry,M., Bancroft,I., Vos,P., Hoheisel,J., Zimmermann,W., Wedler,H., Ridley,P., Langham,S.A., McCullagh,B., Bilham,L., Robben,J., Van der Schueren,J., Grymonprez,B., Chuang,Y.J., Vandenbussche,F., Braeken,M., Weltjens,I., Voet,M., Bastiaens,I., Aert,R., Defoor,E., Weitzenegger,T., Bothe,G., Ramsperger,U., Hilbert,H.,

## References

- Braun,M., Holzer,E., Brandt,A., Peters,S., van Staveren,M., Dirkse,W., Mooijman,P., Lankhorst,R.K., Rose,M., Hauf,J., Kotter,P., Berneiser,S., Hempel,S., Feldpausch,M., Lamberth,S., Van den Daele,H., De Keyser,A., Buysshaert,C., Gielen,J., Villarroel,R., De Clercq,R., Van Montagu,M., Rogers,J., Cronin,A., Quail,M., Bray-Allen,S., Clark,L., Doggett,J., Hall,S., Kay,M., Lennard,N., McLay,K., Mayes,R., Pettett,A., Rajandream,M.A., Lyne,M., Benes,V., Rechmann,S., Borkova,D., Blocker,H., Scharfe,M., Grimm,M., Lohnert,T.H., Dose,S., de Haan,M., Maarse,A., Schafer,M., Muller-Auer,S., Gabel,C., Fuchs,M., Fartmann,B., Granderath,K., Dauner,D., Herzl,A., Neumann,S., Argiriou,A., Vitale,D., Liguori,R., Piravandi,E., Massenet,O., Quigley,F., Clabaud,G., Mundlein,A., Felber,R., Schnabl,S., Hiller,R., Schmidt,W., Lecharny,A., Aubourg,S., Chefdor,F., Cooke,R., Berger,C., Montfort,A., Casacuberta,E., Gibbons,T., Weber,N., Vandenbol,M., Bargues,M., Terol,J., Torres,A., Perez-Perez,A., Purnelle,B., Bent,E., Johnson,S., Tacon,D., Jesse,T., Heijnen,L., Schwarz,S., Scholler,P., Heber,S., Francs,P., Bielke,C., Frishman,D., Haase,D., Lemcke,K., Mewes,H.W., Stocker,S., Zaccaria,P., Bevan,M., Wilson,R.K., de la Bastide,M., Habermann,K., Parnell,L., Dedhia,N., Gnoj,L., Schutz,K., Huang,E., Spiegel,L., Sehkon,M., Murray,J., Sheet,P., Cordes,M., Abu-Threideh,J., Stoneking,T., Kalicki,J., Graves,T., Harmon,G., Edwards,J., Latreille,P., Courtney,L., Cloud,J., Abbott,A., Scott,K., Johnson,D., Minx,P., Bentley,D., Fulton,B., Miller,N., Greco,T., Kemp,K., Kramer,J., Fulton,L., Mardis,E., Dante,M., Pepin,K., Hillier,L., Nelson,J., Spieth,J., Ryan,E., Andrews,S., Geisel,C., Layman,D., Du,H., Ali,J., Berghoff,A., Jones,K., Drone,K., Cotton,M., Joshu,C., Antonoiu,B., Zidanic,M., Strong,C., Sun,H., Lamar,B., Yordan,C., Ma,P., Zhong,J., Preston,R., Vil,D., Shekher,M., Matero,A., Shah,R., Swaby,I.'K., O'Shaughnessy,A., Rodriguez,M., Hoffman,J., Till,S., Granat,S., Shohdy,N., Hasegawa,A., Hameed,A., Lodhi,M., Johnson,A., Chen,E., Marra,M., Martienssen,R., and McCombie,W.R. (1999). Sequence and analysis of chromosome 4 of the plant *Arabidopsis thaliana*. *Nature* *402*, 769-777.
- McNeil,M., Darvill,A.G., Fry,S.C., and Albersheim,P. (1984). Structure and Function of the Primary Cell Walls of Plants. *Annual Review of Biochemistry* *53*, 625-663.
- Menges,M., Hennig,L., Gruissem,W., and Murray,J.A.H. (2002). Cell Cycle-regulated Gene Expression in *Arabidopsis*. *Journal of Biological Chemistry* *277*, 41987-42002.
- Menges,M., Hennig,L., Gruissem,W., and Murray,J.A.H. (2003). Genome-wide gene expression in an *Arabidopsis* cell suspension. *Plant Molecular Biology* *53*, 423-442.
- Meyer,E. (1992). Atomic force microscopy. *Progress in Surface Science* *41*, 3-49.
- Meyerowitz,E. (1987). *In situ* hybridization to RNA in plant tissue. *Plant Molecular Biology Reporter* *5*, 242-250.
- Miller,C.O. (1961). Kinetin and Related Compounds in Plant Growth. *Annual Review of Plant Physiology* *12*, 395-408.
- Mineyuki,Y.I. and Gunning,B.E. (1990). A role for preprophase bands of microtubules in maturation of new cell walls, and a general proposal on the function of preprophase band sites in cell division in higher plants. *J Cell Sci* *97*, 527-537.
- Mok,D.W. and Mok,M.C. (2001). CYTOKININ METABOLISM AND ACTION. *Annual Review of Plant Physiology and Plant Molecular Biology* *52*, 89-118.

## References

- Mordhorst,A.P., Voerman,K.J., Hartog,M.V., Meijer,E.A., van Went,J., Koornneef,M., and de Vries,S.C. (1998). Somatic Embryogenesis in *Arabidopsis thaliana* Is Facilitated by Mutations in Genes Repressing Meristematic Cell Divisions. *Genetics* 149, 549-563.
- Morelli,G. and Ruberti,I. (2002). Light and shade in the photocontrol of *Arabidopsis* growth. *Trends in Plant Science* 7, 399-404.
- Morita, M. T., Kato, T., Nagafusa, K., Saito, C., Ueda, T., Nakano, A. and Tasaka, M. (2002) Involvement of the Vacuoles of the Endodermis in the Early Process of Shoot Gravitropism in *Arabidopsis* *Plant Cell* 14: 47-56.
- Morrow,D.L. and Jones,R.L. (1986). Localization and partial characterization of the extracellular proteins centrifuged from pea internodes. *Physiologia Plantarum* 67, 397-407.
- Mouille, Gregory, Ralet, Marie-Christine, Cavelier , Celine, Cathlene, Eland, Delphine, Effroy, Kian, He maty, Lesley, McCartney, Hoai Nam, Truong, Gaudon, Virginie, Thibault, Jean-Francois, Marchant, Alan, and Hofte, Herman. (2007) Homogalacturonan synthesis in *Arabidopsis thaliana* requires a Golgi-localized protein with a putative methyltransferase domain. *The Plant Journal* 50, 605-614.
- Naill,M.C. and Roberts,S.C. (2004). Preparation of single cells from aggregated *Taxus* suspension cultures for population analysis. *Biotechnol. Bioeng.* 86, 817-826.
- Namdev,P. and Dunlop,E. (1995). Shear sensitivity of plant cells in suspensions present and future. *Applied Biochemistry and Biotechnology* 54, 109-131.
- Neal,G.E. (1965). Changes occurring in the cell walls of strawberries during ripening. *J. Sci. Food Agric.* 16, 604-611.
- Nicol,F. and Hofte,H. (1998). Plant cell expansion: Scaling the wall. *Current Opinion in Plant Biology* 1, 12-17.
- O'Neill,M.A., Ishii,T., Albersheim,P., and Darvill,A.G. (2004). Rhamnogalacturonan II: Structure and Function of a Borate Cross-Linked Cell Wall Pectic Polysaccharide. *Annual Review of Plant Biology* 55, 109-139.
- Olson,A.C., Evans,J.J., Frederick,D.P., and Jansen,E.F. (1969). Plant Suspension Culture Media Macromolecules--Pectic Substances, Protein, and Peroxidase. *Plant Physiol.* 44, 1594-1600.
- Our,P.C. (1973). Plant Cell Walls: New Structural Model. *Nature* 242, 554-555.
- Ossowski, S., Schneeberger, K., Lucas-Lledó, J.I., Warthmann, N., Clark, R.M., Shaw, R.G., Weigel, D., and Michael Lynch (2010). The Rate and Molecular Spectrum of Spontaneous Mutations in *Arabidopsis thaliana*. *Science*: 327 (5961), 92-94.
- Pauly,M. and Keegstra,K. (2010). Plant cell wall polymers as precursors for biofuels. *Current Opinion in Plant Biology* 13, 304-311.

## References

- Pena,M.J., Ryden,P., Madson,M., Smith,A.C., and Carpita,N.C. (2004). The Galactose Residues of Xyloglucan Are Essential to Maintain Mechanical Strength of the Primary Cell Walls in *Arabidopsis* during Growth. *Plant Physiol.* *134*, 443-451.
- Petry,R., Schmitt,M., and Popp,J. (2003). Raman Spectroscopy as a Prospective Tool in the Life Sciences. *Chem. Eur. J. of Chem. Phys.* *4*, 14-30.
- Popper,Z.A. (2008). Evolution and diversity of green plant cell walls. *Current Opinion in Plant Biology* *11*, 286-292.
- Powell,K.T. and Weaver,J.C. (1986). Transient aqueous pores in bilayer membranes: A statistical theory. *Bioelectrochemistry and Bioenergetics* *15*, 211-227.
- Pritchard,J., Williams,G., Jones,R.G., and Tomos,A.D. (1989). Radial Turgor Pressure Profiles in Growing and Mature Zones of Wheat Roots--A Modification of the Pressure Probe. *Journal of Experimental Botany* *40*, 567-571.
- Pujara,P. and Lardner,T.J. (1979). A model for cell division. *Journal of Biomechanics* *12*, 293-299.
- Rabinowitch,E. (1952). Photosynthesis. *Annual Review of Plant Physiology* *3*, 229-264.
- Ragauskas,A.J., Williams,C.K., Davison,B.H., Britovsek,G., Cairney,J., Eckert,C.A., Frederick,W.J., Jr., Hallett,J.P., Leak,D.J., Liotta,C.L., Mielenz,J.R., Murphy,R., Templer,R., and Tschaplinski,T. (2006). The Path Forward for Biofuels and Biomaterials. *Science* *311*, 484-489.
- Ramonell,K.M., Zhang,B., Ewing,R.M., Chen,Y., Xu,D., Stacey,G., and Somerville,S. (2002). Microarray analysis of chitin elicitation in *Arabidopsis thaliana*. *Molecular Plant Pathology* *3*, 301-311.
- Kosala Ranathunge, K. and Schreibe, L. (2011). Water and solute permeabilities of *Arabidopsis* roots in relation to the amount and composition of aliphatic suberin. *Journal of Experimental Botany*, Vol. 62, No. 6, pp. 1961–1974
- Reiter,W.D. (2002). Biosynthesis and properties of the plant cell wall. *Current Opinion in Plant Biology* *5*, 536-542.
- Reiter,W.D., Chapple,C., and Somerville,C.R. (1997). Mutants of *Arabidopsis thaliana* with altered cell wall polysaccharide composition. *The Plant Journal* *12*, 335-345.
- Richard,C., Lescot,M., Inza,D., and De Veylder,L. (2002). Effect of auxin, cytokinin, and sucrose on cell cycle gene expression in *Arabidopsis thaliana* cell suspension cultures. *Plant Cell, Tissue and Organ Culture* *69*, 167-176.
- Richmond,T. (2000). Higher plant cellulose synthases. *Genome Biology* *1*, reviews3001.
- Richmond,T.A. and Somerville,C.R. (2000). The Cellulose Synthase Superfamily. *Plant Physiol.* *124*, 495-498.
- Ridley,B.L., O'Neill,M.A., and Mohnen,D. (2001). Pectins: structure, biosynthesis, and oligogalacturonide-related signaling. *Phytochemistry* *57*, 929-967.

## References

- Rose, J.K., Saladie, M., and Catala, C. (2004). The plot thickens: new perspectives of primary cell wall modification. *Current Opinion in Plant Biology* 7, 296-301.
- SAKAI, T. (1980). Relation between Thickness and Interference Colors of Biological Ultrathin Section. *Journal of Electron Microscopy* 29, 369-375.
- Sakakibara, H. (2006). Cytokinins: Activity, Biosynthesis, and Translocation. *Annual Review of Plant Biology* 57, 431-449.
- Savage, D.F. and Stroud, R.M. (2007). Structural Basis of Aquaporin Inhibition by Mercury. *Journal of Molecular Biology* 368, 607-617.
- Saxena, I. and Brown, R.M. (2005). Cellulose Biosynthesis: Current Views and Evolving Concepts. *Annals of Botany* 96, 9-21.
- Schneitz, K., Sablowski, R., Lemieux, B., Dunwell, J., Sweetlove, L., Fernie, A., Metraux, J.P., Palme, K., McAinsh, M.R., Weisshaar, B., and Berger, F. (2002). Plant biology. *Current Opinion in Plant Biology* 5, 265-274.
- Scragg, A.H., Allan, E.J., and Leckie, F. (1988). Effect of shear on the viability of plant cell suspensions. *Enzyme and Microbial Technology* 10, 361-367.
- Shiu, C., Zhang, Z., and Thomas, C.R. (1999). A novel technique for the study of bacterial cell mechanical properties. *Biotechnology Techniques* 13, 707-713.
- Showalter, A.M. (1993). Structure and Function of Plant Cell Wall Proteins. *Plant Cell* 5, 9-23.
- Smith, A.E., Zhang, Z., Thomas, C.R., Moxham, K.E., and Middelberg, A.P.J. (2000). The mechanical properties of *Saccharomyces cerevisiae*. *Proceedings of the National Academy of Sciences of the United States of America* 97, 9871-9874.
- Smith, L.G. (2001). Plant cell division: building walls in the right places. *Nat Rev Mol Cell Biol* 2, 33-39.
- Smith, L.G. and Oppenheimer, D.G. (2005). Spatial control of cell expansion by the plant cytoskeleton. *Annual Review of Cell and Developmental Biology*, Vol. 21: 271-295
- Smith, L.G. (2003). Cytoskeletal control of plant cell shape: getting the fine points. *Current Opinion in Plant Biology* 6, 63-73.
- Smith, M.M. and McCully, M.E. (1978). Enhancing Aniline Blue Fluorescent Staining of Cell Wall Structures. *Biotechnic & Histochemistry* 53, 79-85.
- Somerville, C. (2006). Cellulose Synthesis in Higher Plants. *Annual Review of Cell and Developmental Biology* 22, 53-78.
- Srivastava, L.M. (2002b). Hormonal Regulation of Cell Division and Cell Growth. In *Plant Growth and Development*, (San Diego: Academic Press), pp. 341-379.
- Srivastava, L.M. (2002a). Cell Wall, Cell Division, and Cell Growth. In *Plant Growth and Development*, (San Diego: Academic Press), pp. 23-74.

## References

- Staiger,C. and Doonan,J. (1993). Cell division in plants. *Current Opinion in Cell Biology* 5, 226-231.
- Stenson,J.D., Thomas,C.R., and Hartley,P. (2009). Modelling the mechanical properties of yeast cells. *Chemical Engineering Science* 64, 1892-1903.
- Stenvik,G.E., Butenko,M.A., Urbanowicz,B.R., Rose,J.K.C., and Aalen,R.B. (2006a). Overexpression of Inflorescence deficient in abscission Activates Cell Separation in Vestigial Abscission Zones in *Arabidopsis*. *Plant Cell tpc*.
- Stenvik,G.E., Butenko,M.A., Urbanowicz,B.R., Rose,J.K.C., and Aalen,R.B. (2006b). Overexpression of Inflorescence deficient in Abscission Activates Cell Separation in Vestigial Abscission Zones in *Arabidopsis*. *Plant Cell tpc*.
- Steudle,E., Zimmermann,U., and Luttge,U. (1977). Effect of Turgor Pressure and Cell Size on the Wall Elasticity of Plant Cells. *Plant Physiol.* 59, 285-289.
- Stevens,B.J.H. and Selvendran,R.R. (1980). The isolation and analysis of cell wall material from the alcohol-insoluble residue of cabbage (*Brassica oleracea* var. capitata). *J. Sci. Food Agric.* 31, 1257-1267.
- Sugimoto,K., Williamson,R.E., and Wasteneys,G.O. (2000). New Techniques Enable Comparative Analysis of Microtubule Orientation, Wall Texture, and Growth Rate in Intact Roots of *Arabidopsis*. *Plant Physiol.* 124, 1493-1506.
- Sussex,I.M., Godoy,J.A., Kerk,N.M., Laskowski,M.J., Nusbaum,H.C., Welsch,J.A., and Williams,M.E. (1995). Cellular and Molecular Events in a Newly Organizing Lateral Root Meristem. *Philosophical Transactions of the Royal Society of London. Series B: Biological Sciences* 350, 39-43.
- Swarbreck, D., Wilks, C., Lamesch, P., Berardini, T.Z., Garcia-Hernandez, M., Foerster, H., Li, D., Meyer, T., Muller, R., Ploetz, L., Radenbaugh, A., Singh, S., Swing, V., Tissier, C., Zhang, P. and Huala, E. The *Arabidopsis* Information Resource (TAIR): gene structure and function annotation (2008) *Nucl. Acids Res.* 36: 1009–1014
- Taiz,L. (1984). Plant Cell Expansion: Regulation of Cell Wall Mechanical Properties. *Annual Review of Plant Physiology* 35, 585-657.
- Talmadge, K.W., Keegstra, K., Bauer, W.D. and Albersheim, P. (1973) The structure of plant cell walls. I. The macromolecular components of the walls of suspension-cultured sycamore cells with a detailed analysis of the pectic polysaccharides. *PlantPhysiol.*51,158-173.
- Tester,M. and Langridge,P. (2010). Breeding Technologies to Increase Crop Production in a Changing World. *Science* 327, 818-822.
- The,A.G., I (2000). Analysis of the genome sequence of the flowering plant *Arabidopsis thaliana*. *Nature* 408, 796-815.
- Theologis,A., Ecker,J.R., Palm,C.J., Federspiel,N.A., Kaul,S., White,O., Alonso,J., Altafi,H., Araujo,R., Bowman,C.L., Brooks,S.Y., Buehler,E., Chan,A., Chao,Q., Chen,H., Cheuk,R.F., Chin,C.W., Chung,M.K., Conn,L., Conway,A.B., Conway,A.R., Creasy,T.H., Dewar,K.,

## References

- Dunn,P., Etgu,P., Feldblyum,T.V., Feng,J., Fong,B., Fujii,C.Y., Gill,J.E., Goldsmith,A.D., Haas,B., Hansen,N.F., Hughes,B., Huizar,L., Hunter,J.L., Jenkins,J., Johnson-Hopson,C., Khan,S., Khaykin,E., Kim,C.J., Koo,H.L., Kremenetskaia,I., Kurtz,D.B., Kwan,A., Lam,B., Langin-Hooper,S., Lee,A., Lee,J.M., Lenz,C.A., Li,J., Li,Y., Lin,X., Liu,S.X., Liu,Z.A., Luross,J.S., Maiti,R., Marzali,A., Militscher,J., Miranda,M., Nguyen,M., Nierman,W.C., Osborne,B.I., Pai,G., Peterson,J., Pham,P.K., Rizzo,M., Rooney,T., Rowley,D., Sakano,H., Salzberg,S.L., Schwartz,J.R., Shinn,P., Southwick,A.M., Sun,H., Tallon,L.J., Tambunga,G., Toriumi,M.J., Town,C.D., Utterback,T., Van Aken,S., Vaysberg,M., Vysotskaia,V.S., Walker,M., Wu,D., Yu,G., Fraser,C.M., Venter,J.C., and Davis,R.W. (2000). Sequence and analysis of chromosome 1 of the plant *Arabidopsis thaliana*. *Nature* 408, 816-820.
- Thomas,C.R., Zhang,Z., and Cowen,C. (2000). Micromanipulation measurements of biological materials. *Biotechnology Letters* 22, 531-537.
- Thomas,C.R. and Paul,G.C. (1996). Applications of image analysis in cell technology. *Current Opinion in Biotechnology* 7, 35-45.
- Thomson,J.A., Mundree,S.G., and Farrant,J.M. (2007). The development of genetically modified maize for abiotic stress tolerance. *South African Journal of Botany* 73, 494-495.
- Tierney,M.L. and Varner,J.E. (1987). The Extensins. *Plant Physiol.* 84, 1-2.
- Tilman,D., Fargione,J., Wolff,B., D'Antonio,C., Dobson,A., Howarth,R., Schindler,D., Schlesinger,W.H., Simberloff,D., and Swackhamer,D. (2001). Forecasting Agriculturally Driven Global Environmental Change. *Science* 292, 281-284.
- Tomos D (2000). The plant cell pressure probe. *Biotechnology Letters* 22, 437-442.
- Tomos,A.D. and Leigh,R.A. (1999). The Pressure Probe: A Versatile Tool in Plant Cell Physiology. *Annual Review of Plant Physiology and Plant Molecular Biology* 50, 447-472.
- Torrey,J.G. (1976). Root Hormones and Plant Growth. *Annual Review of Plant Physiology* 27, 435-459.
- Trewavas,A.J. (1982). Growth substance sensitivity: The limiting factor in plant development. *Physiologia Plantarum* 55, 60-72.
- Turgeon,R. (1996). Phloem loading and plasmodesmata. *Trends in Plant Science* 1, 418-423.
- Turner,S.R., Taylor,N.G., and Jones,L. (2001). Analysis of secondary cell wall formation in *Arabidopsis*. In *Progress in Biotechnology Molecular Breeding of Woody Plants, Proceedings of the International Wood Biotechnology Symposium (IWBS)*, Noriyuki Morohoshi and Atsushi Komamine, ed. Elsevier), pp. 85-92.
- Uslu,A., Faaij,A.P.C., and Bergman,P.C.A. (2008). Pre-treatment technologies, and their effect on international bioenergy supply chain logistics. *Techno-economic evaluation of torrefaction, fast pyrolysis and pelletisation. Energy* 33, 1206-1223.
- Valent,B.S. and Albersheim,P. (1974) The structure of plant cell walls. V. On the binding of xyloglucan to cellulose fibers. *Plant Physiol.* 54, 105-108.

## References

- Valliyodan, B. and Nguyen, H.T. (2006). Understanding regulatory networks and engineering for enhanced drought tolerance in plants. *Current Opinion in Plant Biology* 9, 189-195.
- Valvekens, D., Van Montagu, M., Lijsebettens, M.V. (1988) *Agrobacterium tumefaciens*-mediated transformation of *Arabidopsis thaliana* root explants by using kanamycin selection. *Proc Natl Acad Sci USA* 85: 5536–554
- van der Weele, C.M., Jiang, H.S., Palaniappan, K.K., Ivanov, V.B., Palaniappan, K., and Baskin, T.I. (2003). A New Algorithm for Computational Image Analysis of Deformable Motion at High Spatial and Temporal Resolution Applied to Root Growth. Roughly Uniform Elongation in the Meristem and Also, after an Abrupt Acceleration, in the Elongation Zone. *Plant Physiol.* 132, 1138-1148.
- Vanzin, G.F., Madson, M., Carpita, N.C., Raikhel, N.V., Keegstra, K., and Reiter, W.D. (2002). The mur2 mutant of *Arabidopsis thaliana* lacks fucosylated xyloglucan because of a lesion in fucosyltransferase AtFUT1. *PNAS* 99, 3340-3345.
- Vincken J-P, Schols H.A., Oomen R.J.F.J., McCann M.C., Ulvskov P., Voragen A.G.J., Visser R.G.F. (2003). If homogalacturonan were a side chain of rhamnogalacturonan. I. Implications for cell wall architecture. *Plant Physiology* 132, 1781–1789.
- Vinocur, B. and Altman, A. (2005). Recent advances in engineering plant tolerance to abiotic stress: achievements and limitations. *Current Opinion in Biotechnology* 16, 123-132.
- Vogel, J.P., Raab, T.K., Schiff, C., and Somerville, S.C. (2002). PMR6, a Pectate Lyase-Like Gene Required for Powdery Mildew Susceptibility in *Arabidopsis*. *Plant Cell* 14, 2095-2106.
- Vorwerk, S., Somerville, S., and Somerville, C. (2004). The role of plant cell wall polysaccharide composition in disease resistance. *Trends in Plant Science* 9, 203-209.
- Wang, C., Cowen, C., Zhang, Z., and Thomas, C.R. (2005). High-speed compression of single alginate microspheres. *Chemical Engineering Science* 60, 6649-6657.
- Wang, C., Wang, L., and Thomas, C.R. (2004). Modelling the Mechanical Properties of Single Suspension-Cultured Tomato Cells. *Annals of Botany* 93, 443-453.
- Wang, L., Hukin, D., Pritchard, J., and Thomas, C. (2006). Comparison of plant cell turgor pressure measurement by pressure probe and micromanipulation. *Biotechnology Letters* 28, 1147-1150.
- Hukin D. (2002). Water relations and biophysics of plant cells. PhD Thesis, University of Birmingham, UK.
- Went, F.W. (1958). The Experimental Control of Plant Growth. *Soil Science* 85.
- Whitney, S.E.C., Gothard, M.G.E., Mitchell, J.T., and Gidley, M.J. (1999). Roles of Cellulose and Xyloglucan in Determining the Mechanical Properties of Primary Plant Cell Walls. *Plant Physiol.* 121, 657-664.
- Widholm, J.M. (1972). The Use of Fluorescein Diacetate and Phenosafranine for Determining Viability of Cultured Plant Cells. *Biotechnic and Histochemistry* 47, 189-194.

## References

- Wiese,A., Christ,M.M., Virnich,O., Schurr,U., and Walter,A. (2007). Spatio-temporal leaf growth patterns of *Arabidopsis thaliana* and evidence for sugar control of the diel leaf growth cycle. *New Phytologist* *174*, 752-761.
- Willats,W.G.T., McCartney,L., Mackie,W., and Knox,J.P. (2001). Pectin: cell biology and prospects for functional analysis. *Plant Molecular Biology* *47*, 9-27.
- Williams,D.B., Carter,C.B., Williams,D.B., and Carter,C.B. (2009). The Transmission Electron Microscope. In *Transmission Electron Microscopy*, Springer US), pp. 3-22.
- Yamada,T., Arakawa,H., Okajima,T., Shimada,T., and Ikai,A. (2002). Use of AFM for imaging and measurement of the mechanical properties of light-convertible organelles in plants. *Ultramicroscopy* *91*, 261-268.
- Yamaki,S., Machida,Y., and Kakiuchi,N. (1979). Changes in cell wall polysaccharides and monosaccharides during development and ripening of Japanese pear fruit. *Plant Cell Physiol.* *20*, 311-321.
- Yoneda,M.I. (1964). Tension at the Surface of Sea-Urchin Egg: A Critical Examination of Cole's Experiment. *J Exp Biol* *41*, 893-906.
- Yoneda,M.I. and Dan,K.A. (1972). Tension at the Surface of the Dividing Sea-Urchin Egg. *J Exp Biol* *57*, 575-587.
- Yuan,M., Shaw,P.J., Warn,R.M., and Lloyd,C.W. (1994). Dynamic reorientation of cortical microtubules, from transverse to longitudinal, in living plant cells. *Proceedings of the National Academy of Sciences of the United States of America* *91*, 6050-6053.
- Zablackis,E., Huang,J., Muller,B., Darvill,A.G., and Albersheim,P. (1995). Characterization of the Cell-Wall Polysaccharides of *Arabidopsis thaliana* Leaves. *Plant Physiol.* *107*, 1129-1138.
- Zhang,Z., Ferenczi,M.A., Lush,A.C., and Thomas,C.R. (1991). A novel micromanipulation technique for measuring the bursting strength of single mammalian cells. *Applied Microbiology and Biotechnology* *36*, 208-210.
- Zhang,Z., Stenson,J.D., and Thomas,C.R. (2009). Chapter 2 Micromanipulation in Mechanical Characterisation of Single Particles. In *Advances in Chemical Engineering Characterization of Flow, Particles and Interfaces*, L.Jinghai, ed. Academic Press), pp. 29-85.
- Zhao,Y. (2010). Auxin Biosynthesis and Its Role in Plant Development. *Annual Review of Plant Biology* *61*, 49-64.
- Zimmermann,P., Hirsch-Hoffmann,M., Hennig,L., and Grissem,W. (2004). Geneinvestigator. *Arabidopsis* Microarray Database and Analysis Toolbox. *Plant Physiol.* *136*, 2621-2632.
- Zimmermann,U. (1978). Physics of Turgor- and Osmoregulation. *Annual Review of Plant Physiology* *29*, 121-148.
- Zimmermann,U. and Husken,D. (1979). Theoretical and Experimental Exclusion of Errors in the Determination of the Elasticity and Water Transport Parameters of Plant Cells by the Pressure Probe Technique. *Plant Physiol.* *64*, 18-24.

---

## *Appendices*

---

### Appendix 1: Long Ashton Solution

	Compound	Mol. Weight	Nutrient Sol. In 10L (mM)	Molarity (mM)	g/500ml
1	NH <sub>4</sub> H <sub>2</sub> PO <sub>4</sub>	115.04	1.00	400	23.01
2	(NH <sub>4</sub> ) <sub>2</sub> HPO <sub>4</sub>	132.06	1.00	400	26.41
3	NaFe EDTA	367.05	0.02	6	1.1
	H <sub>3</sub> BO <sub>3</sub>	62.83	0.25	100	3.09
4	MnSO <sub>4</sub>	246.48	0.002	0.8	0.01
	CuSO <sub>4</sub>	249.68	0.002	0.8	0.01
	(NH <sub>4</sub> ) <sub>6</sub> Mo <sub>7</sub> O <sub>24</sub> ·4H <sub>2</sub> O	1235.86	0.00025	0.1	0.06
5	KCl	74.56	0.05	20	0.35
6	KNO <sub>3</sub>	101.11	4.00	1600	80.89
7	MgSO <sub>4</sub>	246.48	1.00	400	49.3
8	Ca(NO <sub>3</sub> ) <sub>2</sub>	236.15	4.00	1600	188.92

## **Appendix 2: The Protocols for Surface Sterilisation**

### **Sodium Hypochlorite solution**

Solution consists of 2mls sodium hypochlorite (house-hold bleach); 12.5 µl tween 20 and made up to 25mls with SDW. Place approximately 100 seeds in a 1.5mls microfuge tube and add 1ml of sodium hypochlorite solution, shake for 2 minutes. Allow seeds to settle, remove sodium hypochlorite solution and add 1ml 70% ethanol and shake for 2 minutes. Remove ethanol and wash three times with 1ml SDW. Later steps may require centrifugation to pellet seeds to enable the removal of the solutions without loss of seeds. This method was used to sterilise seed for same day use.

### **Desiccation**

Place a desiccator in a fume cupboard and switch on. Place seeds to be sterilised into an open microfuge tube, next add 100mls of bleach to a 250ml beaker and place both seeds and beaker into the desiccator. Prior to putting the lid on the desiccator add 3mls of concentrated HCl to the bleach. Seal the desiccator and leave for approximately 4 hours.

### **Appendix 3: De-proteinisation by phenol/ acetic acid / water (PAW)**

The samples must firstly undergo de-proteinisation, which destroys all the proteins from the sample. This is important as the actions of any proteins may damage the quality of the polysaccharides yielded thus affecting the results gained. De-proteinisation will allow the samples to be stored for much longer without degradation, which is important because of both the number of samples and the time taken to process each one.

Sample: 200mls of cell suspension culture, pcv ca. 25mls

- 1) Collect cells on 4 layers of muslin in a filter funnel, and wash in 100mls of fresh culture medium.
- 2) Squeeze muslin gently to remove surplus medium.
- 3) Weigh the balls of cells (without muslin) let the weight = Wg
- 4) Plunge the ball of cells into 7x W mls of solution A [ 100mls glacial acetic acid + 250mls 80% (w/v) aqueous phenol.]
- 5) Stir the sample at 25°C for at least 2 hours; overnight incubation is acceptable.
- 6) Filter on sintered glass (phenol dissolves nylon) Mix 1ml of filtrate with 50ul 10% ammonium formate + 5mls acetone: a precipitate indicates protein.
- 7) Re-suspend cell (wall) residue in 5 x W mls of solution B [100mls glacial acetic acid + 250mls 80% (w/v) aqueous phenol + 50mls H<sub>2</sub>O]
- 8) Repeat step 5-7- until filtrate no longer contains protein
- 9) Wash walls thoroughly with 70% ethanol until no longer smell of phenol. From samples from which wall polysaccharides will be isolated – re-suspend in more 70% ethanol and store in a tightly sealed bottle preferably at 0°C.

#### **Appendix 4: Preparation of Alcohol Insoluble Residue (AIR)**

The next stage is to isolate the polysaccharides from the rest of the cellular matter e.g. organelles and plasma membrane, as this is not needed and may interfere with the subsequent stages.

Sample: 20g fresh *Arabidopsis thaliana* roots/leaves.

- 1) To 20g fresh weigh, add 140mls ice cold absolute ethanol + 40mls H<sub>2</sub>O to give a final solvent composition of 200mls 70% ethanol. The tissue is assumed to contain about 20mls H<sub>2</sub>O.
- 2) Liquidise the tissue by 5 1-minute bursts at full power in a liquidiser e.g. Polytron, ultra-turrax or Sorvall 'OmniMixer' with cooling to 0°C between each burst. An IKA T25 digital ultra Turrax homogeniser was used for this investigation. With the maximum speed being 24,000 rpm.
- 3) For complete extraction of low Mr cell components, stir the suspension at 0°C with a magnetic stirrer bar for several hours.
- 4) Collect the AIR on a filter (e.g. sintered glass funnel or fine nylon gauze.) Wash with several 100ml aliquots of 70% ethanol. To monitor the progress of removal of low Mr compounds measure the A<sub>280</sub> of a sample from each filtrate.
- 5) For samples from which wall polysaccharides will be isolated – re-suspend the final residue in more 70% ethanol and store in a tightly sealing container, preferably at 0°C.

### **Appendix 5: Sequential Extraction of Polysaccharide from Primary Walls**

For the purposes of this analysis it is important to extract the polysaccharides gradually, so a bulk extraction is not suitable. This will allow the analysis of the individual components to be more accurate. This protocol has the benefit of minimal degradation until stage 5. Giving a true representation of what is present in the cell wall.

Sample: As prepared above

#### **DMSO**

Extracts starch + traces of native hemicellulose

Suspend cell walls (equivalent to 1g dry weight, but still moist with 70% ethanol) in 90% DMSO 100mls. Stir for 16h at 25<sup>0</sup>C. Centrifuge (5mins at 2,500g) carefully pour the supernatant from pellet. Assay supernatant for polymer by Anthrone or Ethanol test (see later). Re-suspend wall pellet in 50mls 90% DMSO, centrifuge and pool supernatants. Repeat DMSO extraction until supernatants contain negligible polymer. Remove residual DMSO by re-suspending final pellet in water and centrifuging.

#### **CTDA**

Extracts some Pectin

CTDA- Trans-1,2-diaminocyclohexane-N,N,N,N-tetra acetic acid monohydrate.

Re-suspend pellet from step 1 whilst still wet in 100mls 50mm CTDA, pH adjusted to 7.5 with 1M NaOH, and chlorobutol added to 0.005%. Shake or stir 16h at 25<sup>0</sup>C. Centrifuge, pour supernatant

## Appendices

from pellet. Assay polymers by Ethanol or anthrone test. Repeat CDTA extraction until supernatant no longer contains polymer. Re-suspend the final pellet in water and centrifuge.

### **Urea**

Extracts small proportions of Native hemi-cellulose

Re-suspend pellet from step 2, while still wet in 100mls of 8M Urea (buffered to pH 7.5 with 50mM Hepes/ NaOH.) Shake/stir for 16h at 25°C. Centrifuge, pour off the supernatant. Assay polymers by anthrone or ethanol tests. Repeat urea extraction until the supernatant no longer contains polymer. Re-suspend pellet in water and centrifuge.

### **Guanidium thiocyanate (Gdm)**

Extracts some mannose rich hemi-cellulose

Repeat step 3 with 4.5M Gdm in place of 8M urea.

### **NaOH**

Extracts a high proportion of total hemicellulose but with de-acetylation, some pectin with de-esterification.

Repeat step 3 with 6M NaOH containing 1% NaBH<sub>4</sub> in place of urea. Neutralise extracts with HOAc and assay by anthrone or ethanol tests.

### **NaOH/ H<sub>3</sub>BO<sub>3</sub>**

Extracts small proportion of de-acetylated hemicellulose, some de-esterified pectin

Repeat step 5, supplementing the extractant with 4% H<sub>3</sub>BO<sub>3</sub>.

### **Residue**

Contains cellulose, some resistant pectins and hemicelluloses and extensins

Wash final pellet extensively with H<sub>2</sub>O; freeze dry, weight.

### **Appendix 6: De-salting by Dialysis**

Dialysis is a classic technique for removing un-wanted molecules from a solution of high concentration without losing any molecules of interest. The extractant will pass through a semi-permeable membrane into an external solution with a low osmotic potential. The extractants must be removed because they can interfere with the spectrophotometry. The samples collected from steps 5, 6 and 7 must be de-salted using this method.

Sample 200ml of total hemicelluloses extracted by 6M NaOH/ 1% NaBH<sub>4</sub>

- 1) Prepare the dialysis sac by soaking a 65cm length of 5cm wide visking (dialysis tubing) in water. A 5min treatment is adequate: but soaking also gives an opportunity to wash the tubing (e.g. in 1M EDTA, pH 6.5. followed by 1M NaOH and finally wash with copious amounts of water), for work requiring high purity. Tie two knots in one end of the tubing.
- 2) Neutralise the sample (200mls), and adjust the pH to 5 by addition of acetic acid (requires ca. 120ml). Add acid gradually to avoid heating and so that bubbles of H<sub>2</sub> given off by NaBH<sub>4</sub> do not cause excessive frothing. [It is possible at this stage to centrifuge down and collect the precipitate of 'Hemicellulose A' (flocculation of which is favoured by incubation at 37<sup>0</sup>C); 'hemicellulose' B' is the polysaccharide that remains in solution on neutralisation. Alternatively dialyse the whole suspension.]
- 3) Using a funnel, pour the sample into the tubing. Expel air, and tie two more knots at the other end of the sac. [It is unnecessary to leave room for osmotic expansion of the sample, as visking tubing is very resistant to bursting.]

## Appendices

- 4) Place the sac in a 2litre measuring cylinder almost filled with 0.05% chlorobutol. Stir gently for 1h.
- 5) Change chlorobutol solution; stir for a further 1h. Repeat hourly for 6 hours. Finally stir overnight in fresh chlorobutol.
- 6) Open sac with scissors (cautiously, in a large breaker as the sac will be under pressure). Estimate the sodium acetate concentration of the sac content by use of a conductivity meter. If low enough, freeze dry.

### **Appendix 7: Analysis by Spectrophotometry**

Spectrophotometry uses the transmission/absorbance of light to measure the optical density of a liquid. The target molecules react with certain chemicals that take on a specific chirality giving that a distinct colouration. Depending on the depth of colouration highlights the amount of the target molecules present in the solution. Samples are measured against a 'blank' of a known concentration of the target molecule. By using a series of solutions of known concentrations a calibration curve can be drawn for each target molecule. The products from each extraction will be analysed for the specific saccharides that were to be removed at that stage.

### **Cellulose**

Updegraff method used to assay with cellulose standard.

Suspend the sample (containing 0.2-20 mg cellulose) in 3ml 'acetic-nitric reagent' [HOAc/H<sub>2</sub>O/HNO<sub>3</sub>, 8:2:1], cover the tube with a glass marble, and heat in a boiling water bath for 30min to hydrolyse non-cellulosic polysaccharides. Cool. Centrifuge at 2,500g for 5 min. Reject the supernatant. Re-suspend the pellet in 10 ml acetone. Re-centrifuge and reject the supernatant. Dry the pellet, and then re-dissolve it in 1ml of 67% (v/v) H<sub>2</sub>SO<sub>4</sub> with shaking at 25<sup>0</sup>C for 1h. Transfer 1-100ul of the solution (depending on the expected cellulose content. 20-0.2mg) into a clean tube containing 0.5ml H<sub>2</sub>O, add 1ml 0.2% anthrone in conc. H<sub>2</sub>SO<sub>4</sub>. Proceed to next section.

### **Hexose, free and polymer-bound (soluble + insoluble)**

## Appendices

### Anthrone assay with glucose standard

To 0.5ml aqueous solutions or suspension (containing 5-50  $\mu\text{g}$  hexose, add 1ml 0.2% anthrone in conc.  $\text{H}_2\text{SO}_4$ . Mix (careful shaking is required because  $\text{H}_2\text{SO}_4$  is much denser than  $\text{H}_2\text{O}$ . Caution: becomes hot.) Incubate in boiling water for 5 minutes. Cool. Read  $A_{620}$ . Hexose (and 6-deoxyhexose) containing material goes blue; other sugar units give paler, greenish colours.

### **Pentose, free and polymer-bound (soluble and insoluble)**

#### Orcinol assay with a Xylose Standard

Solutions required:

**A** = 6% orcinol in ethanol

**B** = 0.1%  $\text{FeCl}_3 \cdot 6\text{H}_2\text{O}$  in conc.  $\text{HCl}$ .

To 0.5ml of aqueous solution or suspension (containing 1-10  $\mu\text{g}$  pentose) add 67  $\mu\text{l}$  of **A** followed by 1ml of **B**. Mix well. Incubate in a water bath for 20 min. Cool. Mix again. Read  $A_{665}$ . Pentoses give a green to blue colour, depending on concentration.

### **Uronic acid, free and polymer bound (soluble and insoluble)**

#### m-hydroxybiphenyl assay with a galacturonic acid standard

Solutions required:

**A** = 0.5% borax in conc.  $\text{H}_2\text{SO}_4$

**B** = 0.15% m-hydroxybiphenyl [also known as 3-hydroxydiphenyl or m-phenylphenol] in 1M  $\text{NaOH}$ .

To 0.2 ml aqueous solution or suspension (containing 1-20  $\mu\text{g}$  uronic acid) add 1ml **A**. Mix (careful shaking is required because  $\text{H}_2\text{SO}_4$  is much denser than  $\text{H}_2\text{O}$ . Caution: becomes hot.) Incubate in boiling water bath for 5minutes. Cool in a bath of tap water. Read  $A_{520}$ . Then add 20 $\mu\text{l}$  **B**, mix

## Appendices

thoroughly incubate at 25<sup>0</sup>C for 5 minutes, and re-read A<sub>520</sub>. Calculate increase in absorbance (pink colour), which indicates uronic acid content. (SDS interferes badly).

### **6-Deoxyhexose, free and polymer bound (soluble and insoluble)**

Cysteine/H<sub>2</sub>SO<sub>4</sub> assay with a fructose or rhamnose standard.

Solutions required:

**A** = 86% (v/v) H<sub>2</sub>SO<sub>4</sub>

**B** = 3% L-cysteine-hydrochloride monohydrate in water.

To 0.2ml aqueous solution or suspension (containing 1-100ug 6- deoxyhexose) add 1ml ice-cold **A**. Mix well because H<sub>2</sub>SO<sub>4</sub> is much denser than H<sub>2</sub>O. Caution becomes hot). Cool in 25<sup>0</sup>C water bath. Incubate in a boiling water bath for exactly 3minutes. Cool in a 25<sup>0</sup> water bath. Add 20ul **B** and mix well. Incubate at 25<sup>0</sup>C for 2h. Read A<sub>380</sub>, A<sub>396</sub> and A<sub>427</sub>. The difference (A<sub>396</sub> – A<sub>427</sub>) is proportional to 6-deoxyhexose content; (A<sub>427</sub> – A<sub>380</sub>) is an indication of hexose content (but the colour yield for glucose and fructose is about double that for galactose and mannose). If a large excess of hexose interferes with reliable estimation of 6-deoxyhexose, prolong the 100<sup>0</sup>C treatment to 10 minutes: this virtually abolishes colour production by hexoses.

## **Appendix 8: Probe Manufacture**

### **Dimensions Required**

A major assumption of the modelling process is that the cells are compressed by two flat parallel rigid surfaces of infinite size. Therefore it is essential that the surface of the probe tip is flat and perfectly parallel to the base of the chamber.

As the single *Arabidopsis thaliana* cells are approximately 20-40 $\mu\text{m}$  in diameter the tip of the probe must be at least three times that, so a probe tip approximately 100 $\mu\text{m}$  in diameter will be sufficient. This is necessary to accommodate the horizontal expansion of the cells during compression, if the cell were to reach the edge of the probe this would invalidate any models applied. Any larger will make it difficult to position the probe above a cell, due to magnification required and samples with a high cell density and larger cell aggregates will make isolating single cells to compress much more difficult due to the probe tip area.

The probe tip must be perfectly flat otherwise the data acquired will not fit the standard models. The shaft of the tip must be long enough so that it can be attached to the transducer tube but not too long otherwise the probe may not fit in the chamber or may foul on the transducer casing, in addition this a long probe or a tip that is too drawn out will generate higher levels of compliance.

### **Tip Pulling**

The probes are made from solid borosilicate glass fibres that is heated and stretched to approximately 2mm in diameter, made on site by the University glass blower. Using a Narishige PB-7 tip puller (Narishige Co Ltd., London, UK), a short section of the glass fibre is heated around the midpoint and pulled using weights to taper it into a point. The diameter of the tip can be changed through different heat levels and amount of weight added.

### **Tip Shaping**

Once the tip has been pulled it is going to have to be shortened and shaped. The drawn point is too narrow and the probe itself cannot measure more than 2cm once finished.

Once shortened the probe is secured into the Narishige MF-900 microforge (Narishige Co Ltd., London, UK). The microforge is a device that is used to shape the tip end into an approximately flat surface of approximately the correct diameter. It contains a thin wire filament (approximately 100µm in diameter) that is heated, the probe is touched against the filament to melt it. The heating is then stopped and the probe allowed to cool slightly and then drawn out to give the flat surface.

### **Grinding**

There is likely to be slight inconsistencies in the tip surface, which can be removed using a Narishige EG-70 micropipette grinder (Narishige Co Ltd., London, UK). The probe is mounted vertically in the grinder and ground at high speeds on successively finer lapping paper (3µm, 1µm and 0.3µm.) During the process the probe is raised from the paper, rotated by 90° and moved back down onto the paper. This is done every 30-60 minutes to prevent permanent bending of the probe and to ensure the tip is ground evenly. The probe is then assessed under a light microscope at x 40 magnifications from a number of directions to check the diameter and the flatness.

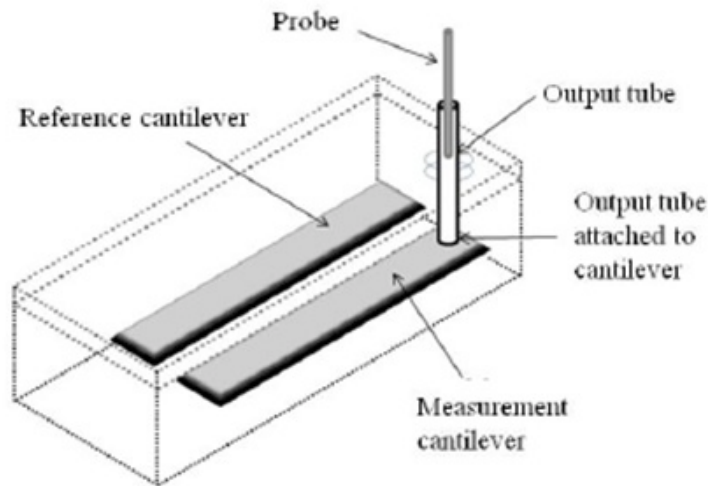
### **Mounting the Probe**

The transducer is secured to a table with the output tube vertically upwards, and the finished probe is fixed using household superglue. Special care must be made to ensure that the probe and the tube are perfectly parallel; which will cause the cells to be moved during compression. To remove the probe it must be submerged in acetone to dissolve the superglue. The transducer is then mounted on the compression rig and lowered to the base of the sample chamber. The contact between the tip and the base is checked to ensure they are parallel.

### **Appendix 9: Force Transducer**

For work with plant cells, initially a 400A force transducer (Aurora Scientific Inc., Ontario, Canada), which is capable of measuring forces of 50mN.

The force transducer contains two silica cantilever beams, a reference cantilever and a measurement cantilever that has an output tube attached. The cantilevers arms are identical in construction, size and mounting within the transducer act as capacitors. If no force is applied to the measurement beam then the capacitance of the beams was equal and the output voltage was zero. If a force is applied to the measurement beam it is deflected and the capacitance is changed. This new capacitance is then compared to that of the reference beam leading to a non-zero result proportional to the deflection hence the force being applied. The resultant force versus time data was recorded by an Amplicon PCI 120 card (Amplicon Liveline Ltd., Brighton, UK). The frequency of voltage sampling and the time can be adjusted. Any thermal effects, mechanical vibrations and electrostatic interference would affect both cantilever beams and should be cancelled out. However, as the output tube increases the weight of the measurement beam this was not the case and mechanical noise was still a problem. Precautions need to be taken which included conducting all experiment on an air cushioned benches to eliminate any unnecessary vibrations. For the data to be analysed the FTC must be calibrated and values for the sensitivity and compliance must be calculated (see appendix X for details).



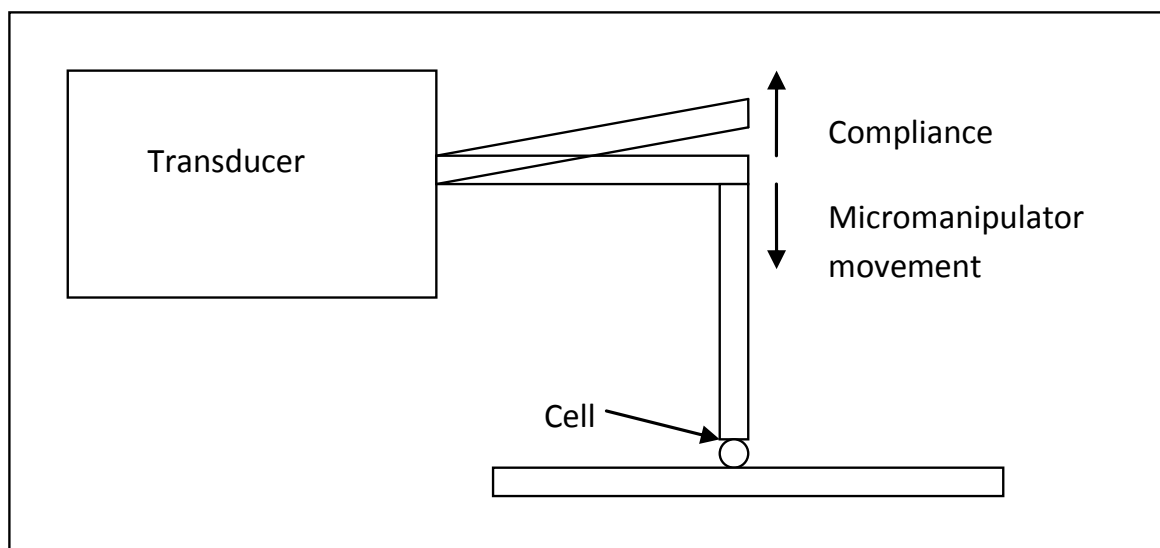
**Appendix 10:  
Calibration - Sensitivity**

**Transducer**

In order to accurately calculate the forces involved, the sensitivity of the transducer must be similar to the manufacturer's limits otherwise the data will be inaccurate. The sensitivity should be checked before each experiment, as this can change throughout the life of the transducer.

Initially using a 5 gram transducer, it is secured on a flat bench with the tube pointing vertically upwards in a room free from draughts. Samples of known weight are balanced on top of the probe to provide a force and the voltage is recorded. This is done using paper for small weights and blue tack for anything above 0.5g. These weights were measured accurately to 0.001g. Prior to the addition of the weight a baseline voltage is recorded, which will be subtracted from the test voltage to get the change. The weights are converted to forces (weight in g x 9.81) and a graph is plotted with voltage against force (mN), with the gradient of the line being the sensitivity (mN/V).

**Appendix 11: Transducer Calibration - Compliance**



The transducer measures the force by the degree of bending of the cantilever arm, this bending is known as the compliance. Compliance is a problem, as the displacement needs to be calculated in order to determine the cell height. The distance the probe has moved can be calculated by multiplying the probe speed and time since the probe started squeezing the cell. Unfortunately, the distance moved is not the actual displacement. This is because the beam bends in the opposite direction in response to the force. Therefore, the compliance had to be calculated and subtracted from the corresponding distance calculation to provide accurate data for force/displacement graphs.

## Appendices

To measure compliance, before taking measurements the probe was pressed against the glass surface and a voltage/time graph was produced. From this graph the  $\Delta t$  and  $\Delta V$  were extrapolated to calculate the compliance.

Calculation:

Speed [ $\mu\text{m/s}$ ]  $\times \Delta t$  = distance moved by the probe [ $\mu\text{m}$ ]

Distance moved by the probe  $\div \Delta V$  =  $\mu\text{m/V}$

$\mu\text{m/V} \div$  sensitivity of the transducer [ $\text{mN/V}$ ] = compliance in  $\mu\text{m/mN}$

## Appendix 12: Compression Rig Control and Calibration

### Control

Hyperterminal is the control programme for the stepping motor. As the step distance is fixed, there are only two controllable variables, the wait between steps and the number of steps moved by the motor.

Command	Action
Version	Returns the version number of the unit. Should return version 2.0 if working correctly.
C	Sets the number of steps for the motor to move (e.g. c,2000). Input 'C' and the number of assigned steps will be returned.
Wait	Sets the delay between the steps which has the effect of controlling the speed of compression. (e.g. wait,50). Input 'wait' and the assigned wait value will be returned.
U	Moves the motor down the by the set number of steps
D	Moves the motor up by the set number of steps
Z	Sets the position to zero
M	Sends the motor to the zero position
P	Returns the position in steps
K	Kills all movement

These commands are confirmed by pressing the enter key, and are the only ones required in order to collect the desired data.

### **Step Distance**

The step motor is used to move the probe up and down, and has a factory specified step distance of  $0.012\mu\text{m}$  per step. It is important to know the stepping distance in order to work out the distance moved by the probe. As theoretically moving the probe 10000 steps should be a displacement of  $120\mu\text{m}$ . The distance moved is required for the calculation of other aspects of the analysis.

To calculate the step distance a  $100\mu\text{m}$  graticule is positioned in the view of the side aspect camera using the  $35\times$  magnification lens. An acetate sheet with the print of a 30cm ruler is affixed to the monitor screen showing the view of the graticule. The corresponding length of  $100\mu\text{m}$  on the ruler is noted as 13.7cm, which equals 16.5cm for  $120\mu\text{m}$  (10000 steps). Hyperterminal is set to  $c=10000$  and  $\text{wait}= 50$ , the probe tip was positioned at 0cm and moved through the full motion and the distance moved is noted.

This was checked through 10 sets of motion; the distance moved each time was 16.5, thus proving that the step distance was  $0.012\mu\text{m}$  as stated by the manufacturers.

### **Motor Speed**

Changing the wait between the steps can alter the speed at which the motor moves the probe. A lower wait will move the probe fast and the opposite for a higher wait. The manipulation of speed may be necessary in order to assess different aspects of the cell wall physiology, for the rupture force analysis high speeds are not required, however in order to assess water relations a high speed is required which this motor may not be able to provide.

To calculate a different range of speeds the motor was timed over a known distance at different wait values, this will enable the calculation of the speed. Using 10000 steps ( $120\mu\text{m}$ ) as the known distance the motor was set through its motion 15 times at different wait values.

Calculation:

$$\Delta t \text{ [s]} \div \text{number of steps moved} = \text{seconds/step}$$

$$0.012\mu\text{m/step} \div \text{seconds/step} = \text{speed } [\mu\text{m/s}]$$

Wait	Average t(s)	sec/step	speed ( $\mu\text{m/s}$ )
50	1.82	0.000182	65.94
100	2.56	0.000256	46.9
150	3.44	0.000344	34.9
200	4.264	0.000426	28.16
250	5.122	0.000512	23.43
300	5.916	0.000592	20.29

## **Appendix 13: Immunolocalisation TEM staining**

### **Fixing material**

Samples were placed in a solution of 2% paraformaldehyde; 0.1% glutaraldehyde in 0.1M sodium cacodylate buffer. Tissue is left in this solution to fix overnight.

### **Dehydration**

Tissue was transferred to different ethanol concentrations, left for 15 min in each solution, 30%; 50%; 70% and 90%.

### **Embedding**

Tissue was transferred to a vial containing 5 ml (1:1) 90% ethanol: LR white (hard grade). The vial was left for 2 hours on a rotor the movement prevents the resin setting. This was repeated with fresh mix. The tissue was then transferred to 5ml of 100% LR white and left overnight on the rotor. The tissue was transferred to fresh 100% LR white and left for approximately 7 h.

## Appendices

Gelatine capsules were filled with LR white. The tissue was placed in the capsule and orientated into position using a seeker. Care must be taken to remove any air bubbles that may have become trapped; these will cause the resin to crack as it dries. The lids were placed in the capsules and they were placed under UV light ( $\lambda = 366 \text{ nm}$ ) for 2 days to polymerise the resin.

### Sectioning

The gelatine capsule was removed using a razor blade. The block end was trimmed and faced up using a razor blade (to a trapezium shape.) The block end was smoothed off using a glass knife. 2-micron sections were cut using the glass knife and collected on to polylysine glass microscope slides. These sections were stained with 1% toluidine blue to ensure the samples were at the face. This process was repeated with the faced blocks with a diamond knife and an ultramicrotome. These samples were transferred to formvar coated sample support mesh grids.

### Staining for TEM

Transfer grids to be stained into slotted grid carrier. Using a glass fill the centre of the reservoir with 30% uranyl acetate overfill so a meniscus bulges on top. Remove any air bubbles. Drop grid carefully on top eliminating any air bubbles. Leave for 7 minutes. Place grids in a beaker containing sonicated ultrapure water. Swirl around and empty water down radioactive sink. Empty and refill at least 3 times. Rinse reservoir in water and dry. Remove excess water from grids with filter paper. Using a syringe suck up 7 ml of lead citrate (this should be clear – do not use if not) and filter into the reservoir so a meniscus bulges. Drop grids carefully on top eliminating any air bubbles. Leave for 7 min. Tip used stain down the sink, do not re-use. Remove grids and swish around in a beaker of sonicated water containing one pellet of sodium hydroxide for about 30 seconds. Remove and place in a beaker of sonicated water – rinse 3 times with ultrapure water. Remove excess water with filter paper and put grids back in grid box while still damp. Do not allow grids to dry, as this will tear the formvar film when moving.